ULTRASTRUCTURAL AND CYTOCHEMICAL STUDIES OF GONADAL ORGANIZATION, SPERMATOGENESIS AND SPERMATOZOA OF MOLLUSCS

By

Sheng Tao Hou BSc, MSc

Thesis submitted in canditure for the degree of Doctor of Philosophy in the Faculty of Medicine, University of Glasgow.

Department of Anatomy

University of Glasgow

September, 1991

ProQuest LLC.
789 East Eisenhower Parkway
P.O. Box 1346
Ann Arbor, MI 48106 – 1346

DEDICATION

This thesis is dedicated to my wife Qiubo, with love and respect, for her understanding, full support, encouragement and secretarial assistance.

DECLARATION

I hereby declare that this thesis is my own composition, except where duly acknowledged, and has not been submitted for consideration of any other degree in this or any other Universities.

Sheng Tao Hou

ACKNOWLEDGEMENTS

It is a pleasure to thank the many people whose assistance has been invaluable throughout this project.

It is not possible to adequately thank my supervisor Dr W. L. Maxwell, for his continued interest, guidance, encouragement, constructive criticism and incredible patience throughout the course of my research. He has been always willing to give up his time to discuss the work, to help with collecting specimen, and to read and comment on many drafts both for publication and this thesis. The idea of this work stemmed from his teaching, for which I shall always be grateful.

I wish to express my sincere gratitute to Professor R. J. Scothorne, F.R.S.E., for providing facilities for my research in the Department of Anatomy, University of Glasgow.

I thank all of the technical staff in the Department for their help during my time in the department. Particularly, I am indebted to Mr J. McGadey, Mr D. Russell, Mr R. Kerr and Mr O. Reid for their valuable instruction and assistance with SEM and TEM; to Ms M. Hughes and Mrs M. Houston for photographic help and Mrs C. Crossan for artistic assistance.

My thanks are also due to Dr L. Tetley (Department of Zoology) for permission to use the freeze-fracture apparatus in the centralised laboratory of the University of Glasgow; Mrs A. Sim, for her excellent technical help

with freeze-fracture and glycogen cytochemistry, and Dr D. Jiang (Aeronautics Department, University of Glasgow) for his help with statistical analysis.

I am extremely grateful to Professor J. Allen in the University Marine Biological Station (Millport, Isle of Cumbrae, Scotland) for his timingly supply of materials (listed in Section **Materials** A, B and C), and Mr C. P. Palmer in the Department of Palaeontology, British Museum (Natural History), London, for species identification (Scaphopoda, Antalis entalis).

I especially thank Dr A. P. Payne, for his constant encouragement and strong support; Dr R. A Smith for his encouragement, stimulating discussion and spending time helping me with introductory literature concerning microtubular studies. I am also grateful to Mr G. Gillepie, Mrs L. Peedle and Ms. B. Robinson, for their ever kindly help during my study in the department, and Dr D. Badran for his companionship over the past three years.

Special thanks are due to Mrs D. Maxwell, for her hospitality, generosity and encouragement throughout this period, to which I am indebted and shall always remember.

Lastly, I owe a considerable debt of gratitude to my wife, parents and parents-in-law, for their love, endless and wholehearted support and encouragement which helped me through to the end.

This research project was supported by a University of Glasgow Postgraduate Research Student Scholarship and an

Overseas Research Student Award. I was extremely honoured to receive these awards for which I am most grateful.

CONTENTS

PART I: TEXT

Page No.

ABSTRACT

The variety of different types of molluscan spermatozoa, spermatogenesis and gonadal organization was demonstrated in this study. The primitive type of spermatozoon was described in Antalis entalis (Scaphopoda); an intermediate type in Rossia macrosoma (Decapoda) and the modified type in Archidoris tuberculata, Tritonia plebeia, Aplysia faciata (Opisthobranchia) and Arion hortensis (Pulmonata).

The spermatozoon of Antalis entalis (Scaphopoda) consisted of a head, midpiece and tail. The acrosome surmounted the nucleus and was membrane-bound. It was formed by an acrosomal granule surrounding an acrosomal fossa into which was invaginated the acrosomal and plasma membranes to form a pit extending to half the acrosomal depth. The nucleus was an elongate truncated cone containing a few nuclear cavities, primarily within the posterior portion. Five large, spherical mitochondria were closely apposed to the nuclear base. There was a proximal and distal centriole orientated perpendicularly within the mid-piece. A discrete satellite complex was associated with the distal centriole. The axoneme was of typical " 9+2 " structure enveloped by the plasmalemma.

During spermatogenesis, the spherical proacrosome was secreted by a single Golgi complex, migrated toward the anterior pole of the spermatid, and there differentiated to

assume the form of an electron-dense collar. Nuclear condensation did not occur until the proacrosome and mitochondria migrated towards the potential anterior and posterior poles of the spermatid. Chromatin condensation occurred by the formation of heterochromatin granules. No manchette of microtubules was observed in the course of nuclear condensation and elongation. Mitochondria achieved their mature spherical shape by decreasing in number and increasing in diameter at an early stage of spermiogenesis. No inter-mitochondrial or mitochondria-nuclear (or centriolar) junctions occurred. Beta glycogen granules appeared late in the development of the spermatid, and were mostly distributed in the centriolar region. This study is the first ultrastructural investigation of Scaphopod spermatogenesis.

The organization of the testis and process of spermiogenesis of the decapod mollusc Rossia macrosoma was investigated by electron microscopy. Cytochemical analysis, by use of the periodic acid-thiosemicarbazide-silver proteinate (PA-TSC-SP) technique, allowed the precise localization of glycogen in the spermatozoon. Nuclear morphogenesis occurred in three stages (termed A, B and C), resulting in the transformation of the nuclear shape from a spherical (stage A) into an elongated form (stages B and C). Prior to elongation of the spermatid nucleus, the sac-

like proacrosome, derived from a single Golgi complex, became located at the apex of the nucleus and further transformed into an elongated structure surrounded by longitudinally orientated microtubules as spermatid elongation occurred. A group of mitochondria assumed an interwoven form in the mitochondrial pocket. Large quantities of glycogen granules, β-particles about 130-145 Å in diameter, were demonstrated in the midpiece in connection with the specialized external plasmamembrane of the mitochondrial sleeve and within or around the axoneme in the tail piece. The most striking feature of the distribution of glycogen was nine rows of intra-gamma-fibres particles, at a spacing of 20-26 μm, along the longitudinal axis. The pattern of glycogen distribution in the spermatozoon was compared with that in octopods and other molluscan groups.

Comparative ultrastructural features of the ovotestes and spermatogenesis of three opisthobranchs, Archidoris tuberculata, Tritonia plebeia and Aplysia faciata, were described. Early stages of spermatogenesis appeared similar among these three species. However, prominent structural differences were demonstrated with respect to later stages of spermiogenesis and spermatozoa. The ovotestis contained two types of somatic cells within the testicular portion: flattened myoepithelial cells defined the outer acinar wall

and accessory cells overlay the basal lamina on the luminal aspect of the male compartment. Early spermatogenesis was similar to that described in other opisthobranchs. In contrast, the late stages of spermiogenesis presented great morphological differences.

Stages of spermatid development were divided into Pre-cup, Cup, and Elongating stages depending on the general shape of the nucleus. Nuclear differentiation involved the formation of anterior and posterior nuclear plaques, condensation of chromatin fibrils into lamellae, the insertion of the centriole into the nuclear fossa and eventually formation of an elongated sperm head. There is a discrete difference of helical form in the three species.

The present study provided evidence to comfirm the existence of an acrosome in opisthobranchs and its origin from the Golgi complex. The detailed processes of the fusion of mitochondria into a large mitochondrial derivative which eventually ensheathed the axoneme, forming a pseudo-paracrystalline periaxonemal sheath, and location of glycogen deposit in the glycogen helix were also described.

Within the ovotestis of the pulmonate, Arion hortensis, desmosome-like junctions between Sertoli-Sertoli and Sertoli-germ cells (spermatogonia, spermatocytes, spermatids and spermatids just prior to spermiation),

together with adjacent long septate junction, were investigated. Desmosome-like junctions were circular when viewed en face and 90-180 nm in diameter. The intercellular space at the junctional site was 15-25nm in width. An intermediate dense line was absent.

Freeze-fracture replicas showed that these junctions formed groups, with one to ten junctions within each group. The most prominent feature of the desmosome-like junction was an electron dense plaque on the cytoplasmic face of the plasmalemma. I described variation in the development of the electron dense plaque on the germ cell side at different stages in the development of the germ cell by analysing serial thin sections. In the spermatogonium and spermatocyte stages, desmosome-like junctions had equally developed electron dense plaques. The plaques were pronounced in junctions between Sertoli cells and spermatocytes/spermatids and less developed in relation to late spermatids where nuclear condensation was complete, and appeared to be lost at spermiation. Finger-like processes arose from the Sertoli cell as desmosome-like junctions are lost at spermiation.

Treatment of the ovotestis with hypertonic fixative solutions containing dextrose demonstrated that the intercellular space between Sertoli cells and germ cells was increased except where the desmosome-like junctions were present. I suggested that desmosome-like junctions

provide strong adhesive sites between Sertoli and germ cells. Furthermore, studies of the ovotestis, treated with different particle sizes electron dense tracers, i.e. lanthanum nitrate, HRP and Ferritin, provided evidence that the desmosome-like junction, together with long septate junction, formed a selective barrier which was only permeable to small molecules.

GENERAL INTRODUCTION

GENERAL INTRODUCTION

A large body of literature of studies of molluscan spermatozoa and spermatogenesis is now available. This includes two prominent aspects: one is the progression of morphological discoveries paralleling the development of research tools; the other is the contemporary one, which spans the very broad range of fine structural, biochemical and biophysical topics of molluscan spermatology. Pertinent literature is voluminous, but it is unsystematic and incomplete. For classes Scaphopoda, Cephalopoda and the subclass Opisthobranchia information is so scanty that valid comparisons with other molluscan groups can not still be made. It is therefore the aim of the present study to investigate those groups which have been poorly studied and to address specific problems which have been highlighted in the recent literature; for example, the permeability of the pulmonate ovotestis.

The presence of spermatozoa within seminal fluid was not recognized until the invention of the microscope by the Dutch investigator Antony van Leeuwenhoek and his student, Ham in 1677. They reported the existence of human spermatozoa and sketched their morphology. However, the first extensive study on the morphology of molluscan sperm, together with those of other metazoan animal species, was undertaken by the Swedish histologist Gustaf Retzius only from 1904. In his outstandingly accurate reports (1904-

1906), he described the organization of the spermatozoa of chitons, bivalves and lower prosobranchs. A bulbous acrosome, columnar nucleus, between four and eight mitochondria and a thin and long flagellum were demonstrated. He even noted the general type of sperm architecture which was common to a great number of lower animals. He called this type of sperm the "primitive" spermatozoon.

Tuzet (1930) using light microscopy studied spermiogenesis of the Gastropoda and was the first investigator to postulate that sperm morphology might be correlated with the biology of propagation, fertilization and phylogenetic relations.

Further extensive, comparative analysis of spermatozoa and spermiogenesis of a very wide variety of molluscan groups by Franzén (1955; 1956) showed that molluscs exhibited perhaps the greatest diversity of spermatozoan form within the Animal Kingdom. He also provided further evidence that molluscan sperm morphology was linked to fertilization biology and phylogenetic affinities.

Using both phase-contrast microscopy and a variety of staining agents, Franzén (1955; 1956) accurately described the spermatozoan morphology of more than 40 molluscan species and developed the concept of the so-called "primitive" and "modified" type of spermatozoon according to the fertilization biology of the species. The primitive

spermatozoa were described in Aplacophora, Polyplacophora, Lamellibranchia and Scaphopoda, all of which have retained the primitive mode of discharging sperm into the surrounding water for external fertilization. This type of sperm consists of a rounded head, a middle piece containing between four and eight spherical mitochondria and a tail formed by a long filament. The so-called modified type of sperm is associated with those molluscan groups practising internal fertilization, for example: Prosobranchia (except Archaeogastropoda), Pulmonata and Opisthobranchia. The major difference from the primitive type of sperm is their elongated head (some even helical), enlarged and transformed mitochondrial derivatives extending along part of, or even the whole of, the tail. As to cephalopod spermatozoa, Franzén (1967) demonstrated features of both primitive and modified types of spermatozoa. He therefore suggested that the cephalopod spermatozoon was of an intermediate type. Retzius (1904-1906) and Franzén (1955-1970), between them, have described the spermatozoa of no less than 242 invertebrate species. Their work forms the broad basis for later electron microscopical investigations.

Invention of the electron microscope in the 1930's and its application to fine structural research of molluscan gametes since the late 1960's has provided an enormous wealth of data (see reviews by Afzelius, 1972; Baccetti and Afzelius, 1976; Roosen-Runge, 1977; Maxwell,

1983; Hodgson, 1986). In particular, detailed studies concerning molluscan spermiogenesis have provided a substantial amount of information for the accurate interpretation of the structure of the mature spermatozoon. The morphology of the male germ cells is so diverse, that there is no identical form between even two closely related species (see reviews by Afzelius, 1972; 1975; Yasuzumi, 1974; Baccetti and Afzelius, 1976; Adiyodi and Adiyodi; 1983; Baccetti, 1986). Baccetti and Afzelius (1976) provided a very comprehensive and authoritive review, in which spermatozoa of about 1000 animal species had been examined by electron microscopy. Ultrastructural information on molluscan spermatozoa confirmed and extended the former light microscopical observations. Extensive studies on spermatozoa have also shown the enormous interspecific variation, demonstrating the species-specificity of spermatozoan morphology.

It would be extremely tedious to review the sperm morphology of every individual molluscan species in this chapter, rather I will summerize the common features and point out some variations.

Available information on molluscan spermatology demonstrates that sperm morphology is useful in determining species systematic and evolutionary phylogeny. However, our knowledge of sperm diversity within the whole molluscan phylum is still sketchy, certainly too imcomplete to propose any detailed molluscan phylogeny. It is only

recently that spermatogenesis of Aplacophora, Polyplacophora and Scaphopoda has been examined by electron microscopy (Hodgson et al., 1988; Buckland-Nicks and Chia, 1989; Hou and Maxwell, 1991) and considerable structural variation within primitive and modified types of spermatozoa have been demonstrated.

(A) Primitive Type of Spermatozoon And Its Spermiogenesis

Recent EM studies have confirmed the occurrence of the primitive type of spermatozoon in Aplacophora (Buckland-Nicks and Chia, 1989), Scaphopoda (Dufresne-Dube et al., 1983; Hou and Maxwell, 1991), Archaeogastropoda (Hodgson and Bernard, 1988; Kohnert and Storch, 1983) and most of the Bivalvia (Popham, 1979); except in Scrobicularia plana and galeommatoidean bivalves Divariscintilla yoyo, D. troglodytes and Scintilla sp., which have the modified type of spermatozoa, described by Sousa et al. (1989) and Eckelbarger et al. (1990). Franzén (1955) classified the spermatozoon of the Polyplacophora as belonging to the primitive type. However, recent ultrastructural studies of this group raise considerable controversy. Russell-Pinto et al. (1984) studied several chiton species and provided evidence that the class Polyplacophora, which practises external fertilization, has the modified type of spermatozoon.

The Aplacophora are a rare group of worm-like molluscs. Their reproductive biology, in particular male

germ cell differentiation, has only been described in detail recently (Buckland-Nicks and Chia, 1989). Earlier studies suggested that Chaetoderma sp. has a sperm type similar in appearance to that of chitons (Retizus, 1904; Hadfield, 1979). However, more recent ultrastructural studies of spermatogenesis demonstrate many unexpected features (Buckland-Nicks and Chia, 1989), indicating that this sperm type is unique among Mollusca. Acrosome formation in Chaetoderma sp. is different from any other molluscs studied. The acrosome itself is relatively undifferentiated. However, the Golgi complex produces an apical horn and apical dense tube in coordination with the acrosome. These structures are unique features, but their functions remain unknown. Another extraordinary feature in Chaetoderma sp. spermiogenesis is the production of two flagella, one from each centriole. The proximal centrole which forms the proximal flagellum is shed anteriorly with residual cytoplasm in late spermiogenesis, leaving only a distal flagellum, derived from the distal centriole, forming the tail piece in the mature spermatozoon. Buckland-Nicks and Chia (1989) suspected that the occurrence of the temporary proximal flagellum might be related to the elongation and deployment of the apical dense tube.

Published studies on species of the class Polyplacophora are very limited, and still, considerable controversy remains. Franzén (1955) examined the

spermatozoa of two chiton species Lepidopleurus asellus and Tonicella marmorea. He placed these sperms into the primitive category. More detailed transmission electron microscopical studies of other chitons, i.e. Onithochiton quercinus, Chiton pelliserpentis and Plaxiphora paeteliana by Sakker (1983; 1984) concurred with Franzén's view. However, Russell-Pinto et al. (1983; 1984) suggested that spermatozoa in Chiton marginatus, Callochitoa septemvaluis, Acanthochitona crinita and Chaetopleura angulata should be classified as the "modified" type. They described modifications to the primitive plan in these chiton spermatozoa, which include lateral positioning of the mitochondria of the midpiece alongside the nucleus and the lack of an acrosome. Hodgson et al. (1988) provided an extensive study of 11 species from the Polyplacophora. Results were thoroughly compared with previous studies. Hodgson and co-workers (1988) confirmed that the structural changes occurring during spermatogenesis in suborders Chitonina and Acathochitonina were similar to those described by Russell-Pinto et al. (1983, 1984) and Sakker (1984). However, they did not agree with the assertion of Sakker (1983, 1984) that chiton sperm should be regarded as of the "primitive" type on the basis that the head, midpiece and the tail region were distinct and mitochondria were similar to those in the primitive type of spermatozoon. They proposed that the strucuture of sperm of the Chitonina and Acanthochitonina appeared to be

transitional between the truly primitive and truly modified types in that the acrosome was lost and there was some displacement of the mitochondria, but the boundaries of the various regions remained distinct. Leptochiton asellus is a member of the more ancient suborder Lepidopleurina and has several aspects of spermatogenesis that are very different. The presence of an acrosome in Leptochiton asellus suggest that in more recent chitons, the acrosome has been secondarily lost. Loss of the acrosome has been proposed to be correlated with variations in egg-coat thickness (Hodgson et al., 1988).

The spermatozoa of the bivalves are generally of the primitve type and structurally conservative. Both marine and fresh water species have retained this type of design (Retzius, 1905; Franzén, 1955, 1956, 1970, 1983; Maxwell, 1974b; Popham, 1979). Published studies on bivalve spermatozoan morphology demonstrate a fairly constant mitochondrial midpiece and tail, but great variation in nuclear length and acrosome shape (Maxwell, 1974b; Popham, 1979; Franzén, 1983; Healy, 1989; Eckelbarger, et al., 1990; Sousa et al., 1989).

The nucleus shows great morphological diversity, ranging from ovoid (Mytilus spp.; Niijima and Dan, 1965; Bourcart et al., 1965), short and conical (Lyrodus pedicellatus; Popham, 1974), nearly spherical (Crassostrea virginica; Galtsoff and Philpott, 1960), barrel-shaped (Spisula solidissima; Longo and Anderson, 1969; Neotrigonia

spp.; Healy, 1989), and elongate rod-shape (Musculus discors and Nucula sulcata; Franzén, 1983; Divariscintilla yoyo, D. troglodytes and Scintilla sp.; Eckelbarger et al., 1990) or long, tapering and curved (Tapes decussatus; Pochon-Masson and Gharagozlou, 1970; Scrobicularia plana; Sousa et al., 1989).

The acrosome, derived from the Golgi complex, also presents substantial morphological differences. For example, as simple as a single or multiple granules in relict bivalves Neotrigonia (Healy, 1989); or the most complex consisting of numerous substructures characteristically disposed within the acrosome (reviewed by Popham, 1979; Eckelbarger et al., 1990). Franzén (1983) stated that no two bivalve species are likely to have spermatozoa of identical morphology and thus this variation may be used for taxonomic purposes. This proposal is supported by recent further ultrastructural studies in a wide variety of bivalves (Healy, 1989; Sousa et al., 1989; Hodgson et al., 1990; Eckelbarger et al., 1990). Popham (1979) and Franzén (1983) also suggested that bivalve spermatozoan acrosome morphology is correlated with features of the egg envelope .

Relatively, scaphopod spermatozoa and spermatogenesis have received scant attention and leave a large gap in our knowledge concerning molluscan spermatology. Retzius (1905) classified scaphopod spermatozoa as of the primitive type. Franzén (1955) examined the spermatozoon of Dentalium

entalis using light microscopy and provided a brief account of spermiogenesis. Dufresne-Dube et al. (1983) confirmed the primitive type of spermatozoon in Dentalium vulgare using electron microscopy and demonstrated ultrastructural changes of the acrosome during fertilization. However, the detailed ultrastructural organization of the scaphopod spermatozoon, in particular spermatogenesis, have only very recently been published (Hou and Maxwell, 1991). I studied the organization of the testis, spermatozoon and spermatogenesis of Antalis entalis (Hou and Maxwell, 1991). A more detailed account is provided in this thesis.

(B) Modified Type of Spermatozoon And Its Spermiogenesis

The modified type of spermatozoa occurs in those molluscan groups practising external fertilization, for example, most of the Prosobranchia (except Archaeogastropoda), Opisthobranchia and Pulmonata. A number of publications by Giusti and Selmi (1982), Maxwell (1974b, 1983), Kohnert and Storch (1984a, b), Koike (1985), Afzelius and Dallai (1983, 1987), Afzelius et al. (1989), Healy (1983, 1988a, 1990), Griffond et al. (1991) and many references cited in these papers have expanded our knowledge of spermatozoa and spermatogenesis in prosobranchs and pulmonates. This has provided a sound basis for discussion of family / superfamily interrelationships (Healy, 1988b). However, our knowledge is still patchy concerning opisthobranch spermatology.

Species from Opisthobranchia and Pulmonata are collectively referred to as the euthyneura based upon comparative anatomy. One feature they share is the similar sperm design and features of spermiogenesis. The variety of form of euthyneuran molluscan mature spermatozoa was examined by Thompson (1973). The spermatozoa of Acteon (Bullomorpha), possessing four distinct mitochondrial spiral keels, have been suggested to be the primitive type of euthyneuran spermatozoa from which others have been derived, for example, Aplysia and Bursatella (Aplysiomorpha, with two spiral keels), and nudibranchs (only one spiral keel) (Thompson, 1973). In pulmonates, the spermatozoan organization in the Stylommatophora is similar to that in the nudibranchs. However, a great difference has been shown from that in the Basommatophora, possessing a multiplicity of helical structures in the sperm tail. Healy (1988b) and co-worker Jamieson (1989) provided a detailed review of euthyneuran spermatozoa and spermatogenesis. Only a single type of sperm, i.e. modified type of spermatozoa (capable of fertilization) is produced in euthyneura. In contrast, two types of spermatozoa, i.e. euspermatozoa and paraspermatozoa (Nishiwaki, 1964; Healy and Jamieson, 1981; Giusti and Selmi, 1982; Buckland-Nicks et al., 1983; Afzelius et al., 1989) are produced in meso-, neogastropoda and Neritoides. Healy (1988b) provided evidence in support of the suggestion that euthyneuran spermatozoan structure is useful in determining the position of some systematicly

uncertain groups. He further proposed (1988b) that, in all likelihood, pulmonates had been derived from opisthobranchs. But certainly, our knowledge of opisthobranch spermatology is still sketchy. A more detailed survey of three opisthobranchs from different suborders is therefore presented in Chapter III of this thesis.

(C). Organization of Testis / Ovotestis

The term "testis" applies to dioecious molluscan species, "ovotestis" in hermaphrodite species. Aplacophora, Monoplacophora, Polyplacophora and the majority of Bivalvia (except, for example, Galeommatoidea which are hermaphrodite according to Eckelbarger et al., 1990) are dioecious and their testes are paired (Roosen-Runge, 1977), or otherwise fused into a single lobule. In the Gastropoda, the gonad is always single and usually consists of a number of tubules or acini opening into a common duct. In the prosobranchs, the spermatozoa and ova may develop in the same tubule (as in Rissoella diaphana, Fretter, 1948) or the gonad may be divided into separate male and female lobes (Fretter, 1948). An example of a species that is exclusively dioecious is the dog-whelk Nucella lapillus (Walker and MacGregor, 1968). The testis of this animal consists of numerous tubules, in which spermatogonia lie in groups around the periphery and mature spermatozoa are arranged adjacent to the lumen with their tails directed

toward the centre. Groups of spermatocytes and spermatids are scattered in between.

Hermaphroditism prevails in pulmonates and opisthobranchs. Spermatozoa and ova are produced in separate compartments of an ovotestis. Luchtel (1972a, b) provided an excellent account of gonadal development and sex determination in the pulmonates Arion circumscirptus, A. ater and Deroceras reticulatum. He stated that the time of sex determination into male and female germ cells occurred during the early stages of the life cycle, around the time of hatching. Luchtel (1972a, b) obtained evidence to show that there were no genetic differences between the primordial germ cells. He believed that during the early stages of development (around the time of hatching), two compartments were established within an acinus -- a cortical compartment, in which oogonia differentiate, and a medullary compartment, in which spermatogonia differentiate. It was assumed that the somatic cell layer (Sertoli cells and follicle cells) maintained a tight barrier which separates the two compartments. Some of the primordial germ cells became localized at the cortex of the gonad and some in the medulla. Luchtel (1972a, b) therefore proposed that the primordial germ cells in two isolated compartments were subject to different microenvironments and thus developed into two different cell lines, the male and female germ lines.

Hill (1977) provided an account of the organisation

of the female compartment in Agriolimax reticulatus. Electron microscopical and cytochemical studies showed that the oocyte was encapsulated by a layer of follicle cells. The follicle cells were active in secretion and digestion. Adjacent follicle cells were connected by septate desmosomes and maculae adhaerens (terminology from Hill, 1977). At the time of ovulation, the follicle cell cytoplasm became electron opaque and the cells eventually peeled away from the oocyte leaving it exposed to the lumen. When electron dense tracers (HRP and Ferritin) were applied to the ovotestis, Hill (1977), however, was unable to locate any of these substances inside the follicle cells or in the surrounding intercellular spaces. He, therefore, suggested that, in Agriolimax reticulatus, the inter-follicular septate desmosome and macula adhaerens form a selectively permeable barrier controlling the transport of ions and molecules into and out of the oocytes. Griffond and Gomot (1979) found that, in Viviparus viviparus, septate junctions between oocytes and follicle cells retard the passage of injected HRP through the intercellular space, but they were not completely impermeable to the tracer. Further evidence is urgently required in order to provide better understanding of the ovotesticular organisation, especially, in the hermaphrodite pulmonate. In the present thesis (Chapter IV), I describe the intercellular junctional organizations in the male germinal epithelium of a pulmonate, Arion hortensis, and their

functional singificance in maintaining the blood-testis barrier. Part of the results concerning the desmosome-like junction has been published.

Segregation of different parts of the gonad producing different germ cells is most marked in the opisthobranchs. Considerable variation occurs, either as evaginations from the main gonadal mass containing female germ cells (Fiona), or the peripheral female part is attached by ductules to the central male part (Okadaia), or an individual acinus is either male or female as in Acteon, Pleurobranchaea, Archidoris, Sapha and Pseudovermis (Hyman, 1967; Maxwell, 1983). More recent studies show that the anatomic structures of the ovotestis in Nudibranchia are related to the intimate association established between the ovotestis and the digestive gland (Medina et al., 1986b, 1987). Eckelbarger and colleagues (1981; 1989) reviewed descriptions of the ovotestis of an eolid nudibranch, Spurillar neapolitana, made by several workers (Hyman, 1967; Miller, 1977), and, in addition, demonstrated clear compartmentation of male and female portions in the ovotestis. However, Eckelbarger and co-workers argued that previous reports, stating that outer female and inner male portions were in direct communication (Marcus, 1957; Hyman, 1967; Miller, 1977) were incorrect. Re-examination by electron microscopy demonstrated that the two portions were separated by layers of both accessory and follicular cells (Eckelbarger and Eyster, 1981; Eckelbarger et al., 1989),

suggesting that interpretation of gross ovotestis morphology in opisthobranchs warrants re-examination using electron microscopy. To this end, in the present thesis, I will describe and compare the organization of the ovotestes of Achidoris tuberculata, Tritonia plebei and Aplysia faciata in order to provide further information concerning the ovotestical variation in opisthobranchs.

Cephalopods are exclusively dioecious. The testis is generally a single unit derived from the coelom (Maxwell, 1983). The development and general structure of the decapod and octopod testes have been reviewed by Arnold and Williams-Arnold (1977) and Wells (1977). However, they did not provide any information concerning the microscopical organisation of the cephalopod testis. Arnold (1978) described the so-called Sertoli cell in the testis of Nautilus and its relationship with developing spermatogenic cells. Apart from this limited data, there has been no detailed description of the microscopical anatomy of the decapod testis. Further study is needed.

Afzelius (1970) compared spermatozoan morphology from a wide variety of animals and listed a large number of unsolved problems concerning the relationships of spermatozoan structure, function and physiology. Some of the questions have been answered in past years, but still a great deal of work is needed to provide a satisfactory understanding of molluscan spermatology.

MATERIALS AND METHODS

Materials

A variety of molluscs were examined with particular emphasis on those groups which have not previously been studied or where a specific problem has been highlighted in recent literature. Species from the following groups have been examined:-

(A) Scaphopoda: Antalis entalis. Mature specimens with a shell length of about 40mm were obtained from the University Marine Biological Station, Millport in Feburary and June 1989. Testis was prepared for paraffin embedding and TEM. Spermatozoa were smeared on a glass slide for phase contrast, light microscope and SEM observations.

(B) Decapoda: Rossia macrosoma were obtained from the University Marine Biological Station, Millport in June 1990. Portions of testis were fixed for TEM and paraffin embedding. Spermatozoa squeezed from the vas deferens were smeared onto a coverslip and prepared for SEM.

(C) Opisthobranchia: Archidoris tuberculata, Tritonia plebeia (Nudibranchia) and Aplysia punctata (Aplysiomorpha) were obtained from the University of Glasgow Marine Biological Station at Millport, Isle of Cumbrae, Scotland in June 1989 and May 1990. These specimens were mature adults with extended body length about 40-50 mm in Archidoris tuberculata, 100-120 mm in Tritonia plebeia and 70 mm in Aplysia punctata. Some

specimens were observed copulating while maintained in the aquarium.

(D) Pulmonata: Arion hortensis, terrestial molluscs were obtained from gardens around Glasgow. Adult specimens were collected every month from December 1988 to December 1989 for TEM, SEM and freeze-fracture studies.

Methods

(A). Light Microscopy

Mature spermatozoa were smeared onto a clean coverslip and examined with either a phase contrast or bright field light microscope.

Portions of gonad were fixed with either Bouin's fluid or Karnovsky's fixative and processed for paraffin embedding as follows;

Fix in Bouin's or Karnovsky's solution	(6-24 hrs)
Dehydration through ascending concentrations of ethanol (from 50% to 100%)	(1 hr each)
Absolute ethanol (3 changes)	(30 min each)
Amylacetate (3 changes)	(30min each)
First paraffin wax (56 C°)	(1 hr)
Second paraffin wax (56 C°)	(1 hr)

Embedding in paraffin wax

Specimens were processed in a Reichert-Jung Histokinette (2000) automatic tissue processor. Sections of

5μm thickness were cut and stained with haemotoxylin and eosin. Sections were examined and photographed with a Leitz Vario-Orthomat microscope.

(B). Transmission Electron Microscopy (TEM)

Many published works have shown that the quality of fine structural preservation is affected both by the method of applying the fixative to the tissue and the type of fixative employed (Robinson, 1982).

Fixation by vascular perfusion, for instance, in vertebrate animals with a well developed closed cardiovascular system, is undoubtedly, in many cases, the best method of tissue preservation. However, fixation by immersion is still the most widely used method for invertebrates. In the present study all molluscan materials were processed by in vitro fixation, i.e. immersion of the excised specimen in fixative.

For the fixation of mature spermatozoa. Suspensions of spermatozoa were placed directly into fixative. After fixation, the specimen was centrifuged at 2000 rpm for ten minutes to form pellet. The pellet was further dehydrated and embedded in Araldite resin.

Solutions of fixative have been suggested to influence the quality of preservation through a number of factors, for example, pH, tonicity, temperature, concentration of the fixative and duration of fixation. A variety of different fixatives were employed in this study

and the results provide further evidence that these factors influence the quality of preservation.

a). Fixatives for marine molluscan spermatogenic cells:

The fine structure of marine molluscan gonads is very difficult to preserve. Application of inappropriate fixatives is demonstrated by the failure to preserve fine structure in previously published accounts of spermatogenic cells in marine scaphopods (Carter, 1986). In the present study several fixatives were applied to marine specimens in order to compare the effectiveness of these fixatives. A brief account of these fixatives is given below:-

1). 3% glutaraldehyde buffered in 0.1 M cacodylate buffer with 3% sucrose added to provide 755 mOsm osmolality, pH 7.4.

2). 2.5% glutaraldehyde in sea water (Osmolality = 1,200 mOsm), fixed at room temperature for 2 hours (From Buckland-Nicks and Chia, 1980; Hodgson et al., 1988).

3). 2.5% glutaraldehyde in 0.1 M cacodylate buffer and sea water, pH 7.4, Osmolality = 1059 mOsm. (From Hodgson and Bernard, 1988).

4). 3% glutaraldehyde, 1% formaldehyde in 0.1 M phosphate buffer with 3% NaCl and 4.5% sucrose. pH 7.4, Osmolality = 1,500 (Modified from Eckelbarger and Eyster, 1981).

5). 2% glutaraldehyde in 0.1 M cacodylate buffer containing

5% sucrose and 2.5% NaCl. pH 7.6, Osmolality = 1115. (From Maxwell, 1975a).

Routine fixation containing 3% glutaraldehyde buffered in 0.1 M cacodylate buffer with 5% sucrose fails to preserve spermatogenic cells optimally in Antalis entalis (Scaphopoda). Cells appear swollen, cell membranes are disrupted and cytoplasm is dispersed. This is probably due to low osmolality and inbalanced salt components in the fixative. Fixatives 2, 3, and 5 gave slightly improved fixation. Fixative 4 with slightly increased osmolality and formaldehyde content provided the best fixation. It has been documented that formaldehyde penetrates faster than glutaraldehyde and temporarily stablizes structures which are subsequently more permanently stablized by glutaraldehyde (Karnovsky, 1965). Despite the slight high osmolality, shrinkage is unusual. This fixative has already provided much improved fixation for the germ cells of marine bivalves and opisthobranchs (Eckelbarger and Eyster, 1981; Eckelbarger et al., 1989, 1990).

b). Fixatives for terrestial molluscan spermatogenic cells:

Fixatives for the fine structure of terrestial molluscan spermatogenic cells have been well documented and successfully demonstrate the intact developing germ cells within the gonads of a large variety of molluscan species (see review, Maxwell, 1974b). The following recipe is the one most widely used in recent research (Thompson, 1973;

Takaichi and Dan, 1977; Parivar, 1980; 1981; Rigby, 1982; Healy and Jamieson, 1989; Griffond et al., 1991):- 3% glutaraldehyde in 0.1 M cacodylate buffer with 3% glucose added to make the osmolality 755 mOsm, pH 7.4.

In the present study, the spermatogenic cells in the ovotestis of Arion hortensis were well fixed by this fixative and intercellular relationships were well maintained.

c). Hypertonic fixative:

After study of the structure of acini in the ovotestis of Arion hortensis, a desmosome-like junction (see Chapter IV for details) was observed between Sertoli cells and developing spermatogenic cells. To test whether this junction provides a strong adhesive site, hypertonic fixatives were applied to the ovotestis. Use of hypertonic fixation causes cell shrinkage and exaggerated intercellular spaces. This artefact has been used to study the integrity of intercellular junctions in the mammalian testis (Russell, 1977a). In the present study 10% and 15% dextrose was added to the fixative containing 3% glutaraldehyde in 0.1 M cacodylate buffer with 3% glucose, which resulted in a fixative with an osmolality 1096 mOsm and 1404 mOsm, respectively. Osmolality was recorded in the Model 3L, 3W advanced osmometer (USA). Dextrose was also added to the rinsing buffer to match the osmolality of the fixatives.

d). Tracers and fixatives for blood-testis barrier studies:

Many types of electron dense tracer are now available for barrier permeability studies. For example, natural tracers like chylomicrons and lipoprotein, which are normally present in the body and can be enhanced by modifing the diet of the animal (Al-Jomard, 1987) and foreign tracers like lanthanum nitrate, horse radish peroxidase (HRP), ferritin and colloidal gold particles. Among them, HRP, lanthanum and ferritin are the most extensively used, particularly in studies of the permeability of the blood-testis barrier (Newell and Skelding, 1973; Hill, 1977; Abraham et al, 1980; Waites and Gladwell, 1982; Bergmann, Greven and Schindelmeiser, 1984; Bergmann, Schindelmeiser and Greven, 1984; Jong-Brink et al., 1984; O'Donovan and Abraham, 1987). These tracers have different particle sizes (see Hill, 1977) and their differential permeabilities in the ovotestis of Arion hortensis allowed the visulization and comparsion of the physiological properties of intercellular junctions.

Lanthanum nitrate, HRP and ferritin were all purchased from Sigma. HRP was the type II powder and ferritin was type 1 in 0.15 M NaCl from horse spleen.

In the literature, tracers have been applied to the gonads either by in vivo or in vitro methods (Newell and Skelding, 1973; Hill, 1977; Jong-Brink et al., 1984). The in vivo method involves the injection of 5% ferritin or

lanthanum in saline into the haemocoel of the animal and the gonad is collected 15 minutes, 30 minutes, 1 hour, 2 hours and 3 hours later.

The *In vitro* method was achieved either, first, by incubating the gonad in tracer solution (in saline) for a period of time, followed by routine fixation for ultrastructural studies; or second, direct fixation of the gonad in fixative containing tracers (in the present study, 5% lanthanum nitrate, HRP and Ferritin were used and tissues were immersed in the fixative for 1.5 hours).

Although, these methods appear well established in the literature, my initial experiments employing the *in vivo* technique demonstrated that tracers did not appear in the ovotestis in *Arion hortensis* even 2 hours after injection, possibly because of the poor circulation in the haemocoele. In addition, animals did not survive the injection more than two hours.

The *in vitro* method, however, provides direct contact between gonad and tracer containing medium and my results show a much improved, and rapid impregnation of tracers into the gonad. The first method of *in vitro* treatment mentioned above (Hill, 1977) (incubating gonads in tracer solution first followed by fixation) did not allow good preservation of the fine structure of cells inside the gonad and intercellular relationships appeared disturbed because of poor fixation. Consequently further investigation of the barriers within the ovotestis in *Arion*

hortensis was carried out employing the following technique:- fix the whole intact, living fresh ovotestis in fresh fixative containing 3% glutaraldehyde in 0.1 M cacodylate buffer with 5% lanthanum nitrate or (HRP or ferritin) for 1 or 1.5 hours. Tissues were post-fixed with 1% osmium tetroxide in 0.1 M cacodylate buffer for 1 hour and further dehydrated for routine Araldite resin embedding.

e). Fixation of the microtubular manchette:

It is only possible to demonstrate the ultrastructure of eukaryotic cells after the introduction of glutaraldehyde and osmium tetroxide as fixatives (see reviews, Palade, 1952; Sabatini et al., 1963; Hayat, 1973). Aldehyde fixatives are considered effective in cross-linking proteins, thus minimizing the extraction of the cytoplasmic matrix; whereas osmium is said to preserve more glycogen and react with the double bonds in lipids which leads to cross-linking of adjacent molecules (Robinson, 1982). Cytoplasmic microtubules were discovered only after the introduction of glutaraldehyde (Sabatini et al., 1963). Fixation with osmium tetroxide alone is insufficient for their preservation and has even been shown to be deleterious to the preservation of microtubules (Afzelius et al., 1990). The major breakthrough which provided superb preservation of cytoplasmic microtubules and settled the controversy concerning the exact number of substructures

within the wall of microtubules was the introduction of tannic acid into the glutaraldehyde fixative by Mizuhira and Futaesaku (1974). This glutaraldehyde-tannic acid fixative have since been widely adopted by workers to study ciliary axonemes (Tilney et al., 1973), or cytoplasmic microtubules (see review, Fujiwara and Linck, 1982; Mogensen et al., 1989).

There has been no report of the application of this technique to study the spermatogenic cells in the molluscan gonad, especially the microtubular manchette. Data derived from the present study provides more accurate details of the organization of the microtubular manchette.

The method I used is described here:- Portions of gonad were fixed in 3% glutaraldehyde, 1% tannic acid and 1.8% sucrose in 0.1 M cacodylate buffer (modified from Afzelius et al., 1990) for 1.5 hours, followed by dehydration through ascending concentrations of ethanol and finally embedded in Araldite resin.

f). Araldite embedding:

The specimen is subject to primary fixation by a specific glutaraldehyde fixative selected from the variety of fixatives discussed above and followed by post fixation in 1% osmium tetroxide which is in a buffer corresponding to the one used in the primary fixative (osmium post fixation is ommitted in glutaraldehyde-tannic acid fixation). A brief account of the embedding procedure is

given here:

Fix in buffered glutaraldehyde	(2 hrs)
Rinse in corresponding buffer (3 changes)	(20 min each)
Post-fix in buffered osmium tetroxide (except in tannic acid fixation)	(1.5 hrs)
Rinse in corresponding buffer	(overnight)
Dehydration through 50%, 70%, 90%, 100% ethanol	(20 min each)
Absolute ethanol (3 changes)	(20 min each)
Propylene oxide 1/2 : 1/2 ethanol	(20 min)
Propylene oxide (2 changes)	(20 min each)
Propylene oxide 1/2 : 1/2 Araldite	(6 hrs)
Propylene oxide 1/3 : 2/3 Araldite	(6 hrs)
Araldite	(12 hrs)
Embedding in fresh Araldite in 56 C° oven	(12-36 hrs)

Araldite embedding medium is a kind of epoxy resin, developed by Glauert, Rogers and Glauert (1956). Although the recipe suggested by Glauert and co-workers (1956) has been modified several times, these modifications are basically similar to the original mixture which contains an Araldite resin, a hardener, an accelerator and a plasticiser. Two formulae of Araldite resin were used for the present embedding media:

1).	Araldite CY 212	12.5 ml
	DDSA	12.5 ml
	DMP 30	0.25 ml
	Dibutyl phthalate	0.2 ml

and a more recent formula:

2).	Araldite MY 753	49 g
	DDSA	49 g
	BDMA	1.5 g
	Ditutyl phthalate	2.7 g

All these chemical reagents were purchased from Sigma.

g). Specimen orientation and sectioning:

Blocks were trimmed and sectioned with a Reichert-Jung microtome (Model 2050, made in Germany). Semi-thin sections of 1 μm thickness were cut and stained with 1% toluidine blue. After examining the general structure on the semi-thin section with a light microscope, a specific area of interest on the block was further trimmed with a glass knife.

The following diagram illustrates the technique used in orientation, trimming and sectioning of the specimen. This technique was first described by Buckland-Nicks and Chia (1990) in studing the pallial oviduct of a marine snail. The application of this technique allowed me easily and accurately to locate and section the male germ cells in the ovotestis of pulmonates and opisthobranchs.

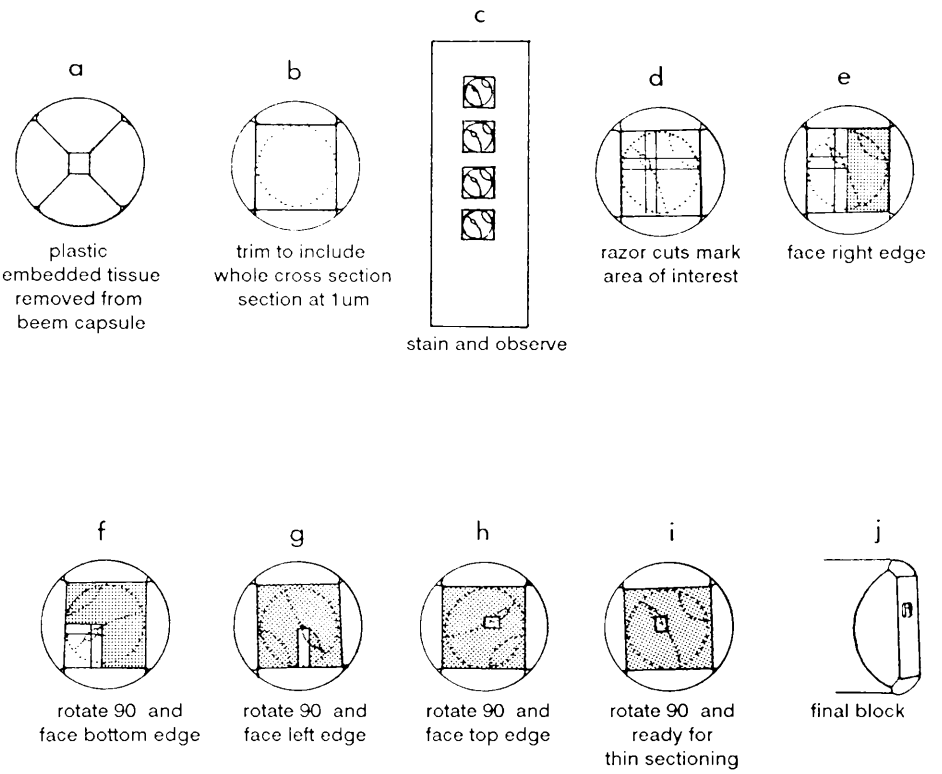

FIGURE. Schematic diagram of technique used to section several areas of interest in a single tissue block with minimal loss of tissue.

(Modified from Buckland-Nicks and Chia, 1990 with acknowledgement)

Serial thin sections (silver and gold colours) were cut on a Reichert-Jung Ultracut microtome, stretched with chloroform vapour and collected either on uncoated 300 mesh copper grids or 300 mesh nickel grids. These loaded grids were air-dried prior to staining.

h). Section staining:

1). Routine UA-LC double staining:

Thin sections on copper grids were stained in saturated uranyl acetate in alcohol for 10 minutes and lead citrate for 8 minutes. After rinsing in distilled water for 2 minutes, grids were air-dried in a dust free area and examined in the transmission electron microscope.

2). Cytochemical staining for glycogen:

The ultrastructural methods for staining glycogen were reviewed by Thiéry (1967). The introduction of silver proteinate by Thiéry (1967) greatly increased the convenience of the method and revealed a definite substructure in the glycogen particules (Vye and Fischman, 1971). Utilizing control tests (for example, omitting various reagents in the Thiéry's method or including aldehyde blocking agents), Robertson and co-workers (1975) confirmed the specificity of the staining. It has been suggested that the polysaccharide contains many diol groups and should thus be the major component that is stained (Vye and Fischman, 1971; Maxwell et al., 1990).

In the present study, gonads of Antalis entalis, Archidoris tuberculata, Tritonia plebeia and Rossia macrosoma were stained for glycogen following the modified methods from Vye and Fischman (1971) and Maxwell et al. (1990). Thin sections on nickel grids were treated with 1% periodic acid (PA) for 40-50 minutes, rinsed in distilled water for 10 minutes, floated on a solution of 1% thiosemicarbazide (TSC) in 10% acetic acid for 50-60 minutes, rinsed in distilled water for 10 minutes and finally incubated in the dark for 30-40 minutes in a fresh solution of 1% silver proteinate in distilled water. Before drying, the section was thoroughly rinsed in distilled water (3 changes). Control treatments were carried out by substitution of periodic acid with distilled water, or the section was first subjected to 1% diastase (in water) digestion (at 37 C°) followed by normal PA-TSC-SP treatment. Staining for glycogen was also checked by staining sections of rat liver at the same time.

(C). Freeze-fracture:

Freeze-fracture has been widely applied in a number of fields since it was first devised by Moor and his co-workers in 1961, and is now an accepted standard tool (Thompson, 1971; Maxwell, 1974b; 1977). This technique involves the making of a platinum carbon replica of the fracture face through frozen cells and the replica is examined in the transmission electron microscope.

One aspect of this technique is that it is a purely physical preparation of the specimen. Fixation and dehydration are not necessary and the tissue is prevented from osmotic stress and chemical destruction. However, material can not be directly frozen at the present state of freezing technology since the rate of freezing of material is still too low to prevent the formation of ice crystals within the specimen (Bullivant, 1965). To reduce the damage caused by freezing, cryoprotectant is normally used in the Balzer freeze-fracture apparatus that I used, for example, glycerol as suggested by Moor et al. (1961). Other methods for rapid freezing are available, but not in Glasgow.

This technique is especially useful in revealing the internal organisation of membranous structures, for example, in recent research on the organisation of intercellular junctions in a large number of vertebrate and invertebrate animals (Afzelius et al., 1989; Dallai et al., 1990; Hou and Maxwell, 1990; Pelletier, 1988; 1990).

Material used in this study (Arion hortensis) was unfixed and stored in buffered 25% glycerol at 4 °C for 1 or 2 hours. Then the specimen was frozen rapidly in liquid Freon 22 and fractured at -115 °C on the Balzer 360M Freeze-fracture Unit maintained in the centralized EM facility at the Univeristy of Glasgow. After fracture, surfaces were coated with carbon (12 seconds) and platinum (8 seconds). Replicas were cleaned in 10% sodium hypochlorite for 12 hours followed by concentrated

sulphuric acid for 24 hours. After rinsing in distilled water, the replicas were finally collected on 400-mesh copper grids and examined in a JEOL-100S transmission electron microscope.

(D). Scanning Electron Microscopy (SEM)

Scanning electron microscopy gives scientists a powerful research tool in gaining a rapid appreciation of the gross form of single cells, as exemplified in the studies of molluscan spermatozoa (Maxwell, 1975b; 1983). Technological advances have greatly improved the resolution of SEM from 20 nm to 1.5 nm, and information obtained with modern instruments is far beyond the resolution of the early "steroscans".

The preparative technique for the SEM has also substantially improved and this has expanded the scope of biological materials available for examination (see review by Claugher, 1990). Uncoated or frozen materials can be examined either with the recently developed system known as CFAS (Charge-Free Anticontamination System) or in the SEM with attached cryostage. The most recently developed accessory for SEM is a device that enables the analogue signal to be digitized and images can be manipulated through a computer. This opens a new world to the microscopist.

Although the resolution of the SEM does not match that of TEM, the results in many cases are informative.

In this study, the mature spermatozoa of Antalis entalis, Rossia macrosoma, Archidoris tuberculata, Tritonia plebeia and Aplysia punctata were examined. Spermatozoa collected from the vas deferens were fixed with a glutaraldehyde fixative described in section Method B. a) (Page 22-23). A suspension of fixed spermatozoa was smeared onto a sterile slide and post fixed with 1% osmium tetroxide in buffer. After several rinses in a corresponding buffer, the cover slip was air-dried in a dust-free area and trimmed to the size of the specimen stub. The cover slip was mounted on the stub with double-sided tape and coated with gold in a SEM Coating Unit E5000. The specimen were examined with a JEOL JSM-T300 scanning electron microscope.

CHAPTER I

ULTRASTRUCTURAL STUDIES OF THE SPERMATOZOON AND SPERMATOGENESIS IN *ANTALIS ENTALIS* (SCAPHAPODA, MOLLUSCA)

Introduction

The Scaphopoda or tusk-shells are the smallest and most uniform class of molluscs (Morton, 1959). They are benthic marine animals burrowing in sand of medium to coarse shelly grade. There are about 350 scaphopod species (Barnes, 1980), of which four have been recorded in Scotland (Allen, 1962). Published material relates to their geographical distribution, habitat, taxonomy, feeding apparatus and development (Arvy, 1950; Bilyard, 1974; Carter, 1986; Davis, 1968; Emerson, 1962; Gainey, 1972; Koukouras and Kevrekidis, 1986; Morton, 1959; Palmer, 1974; Poon, 1987; Reverberi, 1970, 1972; Wilson, 1904a, b). However, little is known about germ cell development and differentiation in this deep sea benthic molluscan group.

Wilson (1904a) provided a remarkable account of studies of female germ cells of the dentalioid scaphopod. He investigated the germinal localization and early development of the fertilized Dentalium vulgare eggs. The pattern of the early development of Dentalium eggs has since been used as a model to address the question of cytoplasmic prelocalization in the unsegmented molluscan egg (Wilson, 1904b; Reverberi, 1970). It was not until 1970 that the detailed ultrastructural organization of the ripe oocyte of the dentalioid scaphopod was fully described by Reverberi (1970). His observations were fundamentally in

agreement with those of Wilson (1904a, b). This extended ultrastructural investigation showed that the constitution of the vegetal plasm is particularly interesting. A large amount of mitochondria and small yolk granules were demonstrated in this area. These mitochondria have been suggested to contain specific macromolecules which activate single different genes during the larval mesoderm differentiation.

Spermatogenesis and spermiogenesis in most of the molluscan classes have been studied: for example, Aplacophora (Buckland-Nicks and Chia, 1989), Polyplacophora (Russell-Pinto et al., 1984; Sakker, 1984; Buckland-Nicks et al., 1988; Hodgson et al., 1988), Bivalvia (see review, Popham, 1979), Gastropoda (see review, Maxwell, 1983; Healy, 1988b) and Cepalopoda (Maxwell, 1974a, b; 1975a), leaving a large gap in our knowledge concerning male germ cell differentiation in the scaphopod molluscs.

Rokop (1977) provided the first detailed year-round studies on the seasonal reproduction of a siphonodentalioid scaphopod Cadulus californicus. The testicular follicle and oocyte diameters were used as parameters to provide information concerning reproductive activity. The male testicular follicles occur in parallel arrays perpendicular to the long axis of the body. It was suggested that spermatogenesis was synchronous because of the uniform diameter and appearance of the testicular follicles. Although it has been suggested that the predominant

breeding pattern in the deep-sea environment is year-round reproduction (Rokop, 1974), the scaphopod mollusc Cadulus californicus appears rather an exception. A predicatable annual gametogenic cycle has been demonstrated (Rokop, 1977), which shows that Cadulus californicus spawns in late summer between July and October.

Recent attempts to demonstrate the ultrastructural organization of the male germ cells in the testis of siphodentalioid scaphopod Cadulidae sp. has proven unsuccessful (Carter, 1986). It has been claimed that this may possibly be due to improper handling of the specimens; for instance, long preservation of those specimens. The organization of the spermatozoon demonstrated in scanning micrographs contained in her doctoral thesis appears variable and inconsistant, even within the same species, in Cadulida sp.. Spermatozoa from Cadulida sp. generally parallel those from Polyschides agassizii. Some of the sperm were mechanically activated through accidental damage to the acrosome during processing. However, the intact acrosome has been described as a tyre-like acrosomal ring. Four polar bodies (mitochondria ?) were present at the posterior of the head surrounding the flagellum of the sperm. Carter (1986) further speculated that Cadulidae sperm were noteably different from dentilioid sperm in that the acrosome in dentalioid sperm is flat like a coin, lacking the inflated tyre-like rim and projecting centre seen in Cadulidae sperm. This suggestion contradicts the

observations on the dentalioid sperm provided by other workers (cf. Franzén, 1955; Dufresne-Dube et al., 1983)

Preliminary light microscopical observations of sperm and spermiogenesis in Dentalium entalis (= Antalis entalis Linné 1758, Palmer, personal communication) were provided by Retzius (1905) and Franzén (1955). Franzén (1955), using light microscopy, confirmed and extended the observations made by Retzius (1905). The spermatozoon in Dentalium entalis was classified as belonging to the so-called "primitive" group which has an oval nucleus and a middle piece consisting of five mitochondrial spheres. The tail forms a long thin filament. Franzén (1955) did not describe in detail the process of spermatogenesis. However the acrosome was demonstrated to be a ring of strongly refracting material on the apex of the nucleus.

A brief description of the fine structure of the mature spermatozoon confirming the primitive form of the spermatozoon of Dentalium vulgare and morphological changes occurring during fertilization has been provided by Dufresne-Dube et al. (1983). However, the acrosome contains a central concavity at the apex, rather than a flat coin-shape as suggested by Carter (1986). Ultrastructural information concerning spermatogenesis and spermiogenesis of Scaphopoda is still lacking.

In this Chapter I will describe the organization of the testis, the ultrastructural changes during spermatogenesis of Antalis entalis, and compare the

structure of the spermatozoon with that of Dentalium vulgare and other molluscan groups possessing the "primitive" type of spermatozoon.

Results

(A). Testis

Antalis entalis is dioecous, with a lobular testis located in the dorsal part of the visceral mass that almost reaches the pavilion dorsally. The testis consists of many elongated follicles which lie parallel to the long axis of the body. Several transverse muscle bands divide the testicular follicles into small groups (Figure 1). Each testicular follicle is limited by a complex basement membrane (Figure 2). This consists of an inner well organised fibrillar layer and an outer randomly distributed fibrillar layer (Figure 2 inset). Spermatogonia, spermatocytes, spermatids and spermatozoa occur in small groups within the lumen of the testis (Figures 2 and 3).

Under the light microscope, stages of developing germ cells appear difficult to ascertain morphologically, especially the spermatogonia, spermatocytes and early spermatids. Several male animals were therefore selected for further studies. Semithin sections of their testes were photographed. The shape of the developing germ cells were treated as ellipsoid and their nuclear volumes were calculated using the following formula:

$$V = 1/6 \cdot \pi \cdot L \cdot M^2$$

V = the nuclear volume;

L = major axis of the nucleus;

M = minor axis of the nucleus.

Obtained data was processed by one-way analysis of variance (ANOVA).

Results showed that the volumes of developing germ cells can be classified into three groups (see Graph). The nuclear volumes of spermatogonia, spermatocytes and early spermatid measured about 251.97 ± 79.35, 138.91 ± 28.09 and 34.14 ± 8.84 μm^3 each.

Graph: A quantitative analysis of spermatogenic cells in the testis of *Antalis entalis*

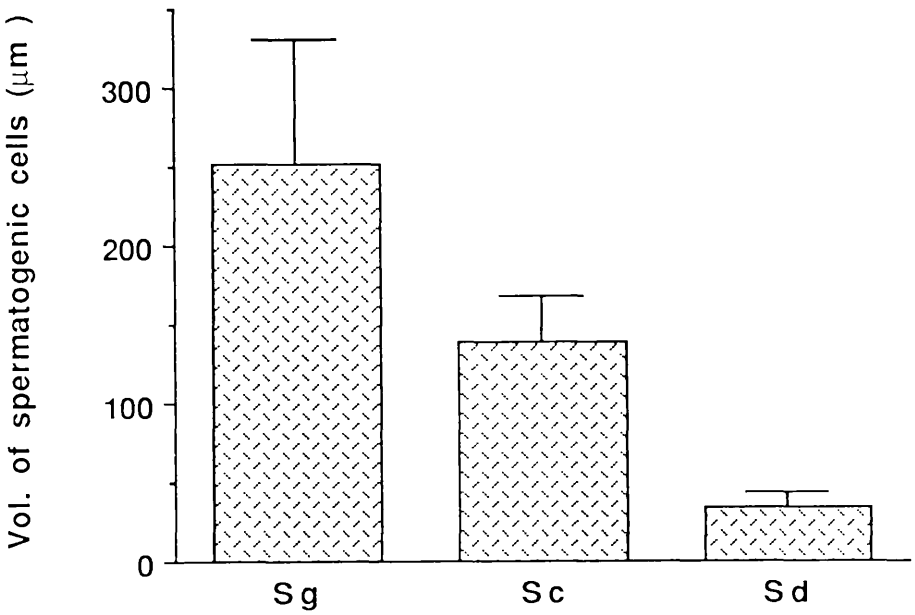

Sg, spermatogonium
Sc, spermatocyte
Sd, spermatid

Table 1 Dimensions of the spermatozoa (measurements in micrometers)

	Acrosome		Nucleus	Head		Author
	L/BDA	R1	L/BDN	R2	R3	
Antalis entalis	0.75/1.6	2.1	5/2.3	2.2	3.3	Present
Dentalium vulgare	0.8/0.55-1.1	1.4	4/1.5	2.7	3.2	Dufresne-Dube et al.

L, length; BDA, basal diameter of acrosome; BDN, basal diameter of nucleus; R1, ratio of L to BDA; R2, ratio of L to BDN; R3, ratio of the length of the head to BDN.

(B). Structure of the Spermatozoon

By phase contrast microscopy, spermatozoa appear thread-like, with a well defined head and long tail. Live spermatozoa actively swim in a progressive manner.

SEM examination of fixed spermatozoa shows the head, mid-piece and tail (Figures 4, 5), comparable to that of Dentalium vulgare (Dufresne-Dube et al., 1983; see Table 1). The spermatozoon falls within the "primitive" type described by Franzén (1955).

The head consists of an apical acrosome and an elongate nucleus (Figures 5 and 6; for measurements see Table 1).

The acrosome is a membrane-bound hollow structure surmounting the nucleus (Figures 5, 6, 7 and 8); it consists of an electron-dense ring of material, the acrosomal granule, surrounding a central, electron-lucent, acrosomal fossa (Figures 7, 8 and 8). On the internal aspect of the acrosomal granule there is a centrally orientated ridge. No axial body or rod occurs either within the central lumen or between the anterior aspect of the nucleus and the acrosomal fossa, nor is there any particulate material in the acrosomal fossa. A slight conical elevation of the anterior tip of the nucleus extends into the acrosomal fossa (Figures 7, 8 and 9).

The nucleus is circular in transverse section (Figure 10); in longitudinal section it appears as a trunctated cone, tapering anteriorly. The nucleus has a length : width

ratio of 2.2 : 1 (Figure 8). The chromatin is homogeneously packed except for a few intra-nuclear cavities (Figures 8, 10 and 12), mostly found in the posterior part of nucleus. The nucleus is indented posteriorly by the mitochondria and proximal centriole. Externally it is enveloped by the nuclear envelope and plasmalemma.

The midpiece is of the primitive type, with five closely apposed large spherical mitochondria (Figures 11, 12, 13 and 14) each about 0.8 ± 0.1 μm in diameter, arranged in a circle around the centriolar complex (Figure 11). They have a discrete external membrane, contain closely packed cristae, and lack inter-mitochondrial bridges or mitochondria-centriolar connections. Associated with the mitochondria and centriolar region are loosely distributed a small number of glycogen granules (Figures 11, 12, 13, 14 and 15). These glycogen granules mostly appear in the midpiece, but I do observe some glycogen granules around the base of the acrosome (Figure 44).

The centriolar complex consists of a pair of centrioles, proximal and distal, each composed of nine typical microtubular triplets surrounded by a homogeneous electron dense matrix (Figure 16). The proximal and distal centrioles are orientated perpendicularly (Figures 12, 13 and 14).

The proximal centriole is apposed laterally to the base of the nucleus. There is a large number of electron dense fibro-filaments, about 1.4 nm in diameter, between

the centriole and the nuclear envelope (Figure 13). The distal centriole, which gives rise to the flagellum, is attached to the adjacent plasmalemma by nine electron dense satellites (centriolar satellite complex) which align with the nine triplets of the distal centriole (Figures 12, 13, 14, 17, 18 and 19). These satellites are 20 nm long and 50 nm wide, and radially arranged around the distal centriole. No striations occur within the satellites which terminate distally in an enlarged, branched tip, closely apposed to the plasmalemma (Figure 19). The satellites lie in association only with the distal centriole, and do not extend into the flagellum (Figures 8 and 12). This system of centriolar satellite or anchoring fibres closely resembles the model of the centriolar satellite complex developed by Summers (1970) and Baccetti and Afzelius (1976).

The flagellum of the spermatozoon measures 108 ± 5.5 μm long, and is limited by the plasmalemma throughout its length (Figures 21 and 22). It has a typical "9+2" axonemal structure (Figure 20), which begins with the appearance of the central doublet at the caudal end of the distal centriole. Nine outer tubular doublets are continuous with the distal centriolar tubules (Figure 12). Rays of spokes (terminology from Baccetti and Afzelius, 1976; Afzelius et al., 1990) are visible between the A tubules and the central doublet (Figures 21 and 22). The 9+2 axonemal structure is lost at the terminal end of the flagellum; the

central doublet is lost first and terminally only two to five irregularly arranged microtubules remain.

(C). Early Spermatogenesis

The spermatogonium is a large spherical cell, and often seen closely related to the basal lamina (Figures 2 inset and 23). Its nearly spherical nucleus measures 8 ± 0.15 μm in diameter and the most prominent feature throughout this stage is the nucleolus (Figures 24 and 25) (0.7 μm in diameter). The nucleus is surrounded by abundant cytoplasm, containing many mitochondria and a Golgi complex. The mitochondria are evenly distributed and about 0.4 μm in diameter. The volume of each is estimated to be about one quarter of that in the mature spermatozoon.

The spermatocyte has a similar size to the spermatogonium (Figure 26). The nucleus is 6 μm in diameter with uniformly distributed heterochromatin throughout the nucleoplasm. The nucleolus is absent. The cytoplasmic organelles are very similar to those of the spermatogonium, and the mitochondria remain the same size as those in the spermatogonium (Figure 26).

(D). Spermiogenesis

The early spermatid is of reduced size but still spherical, with a nuclear diameter of about 4 μm (Figures 27, 28 and 29). Several nuclei of early spermatids occur within a common cytoplasm (Figure 27), in a manner similar to that described in bivalves, for example, Mytilus (Longo

and Dornfeld, 1967), Neotrigonia (Healy, 1989) and Scrobicularia plana (Sousa et al., 1989). No intercellular bridges occur between spermatids. Rather there is a failure of separation of the cytoplasm derived from the spermatocyte, so that several spermatid nuclei are contained within a single cytoplasmic mass. Within the nucleus, the chromatin forms fine fibrils which then aggregate into tiny granules (about 40-95 nm in diameter; Figure 28 and inset); during the process of nuclear elongation in the late spermatid, these granules become closely packed (Figure 29 and inset), without any regular relationship to the long axis of the elongating spermatid. Aggregation of the granules results in a reduction in the numbers of intranuclear cavities, although because of uneven condensation, some small intranuclear cavities remain (Figures 29, 32, 33, 34 and 35) to give rise to the small intranuclear cavities of the spermatozoon (Figure 36). After the close apposition of the mitochondria to the posterior pole and the proacrosome to the anterior (Figures 30 and 31), the longitudinal axis of the spermatid nucleus is established (Figure 32; I call this stage late spermatid) and in synchrony with chromatin condensation the late spermatid nucleus assumes the form of a truncated cone (Figures 33 and 34) as the chromatin finally condenses into an almost homogenouse electron-dense state (Figures 8 and 36).

Using the PA-TSC-SP technique, glycogen granules are

detected at the late spermatid stage (Figure 15). The granules occur in the following areas: peri-acrosomal and peri-mitochondrial. No glycogen occurs in the developing and mature tail piece.

(E). Acrosome and Mid-piece Formation

The proacrosome of Antalis entalis is produced by a single Golgi complex (Figures 37 and 38). In the early spermatid, the Golgi complex lies close to the mitochondria and centrioles (Figure 37). Two types of vesicle arise from the mature face of the Golgi body, one electron-dense, the other electron-lucent (Figure 38). These vesicles fuse (Figure 39) to form the proacrosome, a single, spherical, membranous vesicle with peripheral electron-dense material surrounding a translucent centre containing granular material (Figure 40). Within the electron-dense material is a spherical zone of more marked electron density (Figures 40 and 41). Early in spermiogenesis the proacrosome underlies the plasmalemma, separated from the nucleus but closely related to the mitochondria and developing axoneme (Figures 30, 31 and 40). Later, it migrates to the surface of the nucleus with the spherical electron-dense zone closely apposed to the nuclear membrane (Figures 32, 41 and 42). The proacrosome then assumes the shape of an inverted cup, with a well defined acrosomal fossa (Figures 34, 42 and 43). While the proacrosome is spherical its contents are finely granular but as the final changes in its shape

occur, it becomes more electron dense (Figure 44).

As nuclear condensation occurs the proacrosome migrates to the presumptive apical nuclear pole as the acrosome / centriolar axis is established. At the time of proacrosome formation, mitochondria become reduced in number but increase in size; even when they become apposed to the nuclear surface they still undergo an increase in size, causing deep indentations of the base of the nucleus (Figures 30, 31, 33 and 34). At the early spermatid stage the centrioles lie close to the plasmalemma and lack a prominent centriolar satellite (Figure 37). The developing axoneme forms a spiral in the cytoplasm. It may lie in relation to the nucleus, proacrosome or mitochondria (Figures 30, 37 and 43). The proximal centriole does not become apposed to the nuclear envelope until the late spermatid when the proacrosome/ centriolar axis is established. The axoneme now leaves the cell body to form the flagellum, and a centriolar satellite forms. Excess cytoplasm is shed to leave the truncated cone of the spermatozoan head.

Discussion

(A). Comparative Spermatozoan Structure

Antalis entalis practices external fertilization and its spermatozoan structure falls into the so-called primitive form established by Franzén (1955). The ulrastructure of its mature spermatozoon is very comparable to that of Dentalium vulgare (Dufrsne-Dube et al., 1983). The present studies confirm and extend their observations.

The acrosome of Antalis entalis closely resembles that of Dentalium vulgare (Dufresne-Dube et al., 1983) and in general, is comparable to those of Archaeogastropoda with simple acrosomes (e.g. Type I spermatozoa defined by Hodgson and Bernard, 1988 in patellid limpets and some of the Subtype 1A (Koike, 1985) and those acrosomes with no axial rod in the Veneroida and Myoida bavalves described by Popham in 1979). But there are a number of distinct structural differences. The acrosome does not form a hollow cone, but rather a ring with a centrally orientated ridge. A unique anterior invagination or pit into the central lumen of the acrosome is formed by the external acrosomal membrane and plasmalemma. There is no variation in the electron density of the acrosomal material of the mature spermatozoon, such as occurs in Type II and III spermatozoa of the patellid limpets (Hodgson and Bernard, 1988), other types of spermatozoa in archeogastropods (Koike, 1985) and bivalves (Popham, 1979). Neither is an axial body or rod

present in the subacrosomal space, as, for example, occurs in a wide variety of taxa (Baccetti and Afzelius, 1976), the bivalves (see review, Popham, 1979), e.g. Crassostrea (Galtsoff and Philpott, 1960), Mytilus (Niijima and Dan, 1965; Longo and Dornfeld, 1967; Hodgson and Bernard, 1986), Spisula (Longo and Anderson, 1969), Bankia (Popham et al., 1974), Donax (Hodgson et al., 1990) and Dreissena (Franzén, 1983; Maxwell, 1983). However, the acrosome of A. entalis is more complex than that of Chaetoderma sp., which has been described as an egg-shaped structure, filled with fine granular secretion (Buckland-Nicks and Chia, 1989). Lastly, a conical protrusion of the nucleus extends into the subacrosomal space, rather than a subacrosomal invagination into the nucleus, forming the so-called nuclear tunnel in Musculus discors (Franzén, 1983), and anterior nuclear fossa (e.g. in Pterioida) which is suggested to be correlated with the presence of an axial rod in the acrosome (Popham, 1979).

The occurrence of intra-nuclear cavities has been described in many other bivalve taxa (Maxwell, 1983) and Aaplacophora Chaetoderma sp. (Buckland-Nicks and Chia, 1989). The nuclear cavities in Antalis entalis are very similar to those described in the spermatozoa of the bivalve Spisula (Longo and Anderson, 1969). Nuclear cavities also occur in many other archaeogastropods which are of primitive form (Healy, 1988b; Hodgson and Bernard, 1988; Koike, 1985).

The centriolar satellite complex has been reviewed by Summers (1970), and documented in "primitive" spermatozoa from a wide variety of taxonomic groups. Considerable morphological variation has been noted (Baccetti and Afzelius, 1976). However, there are no detailed descriptions of the centriolar satellite complex in Dentalium vulgare (Dufresne-Dube et al., 1983) except to indicate the presence of proximal and distal centrioles, and the anchoring apparatus of the distal centrioles. In Antalis entalis nine spoke-like satellites extend radially from an electron-dense sleeve surrounding the distal centriole. The satellites are branched at their distal ends where they form Y-shaped terminations. I obtain no evidence of striations within the satellites of the Anatalis entalis spermatozoon. The Y - shaped terminals extend further longitudinally in the spermatozoon of Antalis entalis than do the satellites, since morphologically dissociated terminations are frequently found not connected to satellites but are always closely associated with the plasmalemma. This structural arrangement convinces me that the satellites function as a supporting unit during flagellar motility.

Popham et al. (1974) described a fibrillar proximal centriolar satellite body in the post-nuclear fossa of the spermatozoon of Bankia, and a fibro-granular material was also observed to connect the proximal centriole with the posterior end of the nucleus in Chaetoderma sp. (Buckland-

Nicks and Chia, 1989). Daniels et al. (1971) described a juxtanuclear body (centriolar satellite) in the spermatozoon of Crassostrea virginica, but it was orientated parallel to the proximal centriole and was not attached to the nuclear envelope. In the spermatozoon of Antalis entalis, the proximal centriole is bound to the posterior nuclear envelope by radiating tiny fibro-filaments. These filaments are comparable with the "centriolar satellite body" in Bankia (Popham et al., 1974) and "fibro-granular material" in Chaetoderma sp. (Buckland-Nicks and Chia, 1989), rather than the "juxtanuclear body" in Crassostrea virginica (Daniels et al., 1971). Despite the distinct morphological differences between the "satellite" of the distal and proximal centrioles, the previously used terminology is confusing. In the spermatozoon of Antalis entalis, I refer to the "satellite" of the distal centriole as the centriolar satellite complex possessing nine well organized spoke-like satellite arms connecting the distal centriole with the plasma membrane and the "satellite" of the proximal centriole as fibro-filaments which radiate from the proximal centriole to the posterior aspect of the nuclear envelope.

In recent years many attempts to use sperm morphology as an indicator of phylogenetic affinities within various molluscan groups have been proved valuble and useful (Franzén, 1970, 1983; Healy, 1988b; Hodgson and Bernard, 1986, 1988; Kohnert and Storch, 1983; Koike, 1985; Maxwell,

1983; Popham, 1974, 1979;). The comparision of the mature spermatozoa of Antalis entalis with Dentalium vulgare shows very little difference (See Table 1), suggesting that these two species are closely related as has been demonstrated in species of the genus Donax (Hodgson et al., 1990). But the distinct morphological differences from other molluscan groups also provides supporting evidence for the suggestion that the morphology of molluscan spermatozoa is species-specific (see review, Maxwell, 1983).

(B). Spermatogenesis

Using light microscopy, Franzén (1955) described only minor changes during acrosome formation once the dictyosome came to occupy the apex of the nucleus in Dentalium entalis. Ultrastructural studies in Antalis entalis provide additional information about the differentiation of the proacrosomal vesical produced by the single Golgi complex. Comparison with other molluscs shows that the number of Golgi complexes occurring during spermiogenesis varies between phylogenetic groups. A single Golgi complex is involved in the production of the proacrosome in examples from the Aplacophora (Buckland-Nicks and Chia, 1989), Polyplacophora (Buckland-Nicks et al., 1988) and Archaeogastropoda (Azevedo, 1981, Buckland-Nicks and Chia, 1986, Al-Hajj, 1988; Hodgson and Bernard, 1988). In bivalves, both single and multiple Golgi complexes occur, for example, a single Golgi complex has been described in

Laternula limicola (Kubo, 1977), Neotrigonia (Healy, 1989), Musculus discors, Nucula sulcata, Dreissena polymorpha (Franzén, 1983), Donax (Hodgson et al., 1990) and multiple ones in Mytilus edulis (Longo and Dornfeld, 1967), Spisula solidissima (Longo and Anderson, 1969) and galeommatoid bivalves (Eckelbarger et al., 1990). In mollusc classes with modified spermatozoa, for example, Opisthobranchia (Eckelbarger and Eyster, 1981; Kubo and Ishikawa, 1981; Medina et al., 1985), Pulmonata (Takaichi and Dan, 1977) and Cephalopoda (Maxwell, 1974a, b, 1975a), only multiple Golgi complexes occur. My studies of spermatogenesis in Antalis entalis provide confirmation of the primitive phylogenetic position of the Scaphopoda.

The migration of the proacrosomal granule from the posterior to the anterior pole of the spermatid in Antalis entalis closely parallels the situation observed in other molluscan groups with primitive spermatozoa, for example, the Aplacophora (Buckland-Nicks and Chia 1989), bivalves (Longo and Dornfeld 1967; Longo and Anderson 1969; Popham 1979; Healy 1989; Hodgson et al., 1990) and archaeogastropods (Azevedo 1981; Hodgson and Bernard 1988; Koike 1985). Once the proacrosomal vesicle becomes apposed to the presumptive apex of the nucleus, its form differentiates from spherical to cup-shaped. In contrast, the Golgi complex migrates to the apex of the nucleus and then forms the proacrosomal granule in molluscan groups with modified spermatozoa, for example, opisthobranchs

(Eckelbarger and Eyster, 1981; Kubo and Ishikawa, 1981), pulmonates (Takaichi and Dan, 1977; Rigby, 1982; Griffond et al., 1991) and cephalopods (Maxwell, 1974a, b; 1975a).

In patellid limpets, the Golgi complex often persists in the late spermatid (Hodgson and Bernard 1988). In Chaetoderma sp., the renewed activity of the Golgi body anteriorly even produces an apical horn and an apical tube (Buckland-Nicks and Chia 1989). In Antalis entalis, on the contrary, the Golgi complex is lost once the proacrosome has formed, at the beginning of the late spermatid stage.

Baccetti and Afzelius (1976) suggest that the increasing complexity of the acrosome is aquired progressively throughout evolution. In recent years many attempts to use acrosome morphology as an indicator for phylogenetic affinities within various molluscan groups have proved valuable and useful (Franzén, 1970, 1983; Popham, 1979; Kohnert and Storch, 1983; Maxwell, 1983; Koike, 1985; Hodgson and Bernard, 1986, 1988; Healy, 1988a, b; 1989). Popham (1979) suggests that the organisation of the acrosome in bivalves may reflect the systematic or phylogenetic relationship of species within the group. Comparing the mature spermatozoa of Antalis entalis with Dentalium vulgare shows only minor differences, suggesting that these two species are closely related. My observations on scaphopod spermiogenesis provide further evidence that the process of acrosome formation may be useful in studies of molluscan systematics and evolution.

Once attachment of the mitochondria to the nuclear envelope and the location of the proacrosome has occurred, then spermatid nuclear elongation proceeds. No manchette or any microtubules occur around the nucleus during this stage. The internal force(s) that changes the shape of the spermatid nucleus from spherical to elongate is obscure. In the Aplacophora (Buckland-Nicks and Chia, 1989), bivalves (except Scrobicularia plana, Sousa et al., 1989) (Longo and Dornfeld, 1967; Longo and Anderson, 1969; Popham et al., 1974; Popham, 1979; Maxwell, 1983; Healy, 1989; Hodgson et al., 1990), archaeogastropods (Koike, 1985; Al-Hajj, 1988; Hodgson and Bernard, 1988), all nuclear elongation and chromatin condensation occurs without the presence of a microtubular manchette. The same situation occurs in the scaphopod Antalis entalis. Fawcett et al. (1971) postulated that the pattern of chromatin condensation might be an important process in shaping the sperm head. Hodgson and Bernard (1988) also suggested that nuclear elongation might be brought about by forces within the nucleus. My observations on nuclear development during spermiogenesis in Antalis entalis provide additional support for this hypothesis.

The development of the middle piece resembles that seen in the patellid limpets (Hodgson and Bernard, 1988) and bivalves (Longo and Dornfeld, 1967; Longo and Anderson, 1969; Popham et al., 1974; Franzén, 1983; Healy, 1989; Hodgson et al., 1990). Mitochondria are the first

organelles to become apposed to the nucleus. These apposed mitochondria then increase their size throughout spermiogenesis. Healy (1989) described numerical differences of mitochondria in the spermatozoa of bivalve taxa, for example, in Pteriomorphia, five or six mitochondria occur in Mytiliidae, four or five in Pterioidea, whereas only four in Ostreoidea, Anomioidea and Acroidea. In scaphopods, however, only five spherical mitochondria occur (Franzén, 1955; Dufresne-Dube et al., 1983 and this study).

In the scaphopods, the distal centriolar satellites are structurally similar to those described in a wide variety of primitive spermatozoa in the models developed by Summers (1970) and Baccetti and Afzelius (1976).

In Antalis entalis the axoneme in the flagellum of the spermatozoon consists of a typical "9+2" microtubular structure. My observations on spermiogenesis of the scaphopod allow me to state that, with the exception of the, as yet uninvestigated Monoplacophora, the "9+2" axonemal organization of the spermatozoon is the only form obtained within the phylum Mollusca.

Glycogen granules accumulate only at the later stages of spermatid development in Antalis entalis and are located in the middle piece and close to the acrosome. A perimitochondrial distribution of glycogen has been observed in bivalves (see review, Maxwell, 1983), for example, Nucula sulcata (Franzén, 1983), Donax (Hodgson et

al., 1990), Divariscintilla and Scintilla sp. (Eckelbarger et al., 1990), and the scaphopod Dentalium vulgare (Dufresne-Dube et al., 1983). Glycogen granules occur in the acrosomal region in scaphopods (Dufresne-Dube et al., 1983), bivalves, for example, Donax (Hodgson et al., 1990), Teredinidae (Popham and Dickson, 1975), and octopods (Maxwell 1974b, 1975a). There is no storage of glycogen in the tail piece in the so-called "primitive" type of spermatozoon. I can now confirm a similar glycogen distribution in the spermatozoa of Antalis entalis to that described in Dentalium vulgare. These glycogen granules are probably sources of energy for motility and metabolism (Anderson and Personne 1970, 1976).

To summarize, this is the first ultrastructural investigation of spermatogenensis in a scaphopod. Its primitive spermatozoon and the process of spermatogenesis demonstrate close parallels with those of bivalves and archaeogastropods with "primitive" type of spermatozoon. However, its acrosomal organisation makes it unique in comparison with that described in any other molluscan group. The present investigation demonstrates that the organisation of the microtubular axoneme in scaphopod spermatozoa is exactly comparable to that in other molluscan classes (see reviews, Baccetti and Afzelius 1976; Popham 1979; Maxwell 1983; Koike 1985; Healy 1988b).

CHAPTER II

ULTRASTRUCTURAL AND CYTOCHEMICAL STUDIES OF SPERMIOGENESIS OF THE CUTTLEFISH *ROSSIA MACROSOMA* (MOLLUSCA: DECAPODA)

Introduction

Much research have been devoted to the morphology of the cephalopod spermatophore and the function of its various regions (Austin et al., 1964; Mann et al., 1970; Arnold and Williams-Arnold, 1978; Takahama et al., 1991). There are, however, only a few detailed ultrastructural studies of spermatozoa and spermatogenesis. Franzén (1955, 1956, 1967), after a comprehensive investigation of molluscan spermatozoa using optical microscopy, concluded that, with regard to cephalopod sperm morphology, no correspondence was found among other molluscs. Fields (1965) briefly described the morphology of Loligo opalescens sperm as seen with phase contrast microscopy. It has been demonstrated that decapod spermatozoa possess an elongated head, laterally placed centriole and a so-called mitochondrial pocket (Franzén 1955, 1967,). The arrangement of mitochondria into a separate single "large mass" (termed by Franzén, 1967) is very different from those in the primitive type of spermatozoa which have spherical mitochondria located in the region posterior to the nucleus. Franzén (1955, 1967) also demonstrated great morphological differences of the mature spermatozoa between the two main groups of recent cephalopods, i.e. Decapoda and Octopoda. The octopod spermatozoon, described as atypical by Franzén (1967), has a head and tail, but without a distinct midpiece.

Cephalopod spermatozoa have later been further investigated using electron microscopy in Octopus vulgaris (Galangau and Tuzet, 1968a, b), Octopus bimaculatus (Longo and Anderson, 1970), Eledone cirrhosa (Maxwell, 1974a, b), Eusepia officinalis, Loligo forbesi and Alloteuthis subulata (Maxwell, 1975a), Rossia pacifica (Fields and Thompson, 1976) and Nautilus pompilius (Arnold and Williams-Arnold, 1977; 1978). An elongated acrosome, nucleus, single centriole and a mitochondrial pocket were demonstrated ultrastructurally in the decapod Rossia pacifica spermatozoon (Fields and Thompson, 1976). In octopod spermatozoa, the acrosome is simple but helical, and there occurs only a single centriole. The proximal centriole is lost and mitochondria aggregate around the base of the nucleus forming a mitochondrial sleeve around the proximal end of the axoneme (Galangau and Tuzet, 1968a, b; Maxwell, 1974a).

However, conclusions drawn from these investigations are somehow controversial. Franzén (1955, 1967) and Fields and Thompson (1976) suggested that cephalopod spermatozoa are of an intermediate type between the more primitive invertebrate sperm and highly specialized modified type of spermatozoa. Spermatozoan structure, it is suggested (Franzén, 1967; Fields and Thompson, 1976), is more associated with the specialized mode of copulation, and fertilization biology. However, significant morphological differences of the organization of spermatozoa and

spermiogenesis among examples from the Nautiloida (Arnold and Williams-Arnold, 1978), Octopoda (Franzén, 1955, 1967; Maxwell, 1974a, b) and Decapoda (Maxwell, 1975a; Fields and Thompson, 1976) have led Arnold and Williams-Arnold (1978) to speculate that perhaps genetic drift or other factors may have overridden functional similarities in fertilization biology known in these animals and further detailed examination of other cephalopod species has been suggested.

The decapods have been stated to be unique molluscs because of their telolecithal nonspirally cleaving eggs, eleborate spermatophores and high levels of reproductive specialization (Arnold and Williams-Arnold, 1977). The order Decapoda consists of five families, i.e. Architeuthis, Ommastrephidae, Loliginidae, Sepiidae and Sepiolidae (classification according to Step, 1951). However, the ultrastructure of the spermatozoon in decapoda has been described only in a few species from the following families: Sepiolidae (Rossia pacifica, Fields and Thompson, 1976), Sepiidae (Eusepia officinalis, Maxwell, 1974b, 1975a) and Loliginidae (Loligo forbesi and Alloteuthis subulata, Maxwell, 1974b, 1975a). There has not been enough data gathered to make meaningful comparisons possible.

Within the decapods the process of spermiogenesis has only been described at the ultrastructural level in E. officinalis, L. forbesi and A. subulata (Maxwell, 1975a). There has been no cytochemical analysis of glycogen

deposits in decapod spermatozoa. Fields and Thompson (1976) described some glycogen aggregation in the mitochondrial spur (termed "mitochondrial sleeve" by Maxwell, 1975a) to one side of the posterior end of the sperm head, using PAS staining. There have been no ultrastructural and cytochemical studies to substantiate this finding in order to provide precise glycogen localization in the decapod spermatozoon.

Cephalopod molluscs exhibit some features of higher vertebrates such as eye organization, centralized nervous system and internal fertilization; in contrast to other invertebrates. Recent studies of molecular aspects of spermatogenesis suggest that the testis of decapod molluscs is a good model for studies of changes in chromatin protein composition during spermatogenesis (Kadura and Khrapunov, 1988; Khrapunov et al., 1988; Wouters-Tyrou et al., 1988). The present investigation, by providing a detailed analysis of normal development of the structural and cytochemical features of spermiogenesis in Rossia macrosoma, can only serve to provide a firm basis for further molecular studies of spermiogenesis.

In this chapter I present a description of spermiogenesis in Rossia macrosoma, with particular attention paid to the formation of the elongated acrosome and the precise localization of glycogen in the spermatozoa. The process of spermiogenesis and distribution of glycogen will be compared with that in other molluscs.

Results

(A). Light and Scanning Electron Microscopical Observations

The testis of Rossia macrosoma is a lobulated structure, which contains a number of testicular tubules (Figures 1 and 2). Each testicular tubule is limited by a basement membrane. External to the basement membrane, there occurs a discontinous layer of myoepithelial cells which rest on a thin layer of loose connective tissue (Figure 2). Small blood vessels pass between the tubules in the connective tissue (Figures 2 and 3). A large number of developing spermatogonia, spermatocytes, spermatids and spermatozoa occur in the lumen of the tubule.

Under the light microscope, all stages of developing male gametes can be observed in the same tubule. The spermatogonia lie on the basement membrane with prominent darkly stained nuclei. These cuboidal cells are closely associated with each other (Figure 2). The nuclei of spermatocytes, with punctate heterochromatin, appear lightly stained by toluidine blue in semi-thin sections. The spermatocytes are in close relation to the luminal side of the basal spermatogonia. Spermatid nuclei undergo significant morphogenesis. In the first stage, the nuclei are spherical. Chromatin begins its initial condensation. Spermatid nuclear elongation occurs prior to the final stage of transformation into a feebly bent rod.

Living sperm obtained from the spermatophore appear very active, moving progressively forward in a three-dimensional helical wave. I have measured the dimensions of the acrosome, nucleus, mitochondrial sleeve and the flagellum. The comparison of the dimensions of sperm with those of Rossia pacifica (Fields and Thompson, 1976) shows only slight differences (Table), confirming that these two species are closely related.

Spermatozoa taken from the vas deferens were also examined by scanning electron microscopy (Figure 4). The head is elongate with a prominent rod shaped acrosome (Figure 5). There is no apparent demarcation between the head and mitochondrial sleeve which surrounds the proximal part of the tail (Figure 6). The surface of the spermatozoa appears smooth with no surface specialisations visible under the scanning electron microscope (Figures 4, 5 and 6).

Table:

Measurements of the lengths of Living Spermatozoa (in micrometer)

	Acrosome	Nucleus	Mitochondrial sleeve	Flagellum	Sperm (total)
R. pacifica Fields & Thompson 1976	3.5-4	14	4.2	138	156
R. macrosoma Present	2.4-3	16	2	102	120

(B). Ultrastructure of Spermiogenesis

(1) Nuclear morphogenesis

The spermatid nucleus differentiates from a spherical to an elongate shape, with a length:width ratio (at the base of the nucleus) reaching approximately 6:1 in the spermatozoon. I have divided the course of nuclear morphogenesis into three stages (A,B,C), according to the morphological transformation of the nucleus and the degree of nuclear condensation.

Stage A. A secondary spermatocyte (Figures 7, 8 and 9) possessing a spherical nucleus (without a nucleolus) gives rise to the stage A spermatid (Figure 11). The stage A spermatid nucleus is spherical. Initial stages of chromatin condensation can be summerized as follows:- Small granular concentrations of chromatin about 24 nm in diameter aggregate together into large granules inside the nucleoplasm (Figures 11, 12 and 13). Arrays of microtubules in the cytoplasm become regularly arranged along the nuclear membrane, forming a microtubular manchette (Figures 12 and 13). These microtubules are evenly distributed along the nuclear membrane at a spacing of 40-50 nm (Figures 12 and 13).

Stage B. The chromatin inside the nucleus forms fine fibrils (Figure 14) and further aggregate into thin filament. Initially these fine filaments are not orientated along the longitudinal axis of the nucleus. Most of them

are randomly distributed within the nucleoplasm, some of them appear perpendicularly orientated to the nuclear membrane in a transverse section of the nucleus (Figure 15). The chromatin filaments further condense into thick filaments. These large electron dense filaments are orientated in the longitudinal axis (acrosome-centriole axis) of the elongating spermatid (Figure 16). Intercellular bridges connect adjacent developing spermatids (Figures 10 and inset).

Stage C. The fully elongated nucleus contains groups of large, longitudinally orientated chromatin filaments (Figures 17 and 18). The electron lucent spaces between adjacent chromatin fibers are gradually reduced (Figures 18 and 19). Further chromatin condensation results in the nucleus assuming a homogeneous electron dense form. Arrays of longitudinally orientated microtubules are closely associated with the elongating nucleus. Intermicrotubular bridges connect two adjacent microtubules (Figure 18). The attachment of the centriolar complex to the posterior lateral side of the nucleus results in the formation of the nuclear fossa (Figure 37).

(2) Proacrosome and acrosome formation

Two Golgi complexes occur in the spermatid cytoplasm (Figure 20). However, only one is consistantly associated with the developing proacrosomal granule. The Golgi complex is well differentiated consisting of stacks of five to

seven closely associated cisternae and a number of small transfer vesicles. Endoplasmic reticulum is closely related to the forming face of the cisternea of the Golgi complex (Figure 21). The first sign of acrosome formation is the growth of the cisternea of the maturing face in the stage A spermatid, resulting in the formation of a large sac-like proacrosomal granule (Figures 22 and 23). The proacrosomal granule further develops by addition of small transfer vesicles budded from the Golgi cisternae. As nuclear chromatin condensation begins, the Golgi complex and closely associated proacrosomal granule migrate towards the nuclear apex. The proacrosomal granule then becomes apposed to the anterior surface of the nucleus (Figures 23 and 24). Electron-dense material accumulates inside the proacrosome vesicle. This electron-dense material gradually condenses into a homogeneous state. The Golgi complex is still intimately associated with the proacrosomal granule at this stage (Figures 23 and 24). With further condensation and elongation of the nucleus at stage C of the developing spermatid, the proacrosome transforms from a spherical vesicle into a trapezoid shape when seen in longitudinal section (Figure 25). The Golgi complex is lost at this stage. At the lateral inner side of the proacrosome, electron dense material accumulates. In contrast, the central area of the proacrosome appears less electron dense.

Further differentiation of the internal structure of

the proacrosome results in the formation of an apical electron lucent bulb and a subacrosomal fossa (Figures 26, 27 and 28). The apical acrosomal membrane involutes (Figures 28 and 29), and fuses to give rise to an isolated vesicle (Figures 27 and 29) at the acrosomal apex. Furthermore, the juxtanuclear surface of the proacrosome detaches from the apex of the nucleus forming a subacrosomal fossa (Figures 27, 28, 29 and 30). Between the apical electron lucent bulb and the posterior subacrosomal fossa is electron-dense material, forming an elongate rod (Figure 41).

Prominent structural differentiation occurs within this electron dense rod. In a longitudinal section of the developing acrosome, there is a condensation of electron dense material against the acrosomal membrane, except at the apical region of the rod (Figure 30). This layer of electron dense material first appears at the lateral side of the acrosome, then at the juxtanuclear aspect. At the spermatid stage C, it is about 36 nm thick and appears solid and homogeneous.

A group of longitudinal microtubules occur at this stage forming the manchette around the elongating proacrosome (Figures 28, 29, 30, 31, 32 and 33). These microtubules extend further both anteriorly into the cytoplasm (Figures 30 and 31) and posteriorly into the nuclear region connecting with the microtubular manchette which envelopes the nucleus (Figures 30 and 33).

(3) Mitochondrial midpiece and centriole

Mitochondria are randomly distributed in the spermatocyte cytoplasm without any prominent morphological specializations (Figure 9). As the spermatid nuclear chromatin becomes condensed to form fine filaments, the mitochondria aggregate to assume a tortuously interwoven form (Figures 21 and 35). However, these mitochondria do not fuse. The number of mitochondrial cristae is reduced and the mitochondrial matrix becomes electron dense (Figures 35, 37 and 38). Later, this mitochondrial aggregation migrates towards the posterior pole of the elongating nucleus. With further differentiation of the external plasmalemma of the spermatozoa, the mitochondrial pocket is formed to house the mitochondria (Figures 34 and 38).

Two centrioles are first observed close to the concave side of the mitochondrial derivative in the Stage A spermatid nucleus (Figure 36). However, no direct evidence for a typical triplet centriole was obtained, rather forming nine electron dense masses (Figure 39). The proximal centriole attaches to the lateral side of the nucleus, forming a deep indentation termed the nuclear fossa. The proximal centriole is a rod-like structure, deeply embedded in the nuclear fossa (Figure 37). It is orientated almost parallel to the distal centriole (Figure 37). The distal centriole gives rise to a "9 + 2" axoneme at its distal end (Figures 36, 37, 38, 39 and 40). In the

midpiece region, nine course fibres are present (Figure 40) peripheral to the α-doublets. In longitudinal section, these course fibres are continuous with the electron dense material which surrounds the nine triplets of the distal centriole (Figures 36, 37 and 38). No supporting structures, comparable to centriolar satellites, are observed around both proximal or distal centrioles. During maturation of the spermatid, the axoneme lengthens and becomes surrounded by the plasmalemma throughout its length.

During spermiogenesis, the microtubular manchette also extends into the midpiece region. These microtubules appear less organised than those around the nucleus. In transverse section both single and multiple layers of microtubules occur in the middle piece area (Figure 34).

(C). Ultrastructure of the Spermatozoon

(1). Spermatozoon

Spermatozoa collected from the vas deferens were processed for thin sectioning. An acrosome, nucleus, mitochondrial pocket and a long flagellum are present.

The acrosome is elongate, about 2.2 μm long. A layer of electron dense material fills the juxtanuclear subacrosomal fossa (Figure 42). The apical acrosomal vesicle is membrane bound (Figure 42). In a longitudinal section, the peripheral region of the acrosome is greatly thickened, whereas the internal area appears electron

lucent (with a density similar to that in the subacrosomal fossa). The thickened wall actually consists of arrays of parallel longitudinal filaments extending to the area of the apical vesicle (Figures 42 and 44). In transverse sections these longitudinally orientated filaments assume groups of bundles (Figure 43). Adjacent bundles are separated from each other, rather than connected by circumferential filaments as have been demonstrated in Rossia pacifica (Fields and Thompson, 1976). At places where these filamentous bundles are absent, the acrosomal membrane and external sperm plasmamembrane are clearly recognizable (Figure 43). The microtubular sheath surrounding the elongating proacrosome in the late spermatid disappears in the spermatozoon.

The nucleus in transverse section appears homogenously electron dense (Figures 42 and 46). There is no occurrence of intranuclear cavities such has been demonstrated in a large number of primitive type of spermatozoa (Franzén, 1983; Hou and Maxwell, 1991). The nuclear membrane is closely apposed to the chromatin and in sections is virtually indistinguishable.

The centriole penetrates deeply into the base of the nucleus to lie in the nuclear fossa. The proximal and distal centrioles are embedded in electron opaque material (Figure 46). The distal centriole gives rise to a "9 + 2" axoneme (Figure 47). The proximal end of the flagellum is enveloped by the mitochondrial sleeve (Figure 45). There

are no further changes in the morphology of the mitochondrial pocket in the spermatozoon collected from the vas deferens (Figure 45). Mitochondria are tightly packed. At the tail tip, the axoneme loses its "9 + 2" arrangement (Figure 48) and eventually, microtubules are absent.

(2) Glycogen distribution

The mature spermatozoon of Rossia macrosoma consists of an acrosome, nucleus, mitochondrial middle piece and tail (cf. Maxwell, 1975a; Fields and Thompson, 1976). Treating spermatozoa with PA-TSC-SP staining, glycogen particles are detected around the plasmalemma of the mitochondria in the middle piece and in the tail (Figures 49, 50 and 51). No glycogen deposits are associated with either the nucleus or acrosome.

The glycogen granules are about 130-145 Å in diameter and form β particles according to the structural classification of glycogen described by Drochmans (1962). Control sections incubated in α, β-diastase exhibit a complete absence of glycogen.

In the mitochondrial sleeve (Figure 49) the glycogen particles lie closely related to the plasma membrane of the mitochondrial sleeve and aggregate into small groups. Large amounts of glycogen are deposited in the tail piece within and around the axial filaments (Figures 50 and 51). These peri-axonemal granules are arranged into nine longitudinal rows. Each contains a series of single glycogen particles

regularly located between two adjacent gamma fibres in the axoneme (Figure 51). In longitudinal sections, these granules are regularly spaced at about 20-26nm (Figure 50). In addition, intra-axonemal granules occur around the central doublet of the axoneme but with less regularity than that displayed by the periaxonemal glycogen. This striking feature of inter-axonemal deposition of glycogen makes it remarkably different from the arrangement of glycogen particles within the tail of Octopus bimaculatus (Longo and Anderson, 1970) and Eledone cirrhosa (Maxwell, 1974a), in which glycogen granules form a sheath surrounding the gamma fibres and the 9+2 axoneme.

Discussion

(A). Spermatozoon and Spermiogenesis

The ultrastructure of the spermatozoon of Rossia pacifica was described in detail by Fields and Thompson (1976). In the peripheral region of the acrosome, a meshwork of longitudinal and circumferential filaments forms a peripheral girdle around the stalk-like acrosome. However, in Rossia macrosoma only bundles of longitudinal filaments occur in the acrosome. In addition, during the development of the acrosome, a microtubular sheath also occurs around the proacrosome which is absent in spermatozoa collected from the vas deferens.

There are two centrioles in Rossia (Sepiolidae; Fields and Thompson, 1976; present study), but there is only a single triplet centriole in Eusepia (Sepiidae), Loligo and Allotouthis (Loliginigae) (Maxwell, 1975a).

Sperm structure has been demonstrated to be a valuable character for studing the taxonomic relationships in a variety of molluscan groups at both species and higher levels (see reviews: Popham, 1979; Maxwell, 1983; Healy, 1988a, b; Hodgson and Bernard, 1988; Eckelbarger et al., 1990; Hodgson et al., 1990). Fields and Thompson (1976), however, felt that sperm morphology in the Decapoda is more related to the mode of fertilization than phylogenetic considerations. Franzén (1955, 1967) studied

spermatogenesis and the spermatozoa of a variety of cephalopods using optical microscopy and particularly emphasized phylogenetic differences. The morphological evolution of the sperm and spermiogensis in the cephalopods has been suggested to be associated with difference in either egg size and/or ontogeny. In the present study, comparison of the ultrastructural organization of mature spermatozoa of Rossia pacific and Rossia macrosoma with examples from other decapod families show differences, providing another example to support the suggestion that decapod spermatozoa are useful material to aid in elucidating systematic relationships between different groups.

Freeze-fracture studies of decapod spermatozoa revealed that both the internal and external surfaces of the plasmalemma which limit the axoneme in the midpiece region in Eusepia officinalis, Loligo forbesi and Alloteuthis subulata were highly modified (Maxwell, 1975a). Series of groups of parallel, longitudinally orientated ridges were demonstrated on both internal and external surfaces of the plasmalemma. My study of Rossia macrosoma also demonstrates the occurrence of electron dense deposits on both sides of the plasma membrane in the midpiece area. These deposits have been suggested to serve some role in strenthening the plasmalemma which is closely applied to the axoneme (Maxwell, 1975a).

My observations of the spermatozoa of Rossia

macrosoma, using scanning electron microscopy, did not demonstrate any specialized materials on the surface of the spermatozoon plasmalemma, probably due to the low resolution of SEM.

The structural changes that occur during spermatogenesis in Rossia macrosoma (Sepiolidae) are similar to those described in Loligo forbesi, Alloteuthis subulata (Loliginidae) and Eusepia officinalis (Sepiidae) (Maxwell, 1975a). However the acrosomal morphogenesis appears different and interesting. The acrosome of Rossia macrosoma is elongate with arrays of supporting longitudinal filamentous bundles surrounding the rigid fibrous core rather than a spherical sac-like structure described in other decapods (Maxwell, 1975a). The acrosome of Rossia pacifica is enclosed by a meshwork of longitudinal and circumferential filaments (Fields and Thompson, 1976). I am, however, unable to demonstrate the circumferential layer of filaments described in the acrosome of Rossia pacifica by Fields and Thompson (1976). Rather, groups of separate, longitudinal filaments occur in close relation to the internal aspect of the acrosomal membrane. These filaments have been suggested to provide mechanical support around the acrosome or possibly function in the extension of the acrosomal process during the acrosomal reaction (Fields and Thompson, 1976).

There has been no report of the occurrence of microtubules during development of the acrosome in

cephalopods. In Rossia macrosoma, a longitudinally orientated microtubular sheath is closely associated with the elongating proacrosomal granule. This proacrosomal microtubular sheath is associated with the microtubular manchette around the nucleus and lost in those spermatozoa obtained from the vas deferens. The close association of microtubules with the elongating proacrosome indicates that microtubules may be involved in the shaping of the acrosome.

The Golgi cisternae at the maturing face swell and the internal contents become condensed, giving rise to a proacrosomal granule. Prior to the transformation of the spherical proacrosomal granule into an elongate form, this large granule first settles at the apex of the nucleus with the Golgi complex still closely associated. Later, a sheath of microtubules develops in association with the elongated acrosome. This process of acrosomal development is comparable to that in the modified type of spermatozoa, but differs from those of the primitive spermatozoa (see reviews by Buckland-Nicks and Chia, 1989; Healy, 1989; Eckelbarger et al., 1990; Hou and Maxwell, 1991), in which the proacrosome, secreted by the Golgi complex, will migrate independently to the apex of the nucleus prior to nuclear elongation.

Patterns of nuclear chromatin condensation have been described in both primitive and modified types of spermatozoa (see review by Maxwell, 1983). The shape of the

nucleus in Rossia macrosoma changes from a spherical into an elongate form during the process of spermiogenesis. Chromatin displays a similar packing system to that described in other decapods (Maxwell, 1975a, 1983). However, the nuclear chromatin in Rossia macrosoma condenses into much thicker filaments than that demonstrated in Alloteuthis and Eusepia (Maxwell, 1975a). In Nautilus, nuclear chromatin has been shown to be packed into longitudinal sheet-like arrays (Arnold and Williams-Arnold, 1978). Freeze-fracture of the decapod spermatozoan nucleus (Maxwell, 1975a) demonstrated an organization of the chromatin more complex than the simple irregular packing of human chromatin, but not as complex as that in the bull or rabbit spermatozoan head. This nuclear chromatin packing system has been termed "pseudolaminar" packing (Maxwell, 1975a, 1983).

During spermiogenesis, mitochondria elongate and assume a tortuously interwoven form when spermatid nuclear chromatin condensation occurs. This mitochondrial aggregate is structurally similar to that described in an insect Trialeyrodes vaporariorum (Baccetti and Dallai, 1977), but structurally different from those giant mitochondria which at certain stages in sperm morphogenesis form a complex onion-like structure called the "Nebenkern" (e.g. in the spermiogenesis of euthyneuran gastropods, Walker and MacGregor, 1968; Giusti, 1971; and insects, Baccetti and Afzelius, 1976). The mitochondria in Rossia macrosoma,

without further fusion into two large mitochondria, are loosely packed in the mitochondrial sleeve. Fields and Thompson (1976) postulated that the mitochondrial sleeve may be a mechanical aid to the locomotion of spermatozoa and assist the spermatozoon in passing through the egg jelly.

Rossia macrosoma practises external fertilization (Racovitza, 1894). Franzén (1955, 1967) suggested that it was the biology of fertilization that determined the modification of sperm into two groups. The primitive type of spermatozoa usually occurs in species practising external fertilization, whereas the modified type of spermatozoon is present in species fertilizing internally. However, spermiogenesis of Rossia macrosoma shows features of both modified and primitive types. For example, features suggestive of the modified type: 1). the Golgi complex moves first to the apex of the spermatid nucleus prior to the formation of a proacrosomal granule, 2). the early stages of proacrosome differentiation occur at the apex of the nucleus with close association of the Golgi complex, 3). the elongate nucleus and its surrounding microtubular manchette, and 4). the occurrence of glycogen in the tail piece. These characters parallel those described during spermiogenesis in the euthyneuran molluscs possessing the modified type of spermatoon (see review by Healy and Jamieson, 1989). On the contrary, primitive features are: 1). only a spherical proacrosomal granule occurs without

further development of a acrosomal pedestal which usually occurs in the modified type of spermatozoon; as summerised by Healy and Jamieson (1989); 2). a cluster of mitochondria gathers around the posterior end of the head, 3) there is no occurrence of anterior and posterior nuclear membrane specializations, and 4). a large amount of β-glycogen granules occur in the mitochondrial sleeve. These features are comparable to those described in the molluscan groups with the primitive type of spermatozoon (see reviews by Popham, 1979; Franzén, 1983; Healy, 1989; Eckelbarger et al., 1990; Hou and Maxwell, 1991).

(B). Glycogen deposition

Glycogen deposits within molluscan spermatozoa are well documented (see reviews: Anderson and Personne, 1970; Maxwell, 1983). Using Best's carmine staining, high levels of carbohydrate have been demonstrated in the semen of octopods, most of it glycogen (Mann et al., 1970). However, the reported distribution of glycogen in the spermatozoa of octopods varies between species. Martin et al. (1970) and Mann et al. (1970) demonstrated large amounts of glycogen near the surface of the sperm head in Octopus dofleini by using Best's carmine and PAS techniques. With the development of the periodic acid-thiosemicarbazide-silver proteinate (PA-TSC-SP) technique for the detection of polysaccharides in thin sections (Thiéry, 1967; Vye & Fischman, 1971), a more precise, ultrastructural,

localization of glycogen within the spermatozoa of Octopus bimaculatus and Eledone cirrhosa was described by Longo and Anderson (1970) and Maxwell (1974a). Most of the glycogen particles appear loosely packed in the intracellular space between the plasma membrane and the outer fibers of the sperm tail. No glycogen was detected in the head and midpiece. No explanation of the positive PAS reaction within the head of the spermatozoa as observed by Martin et al. (1970) and Mann et al. (1970) under the light microscope has been provided in the literature.

Using light microscopy a positive PAS reaction has been detected around the nucleus and in the mitochondrial sleeve in Rossia pacifica (Fields and Thompson, 1976). Fields and Thompson (1976), however, were unable to demonstrate ultrastructurally any glycogen in the tail piece. Judging by the close association of glycogen with both mitochondria and the sperm head, Fields and Thompson (1976) suggested that glycogen was thereby convenient to the mitochondria for energy production. In their micrographs (number 22, 23 and 24), accessory filaments were described in the region between adjacent coarse outer fibres in transverse sections of the flagellum and electron dense particulate material described between the course fibres and the plasmalemma in longitudinal sections of the flagellum. In the present study, these accessory filaments, however, are positive to PA-TSC-SP staining which suggests that the so-called accessory filaments

described by Fields and Thompson (1976) are in fact rows of intra-axonemal glycogen particles. I am, however, unable to demonstrate any glycogen in the acrosomal and nuclear areas. My study shows that the glycogen occurs in the mitochondrial pocket underlying the plasma membrane and in the flagellum.

The present ultrastructural studies of the Rossia macrosoma spermatozoa and spermiogenesis reveal that they are structurally different from both the primitive and modified spermatozoa. Indeed, comparison of the distribution of stored glycogen in the spermatozoa of Rossia macrosoma demonstrates an apparent difference between these two types. In those molluscan groups with the primitive type of spermatozoon, for example, Aplacophora (Buckland-Nicks and Chia, 1989), Bivalvia (Popham and Dickson, 1975; Popham, 1979), Scaphopoda (Hou and Maxwell, 1991) and Archaeogastropoda (Koike, 1985; Hodgson and Bernard, 1988), β-glycogen particles mainly occur in the head and middle piece. Glycogen deposits never occur in the flagellum. On the contrary, glycogen in the modified type of euthyneuran spermatozoa is highly compacted and incorporated into helical compartments within the mitochondrial derivative (see reviews by Maxwell, 1980; 1983; Healy, 1982a, 1988a, b; Healy and Willan, 1984; Healy and Jamieson, 1989). In the euspermatozoa of meso- and neogastropods (Prosobranchia), glycogen occurs in a distinct glycogen piece posterior from the midpiece

(Buckland-Nicks, 1973; Kitajima and Paraense, 1976; Griffond, 1980; Healy, 1982b). However, there have been descriptions of an irregularly arranged intra-axonemal distribution of glycogen within the tail of prosobranchs and opisthobranchs (Thompson, 1973; Healy, 1982a, b; Minniti and D'Andrea, 1989). The pattern of glycogen distribution in Rossia macrosoma lends further surpport to the suggestion that decapod spermatozoa are of an intermediate type.

In summary, the present study of Rossia macrosoma spermiogenesis confirms previous light microscopical studies (Franzén, 1955, 1967) that the decapod spermatozoon and spermiogenesis possess features of both primitive and modified types of spermatozoa and it would be more appropriate to classify them as an intermediate group.

CHAPTER III

SPERMATOGENESIS OF *ARCHIDORIS TUBERCULATA*, *TRITONIA PLEBEIA* AND *APLYSIA FACIATA* (MOLLUSCA: OPISTHOBRANCHIA)

Introduction

The subclass Opisthobranchia represents a large and diverse molluscan group comprising nine orders (systematic classification according to Thompson, 1976), i.e. Bullomorpha, Pyramidellomorpha, Thecosomata, Gymnosomata, Aplysiomorpha, Pleurobranchomorpha, Acochlidiacea, Sacoglossa and Nudibranchia, representing the majority of 15 orders within the Gastropoda.

The general classification of the external and internal reproductive system of opisthobranchs have been described (Pruvot-Fol, 1960; Ghiselin, 1966; Hyman, 1967; Franc, 1968; Thompson and Bebbington, 1969; Beeman, 1970a; Thompson, 1976). The reproductive system of opisthobranchs consists of an ovotestis and a complex gonoduct, the form of which varies considerably between different suborders and families (see review Thompson, 1976). Ghiselin (1966) analysed the structural and functional variations of the opisthobranch gonoduct; which by later authors has been used as an important parameter for the elucidation of the systematics of opisthobranchs (see review by Beeman, 1977). However, many aspects of the histology and fine structure of the ovotestis in opisthobranchs, particularly male germ cell differentiation, are still poorly known.

Previous investigations have demonstrated great variation in the histology of the ovotestes between nudibranch species (Medina et al., 1986b, 1987). The

nudibranchs have been commonly divided into two groups, i.e. "dorid nudibranchs" and "eolid nudibranchs" (Thompson, 1976; Beeman, 1977). The first group refers to the suborder Doridacea, whereas the latter is a collective term applied to suborders Dendronotacea, Arminacea and Aeolidiacea. The ovotestes in the suborders Doridacea and Dendronotacea, for example, Archidoris pseudoargus (Thompson, 1966), Tritonia hombergi (Thompson, 1961), Hypselodoris tricolor (Medina et al., 1986b, 1987), extend over a larger area of the digestive gland, to which it is closely attached. This is quite different from the arrangment in other suborders of nudibranchs, for example, Aeolidacea and Arminacea (Medina et al., 1987), in which the gonads lie freely in the haemocoelomic cavity; except, however, Spurillar neapolitana in which the ovotestis occurs in close association with the underlying digestive gland (Eckelbarger et al., 1981).

The location of germ cell lines (male/female) within an acinus in the ovotestis also shows a great diversity and does not appear to follow a fixed pattern (Hyman, 1967). In nudibranchs, in those suborders in which the ovotestes are closely associated with the underlying digestive glands, the male and female developing germ cells occur within the same acinus. In the gill-less dorids Okadai (Baba, 1931, 1937; Hyman, 1967) and the eolids Fiona, Embletonia, Eubranchus and Dondice (Hyman, 1967; Beeman, 1977), male and female germ cells develop within separate acini. In those groups which have an ovotestis separated from the

digestive gland, for example, Godiva banyulensis (Medina, et al., 1986b), the male germ cells occur in the central lumen and the female cells are contained in a set of peripherial diverticula. In other opithobranchs possessing an ovotestis histologically detached from the digestive gland, such as the notospideans Aplysia (Thompson and Bebbington, 1969; Dudek et al., 1980) and Phyllaplysia taylori (Beeman, 1970a, b), the arrangement of the ovotestis, however, is similar in that female germ cells lie peripheral to the centrally located male germ cells all within a single acinus (Medina et al., 1986b, 1987).

Prior to electron microscopical studies of spermatogenesis, Robert (1888), Retzius (1906) and Tuzet (1939) provided preliminary notes on some general features of the process of spermatogenesis in a variety of families of opisthobranchs using bright field light microscopy. Schitz (1925) provided very detailed descriptions of the early stages of spermatogenesis in the highly specialized pelagic pteropods. Using phase contrast microscopy, Franzén (1955) examined the spermatozoa and spermatogenesis of a large number of opisthobranchs and provided a few excellent drawings of the developmental stages. Beeman (1970b), using autoradiography and phase contrast light microscopy, provided the first detailed account of spermatogenesis of a notaspidean opisthobranch, Phyliaplysia taylori, and also described the time scale for a single spermatogenic cycle. The minimum time scale for the entire process of

spermatogenesis is about 20 days. It took approximately ten days for a primary spermatocyte to develop into a mature spermatozoon.

The process of spermatogenesis in opisthobranchs has only recently been described at the ultrastructural level in a small number of species. These species include: Aplysiomorpha, Phyllaplysia taylori, Aplysia californica (Beeman, 1970a, b, 1977), Aplysia kurodai (Kubo and Ishikawa, 1981), Bursatella leachi (Thompson, 1975); Pyramidellomorpha, Turbonille sp., Pyrgulina sp., Cingulina sp., and Hinemoa sp., (Healy, 1988a), and Nudibranchia, Spurilla neapolitana (suborder: Aeolidacea) (Eckelbarger and Eyster, 1981), Hypselodoris tricolor (suborder: Doridacea) (Medina et al., 1985, 1986a, 1988). Clearly more detailed information is needed to further substantiate these findings and provide a broad basis for future comparison.

Initial ultrastructural studies on aplysiid spermatozoa were unable to demonstrate the acrosome (Thompson and Bebbington, 1969, 1970; Beeman, 1977). It is only after further detailed observations on spermatogenesis of Aplysia furodi by Kubo and Ishikawa (1981), that the presence of a small acrosome has been demonstrated. Kubo and Ishikawa (1981) also provided evidence that the proacrosome is formed by fusion of vesicles derived from the Golgi complex. Recent studies on acrosome formation in the Aeolidacea nudibranchs Spurilla neapolitana and

Doridacea Hypselodoris tricolor, on the contrary, failed to demonstrate the involvment of the Golgi complex in the production of the proacrosome (Eckelbarger and Eyster, 1981; Medina et al., 1985).

Detailed information on the spermatozoa and spermatogenesis of opisthobranchs have provided convincing evidence to contribute to the resolution of the taxonomic positions of those systematically uncertain molluscan groups (Healy, 1988a; Minniti and D'Andrea, 1989). For instance, the systematic positions of the Architectonicidae and Pyramidellidae within the Gastropoda have long been a subjet for debate among malacologists and palaeontologists (Fretter and Graham, 1949, 1962; Robertson, 1973, 1978; Ponder, 1973). This uncertainty is mainly due to the lack of anatomical observations concerning these groups, involving not only genera, but even orders and subclasses (Healy, 1988a; Minniti and D'Andrea, 1989). The shell morphology has often been suggested as evidence of their prosobranch affinity. However, studies of their soft part anatomy, in particular the structure of the reproductive system and sensory organs, indicate that these gastropods are most appropriately referred to the subclass Opisthobranchia (Fretter and Graham, 1962; Ghiselin, 1966). Recent electron microscopical studies of gastropod spermatozoa and spermatogenesis have provide further evidence to show significant differences between meso/neogastropods and euthyneurans (see review by Healy,

1988b). The most prominent difference has been demonstrated to occur during the formation of the midpiece and the acrosome (Healy, 1982a; b; 1988a, b; Minniti and D'Andrea, 1989). Further detailed studies of the ultrastructural organization of spermatozoa and spermatogenesis of Architectonicidae (Philippia hybrida, Minniti and D'Adrea, 1989) and Pyramidelloidea (Cingulina sp., Pyrgulina sp., Turbonilla sp., and Hinemoa sp. Healy, 1988a) confirm that the features of developing and mature spermatozoa follow the pattern observed in opisthobranchs, for example, 1). an acrosome with apical vesicle and acrosomal pedestal; 2). formation of the midpiece by a mitochondrial wrapping around the axonemal/course fibres complex; 3). formation of a glycogen filled helix within the mitochondrial derivative (via a second wrapping of mitochondria); and 4). the nucleus further condensing into a helically-keeled shape.

However, this information covers only a limited number of opisthobranch groups and yet prominent structural differences between species even from the same systematic group, for example, superfamily or family, have been demonstrated (see Thompson, 1973, 1976; Healy, 1988b), which strongly suggests that further extended research on the opisthobranchs is needed and would also contribute greatly to our knowledge of their systematics.

The functional organization of the reproductive system and spermatozoan ultrastructure of Archidoris pseudoargus, Tritonia hombergi, Aplysia depilans, Aplysia

faciata and Aplysia punctata have been thoroughly investigated by Thompson and co-workers (Thompson, 1961, 1966; Thompson and Bebbington, 1969, 1970). The process of acrosome formation in Aplysia kurodi has been described by Kubo and Ishikawa (1981). However, there has been no investigation of spermatogenesis of these species. The present investigation analysed ultrastructural changes during spermatogenesis in Archidoris tuberculata, Tritonia plebeia and Aplysia faciata. Results obtained will also be compared with previous studies. Specific problems which have been highlighted in the recent literature, for example, the origin of the acrosome, will be discussed.

Results

(A). Organization of the Ovotestis and Spermatozoon

The ovotestes of Archidoris tuberculata, Tritonia plebeia and Aplysia faciata are posterior and intimately associated with the underlying digestive glands. Each ovotestis consists of a number of sac-like acini (Figures 1, 2 and 3) which are outlined by a very complex wall and a layer of loose connective tissue (cf. Figures 15, 16, 17 and 18). Developing oocytes and spermatozoa occur simultaneously within each acinus.

The acinar wall consists of two layers, an outer myoepithelial layer (terminology from Eckelbarger and Eyster, 1981; Figures 15-18) and an inner thickened basal lamina (Figures 15-18). The myoepithelial cell possesses a centrally located, small, dark nucleus (Figure 19). In the cytoplasm, numerous myofilaments are arranged parallel to the basal lamina. A few mitochondria are loosely distributed among these filaments (Figure 18). The basal lamina, measured about 0.3-0.45 μm thick in Archidoris tuberculata and Tritonia plebeia, but only 0.15 μm in Aplysia faciata (Table 2), provides direct contact with accessory cells (terminology from Eckelbarger and Eyster, 1981). The basal lamina consists of only dense fine fibrils (Figure 15). The accessory cells overlie the basal lamina (Figure 19). It contains a large irregular shaped nucleus (Figure 20). In the cytoplasm of the accessory cell,

abundant electron dense granules, morphologically resembling clusters of glycogen, and lipid droplets occur (Figure 21). Developing male germ cells are closely associated on the luminal side of the accessory cells (Figures 19 and 20).

Within each acinus in the ovotestis of Achidoris tuberculata, male germ cells occur proximal to the underlying digestive gland whereas female cells are mostly distributed distally, near the surface of the ovotestis (Figure 1). The organization of male and female germ cells, however, is different in the ovotestis of Aplysia faciata and Tritonia plebeia. Serial sections of the whole ovotestis demonstrate that male germ cells occur in the central part of the acinus and are surrounded by peripheral developing female germ cells (Figures 2 and 3).

The mature spermatozoa of Archidoris pseudoargus and Tritonia hombergi have been examined by Thompson (1961, 1966), using phase contrast and transmission electron microscopy. To appreciate the three-dimensional organization of these spermatozoa, I carried out further study using scanning electron microscopy. The spermatozoa of Archidoris tuberculata, Aplysia faciata and Tritonia plebeia show significant differences both in dimension and organization (see Table 1 and Figures 4-14). The length of the head and total sperm of Achidoris tuberculata is much longer than that of Archidoris pseudoargus (Thompson, 1966) (Table 1), although the body size of these two species are

very similar, 120mm (Thompson, 1966).

My scanning electron microscopical observations of spermatozoa from Archidoris tuberculata, Aplysia faciata and Tritonia plebeia confirm previous descriptions made by a number of workers (Franzén, 1955; Thompson, 1966; Thompson and Bebbington, 1969; Beeman, 1970b, 1977). The head in the spermatozoon of Achidoris tuberculata is filiform (Figures 4, 5 and 12). A minute helical keel spirals along the head (Figure 4) and is continuous with the large glycogen keel in the tail. Measurement of the length of the spiral pitchs in the spermatozoa show prominent differences between the three species (Table 3). The pitch length in the head region is shorter than that in the tail in Tritonia plebeia and Aplysia faciata, but longer in Archidoris tuberculata (Table 3). The spiral keel winds around the spermatozoan head and flagellum in a dextral direction. (Figures 12, 13 and 14). There is no clear demarcation between the head and flagellum in Tritonia plebeia and Aplysia faciata (Figures 7-11). The head of the Tritonia spermatozoon is twisted like a corkscrew (Figures 7, 13), whereas a very prominent helix, originating just behind the anterior extremity of the head, extends over nearly the whole length of the spermatozoan flagellum in Aplysia faciata (Figures 10, 11 and 14). An acrosomal granule is visible on the apex of the nucleus of the three species examined (Figures 11, 12, 13 and 14).

Table 1

Comparison of the Length of the Spermatozoa (μm)

Species	Acrosome	Nucleus	Tail	Total	Author
Archidoris pseudoargus	0.36	9	199-200	208-210	Thompson 1966
A. tuberculata	1.00	12	375	388-390	Present
Tritonia hombergi	—	10	—	280	Thompson 1961
T. festiva	—	—	—	180-190	Thompson 1961
T. plebeia	0.8	9	170	185	Present
Aplysia faciata	0.7	20	163	185	Present Thompson and Bebbington (1969)
A. depilans	—	25	—	158	Thompson and Bebbington (1969)
A. punctata	—	20	—	220	Thompson and Bebbington (1969)

— data not available

Table 2

Dimension of spermatogenic cells and basal lamina (μm)

species	Family	Basal lamina	Sg (N) (ϕ)	Sc (N) (ϕ)
Archidoris tuberculata	Archidorididae	0.3	5.6±0.1	6.6±0.1
Tritonia pleibeia	Tritoniidae	0.45	5.7±0.1	7.4±0.2
Aplysia faciata	Aplysiidae	0.15	5.4±0.2	4.6±0.2

Sg, spermatogonium; Sc, spermatocyte; N, nucleus;

ϕ, diameter.

Table 3

Measurement of spermatozoan helical pitch (μm)

species	Head region	Tail region
Archidoris tuberculata	1.3	0.8
Tritonia plebeia	1.3	1.8
Aplysia faciata	3.5	4.8

(B). Early Spermatogenesis

An analysis of acrosomal development and related stages of spermiogenesis in Aplysia kurdai has been provided by Kubo and Ishikawa (1981). In the present thesis I will describe the early stages of spermatogenesis of Aplysia faciata and compare the late stages of spermiogenesis with that in Aplysia kurodai. The early stages of spermatogensis in Archidoris, Aplysia and Tritonia are very similar. Therefore, unless otherwise noted, the following description applies to all three species.

The spermatogonia in Archidoris tuberculata, Tritonia plebeia and Aplysia faciata are spherical cells with a large, centrally located nucleus measuring about 5.6 μm in Archidoris tuberculata, 5.7 μm in Tritonia plebeia and 5.4 in Aplysia faciata (Figures 22-24; Table 2). A common feature of developing spermatogonia is the prominent nucleolus measuring around 1.4-1.5 μm in the three species. There is a thin layer of cytoplasm around the nucleus which contains small, spherical and rod-shaped mitochondria (Figures 22-24). The spherical mitochondria measure 0.2 - 0.4 μm in diameter whereas rod-like ones measure 0.9 - 1.1 μm long. The matrix is electron-dense with arrays of intramitochondrial cristae. A large number of spermatogonia form small groups on the luminal side either directly overlying the basal lamina or in close association with the accessory cell in the male portion. They are connected by

intercellular bridges (Figure 25).

Primary spermatocytes are very similar to spermatogonia. However, the nuclear diameters are larger than those in the spermatogonia (except Aplysia faciata) (6.6 and 7.4 μm in Archidoris and Tritonia; see Table 2). The nucleolus is no longer present and heterochromatin is diffuse (Figures 26-29). In the nucleoplasm, synaptonemal complexes (Figures 30-31), which represent the zygotene or pachytene stages of meiosis, occur. In the cytoplasm, mitochondria remain similar to those in the spermatogonia, but electron dense material starts to build up within the mitochondrial matrix (Figures 84, 85 and 86).

(C). Spermiogenesis

(1). Nuclear morphogenesis

A similar process of nuclear structural transformation has been observed in other opisthobranchs. To facilitate description, I also divide spermiogenesis into three stages, i.e. pre-cup stage, cup stage, and elongating stage according to the descriptions provided in the other opisthobranchs by Eckelbarger and Eyster (1981) and Healy (1988a).

Pre-cup stage

The nucleus in this stage is spherical (2.3 - 3.0 μm in diameter) with evenly distributed finely granular chromatin (Figures 32-34). Intercellular bridges still remain in the spermatid stage (Figure 32). A prominent

characteristic throughout this stage is the development of an electron dense anterior and posterior plaque. Later, the proacrosome and centriolar complex will become closely associated with the anterior plaque and posterior plaque (Figure 35). Serial thin sections show that the anterior plaque forms first in Archidoris tuberculata and Tritonia plebeia and involves the deposition of electron dense material on both sides of the nuclear membrane (Figures 35, 37). The anterior plaque measures about 50 nm thick in Archidoris tuberculata and Tritonia plebeia. The posterior plaque is different from the anterior plaque in that only a single layer of electron-dense material (about 24 nm thick) is deposited at the internal surface of the nuclear envelope (Figures 33, 36, 40 and 41). However, in Aplysia faciata, the posterior plaque forms first (Figure 34) and measures about 0.3 μm thick. The appearance of the nuclear plaques establishes the anterior and posterior polarity of the developing spermatid nucleus.

Cup stage:

Further differentiation of the nucleus results in the shortening of the anterior/posterior axis of the spermatid so that the posterior and anterior plaques move closer (Figures 34-42). As a result of the inward curving of the anterior plaque, the spermatid nucleus assumes the form of a concave, cup shape (Figures 38, 39 and 40). Chromatin forms thin fibrils which are most numerous near the

anterior and posterior plaques (Figures 40, 41) in Tritonia plebeia.

At this stage, however, I was unable to detect any microtubules in relation to the nucleus. Shortening of the anterior/posterior axis of the nucleus apparently occurs without the involvement of microtubules.

Elongating stage:

The nucleus loses its cup shape and undergoes elongation along the anterior/posterior axis (Figures 43, 45, 48 and 52). Dramatic changes of nuclear shape occur at this stage. The nucleus transforms from a cup shape into an elongate helicoid; great morphological differences occur in the nucleus between the three species.

Chromatin condenses into fine filaments in the nucleoplasm (Figures 45, 48 and 53). A group of filaments lying in the same plane aggregate into lamellae (Figures 49 and 51). Oblique sections through the periphery of the nucleus reveal a banded pattern of chromatin lamellae (Figures 62 and 63). In Aplysia faciata, many tubular structures similar to those described in Aplysia kurodi (Kubo and Ishikawa, 1981) also occur in the nucleus (Figure 64). The diameter of a single tubule is about 21 nm.

As the nucleus undergoes the final stage of condensation, longitudinally oriented microtubules become regularly arranged around the elongating nucleus, forming a manchette. These microtubules, measured about 10-15 nm in diameter, are closely associated with the nuclear envelope

and embedded in a filamentous matrix (Figure 62). Tannic acid fixed material reveals inter-microtubular bridges between adjacent microtubules (Figures 68, 69 and 70).

In the process of spermatid nuclear transformation, from a cup-shape into elongate form, major nuclear morphological differences occur between Archidoris tuberculata (Figures 43-47), Tritonia plebeia (Figures 48-50), and Aplysia faciata (Figures 51-54). In Tritonia plebeia, the early spherical spermatid nucleus first elongates along the anterior/posterior axis then assumes a spiral shape (Figures 49 and 50). Condensing chromatin lamellae become helical arranged within the nucleus (Figure 49), resulting in the formation of a prominent nuclear keel (Figures 7, 13, 67 and 81). In a transverse section of the nucleus, some of the chromatin lamellae and corresponding microtubules are transversely cut, whereas the remainder are obliquely sectioned (Figure 62). Chromatin lamellae further condense into a homogeneous state (Figure 67). In contrast, in Archidoris tuberculata, a nuclear keel is not found (Figure 66), rather chromatin lamellae aggregate into a homogeneous state (Figures 60, 66 and 80). Spermatid chromatin filaments of Aplysia faciata at the elongating stage also arrange themselves helically with respect to the longitudinal axis of the nucleus (Figure 53). But the nucleus initially has a very irregular shape (Figure 51) and later elongates along the anterior/posterior axis and coils around the flagellum (Figures 52, 65, 71 and 72).

(2). Acrosome differentiation:

There are more than two Golgi complexes in the primary spermatocyte (Figures 73 and 74), however only one is constantly related to the developing proacrosomal granule (Figures 75-78). The electron dense proacrosomal granule is spherical and membrane bound, measuring 0.25-0.3 μm in diameter. It first appears on the concave side of the Golgi complex in close relation to dilated Golgi cisternae and adjacent endoplasmic reticulum (Figures 74-76), suggesting that the proacrosomal granule is indeed derived from the Golgi cisternae. As the anterior and posterior plaques develop on the spermatid nuclear envelope, this proacrosomal granule settles at the apex of the nucleus assuming an ellipsoid shape (Figures 42, 44 and 78). Further differentiation of the proacrosomal granule occurs when the nucleus transforms into a cup-shape. Electron dense material accumulates underneath the proacrosomal granule, forming a supporting acrosomal pedestal (Figures 43, 44 and 79). This pedestal extends upward to surround almost the entire lateral wall of the proacrosomal granule, leaving, however, only the anterior tip of the granule uncovered (Figures 79, 80, 81 and 82). As the nucleus elongates and condenses, excess cytoplasm is lost from the midpiece and tail. At this stage, the acrosomal pedestal forms a layer of homogeneous electron dense material surrounding the peripherial and basal aspects of the acrosome. The apex of the acrosome is, however, only

covered by the acrosomal membrane and the plasmalemma of the spermatozoon.

(3). Midpiece and tail formation:

Mitochondria in the spermatogonia are small, rod-shaped with arrays of parallel arranged cristae in the matrix (Figure 83). However, mitochondrial cristae lose their regular arrangement and decrease in number. The mitochondria increase in size as the spermatogonium differentiates into spermatocyte and spermatid (Figures 84-86). A flocculent electron dense material replaces the mitochondrial cristae within the mitochondrial matrix of the spermatid in Tritonia plebei (Figure 84). However, in Archidoris tuberculata and Aplysia faciata, electron dense dark intracristal bodies occur within the mitochondrial matrix (Figures 85 and 86). Prior to nuclear elongation, mitochondria cluster around the proximal region of the axoneme (Figures 87-90), where they begin to fuse into a single sheath around that axoneme (termed primary wrapping phase; Figures 87, 88, 90 and 91; terminology from Healy, 1988a). The number of mitochondrial cristae is reduced and forms a membranous network. The mitochondria at this stage are structurally comparable to "lamellar vesicles" described in Hypselodoris tricolor by Medina et al. (1988). The process of mitochondrial fusion spreads posteriorly (Figures 87 and 91) and after the primary wrapping is complete, a secondary wrapping phase begins. At this

stage, intracristal bodies become mixed with the mitochondrial matrix. Inner mitochondrial cristae appear disordered and are replaced by "pseudo-paracrystalline" structures (Figures 60, 92 and 94). Furthermore, these mitochondria surround the axoneme and its primary mitochondrial sheath. The secondary wrapping forms a helical keel in which large amount of glycogen are deposited (Figures 94-97). In longitudinal sections through the midpiece, "pseudo-paracrystalline" material assumes 55 - 70 nm wide bands arranged spirally around the axoneme (Figures 98, 99 and 100). In transverse sections, however, "pseudo-paracrystalline" material appears electron dense and homogeneous (Figures 95, 96 and 97). The "pseudo-paracrystalline" material which envelopes the glycogen helix is more densely packed than that around the axoneme and measures about 25 - 30 nm thick in transverse section.

External to the secondary mitochondrial sheath are rows of equally spaced, helically orientated microtubules (Figures 95 and 96). Adjacent microtubules are spaced at about 7 nm. The secondary mitochondrial sheath and microtubules disappear near the distal tip of the flagellum. Transverse sections close to the end of the flagellum show only the axoneme and a thin layer of periaxonemal mitochondrial sheath (Figure 105). The axoneme loses its "9+2" arrangement at the distal tip of the flagellum (Figure 105).

The helical keel contains electron dense granules

(Figures 101, 102, 103 and 104). Cytochemical staining with PA-TSC-SP, and control sections pre-digested with α, β-diastase, demonstrates that these electron dense granules are glycogen (Figures 101, 102, 103 and 104). The glycogen specific staining provides further evidence that the helical keel is a glycogen helix as has been suggested in other opisthobranchs, but derived from morphological studies lacking the use of cytochemical techniques (Eckelbarger and Eyster, 1981; Healy, 1988a). Only one glycogen helix occurs in Archidoris, Tritonia and Aplysia. Glycogen granules are also detected within the axoneme. However, the glycogen is irregularly arranged both around the central and peripheral doublets (Figures 101, 102, 103 and 104).

At the stage of spermatid nuclear elongation, the centriole attaches to the basal region of the nuclear envelope, resulting in the formation of an indentation called the nuclear fossa (Figures 43, 47, 48 and 52). A centriolar adjunct (terminology from Eckelbarger and Eyster, 1981), which is in close association with the proximal end of the axoneme, occurs at the junction of the axoneme and the electron dense centriolar derivative (terminology from Healy, 1988a) in Archidoris tuberculata and Tritonia plebei. This electron dense centriolar adjunct is a ring-like structure in transverse section and resembles two equilateral triangles in longitudinal section (Figure 47). However, there is no centriolar adjunct in

Aplysia faciata (Figures 52, 53 and 54). The centriolar derivative is cap-shaped, closely located in the nuclear fossa. A typical "9 + 2" microtubular axoneme and its peripheral coarse accessory fibres descends from the centriolar derivative (Figures 47, 50 and 54).

A multivesicular body with structure similar to that described in Spurilla neapolitana by Eckelbarger and Eyster (1981), Eckelbarger (1982) is secreted from the Golgi complex (Figures 55 and 56). This multivesicular body first appears on the concave side of the Golgi complex. A few small vesicles are enveloped by a common external membrane (Figure 56). Later, this multivesicular body is released from the Golgi complex and migrates to the nuclear base in close relation to the centriolar derivative and nucleus (Figures 57 and 58). The external membrane breaks down (Figure 57) and the contained small vesicles are gradually lost. After extensive investigation, I can only demonstrate this multivesicular body in Archidoris tuberculata and Tritonia plebei. The multivesicular body disappears prior to the formation of the centriolar adjunct.

Discussion

(A). The organization of Ovotestis

The anatomy of the reproductive system of opisthobranchs has been extensively studied (for review see Thompson, 1976; Beeman, 1977; Medina et al., 1986b). All opisthobranchs so far investigated possess a single lobulated ovotestis and are simultaneous hermaphrodites. Both female and male germ cells differentiate and develop in the same acinus. However, marked variability in the organization of the ovotestis occurs within the opisthobranchs, even among specimens belonging to the same species (Pruvot-Fol, 1960; Medina et al., 1986b, 1987). The mature ovotestis of Archidoris pseudoargus and Tritonia hombergi has been described by Thompson (1961, 1966). The ovotestis in Archidoris pseudoargus forms a layer overlying the digestive gland. The female compartment opens into the male compartment. This ovotesticular arrangement is very similar to the present finding in Archidoris tuberculata, but apparently different from that in Archidoris montereyensis (McGowan and Pratt, 1954), in which an anterior exclusively male zone and a posterior entirely female area occurs. Medina et al. (1986b, 1987) suggested that the different histological arrangement of the ovotestis is probably due to some extent to the relationship between the ovotestis and the digestive gland. In those groups in which the ovotestis is intimately

associated with the digestive gland (for example, Hypselodoris tricolor; suborder: Doridacea), the ovotestis acini are arranged rather irregularly (Medina et al., 1986b; 1987), probably due to the spatial limitations imposed by the digestive gland. My present observations of ovotesticular organization in species from different suborders, Archidoris tuberculata (Doridacea) show major structural differences from that in Tritonia plebeia (Dendronotacea) and Aplysia faciata (Aplysiomorpha), providing further examples of variance in the segregation of different parts of the gonad producing different germ cells within the opisthobranchs. My observations strengthen the suggestion that further morphological studies of ovotestis structure are required.

(B). Comparative Spermatogenesis

The present study provides the first ultrastructural and cytochemical studies of spermatogenesis of Archidoris tuberculata and Tritonia plebeia. The early stages of spermatogenesis in Aplysia faciata are also described for the first time.

(1). Nutritive cell

Developing spermatogenic cells have been observed in close association with a somatic cell in Archidoris tuberculata, Tritonia plebeia and Aplysia faciata. In previous studies, this cell in nudibranchs has been given a variety of names, for example, "nutritive cells" (Chambers,

1934), a central mass of "plasm" (Franzén, 1955), "nurse cell" (DeVries, 1963) and "accessory cells" (Ekelbarger and Eyster, 1981). Similar cells have also been described in aplysiid ovotestes and have been referred to as "nurse cells" (Thompson and Bebbington, 1969) and "phagocytic cells" (Beeman, 1970b). Thomas (1975) described the occurrence of "supporting cells" between the spermatogonia and basal lamina, but he did not demonstrate the association of late spermatids with this cell. Eckelbarger and Eyster (1981) studied the organization of the ovotestis in a eolid nudibranch Spurilla neapolitana (suborder: Arminacea). The somatic cell, with which developing spermatogenic cells are closely associated, have been termed "accessory cells". The presence of lipid droplets, α- and β-glycogen particles, RER, Golgi complex, lysosome-like bodies, heterophagic vacules and ocytotic vesicles led Eckelbarger and Eyster (1981) to suggest that probably these cells were involved in the digestion of exogenous cellular components and may serve both a nutritive and phagocytic function.

(2). Golgi complex and acrosome formation

Early light and electron microscopical studies on acrosome formation have left little doubt that the acrosome in the mammal is wholly a product of the Golgi complex (Bowen, 1924; Burgos and Fawcett, 1955; Roosen-Runge, 1977) and the involvement of the Golgi complex in the production

of the proacrosome has been documented in examples from a variety of molluscs, for example, Aplacophora (Buckland-Nicks and Chia, 1989), Bivalvia (Longo and Dornfeld, 1967; Kubo, 1977; Popham, 1979; Hodgson and Bernard, 1986; Sousa et al., 1989; Hodgson et al., 1990), Scaphopoda (Hou and Maxwell, 1991), Prosobranchia (Buchland-Nicks and Chia, 1976; Azevedo, 1981; Azevedo et al., 1985), Pulmonata (Jong-Brink et al., 1977; Takaichi and Dan, 1977) and Cephalopoda (Maxwell, 1974a, b, 1975a; Arnold and Williams-Arnold, 1978).

However, the definitive origin of the proacrosomal vesicle in opisthobranchs has been controversial. Previous studies of the process of spermatogensis of opisthobranchs by Thompson and Bebbington (1969, 1970) and Beeman (1970b, 1977) were unable to demonstrate the presence of an acrosome in the spermatozoa of Aplysia depilans, A. faciata, A. punctata (Thompson and Bebbington, 1969, 1970) and Phyllaphsia taylori (Beeman, 1970b, 1977). Later, three published reports concerning the ultrastructure of the acrosome confirmed the existance of an acrosome in Aplysia kurodi (Kubo and Ishikawa, 1981), Spurillar neapolitana (Eckelbarger and Eyster, 1981) and Hypselodoris tricolor (Medina et al., 1985). More recent ultrastructural studies of pyramidellid gastropods (opisthobranchs) (Healy, 1988a) and Phyilippia hybrida (Minniti and D'Andrea, 1989) have also demonstrated an acrosome. This, strengthened by my own findings, allows the suggestion that the acrosome is an

integral component in opisthobranch spermatozoa.

Despite extensive ultrastructural observations of Golgi complex activity in the spermatids of Spurillar neapolitana, Eckelbarger and Eyster (1981) were unable to demonstrate structural association of the Golgi complex with the putative acrosome. When the acrosome becomes apposed to the nuclear surface, the Golgi complex is always found in relation to the centriole. It has not therefore been documented whether the Golgi complex is involved in formation of the acrosome (Eckelbarger and Eyster, 1981). Recent analyses of acrosome formation in Hypselodoris tricolor (Medina et al., 1985) and pyramidellid gastropod (opisthobranchs) (Healy, 1988a) confirm the finding in Spurillar neapolitana (Eckelbarger and Eyster, 1981), that the proacrosome originates at a considerable distance from the zone where the Golgi complex is located. Medina et al. (1985) therefore postulated that some form of membranous system might be established to communicate between the proacrosome and the Golgi complex cisternae. In addition, Healy (1988a) suggested that the proacrosomal granule might be derived from some modified Golgi apparatus. My studies allow me to demonstrate a close structural association of one Golgi complex, and transfer vesicles with the proacrosomal vesicle in the process of acrosome formation in Archidoris tuberculata, Tritonia plebeia and Aplysia faciata. The present study also provides evidence to show that the Golgi complex with its discrete secretion

(proacrosomal granule) becomes located at the apex of the nucleus close to the anterior plaque at the pre-cup stage (Figure 35). Prior to further differentiation of the proacrosome, the Golgi complex then degenerates and eventually disappears.

The mature acrosome in Archidoris tuberculata, Tritonia plebeia and Aplysia faciata consists of an apical vesicle and an acrosomal pedestal. The organization is in agreement with that described in Aplysia kurodai (Kubo and Ishikawa, 1981), pyramidellid gastropods (opisthobranchs) (Healy, 1988a) and Philippia hybrida (Minniti and D'Andrea, 1989), but different from that in Hypselodoris tricolor (Medina et al., 1985) in which an extremely elongate subacrosomal substance (SS) (comparable to acrosomal pedestal) and lamellar component occur in addition to the acrosomal vesicle. Various shaped acrosomal pedestals have also been demonstrated in other pulmonates (Healy and Jamieson, 1989). Medina et al. (1985) suggested that the Golgi complex is not involved in the secretion of the subacrosomal substance in Hypselodoris tricolor due to the fact that this element is not limited by a membrane. On the contrary, Minniti and D'Andrea (1989) argued that the granular material lining one side of the acrosomal vesicle represents the earliest stage of the developing acrosomal pedestal which is derived from the Golgi complex in Philippia. Furthermore, this acrosomal pedestal may be homologous with the basal plate of the acrosomes of meso-

and neogastropod euspermatozoa (Minniti and D'Andrea, 1989). The result obtained in the present study encourages me to agree with Medina and co-workers (1985). I found no indication of the involvement of the Golgi complex in the formation of the acrosomal pedestal, rather I have obtained evidence suggesting that probably the electron dense material at a specific region on the anterior nuclear plaque might contribute to the formation of the acrosomal pedestal. However, the exact origin of this electron dense material at the external surface of the anterior nuclear plaque is still unknown.

The Golgi complex has been demonstrated to produce a variety of secretions during nudibranch spermatogenesis, including one to several multivesicular bodies and membrane-limited electron-dense rods and ring-like structures (Ekelbarger and Eyster, 1981; Eckelbarger, 1982). The multivesicular body described in the present study shows great similarity to that demonstrated in Spurilla neapolitana (Ekelbarger and Eyster, 1981). It is secreted by the Golgi complex and later migrates to the base of the nucleus to form a close association with the centriolar-nucleus junction. However, I did not find any evidence to confirm the occurrence of membrane-limited electron-dense rods and ring-like structures reported in Spurilla neapolitana (Eckelbarger and Eyster, 1981). Healy (1988a) postulated that the close association of a well-developed Golgi complex during midpiece formation indicated

that the Golgi complex itself may be involved in facilitating fusion of mitochondria and therefore contribute to their differentiation during spermatogenesis. In Archidoris tuberculata and Tritonia plebeia, multivesicular bodies are lost prior to the formation of the centriolar adjunct, whereas in Aplysia faciata I have found no evidence for the occurrence of multivesicular bodies. The presence of a multivesicular body in opisthobranch species possessing a centriolar adjunct suggests that the multivesicular body may be involved in the formation of that centriolar adjunct.

(3). Nuclear morphogenesis

A prominent cytological event occurring during nuclear transformation is the formation of anterior and posterior plaques. Electron dense material is deposited on both sides of the nuclear membrane at the anterior plaque, but only on the internal side at the posterior plaque in the spermatid of Archidoris tuberculata, Tritonia plebeia and Aplysia faciata. However, in Aplysia kurodai, electron dense material occurs only on the outer nuclear membrane (Kubo and Ishikawa, 1981). Great structural variation of nuclear plaques occurs in different euthyneuran molluscs. In opisthobranchs, the anterior plaque occurs prior to the posterior plaque (Eckelbarger and Eyster, 1981; Kubo and Ishikawa, 1981; Healy, 1988a; Medina et al., 1986a; and the present study) and electron dense material is deposited on

either both sides of the nuclear envelope or just on the outer nuclear envelope at the anterior plaque. In Archidoris tuberculata, Tritonia plebeia and Aplysia faciata and most reported opisthobranch species, there occurs only an internal layer of electron dense material at the posterior plaque. However, Eckelbarger and Eyster (1981) demonstrated an external layer of electron dense material at the posterior plaque in Spurillar neapolitana. Variation has also been demonstrated in pulmonates, for example, in Euhadra hickonis (Takaichi and Dan, 1977; Dan and Takaichi, 1979), the posterior plaque forms first and the electron dense material of the anterior plaque lies only on the internal aspect of the nuclear envelope. The occurrence of nuclear plaques is common in euthyneuran molluscan seprmatids but their functions are unknown. Medina et al. (1985, 1986a) suggested that formation of the anterior plaque could faciliate the adhesion of the acrosomal complex, whereas the centriolar derivative is attached directly to the nuclear envelope at the posterior plaque. The present study provides evidence to suggest that the electron dense material at the anterior nuclear plaque probably also contributes to the formation of the acrosomal pedestal.

Kubo and Ishikawa (1981) described many tubular structures within the intranuclear space in Aplysia kurodai, which have similarly been demonstrated in Aplysia faciata (the present study). Kubo and Ishikawa (1981)

suggested that these tubules could form a centre during condensation of nuclear chromatin and thus contribute to nuclear shaping. However, the exact role of these tubular structures is still unclear.

The microtubular manchette occurs during the late stage of spermiogenesis in all investigated opisthobranchs (Eckelbarger and Eyster, 1981; Kubo and Ishikawa, 1981; Medina et al., 1986a; Healy, 1988a; the present study). Microtubules become closely associated with the nucleus at the beginning of the elongation stage in the three species. It is the most widely held view that the microtubular manchette associated with the spermatid nucleus plays an extremely important role in the shaping of the nucleus. However, transformation of the spherical spermatid nucleus into a cup shape occurs without the presence of a microtubular manchette. This provides evidence supporting the argument that it is the internal force(s) which shapes the nucleus (Fawcett et al., 1971; Dooher and Bennett, 1973; Hodgson and Bernard, 1988). The exact mechanism of action of the manchette has aroused a considerable controversy and will be further discussed in the **GENERAL DISCUSSION.**

(4). Pseudo-paracrystalline materials and midpiece formation

The process of midpiece formation in euthyneurans has been well established both light microscopically (Franzén, 1955) and ultrastructurally (see reviews by André, 1962;

Maxwell, 1974b, 1983; Baccetti and Afzelius, 1976; Dan and Takaichi, 1979; Healy, 1988a, b). The intracristal bodies first appear at the spermatocyte stage in Archidoris tuberculata, Tritonia plebei and Aplysia faciata. However, these granules appear more electron dense in Aplysia faciata and Archidoris tuberculata. In Tritonia plebei, intracristal bodies are rather electon lucent and are described as flocculent in the present study. These intracristal bodies will mix with the inner membranes and matrix of the mitochondrial sheath later in maturation of the spermatozoa. This is a difference from Spurilla neapolitana where intracristal bodies appear late in spermatogenesis. Kubo and Ishikawa (1981) did not report intracristal bodies during their study of Aplysia kurodai. The fate of the intracristal body in Spurilla neapolitana is also unknown (Eckelbarger and Eyster, 1981). Medina et al. (1988) provided a detailed account of differentiation of the spermatozoan tail in Hypselodoris tricolor. They noted a structural difference between the intracristal bodies of Hypselodoris tricolor and Spurilla neapolitana (Eckelbarger and Eyster, 1981); in Hypselodoris tricolor, in particular, intracristal bodies appeared early at the spermatocyte stage.

My studies of spermatogenesis in Archidoris tuberculata, Tritonia plebeia and Aplysia faciata allow me to demonstrate the occurrence of primary and secondary wrapping phases during mitochondrial differentiation and

midpiece formation. Similar patterns of mitochondrial differentiation and midpiece formation have been described in other opisthobranchs, for example, Spurillar neapolitana (Eckelbarger and Eyster, 1981), Aplysia kurodai (Kubo and Ishikawa, 1981), Hypselodoris tricolor (Medina et al., 1988), pyramidellid gastropods (Healy, 1988a) and Philippia hybrida (Minniti and D'Adrea, 1989). During the secondary wrapping phase, electron dense material, otherwise termed intracristal bodies (Eckelbarger and Eyster, 1981) or "lamellar vesicles" (Medina et al., 1988) accummulates inside the mitochondrial cristae. My study confirms the occurrence of this structure in the mitochondria of Archidoris tuberculata, Tritonia plebei and Aplysia faciata spermatocytes and spermatids. But my detailed analyses of mitochondrial differentiation in three suborders of Opisthobranchia allow me to demonstrate detailed differences of patterns of mitochondrial reorganization not previously suspected in analyses concerning studies of a single species.

At the end of spermatogenesis, mitochondrial cristae and intracristal bodies differentiate into a structure that I term "pseudo-paracrystalline" mitochondrial derivative. André (1962) described a so-called paracrystalline structure in a variety of pulmonate spermatozoa. Further studies by a number of workers suggested that the mitochondrial derivative represented a highly effective form of mitochondria where respiratory enzymes are packed

into crystals (André, 1962; Anderson et al., 1968; Favard and André, 1970; Anderson and Personne, 1976; Maxwell, 1983). The paracrystalline materials in pulmonates are believed to be proteinaceous and consists of networks of hollow rodlets measuring 90 Å in diameter (André, 1962; Personne, 1971). Maxwell (1974b) obtained evidence from freeze-factured spermatozoa of Arion and Lymnea to suggest that the sub-units of the paracrystalline material of pulmonate spermatozoa are quasi-equivalently bonded to each other; both in the same and in the layers immediately above and beneath them. These sub-units of the paracrystalline material assume a helical organization. However, the present study of mitochondrial morphogenesis during spermatogenesis in three opisthobranchs can not demonstrate a clear cut paracrystalline structure comparable to that described in pulmonates. Rather, in longitudinal sections, the mitochondrial derivative forms helical bands spiralling around the axoneme. These bands are 55 - 70 nm thick and membrane bound. In transverse section, the mitochondrial derivative appears flocculent and homogeneous. I am unable to demonstrate any sub-structures within this material. Since these materials have a comparable origin to that paracrystalline material described in pulmonates, I propose to name this mitochondrial derivative "pseudo-paracrystalline" material. A similar arrangement of mitochondrial derivative has also been demonstrated in micrograngphs from studies of Spurilla neapolitana

(Eckelbarger and Eyster, 1981) and pyramidellid gastropods (Healy, 1988a). Healy (1988b) suggested that it is likely that pulmonates have been derived from opisthobranchs. The present comparative studies of mitochondrial transformation in three opisthobranchs provide further evidence to support Healy's proposal in that the highly regularly arranged paracrystalline material in pulmonate spermatozoa might be derived from the less highly ordered "pseudo-paracrystalline" materials in opisthobranch spermatozoa. Clearly, further detailed studies are needed.

(5). Glycogen distribution

The "pseudo-paracrystalline" mitochondrial derivative in Archidoris tuberculata, Tritonia plebeia and Aplysia faciata encloses a helical compartment filled with glycogen (termed glycogen helix in opisthobranchs by Healy, 1988a, b; and major helix in pulmonates by Maxwell, 1980; 1983). Specific staining for glycogen demonstrates that glycogen occurs only in the glycogen helix and axoneme. The pattern of glycogen distribution in Archidoris and Tritonia is very similar that in other opisthobranchs (Thompson, 1973; Eckelbarger and Eyster, 1981; Kubo and Ishikawa, 1981; Healy, 1982a, b; Healy and Willan, 1984; Healy, 1988a, b; Medina et al., 1988; Minniti and D'Adrea, 1989), and also coincides with that in a large number of pulmonates (Personne and André, 1964; Anderson and Personne, 1970; Bayne, 1970; Personne and Anderson, 1970; Personne, 1971;

Thompson, 1973; Maxwell, 1980, 1983; Healy and Jamieson, 1989). Only one glycogen helix occurs in the majority of nudibranchs (Thompson, 1973; Eckelbarger and Eyster, 1981; Healy, 1988b; Medina et al., 1988; Minniti and D'Andrea, 1989; present study). Thompson (1973) and Maxwell (1983) pointed out that there is an apparent reduction of helix number within opisthobranchs, for example, four helices in the spermatozoa of Acteon (Acteonidae, Bullomorpha); two in Aplysia (Aplysiisae, Aplysiomorpha) and one in the majority of nudibranchs. Healy and Willan (1984) also noted that there is a tendency towards a reduction in number of glycogen helices in euthyneuran spermatozoa.

(6). Centriolar adjunct

Thompson (1966) described the detailed organization of the mature spermatozoa of Archidoris pseudoargus and tentatively interpretated the ultrastructural organization of the neck region. Two centrioles (proximal and distal centrioles) and an electron translucent annulus in the spermatozoan neck were described. Medina et al. (1988) compared the spermatozoan centriolar organization of Hypsedoris tricolor with that in Archidoris pseudoargus. Their findings led them to state that Figure 3E in Thompson's paper (1966) cannot be identified in the photographs, suggesting that the previous description given by Thompson (1966) is incorrect. The present study provides further evidence that during the process of spermatogenesis

in Archidoris, Tritonia and Aplysia, there occurs only a single centriole which assumes an electron dense cap shape. This centriolar derivative has been named "basal body" (Medina et al., 1988) or "centriolar derivative" (Healy, 1988a) in other opisthobranchs. I am unable to demonstrate the occurrence of the annulus described in the mature spermatozoon by Thompson (1966). Rather a centriolar adjunct occurs at the junction between the centriolar derivative and the axoneme. The centriolar adjunct has been widely reported during spermiogenesis in pulmonates (Takaichi and Sawada, 1973; Maxwell, 1974b; Yasuzumi et al., 1974; Dan and Takaichi, 1979; Healy and Jamieson, 1989; Griffond et al., 1991), insects and mammals (see reviews by Phillips, 1970; Baccetti and Afzelius, 1976), but only first described in a nudibranch Spurillar neapolitana by Eckelbarger and Eyster only as late as 1981. The centriolar adjunct appears triangular in longitudinal section in the Archidoris tuberculata, Tritonia plebeia and Aplysia faciata developing spermatid and structurally similar to that in Spurillar neapolitana (Eckelbarger and Eyster, 1981). However, the centriolar adjunct is different from the so-called "centriolar adjunct-like" structure in Hypselodoris tricolor (Medina et al., 1988), which forms two transverse electron dense lines in longitudinal section and a ring around the junction of cap-shaped centriolar derivative and axoneme in transverse section. Both the centriolar adjunct and adjunct-like structures degenerate

and disappear during the course of spermiogenesis, suggesting that there is no prominent role for this structure in the mature spermatozoon (Phillips, 1970; Maxwell, 1976; Dan and Takaichi, 1979; Eckelbarger and Eyster, 1981; Healy, 1988a; Medina et al., 1988). Medina et al. (1988) postulated that the centriolar adjunct in the early spermatid stage could serve to attach the axonemal complex to the nucleus and further strengthen the junction between the nucleus, axial complex and mitochondrial sheath. The present studies of Archidoris tuberculata and Tritonia plebei demonstrate that the centriole attaches to the nuclear base prior to formation of the centriolar adjunct. I provide evidence that it is probably the multivesicular body which plays an important role in the formation of the centriolar adjunct.

(7). Systematic considerations

Studies of spermatogenesis and spermatozoan morphology have been demonstrated to be of great value in elucidating systematic relationships in a variety of euthyneuran molluscan groups (see reviews by Baccetti and Afzelius, 1976; Popham, 1979; Maxwell, 1983; Healy, 1988a, b; Minniti and D'Andrea 1989; Hodgson et al., 1990). The present study of spermatogenesis of three opisthobranchs from different families shows some similarity with other opisthobranchs, but also demonstrates distinct differences even from those reported in closely related species, for

example, Aplysia faciata and Aplysia kurodai (Kubo and Ishikawa, 1981) and provides further examples for future comparison. Our knowledge of the diversity of spermatogenesis and spermatozoa within the Opisthobranchia is, however, still patchy. There is a great need for a wide based analysis of spermatogenesis and spermatozoan structure throughout the largest gastropod subclass before any systematic and phylogentic conclusions can be drawn.

CHAPTER IV

DESMOSOME-LIKE JUNCTIONS BETWEEN SERTOLI-SERTOLI AND SERTOLI-GERM CELLS IN THE OVOTESTIS OF *ARION HORTENSIS* (MOLLUSCA: PULMONATA)

Introduction

The functional organization of the ovotestis in pulmonates has been extensively studied. Joosse and Teitz (1969), using light microscopy, described the organization of the ovotestis in Lymnaea stagnalis. Developing male germ cells were shown to be in continuity and in contact with the Sertoli cells. These cells together forming an epithelial layer overlying the basal lamina in the male compartment of the ovotestis. Joosse and Teitz (1969) speculated that Sertoli cells were always in close contact with each other, and therefore divided the lumen of the acinus into a female and male compartment.

Further ultrastructural and physiological evidence has been obtained more recently to provide detailed information concerning the functional basis of this compartmentation in pulmonate gonads. It is now well established that in the pulmonate molluscan ovotestis, male and female germ cells develop within the same acinus and Sertoli cells form a continuous layer overlying the follicular cells which surround the oocyte (Maxwell, 1974b; 1983; Jong-Brink et al., 1976; 1977; 1984; Rigby, 1982; Hou and Maxwell, 1990; Griffond, et al., 1991).

A number of intercellular membranous specializations, including gap junctions, septate junctions and desmosomes have been described between follicle cells and oocytes in a variety of pulmonates during the later part of oocyte

maturation (Anderson, 1974; Jong-Brink et al., 1976; Hill, 1977; Griffond and Gomot, 1979; Saleuddin et al., 1980; Khan and Saleuddin, 1983). It has been suggested that this allows possible development of a microenvironment for optimal growth of the oocyte, perhaps associated with heterocellular communication (Jong-Brink et al., 1976; 1984; Khan and Saleuddin, 1983).

In the male compartment of the pulmonate molluscan ovotestis, all the spermatogenic cells differentiate and develop in close relation to the luminal aspect of the Sertoli cell. Adjacent Sertoli cells are connected by a variety of intercellular junctions, for example, desmosomes, septate junctions, gap junctions, punctate tight junctions (see reviews by Bergmann, Greven and Schindelmeiser, 1984; O'Donovan and Abraham, 1987). Septate junctions have often been described as maintaining a structural barrier which prevents large molecules in the haemolymph from entering the male compartment. This structural barrier has been termed the blood-testis barrier in pulmonates (Jong-Brink et al., 1984; Buckland-Nicks and Chia, 1986; O'Donovan and Abraham, 1987). A desmosome is always seen in close association with the long septate junction at its luminal terminal (Jong-Brink et al., 1984; O'Donovan and Abraham, 1987). Gap junctions, tight junctions and desmosomes occur either between Sertoli cells (Bergmann, Greven and Schindelmeiser, 1984; O'Donovan and Abraham, 1987), or Sertoli and germ cells (Parivar, 1980;

Rigby, 1982).

A variety of electron dense tracers have been employed to study the permeability of inter-Sertoli cellular junctions. However, results obtained are rather inconsistant. Impregnation of the ovotestis with colloidal gold, HRP and lanthanum shows that the basal lamina around the ovotestis acinus hardly forms a barrier, only the larger colloidal gold particles do not pass through this lamina (Jong-Brink et al., 1984; O'Donovan and Abraham, 1987).

Septate junctions occurring between Sertoli cells have been described in a number of molluscs, for example, Lymnaea stagnalis (Jong-Brink et al., 1984; Bergman, Greven and Schindelmeiser, 1984; Anelli et al., 1985), Levantina hierosolyma (O'Donovan and Abraham, 1987) and three marine snails, Fusitriton oregonensis, Ceratostoma foliolatum and Littorina sitkana (Buckland-Nicks and Chia, 1986). In testing for a blood-testis barrier in marine snails, Buckland-Nicks and Chia (1986) obtained evidence to show that the tracer lanthanum was taken up by testicular tissue, became concentrated in the basal aspect of Sertoli cells, but was blocked at the inter-Sertoli septate junction and thus failed to reach the germ cell layer. However, lanthanum also penetrated the septate junction partway, which indicated that the septate junction was an incomplete barrier to the tracer (Buckland-Nicks and Chia, 1986). Bergmann, Greven and Schindelmeiser (1984), on the

contrary, demonstrated that lanthanum tracer penetrated the whole length of septate junctions in a pond snail, Lymnaea stagnalis, but was stopped by tight junctions, indicating that it was the tight junction which formed the blood-testis barrier. This contradicts the previous studies on the nature of the blood-testis barrier (Jong-Brink et al., 1984; Anelli et al., 1985) and also does not substantiate the notion that the septate junction is a structural tight junction. However, Bergman, Greven and Schindelmeiser (1984) suggested that demonstration of intercellular junctions was highly dependent upon the fixation technique employed.

In the mammalian semeniferous tubule, two types of junction have been described between Sertoli cells and germ cells. First, tight junctions forming the inter-Sertoli junction (Flickinger and Fawcett, 1967), believed to maintain the blood-testis barrier (Neaves, 1973; Dym and Fawcett, 1970; Ross, 1977), and the junctional specialization present throughout the last stage of spermiogenesis (Ross, 1976). Second, desmosome-like junctions present between the Sertoli cells and spermatogonia, spermatocytes and non-elongated spermatids (Russell, 1977a) which have been suggested as sites of strong adhesion between Sertoli cells and germ cells (Ross, 1976, 1977; Russell, 1977a, b).

No detailed information concerning the temporal occurrence of junctions between Sertoli and germ cells

during spermatogenesis in pulmonate mollucs has been provided. It is the aim of the present study to examine the structure and function of intercellular junctions in the pulmonate ovotestis and to provide evidence in order to clarify the controversy regarding the blood-testis barrier in these molluscs.

Results

(A). Sertoli-Sertoli Junctions

The ovotestis of Arion hortensis consists of at least 3 lobules (Figure 1). There are many acini within each lobule (Figure 2). Each acinus is surrounded by a complex basement membrane similar to that described in Lymnaea stagnalis (Jong-Brink et al., 1977, 1984). Developing male and female germ cells occur simultaneously within a single acinus (Figures 5 and 6). Sertoli cells form a continuous layer overlying the basal lamina (Figures 3, 4 and 7). The basal lamina is 100 nm thick, and provides direct contact with Sertoli cells on the luminal side. External to the basal lamina is a layer of connective tissue. A single layer of myoepithelial cells envelopes the acinus (Figure 7). All germ cells, including spermatogonia, are located on the luminal aspect of the Sertoli cell surface (Figures 3, 4 and 7). This organization differs considerably from that in the mammalian testicular germinal epithelium.

Sertoli cells form an irregular profile of a low cuboidal epithelium with an oval central nucleus, and numerous processes extending into the acinar lumen (Figure 7). The Sertoli cells form a discrete epithelium, with adjacent cells or cell processes connected by intercellular junctions (Figure 8), rather than occurring as isolated cells scattered over the wall of the acini, as described in Arion ater (Parivar, 1980). Sertoli cell nuclei are

approximately 10μm in diameter, possess punctate heterochromatin and deep nuclear clefts. Their cytoplasm contains large amounts of glycogen granules arranged in β rosettes (Figures 8 and 11), ribosomes, polyribosomes and lipid droplets comparable to the description given for Biomphalaria glabrata (Jong-Brink et al., 1977), A. ater (Parivar, 1980) and Lymnaea stagnalis (Rigby, 1982). Intercellular processes are connected to those of neighbouring cells by a kind of maculae adherens junction (Figure 8 and inset). Careful examination shows that junctions between the bodies of Sertoli cells are rare. Thin sections show that intercellular spaces between Sertoli cells at the junctional sites are discretely narrowed (ranging from 15nm to 25nm) and filled with electron dense material, but the intermediate dense line of a typical desmosome (Farquhar and Palade, 1963) is absent. Cytoplasmic dense plaques are equally developed within each partner in the junction (see Graph). Aggregates of tonofilaments tend to be masked by the electron density of the Sertoli cytoplasm. I suggest that these junctions should be described as desmosome-like since they are structurally identical to similar junctions described in the prosobranch molluscs, Ceratostoma foliolatum, Fusitriton oregonensis and Littoria sitkana (Buckland-Nicks and Chia, 1986) and the rat seminiferous epithelium (Russell, 1977a).

Serial sections and freeze fracture replicas of the

Sertoli cells' surface reveal that these junctions are spot-like with a diameter of 90-180nm. They are scattered on the Sertoli cell surface in groups, ranging from one to ten in each group (Figures 9 and inset).

(B). Sertoli-Germ Cells Junctions

Spermatogonia, spermatocytes and spermatids all differentiate on the luminal aspect of the Sertoli cells. I am unable to confirm the presence of either gap junctions or tight junctions between Sertoli and germ cells such as those described in other molluscs, for example, Lymnaea stagnalis (Rigby, 1982) and Levantina hievosolyma (O'Donovan and Abraham, 1987). The only junctions I am able to demonstrate between Sertoli and germ cells in the ovotestis of Arion hortensis are desmosome-like junctions.

Spermatogonia are ovoid, with a rounded nucleus approximately 6μm in diameter. Ribosomes and large mitochondria are packed within a narrow band of cytoplasm. Spermatogonia are juxtaposed to the surface of the Sertoli cell. The intercellular space is discrete at the junctional site and the intermediate dense line is lacking (Figures 10 and inset).

Spermatocytes have a rounded nucleus approximately 8 μm in diameter. The cytoplasm is more extensive with large numbers of mitochondria and Golgi apparatus (Figure 11). Spermatocytes are closely associated with the cytoplasmic processes of Sertoli cells where desmosome-like junctions

occur (Figures 11 and inset). The cytoplasmic plaques are equally developed on both sides at the junctional site. Although this is comparable to the structure described in Lymnaea stagnalis (Rigby, 1982) and which she termed a tight junction, I can demonstrate a clear intercellular space between the apposed plasmalemma of the junction (Figure 11 inset) and therefore suggest that it is desmosome-like, rather than a tight junction.

Sertoli-germ cell desmosome-like junctions are perhaps best developed in relation to spermatogonia, spermatocytes and early spermatids. The spermatids undergo marked changes of shape during spermiogenesis (Maxwell, 1983). The head of early spermatids is enveloped by the Sertoli cell and numerous desmosome-like junctions occur in this region. Their structure is very similar to that described in relation to spermatocytes (Figure 12), although in maturing spermatids structural changes appear (Figure 13). The electron dense plaque is now more pronounced on the Sertoli side of the junction. On the germ cell side (Figures 13 and inset) the cytoplasmic density is reduced (see Graph). Further reduction occurs as the germ cell continues its differentiation, but the localization of these junctions to the area adjacent to the developing head is maintained throughout spermatid maturation (Figures 14 and 15).

Following nuclear condensation, at a stage that I shall describe as the late spermatid, that is prior to

Graph: Variations of the electron-dense plaque of desmosome-like junction during male germ cell development

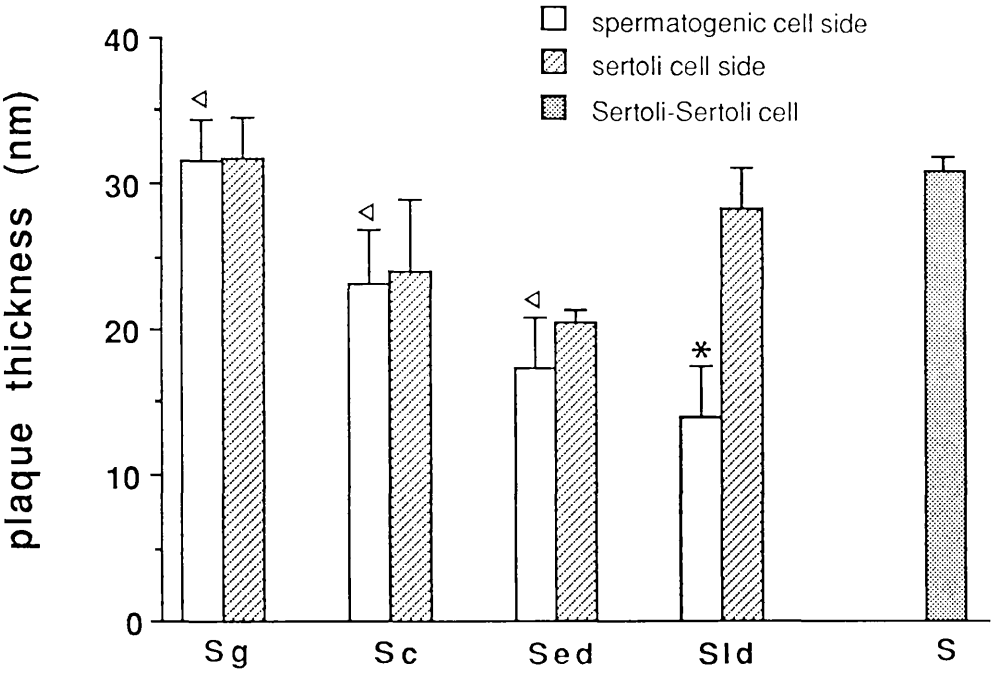

*: significant decrease of plaque thickness compared to that on the Sertoli cell side ($p < 0.01$) ANOVA.

◁: no significant difference ($p > 0.05$).

Sg, spermatogonium
Sc, spermatocyte
Sed, early spermatid
Sld, elongate spermatid
S, Sertoli cell

spermiation, there is at first a marked loss of electron density of the electron dense plaque on the spermatid side of the junction (Figures 15 and inset), and later a numerical loss of junctions, until they are absent at the time of spermiation. During this period of loss of desmosome-like junctions, numerous finger-like processes develop on the luminal aspect of the Sertoli cell and lie in close relation to the head of the spermatozoon (Figures 15, 16, 17, 18, 19 and 20). Micrographs number 16 to 18, and 19, 20 are serial thin sections through the heads of two spermatozoa, showing the finger-like processes and spermiation.

(C). Fixation with Hypertonic Solutions

(1). Junctions between Sertoli and germ cells

In the Arion hortensis ovotestis, fixative containing 3% glucose (755mOsM) shows perfect relationships of cells within acini. In contrast, the addition of 10% or 15% dextrose results in a prominent shrinkage of cells and the exaggeration of intercellular spaces (Figure 21). When 15% dextrose is added to the fixative (1404mOsM) all cell cytoplasm within the Arion hortensis ovotestis is highly condensed and the intercellular space is greatly enlarged. The germ cells remain in contact with the Sertoli cells only at the desmosome-like junctions (Figure 22). Because of the strong shrinkage forces between cells, small

cytoplasmic fragments of Sertoli cell and spermatocyte are often separated from their cell body. Careful examination of these fragments shows that they are attached by desmosome-like junctions (Figures 22 and inset). This demonstrates that the desmosome-like junctions provide strong adhesive sites between Sertoli cells and germ cells.

(2). Junctions between Sertoli cells

A number of inter-Sertoli junctions occur between adjacent Sertoli cells. Towards the luminal side of the acinus, Sertoli cytoplasmic processes are connected by a desmosome-like junction and a long septate junction (Figures 8 and 23). Septate junctions measure 600 - 650 nm in length, with an intercellular space at 40 nm. Electron dense septal bars measure about 9 nm in width. Punctate tight junctions occur between desmosome-like junctions and septate junctions, whereas gap junctions are found near the basal lamina and more distal to the acinar lumen than the septate junction (Figures 8 and 23). These junctions are frequently seen in close association with a desmosome-like junction (Figures 8, 23 and insets), and they strongly bind adjacent Sertoli cells together so that the discrete Sertoli cell layer is virtually undisrupted by a hypertonic fixative solution (Figure 23). However, the basal lamina appears highly folded due to shrinkage of the acinus.

(D). Permeability of Inter-Sertoli Junctions in the Male Compartment

When lanthanum is applied to the ovotestis, it penetrates the acinus wall rapidly and appears in the acinar lumen around the developing germ cells (Figures 24-30). However, HRP can only cross the basal lamina, enter a short distance into the basal part of the inter-Sertoli space. It is stopped by the inter-Sertoli septate junction (Figures 31-35). Ferritin, with a particle size larger than lanthanum and HRP, penetrates between the myoepithelial layer and the basal lamina. Some of the Ferritin particles appear bound to the external surface of the myoepithelial cells and some trapped in the space between the myoepithelial layer and basal lamina (Figures 36 and 37).

These results were obtained under the condition that the ovotestis was incubated in fixatives containing the same amount of tracers (5%) and treated for an equal time (1 or 1.5 hours). I further increased the time of incubation in HRP and Ferritin to 2 and 3 hours. However, I was still unable to detect any HRP crossing the septate junction into the lumen and Ferritin in the inter-Sertoli spaces.

Discussion

(A). Desmosome-like Junction

Desmosome-like junctions, often containing an intermediate dense line, occur between Sertoli and germ cells within the rat testis (Russell, 1977a). They are best developed between the pachytene spermatocyte and Sertoli cell at a level just adluminal to the Sertoli-Sertoli occluding junctions. There is a greater development of the electron dense plaque on the Sertoli side of the junction. Russell (1977a) also showed that the form of this junction varied in relation to different developmental stages of the associated germ cells with, at first, a gradual loss of subsurface density on the Sertoli side of the junction and, later, loss of the intermediate dense line. The last developmental stage at which these junctions occur is the non-elongate spermatid.

In Arion hortensis there are a number of differences compared with the rat in the structure and relations of desmosome-like junctions between Sertoli cells and the germ cells. First, there is no intermediate dense line at the junctional site. This has been described as being poorly represented in the rat (Russell, 1977a). In contrast, I observed electron dense filaments bridging the adjacent plasmalemmae in Arion hortensis. Second, desmosome-like junctions are present throughout a greater number of

developmental stages of the germ cells; i.e. from spermatogonia to spermatids just prior to spermiation. Third, there are changes in the relationships of the components of these junctions as the germ cells develop. In particular there is an equal development of the spermatocyte and Sertoli cell subsurface density; rather than a greater electron density on the Sertoli side of the junction as described in the rat (Russell, 1977a). The subsurface density on the maturing spermatid side is then reduced until final loss just prior to spermiation. In the rat, desmosome-like junctions are lost prior to spermatid elongation but also occur in association with Sertoli junctional specialisations (Fawcett, 1975; Ross and Dobler, 1975). Russell (1977a) suggested that the continued presence of desmosome-like junctions did not allow for shaping and/or movement of spermatids within the seminiferous epithelium. In A. hortensis, however, there is no development of junctions comparable to the Sertoli junctional specialisation. Rather only desmosome-like junctions occur between Sertoli and germ cells until spermiation. I note that the desmosome-like junctions are most numerous in relation to the developing head. The presence of desmosome-like junctions throughout the period of change in nuclear form in spermatids of Arion hortensis shows that they do not preclude spermatid elongation or spiralization but probably serve as attachment sites for the spermatids to the luminal surface of the Sertoli cells.

The fact that these junctions are only lost at the time of spermiation lends further support to this argument. In addition no structures comparable to the tubulobulbar complexes (Russell and Clermont, 1976) present between germ and Sertoli cells of mammals occur in Arion hortensis. I have demonstrated that desmosome-like junctions are the only form of attachment device present throughout the differentiation and development of the male gamete in Arion hortensis. In addition I suggest that they allow complex changes in nuclear form in the final stages of spermiogenesis instead of being lost before these changes take place; as have been documented in the rat (Russell, 1977a).

The present study provides evidence to demonstrate that desmosome-like junctions between adjacent Sertoli cells occur in Arion hortensis on the luminal side of the long, laterally interconnected septate junctions. Both junctions form a strong adhesive structural barrier which possibly maintains the microenvironment within the acinus.

In addition use of freeze-fracture allows me to demonstrate that desmosome-like junctions are numerous between Sertoli cell and germ cells, forming groups of one to ten junctions.

Use of hypertonic fixative solutions results in marked shrinkage of all cells within the testis (ovotestis), with widening of the intercellular spaces. In mammals this cell separation artefact (Russell, 1977a) led

to the suggestion that desmosome-like junctions provide a stable attachment between Sertoli cells and germ cells. In Arion hortensis, this technique was useful in demonstration of the integrity of the junctions. The germ cells were widely separated from Sertoli cells except where desmosome-like junctions were present. This enlargement of the intercellular space did not disrupt the desmosome-like junctions, indicating that the junctions provide strong intercellular adhesion.

The classical description of desmosome structure in mammals was given by Farquhar and Palade (1963). A conspicuous component of the desmosome is the intermediate dense line which lies centrally in the intercellular space within the junction. In the Arion hortensis ovotestis the intermediate line is absent. However, there are parallels with the organisation of the mammalian desmosome in that this junction is spot- or plaque-like, differing from the tight junction (zonula occludens) and zonula adherens. In the ovotestis of Arion hortensis it is clear that the desmosome-like junction is neither a typical desmosome nor a tight junction, as has been reported in the ovotestis of Arion ater (Parivar, 1980) and Lymnaea stagnalis (Rigby, 1982). Desmosome-like junctions between Sertoli cells have been described in the testes of prosobranch molluscs by Buckland-Nicks and Chia (1986). I can now demonstrate the occurrence of these junctions between Sertoli and germ cells within the pulmonate molluscan ovotestis.

In conclusion, desmosome-like junctions in the ovotestis of Arion hortensis are present between Sertoli cells and germ cells throughout spermatogenesis and probably provide strong attachment sites. The electron density of the plaques of the junction varies during the developmental stages of the germ cells and the close relation of the junctions with the developing head suggests that desmosome-like junctions do not preclude changes in the shape of the developing head of the spermatozoon, contrary to that suggestion made in mammals (Russell, 1977a).

(B). Permeability of Inter-Sertoli Junctions

The mammalian testis shows a distinct compartmention in the seminiferous epithelium. This compartmentation has been demonstrated physiologically (see reviews by Setchell and Waites, 1975; Waites and Gladwell, 1982) and morphologically by means of electron dense tracers and freeze-fracture techniques (see reviews by Fawcett, 1975; Setchell, 1980; Waites and Gladwell, 1982; Bergmann, Greven and Schindelmeiser, 1984). Inter-Sertoli tight junctions in the seminiferous tubules of mammals have been demonstrated to be the structural basis of this compartmentation which divides the seminiferous epithelium into a basal "open" compartment and an adluminal "tight" compartment (Bawa, 1963; Brökelmann, 1963; Dym and Fawcett, 1970; Fawcett, 1975; Fawcett et al., 1970; Ross, 1976).

Russell (1977b) demonstrated the transient break-down in the mammalian testis of the junctional specialization to permit the passage of spermatocytes from the basal to the adluminal compartment. Camatini et al. (1982) further substantiated this finding in the testes of monkeys (Cercopitheus aetiops) with freeze-facture and tracer studies. This transient breakdown is faciliated by the plasminogen activator (Lacroix et al., 1977).

The blood-testis barrier in the rat first appears in the postnatal rat between 16 and 19 days when occluding junctions between Sertoli cells apppear and a lumen develops in the centre of the seminiferous cord. Once formed, the tight junction between Sertoli cells is able to resist the effects of experimental cryptorchidism (Hagenäs et al., 1977), gonadotropin supression (Chemes et al., 1979), heat (Gladwell, 1977), osmotic shock (Everett and Simmons, 1958) and a wide range of drugs (Vitale et al., 1973). In mammals, the blood-testis barrier also constitutes an effective immunological barrier (Johnson and Setchel, 1968; Johnson, 1970; 1973; O'Rand and Romrell, 1977; Tung and Fritz, 1978; Pelletier et al., 1981).

In other vertebrates, a distinct compartmentation have also been demonstrated, for example, teleosts (Billard, 1970; Abraham et al., 1980), amphibians (Franchi et al., 1982; Bergmann et al., 1983; Cavicchia and Moviglia, 1983), reptiles (Baccetti et al., 1983; Bergmann, Schindelmeiser and Greven, 1984) and birds (Cooksey and

Rothwell, 1973; Setchell and Waites, 1975; Osman et al., 1980; Bergmann and Schindelmeiser, 1987; Pelletier, 1990). Inter-Sertoli tight junctions are generally accepted to be the structural basis of the compartmentation in these vertebrates. The tightness of a junction has been suggested to be related to the number of its strands, visualized in freeze-fracture replicas, (Claude and Goodenough, 1973; Pricam et al., 1974; Wade and Karnovsky, 1974; Claude, 1978; Easter et al., 1983; Madara and Dharmsathaphorn, 1985). The higher the number of strands, the higher would be the transepithelial resistance. However, in the mink (Mustela vison), a seasonal breeder, during the testicular regression period, inter-Sertoli junctions composed of numerous strands were permeable to tracers (Pelletier, 1988), whereas in the duck, during the same period, the number of strands was considerably reduced, but remain impermeable (Pelletier, 1990). It was therefore suggested that inter-Sertoli junctions were more a selective barrier, rather than an impervious seal (Setchell and Waites, 1975; Setchell, 1980; Setchell and Brooks, 1988; Pelletier, 1990).

In invertebrates, septate junctions have been described as an effective barrier, for example, in nematodes (Marcaillou and Szöllösi, 1980), molluscs (Bergman, Greven and Schindelmeiser, 1984; Jong-Brink et al., 1984; Anelli et al., 1985; Buckland-Nicks and Chia, 1986; O'Donovan and Abraham, 1987), and insects (Marcaillou

and Szöllösi, 1975; Szöllösi and Marcaillou, 1977; Jones, 1978). The present study employing electron opaque tracers with different particle sizes shows that the basal lamina does not form a barrier to small particles such as lanthanum and HRP. Only Ferritin particles were retarded by the basal lamina. In Lymnaea stagnalis (Jong-Brink et al., 1984) and Viviparus viviparus (Griffond and Gomot, 1979), both freshwater species, HRP crossed the basal lamina, whereas in terrestial pulmonates, for example, Agriolimax reticulatus (Hill, 1977) and Levantina hierosolyma (O'Donovan and Abraham, 1987), HRP were barred from the acinus basal lamina. Differences in the thickness of the basal lamina range from 7-18 nm in Lymnaea stagnalis (Jong-Brink et al., 1984) to 100-120 nm in Levantina hierosolyma (O'Donovan and Abraham, 1987), Helix aspersa (Guyard, 1971) and Arion hortensis (present study). O'Donovan and Abraham (1987) proposed that the significance of this difference in size and tightness of the basal lamina was not intrinsic in maintaining a barrier, rather, probably more related to osmoregulation. Results derived from the present study on the terrestial pulmonate, Arion hortensis, agree with the view that the basal lamina only forms a primary barrier to large molecules and the septate junctions between adjacent Sertoli cells constitute a barrier to smaller particles.

GENERAL DISCUSSION

GENERAL DISCUSSION

Specific details concerning the spermatozoon and spermatogenesis have been fully discussed in the section **Discussion** of each chapter. However, there are two additional general aspects worth comment. These will be discussed in this section.

(A). The Microtubular Manchette And Nuclear Shaping

The microtubular manchette which occurs in spermatids during spermiogenesis in a large number of animal species has been suggested as a major motive force which shapes the spermatid nucleus, and thus influences the morphology of the sperm head.

The shaping of the sperm head is a very precise and intricate process that usually occurs during development of the late spermatid. Although there is abundent evidence based upon studies of metazoa that several factors are involved in the determination of the specific shape of the sperm head, the mechanisms responsible for the morphogenesis of the sperm head are still not known (Cole et al., 1988, Meistrich et al., 1990). Up to now, based upon ultrastructural studies, several potential mechanisms have been suggested to elucidate the possible course of nuclear shaping. It is considered that the following factors may be involved:

(1). The microtubular manchette (Clarke, 1967; McIntosh and Porter, 1967; Kessel, 1970; Baccetti and Afzelius, 1976; Wolosewick and Bryan, 1977; Arnold and Williams-Arnold, 1978; Maxwell, 1983; Cherry and Hsu, 1984; Cole et al., 1988; Afzelius et al., 1989; Meistrich et al.,1990).

(2) The aggregation of DNA-neucleoprotein complex within the nucleus (Fawcett et al., 1971; Phillips, 1974), and the location of chromosomes to specific regions on the nuclear envelope (Dooher and Bennett, 1973).

(3) Cytoskeletal elements (filamentous actin) in the subacrosomal space and post-acrosomal region of the sperm head and midpiece of early elongating spermatids (Clarke, et al., 1982; Welch and O'Rand, 1985; Afzelius et al., 1989).

(4) the ectoplasmic actinous filaments of Sertoli cells, known as the mantle (Flickinger and Fawcett, 1967; Russell, 1977a; Vogl and Soucy, 1985).

It has been repeatedly suggested in the literature that the microtubular manchette is the major force which shapes the spermatid nucleus (Dooher and Bennett, 1973; Butler and Gabri, 1984; Okamura and Nishiyama, 1976; McIntosh and Porter, 1967; Maxwell, 1983). These microtubules (MTS) of manchette may be one or a number of units wide and form a transient ensheathing ring which surrounds the posterior third of the spermatid nucleus in

mammals (Fawcett et al., 1971; Rattner and Brinkley, 1972; Dooher and Bennett, 1973) or forms, initially, a low-pitch circumferential helix around the nucleus, and later, a high-pitch helix as nuclear elongation proceeds in, for example, the domestic fowl and lizards (Clark, 1967; McIntosh and Porter, 1967; Butler and Gabri, 1984). In invertebrates, this microtubular manchette occurs in the modified type of spermatozoa during late spermiogenesis (see review Adiyodi and Adiyodi, 1983) and is oriented parallel to the elongating nucleus (Anderson, 1967; Phillips, 1970; Fawcett et al., 1971; Baccetti and Afzelius, 1976; Maxwell, 1983).

A novel finding in this study is the demonstration of a microtubular manchette in close association with the developing acrosome during spermiogenesis in Rossia macrosoma (Decapoda). These microtubules are not present in sperm collected from the vas deferens. I therefore suggest that the microtubular manchette is also involved in development of the elongate acrosome of the R. macrosoma spermatozoon.

Connections between microtubules, between microtubules and the nuclear envelope (Maxwell, 1983; Meistrich et al., 1990; personnal observations) and the peripherial chromatin fibres of the nucleus (Arnold and Williams-Arnold, 1978) have been demonstrated. These topographical relationships of the manchette to the nucleus have led several workers to suggest that these microtubules

exert forces on the nuclear envelope. Sterile mutants of Drosophila, which lack microtubules around the nucleus, show chromatin condensation but the nucleus remains rounded (Shoup, 1967). Recent studies on the azh/azh mutant mouse (Cole et al., 1988; Meistrich et al., 1990) revealed that abnormal positioning of the microtubular manchette in the spermatid results in a deformation of the shape of the nucleus. Furthermore, observations in the normal mouse, where the manchette appears just before the onset of nuclear condensation and remains associated with it during normal morphogensis but disappears soon after the nucleus has attained its definitive form, lend further support to the suggestion that the manchette is playing a "moulding" or supportive role during nuclear morphogenesis (Rattner and Brinkley 1972; Maxwell 1983; Butler and Gabri, 1984; Meistrich et al., 1990).

To further test these hypotheses, anti-microtubule drugs, e.g. cholchicine, were applied in vivo to the ovotestis of a pulmonate mollusc Arion hortensis (Maxwell, 1983). Preliminary observations did show that the sperm head did not assume a helical form after elongation.

Antitubulin immunofluorescence labelling of the manchette (Cherry and Hsu, 1984; Cole et al., 1988) provides a greater specificity and visulization of its 3-dimentional structure in mammals. Afzelius et al. (1989) provides an excellent account of an immunofluorence study of α-tubulin and actin microfilaments (RH-Ph staining) in a

mesogastropod Melanopsis dufouri etrusca. A large amount of α-tubulin is found around the nuclear and mitochondrial region. Most of the actin filaments occur in the subacrosomal space, in the perinuclear and the mitochondrial regions. This initial study make it technically feasible in the future studies to examine drug induced abnormal morphogenesis of sperm head development during spermiogenesis.

However, the suggested sperm head shaping mechanism described above has been challenged by those workers who believe that intrinsic genetic control of DNA-nucleoprotein aggregation directly influences the process of chromatin condensation (Fawcett et al., 1971). Fawcett et al. (1971) critically reviewed the suggestion that the manchette could actually generate forces to shape the nucleus in vertebrates (Clark, 1967; McIntosh and Porter, 1967) and large number of invertebrates (Shoup, 1967; Kessel, 1970). Fawcett et al. (1971) suggested that microtubules may be essential for the redistribution of cytoplasm that takes place during spermatid elongation but that they are probably not directly involved in shaping of the nucleus.

In decapods (Maxwell, 1975a), widely spaced microtubules become closely apposed only near the completion of chromatin condensation. In all examples of the primitive type of spermatozoa (Franzén, 1983; Buckland-Nicks and Chia, 1989; Hodgson et al., 1988; Hodgson et al.,

1990; Hou and Maxwell, 1991), no microtubular manchette occurs during spermiogenesis (Baccetti and Afzelius, 1976; Adiyodi and Adiyodi, 1983; and this study). However, despite this, the nuclei of the spermatids of some animals transform dramatically from a spherical to an elongate shape. Furthermore, during the early stage of spermiogenesis in the modified type of spermatozoa, particularly in the opisthobranchs and pulmonates, there is a stage when the spermatid nucleus transforms from a spherical into an inverted cup shape (see Chapter III). This morphogenic process occurs without the presence of a microtubular manchette. What internal and external forces shape the nucleus are not clear (Maxwell, 1983; Hodgson and Bernard, 1988).

In the spermatids of some Annelida (Donin and Lanzacecchia, 1974; Webster and Richards 1977) and Opisthobranchia (e.g. Aplysia, Kubo and Ishikawa, 1981; the present study) a noteable tubular substructure occurs within the nucleus during the stage of spermatid elongation and chromatin condensation. This spiral substructure might be an internal frame for chromatin condensation.

The structure of molluscan spermatozoa, the modified type in particular, presents such a species-specific variety (Thompson, 1973; Baccetti and Afzelius, 1976; Maxwell, 1983; the present study) that my studies on spermatogenesis in examples from opisthobranch, decapod and scaphopod molluscs convinces me that spermatid nuclear

morphogenesis may be controlled by a number of factors. The manchette always appears in close association with the onset of chromatin condensation and elongation. Tannic acid containing fixation preserved spermatids clearly demonstrate that microtubules in the manchette are highly organized and linked by cross bridges (comparable to structures described in mouse spermatids, Wolosewick and Bryan, 1977). These arrays of microtubules concomitantly assume a 3-dimensional organization which mimics that of the nucleus.

In addition, in my study on the ovotestis of a pulmonate mollusc, Arion hortensis, I have described the temporal occurrence of desmosome-like junctions between Sertoli and developing germ cells (Hou and Maxwell, 1990), showing that unlike the Sertoli junctional specializations and desmosome-like junctions in the rat (Fawcett, 1975; Ross and Dobler, 1975; Russell, 1977b), this form of junction between Sertoli and germ cells in the ovotestis of Arion hortensis is present throughout spermatogenesis. I therefore suggest that the desmosome-like junction does not preclude sperm head shaping, as originally suggested by Russell (1977a). More information is needed to demonstrate whether, either internal forces within the nucleus or external forces mediated by (i) the microtubular manchette; (ii) cytoplasmic filaments within the developinmg spermatid and (iii) forces induced by Sertoli cells contribute to head shaping either individually or in conbination.

(B). "Sertoli Cell" in Molluscan Gonads — Its Structure and Function

Developing spermatogenic cells in a variety of molluscan groups have been demonstrated in close association with a somatic cell within the male germinal epithelium. Published examples include: bivalves (Sousa et al., 1989; Eckelbarger et al., 1990), prosobranchs (except Archaeogastropoda) (Buckland-Nicks and Chia, 1986), pulmonates (Jong-Brink et al., 1977, 1981, 1984; Parivar, 1980; Rigby, 1982; Bergman et al., 1984; Hou and Maxwell, 1990; Griffond et al., 1991), Opisthobranchs (Chambers, 1934; Eckelbarger and Eyster, 1981; the present study) and cephalopods (Arnold and Williams-Arnold, 1978). Numerous terms have been ascribed to this type of cell in the male compartment, for example, "accessory cell" (Eckelbarger and Eyster, 1981; Eckelbarger et al., 1990; the present study), "basal cells" (Sachwatkin, 1920; Woodard, 1940); "nurse cells" (Reinke, 1912), "free cells" (Nishiwaki, 1964), "nutritive cells" (Yasuzumi et al., 1960; Yasuzumi, 1974), "support cells" (Sousa et al., 1989), "pleomorphic follicle cells" (Eckelbarger et al.,1990) and "Sertoli cells" (Jong-Brink et al., 1977, 1981, 1984; Parivar, 1980; Bergmann et al., 1984; Buckland-Nicks and Chia, 1986; Hou and Maxwell, 1990).

Limited ultrastructural, cytochemical and physiological studies of prosobranchs and pulmonates (see Jong-Brink et al., 1977, 1981, 1984; Buckland-Nicks and

Chia, 1986; Hou and Maxwell, 1990) have revealed that this type of somatic cell is structurally and functionally similar to the Sertoli cell (named after Sertoli, 1865) described in the mammalian seminiferous epithelium (see reviews by Fawcett, 1975; Waites and Gladwell, 1982). To simplify the terminology, the term "Sertoli cell" has since been widely accepted and used in studies of prosobranchs, pulmonates and cephalopods (Roosen-Runge, 1977; Arnold, 1978; Parivar, 1980, 1981; Rigby, 1982; Maxwell, 1983; Griffond et al., 1991; Hodgson et al., 1991). However, in the cases of the opisthobranchs and bivalves, the structure and function of the nongerminal cells within the germinal epithelium have been poorly documented. Ecklebarger and co-workers (1981, 1990) suggested that the highly specialized functions and characteristic ultrastructural features (Fawcett, 1975) of Sertoli cells in vertebrates may not be homologous in opisthobranchs and bivalves. The term "Sertoli cells" should, therefore, be used cautiously in conjunction with opisthobranch and bivalve gonads. Eckelbarger and colleagus felt that "follicle cells" or "accessory nutritive cells" would be most appropriate. In the present investigation of three opisthobranchs, without further functional evidence, it would only be safe to name the somatic cells in the germinal epithelium "accessory cells".

The Sertoli cell in male dioecious prosobranchs has been suggested to be related to the production of different

types of sperm. Developing eupyrene (typical) spermatids are enveloped by the elongated Sertoli cell cytoplasmic process (termed pseudopodia in the pond snail Cipangulopaludina malleata by Yasuzumi et al., 1960). These pseudopodia have been suggested to form a conducting system for nutritive supply from Sertoli cells to the developing eupyrene spermatids. However, apyrene (atypical) spermatids, which occur widely in meso- and neogastropods (Giusti and Selmi, 1982; Healy, 1982b, 1986, 1988a; Afzelius et al., 1989), are only lodged in a deep indentation of the Sertoli cell surface without being surrounded by pseudopodia (Yasuzumi et al., 1960). It is also interesting to note that the occurrence of somatic cells in the male germinal epithelium is always associated with the production of the modified type of fertilizing spermatozoon. Published information demonstrates that in those molluscan groups where the primitive type of spermatozoa occur, i.e. Aplacophora, Polyplacophora, most of the Bivalvia, Scaphopoda and Archaeogastropoda, there is no occurrence of somatic supporting cells in the germinal epithelium. On the contrary, in those groups, i.e. some of the Bivalvia (e.g. Galeommatoidea, Ekelbarger et al., 1990 and Scrobicularia plana, Sousa et al., 1989), Prosobranchia (except Archaeogastropoda), Opisthobranchia, Pulmonata and Cephalopoda, somatic cells always occur in association with the production of the modified type of spermatozoa. In the present study of the ovotestis of the pulmonate Arion

hortenesis, a large number of finger-like Sertoli cell cytoplasmic processes have also been described at the late stage of spermiogenesis and suggested to be involved in spermiation (Hou and Maxwell, 1990). These finger-like process may be homologous to the pseudopodia in the prosobranchs.

The presence of large amounts of glycogen in Sertoli cells suggests that they provide nutrition to developing spermatogenic cells (Jong-Brink et al.,1977). At the end of the spermatogenic cycle in pulmonates, the Sertoli cell dies and is subsequently replaced (Jong-Brink et al., 1977). Jong-Brink et al. (1977) demonstrate that glycogen deposition within the Sertoli cell declines as its associated spermatogenic cells mature. Parivar (1980) provides evidence to demonstrate that the Sertoli cell differentiates before and after spermiation in Arion ater, but he did not mention any quantitive changes of glycogen content. If indeed the Sertoli cell provides "nutrition" to associated spermatogenic cells, it may be expected that there should be a correlation between the glycogen content within the Seroli cell and stages of spermatogenesis. Maxwell (1980) made the first attempt to quantitively characterise glycogen deposition in the euthyneuran sperm tail. A non-liner disposition of glycogen is demonstrated and about 90% of the glycogen is present in the posterior 75% of the sperm length in Arion hortensis (Maxwell, 1980). This raises a further question about how glycogen is

transferred from the Sertoli cell to the developing spermatogenic cells, and its catabolism within the spermatozoon. Further investigation is required.

Several other functions of Sertoli cells have been described, for example, phagocytosis, secretion of steroid hormones, involvement in spermiation and maintainance of the blood-testis barrier (Jong-Brink et al., 1977, 1981, 1984; Buckland-Nicks and Chia, 1986). Among these, maintaining the blood-testis barrier is perhaps the most important characteristic of Sertoli cells. It provides a mechanism by which the environment of the male germ cells can be regulated (Buckland-Nicks and Chia, 1986). Jong-Brink et al. (1984) studied the physiological properties of the blood-testis barrier in a freshwater pulmonate Lymnaea stagnalis, using the micropuncture technique. Samples of blood and gonadal fluid from the male compartment were collected and the osmolarity, protein content and ionic and amino acid composition of these fluids were measured. Gonadal fluid differed in many respects from the haemolymph, not only in the content of organic materials such as proteins and amino acids, but also in the concentrations of ions, for example, Na^{+}, Ca^{++}, Mg^{++} and K^{+}, resulting in a high osmolarity. Jong-Brink et al. (1984) suggested that the high concentration of K^{+} in gonadal fluid of Lymnaea stagnalis might be responsible for the induction and/or maintainance of motility of spermatozoa (in Lymnaea stagnalis, spermatozoa appear

already motile within the acinus, Jong-Brink et al., 1984). In addition the high osmolarity of the gonadal fluid will attract water and thus either induce a positive transmural pressure to maintain the fluid architecture of the gonadal system, and /or induce a water current, beneficial for the transport of sperm and oocytes. An increase of this influx, for example, by hormonal action, might contribute to the process of spermiation and ovulation.

There is evidence in insects that certain hormones are involved in the regulation of the formation of the blood-testis barrier (Jones, 1978). The establishment of a blood-testis barrier in Schistocerca gregaria is altered by treatment in vitro with ecdysterone, which stimulates the formation of the inter-Sertoli cellular junctions (Jones, 1978). This effect is antagonized by juvenile hormones. The balance of these hormones may be critical for the formation of the barrier and the subsequent onset of meiosis (Jones, 1978).

Although, it is now well known that pulmonate molluscan reproduction is under control of the nervous system (see reviews: Saleuddin et al., 1980; Joosse, 1988; Takeda, 1989), information is still lacking concerning the hormonal regulation of the establishment of the blood-testis barrier in molluscs.

As suggested by Setchell (1980), the term blood-testis barrier is somewhat misleading. In the mammalian seminiferous tubule, the effective barrier separates the

luminal contents of the seminiferous tubule from the peripheral fluid and not from the blood. Originally, Marcaillou and Szöllösi (1980) suggested that the term "blood-testis barrier" should be used even in the case of Mollusca. Abraham et al. (1980), working on fish, argued that the barrier is not between the blood and the testis as a whole. He therefore proposed the term "blood-male gonocyte barrier". Furthermore, O'Donovan and Abraham (1987) suggested that in the Platyhelminthes, the term "somatic tissue-male germ cell barrier" would be most suitable, since there is no blood in these animals. They thus proposed to apply this term to embrace animals without a circulatory system. In the present investigation of the pulmonate mollusc Arion hortensis, a barrier is established between haemolymph and spermatogenic cells in the male compartment. According to the rule of O'Donovan and Abraham (1987), a term like "haemolyph-male germ cell barrier" seems accurate, but it would not adequately describe the situation in other molluscan groups, for example, cephalopods, in which the blood is contained in a closed circulatory system. I therefore agree with Marcaillou and Szöllösi (1980) that to avoid further confusion, the term "blood-testis" barrier should be used in reference to molluscs.

In conclusion, the present studies of male germ cell differentiation and development in a variety of molluscs (see Chapters I, II, III and IV) provide additional

information demonstrating the diversity of molluscan male germ cell production. However, certain problems still remain unsolved. Further research along these lines is necessary.

REFERENCES

ABRAHAM, M. E., TIBIKA, R. H., GOLENSER, E. AND KIESELSTEIN, M. (1980) The blood-testis barrier in Aphanius dispar (Teleostei). Cell Tissue Res. **211**, 207-214.

ADIYODI, K. G. AND ADIYODI, R. G. (eds.) (1983) Reproductive Biology of Invertebrates. Vol. II Spermatogenesis and Sperm Function. John Wiley and Sons.

AFZELIUS, B. A. (1955) The fine structure of the sea urchin spermatozoa as revealed be the elctron microscope. Z. Zellforsch. Mikrosk. Anat. **42**, 134-148.

AFZELIUS, B. A. (1970) Thoughts on comparative spermatology. In: Comparative Spermatology, (Ed: B. Baccetti). Academic Press, New York, London. pp. 565-573.

AFZELIUS, B. A. (1972) Sperm morphology and fertilization. In: The Genetics of the Spermatozoon, (Eds: R. A. Beatty and S. Gluecksohnwaelsch). Edinburgh and New York. pp. 131-143.

AFZELIUS, B. A. (1975) The functional anatomy of the spermatozoon. Pergamon Press, Oxford.

AFZELIUS, B. A. AND DALLAI, R. (1983) The paired spermatozoa of the marine snail Turritella communis Lamark (Mollusca, Mesogastropoda). J. Ultrastruct. Res.. **85**, 311-319.

AFZELIUS, B. A. AND DALLAI, R. (1987) Conjugated spermatozoa. In: New Horizons in Sperm Cell Research, (Ed: H. Mohri). Japan Sci. Soc. Press. Tokyo/Gordon and Breach Sci. Publ.. New York. pp. 349-355.

AFZELIUS, B. A., DALLAI, R. AND CALLAINI, G. (1989) Spermiogenesis and spermatozoa in Melanopsis (Mesogastropoda, Mollusca). J. Submicrosc. Cytol. Pathol. **21**, 187-200.

AFZELIUS, B. A., BELLON, P. L. AND LANZAVECCHIA, S. (1990) Microtubules and their protofilaments in the flagellum of an insect spermatozoon. J. Cell Sci. **95**, 207-217.

ALLEN, J. A. (1962) The Fauna of the Clyde Sea area, Mollusca. Scottish Marine Biological Association Millport. pp. 49-50.

AL-HAJJ, H. A. (1988) Ultrastructural analysis of sperm head development in Nerita polita (Mollusca: Archaeogastropoda) from the Jordan Gulf of Aqaba (Red Sea). Internat. J. Invert. Rep. Dev. **13**, 281-295.

AL-JOMARD, R. (1987) Studies of the lymphatics of the liver and the uptake of interstitial fluid from the space of Disse. PhD Thesis, University of Glasgow. pp. 76-81.

ANDERSON, E. (1974) Comparative aspects of the ultrastructure of the female gamete. Int. Rev. Cytol. **4**, 1-70.

ANDERSON, W. A. (1967) Cytodifferentiation of spermatozoa in Drosophilia melanogaster: the effect of elevated temperature on spermiogenesis. Mol. Gen. Genet. **99**, 257-273.

ANDERSON, W. A., AND PERSONNE, P. (1970) The localisation of glycogen in the spermatozoa of various invertebrate and vertebrate species. J. Cell Biol. **44**, 29-51.

ANDERSON, W. A. AND PERSONNE, P. (1976) The molluscan spermatozoon; dynamic aspects of its structure and function. Am. Zool. **16**, 293-313.

ANDERSON, W. A., PERSONNE, P. AND ANDRÉ, J. (1968) Chemical compartmentalisation in Helix spermatozoa. J. Microsc. **7**, 367-390.

ANDRÉ, J. (1962) Contribution a la connaissance du chondriome - Étude de ses modifications ultrastructurales pendant la spermatogenèse. J. Ultrastr. Res. suppl. 3. pp. 1-185.

ANELLI, G., FRANCHI, F. AND CAMATINI, M. (1985) Structure and possible functional role of septate junctions in the ovotestis of a pond snail: inter-Sertoli junctions. J. Submicrosc. Cytol. **19**, 213-222.

ARNOLD, J. M. (1978) Spermiogenesis in Nautilus pompilius. II. Sertoli cell-spermatid junctional complexes. Anat. Rec. **191**, 261-268.

ARNOLD, J. M., AND WILLAMS-ARNOLD, L. D. (1977) Cephalopoda, Decapoda. In: Reproduction of marine invertebrates. (Eds: A. Giese and J. Pearse, eds.). Academic Press, pp. 243-290.

ARNOLD, J. M., AND WILLIAMS-ARNOLD, L. D. (1978) Spermiogenesis of Nautilus pompilius. I. General survey. J. Exp. Zool. **205**, 13-26.

ARVY, L. (1950) Données histologiques sur L'ovogénèse chez Dentalium entale Deshayes. Arch. Biol. **61**, 187-195.

AUSTIN, C. R., LUTWAK-MANN, C. AND MANN, T. (1964) Spermatophores and spermatozoa of the squid Loligo pealii. Proc. Roy. Soc. Lond. B. **161**, 143-152.

AZEVEDO, C. (1981) The fine structure of the spermatozoon of Patella lusitarica (Gastropoda: Prosobranchia), with special reference to acrosome formation. J. Submicrosc. Cytol. **13**, 47-56.

AZEVEDO, C., LOBO-DA-CUNHA, A. AND OLIVEIRA, E. (1985) Ultrastructure of spermatozoon in Gibbula umbilicalis (Gastropoda, Prosobranchia), with special reference to acrosome formation. J. Submicrosc. Cytol. **17**, 609-614.

BABA, K. (1931) A noteworthy gill-less holohepatic nudibranch Okadaia elegans Baba, with special reference to its internal anatomy. Annot. Zool. Jpn. **13**, 63-88.

BABA, K. (1937) Contribution to the knowledge of a nudibranch Okadaia elegans Baba. Jpn. J. Zool. **7**, 147-190.

BACCETTI, B. AND AFZELIUS, B. A. (1976) The Biology of Sperm Cell, Monographs in Developmental Biology, 10 (Ed. A. Wolsky), S. Karger, Basel. pp. 65-81.

BACCETTI, B. AND DALLAI, R. (1977) The spermatozoa of Arthropoda, XXIX. The degenerated axoneme and branched acrosome of Aleyrodids. J. Ultrastruct. Res. **61**, 26-70.

BACCETTI, B., BIGLIARDS, E., TALLURI, M. V. AND BURRINI, A. G. (1983) The Sertoli cell in lizards. J. Ultrastruct. Res. **85**, 11-23.

BACCETTI, B. (1986) Evolution trends in sperm structure. Comp. Biochem. Physiol. **85A**, 29-36.

BARNES, R. D. (1980) Invertebrate Zoology. 4th edition. Saunders College, Philadephia. pp. 432-434.

BAWA, S. R. (1963) Fine structure of the Sertoli cell of the human testis. J. Ultrastruct. Res. **91**, 459-473.

BAYNE, C. J. (1970) Organization of the spermatozoon of Agririolimax reticulatus, the grey field slug (Pulmonata, Stylommatophora). Z. Zellforsch. **103**, 75-89.

BEEMAN, R. D. (1970a) The anatomy and functional morphology of the reproductive system in the opisthobranch mollusk Phyllaplysia taylori Dall, 1900. Veliger **13**, 1-13.

BEEMAN, R. D. (1970b) An autoradiographic and phase contrast study of spermatogenesis in the anaspidean opisthobranch Phyllaplysia taylori Dall, 1900 (Gastropoda: Opisthobranchia). Arch. Zool. Exp. Gen. **111**, 5-22.

BEEMAN, R. D. (1977) Gastropoda: Opisthobranchia. In "Reproduction of marine invertebrates" (eds: A. C. Giese and J. S. Pearse). Vol. VI. Molluscs: Gastropods and Cephalopods. New York: Academic Press. pp. 115-172.

BERGMANN, M., GREVEN, H. AND SCHINDELMEISER, J. (1983) Observations on the blood-testis barrier in a frog and a salamander. Cell Tissue Res. **232**, 189-200.

BERGMANN, M., GREVEN, H. AND SCHINDELMEISER, J. (1984) Tight junction in the ovotestis of the pond snail Lymnaea stagnalis (L.) (Gastropoda, Basommatophora). Internat. J. Invert. Reprod. Develop. **7**, 291-296.

BERGMANN, M., SCHINDELMEISER, J. AND GREVEN, H. (1984) The blood-testis barrier in vertebrates having different testicular organization. Cell Tissue Res. **238**, 145-150.

BERGMANN, M. AND SCHINDELMEISER, J. (1987) Development of the blood-testis barrier in the domestic fowl (Gallus domesticus). Int. J. Androl. **10**, 481-488.

BILLARD, R. (1970) La spermatogenèse de Poecilia reticulata. III. Ultrastructure des cellules de Sertoli. Ann. Biol. Anim. Biochim. Biophys. **10**, 37-50.

BILYARD, G. R. (1974) The feeding habits and ecology of Dentalium entalis stimpsoni Henderson (Mollusca: Scaphopoda) Veliger **17**, 126-138.

BOURCART, C., LAVALLARD, R. AND LUBET, P. (1965) Ultrastructure du spermatozoïde de la moule (Mytilus parma von Ihering). C. R. Hebd. Séanc. Acad. Sci. Paris, sér. D. **260**, 5096-5099.

BOWEN, R. H. (1924) On the acrosome of the animal sperm. Anat. Rec. **28**, 1-13.

BRÖKELMANN, J. (1963) Fine structure of germ cells and Sertoli cells during the cycle of the seminiferous epithelium in the rat. Z. Zellforsch. Mikrosk. Anat. **59**, 820-850.

BUCKLAND-NICKS, J. A. (1973) The fine structure of the spermatozoon of Littorina (Gastropoda, Prosobranchia), with special reference to sperm motility. Z. Zellforsch. Mikrosk. Anat. **144**, 11-29.

BUCKLAND-NICKS, J. AND CHIA, F. S. (1976) Spermatogenesis of a marine snail Littorina sitkana. Cell Tiss. Res. **170**, 455-475.

BUCKLAND-NICKS, J. AND CHIA, F. S. (1980) Fine structure of Sertoli cells in three marine snails with discussion on the functional morphology of Sertoli cells in general. Cell and Tissue Res. **245**, 305-313.

BUCKLAND-NICKS, J., WILLIAMS, D., CHIA, F. S. AND FONTAINE, A. (1983) Studies on the polymorphic spermatozoa of a marine snail. Gamete Res. **7**, 19-37.

BUCKLAND-NICKS, J., AND CHIA, F. S. (1986) Fine structure of Sertoli cells in three marine snails with a discussion on the functional morphology of Sertoli cells in general. Cell Tiss. Res. **245**, 305-313.

BUCKLAND-NICKS, J., AND CHIA, F. S. (1989) Spermiogenesis in Chaetoderma sp. (Aplacophora). J. Exp. Zool. **252**, 308-317.

BUCKLAND-NICKS, J. AND CHIA, F. S. (1990) Egg capsule formation and hatching in the marine snail Littorina sitkana. Phil. Trans. Roy. Soc. Lond. B. **326**, 159-176.

BUCKLAND-NICKS, J., KOSS, R. AND CHIA, F. S. (1988) The elusive acrosome of chiton sperm. Internat. J. Invert. Reprod. Dev. **13**, 193-198.

BULLIVANT, S. (1965) Freeze-substitution and supporting techniques. Lab. Invest. **14**, 1178-1195.

BURGOS, M. H. AND FAWCETT, D. W. (1955) Studies on the fine structure of the mammalian testis. J. Biophys. Biochem. Cytol. **1**, 287-315.

BUTLER, R. D. AND GABRI, M. S. (1984) Structure and development of the sperm head in the lizard Podarcis (=Lacerta) taurica. J. Ultrastruct. Res. **88**, 261-274.

CAMATINI, M., CURTIS, I. D. AND FRANCHI, E. (1982) Dynamic aspect of inter-Sertoli junctions in monkeys. J. Ultrastruct. Res. **79**, 314-326.

CARTER, M. S. (1986) Interrelation of shell form, soft part anatomy and ecology in the siphonodentalioida (Mollusca, Scaphopoda) of the Northwest Atlantic continental shelf and slope. PhD Thesis, University of Delware, Lewes, Delware. pp. xvi+214.

CAVICCHIA, J. C. AND MOVIGLIA, G. A. (1983) The blood-testis barrier in the toad (Bufo arenarum Hensel): a freeze-fracture and lanthanum tracer study. Anat. Rec. **205**, 387-396.

CHEMES, H. E., DYM, M. AND RAJ, H. G. M. (1979) Hormonal regulation of Sertoli cell differentiation. Biol. Reprod. **21**, 251-262.

CHAMBERS, L. A. (1934) Studies on the organs of reproduction in the nudibranchiata molluska. Bull. Am. Mus. Nat. Hist. **66**, 599-641.

CHERRY, L. M. AND HSU, T. C. (1984) Antitubulin immunofluorescence studies of spermatogenesis in the mouse. Chromosoma (Berl). **90**, 265-274.

CLARK, A. W. (1967) Some aspects of spermiogenesis in a lizard. Am. J. Anat. **121**, 369-400.

CLARKE, G. N., CLARKE, F. M. AND WILSON, S. (1982) Actin in human spermatozoa. Biol. Reprod. **26**, 319-327.

CLAUDE, P. AND GOODENOUGH, D. A. (1973) Freeze-fracture faces of zonulae occludentes from "tight" and "leaky" epithelia. J. Cell Biol. **58**, 390-400.

CLAUDE, P. (1978) Morphological factors influencing transepithelial permeability: a model for the resistance of the zonula occludens. J. Membr. Biol. **39**, 219-232.

CLAUGHER, D. (1990) Scanning electron microscopy in taxonomy and functional morphology. Systematic association special volume No. 41. Clarendon Press, Oxford. The Systematic Association. pp.315.

COLE, A., MEISTRICK, M. L., CHERRY, L. M. AND TROSTLE-WEIGE, P.K., (1988) Nuclear and manchette development in spermatids of normal and azh/azh mutant mice. Biol. Reprod. **38**, 385-401.

COOKSEY, E. J. AND ROTHWELL, B. (1973) The ultrastructure of the Sertoli cell and its differentiation in the domestic fowl (Gallus domesticus). J. Anat. **114**, 329-345.

DALLAI, R., BIGLIARDI, E. AND LANE, N. J. (1990) Intercellular junction in myriapods. Tissue & Cell **22**, 359-369.

DAN, J. C. AND TAKAICHI, S. (1979) Spermiogenesis in the pulmonate snail Euhadra hickonis, III. Flagellum formation. Develop. Growth and Differ. **21**, 71-86.

DANIELS, E. W., LONGWELL, A. C., MCNIFF, J. M. AND WOLFGANG, R. W. (1971) Ultrastructure of spermatozoa from the American oyster Crassostrea virginica. Trans. Amer. Micros. Soc. **90**, 275-282.

DAVIS, J. D. (1968) A note on the behaviour of the scaphopod, Cadulus quadridentalus (Dall) 1881. Proc. Malacol. Soc. Lond. **38**, 135-138.

DEVRIES, J. (1963) Contribution to the morphology and histology of the nudibranch Melibe roseo. Rang. Ann. Univ. Stellenbosch. **38** (Ser. A.), 105-153.

DONIN, C. L. L. AND LANZACECCHIA, G. (1974) Morphogenetic effects of microtubules. III Spermiogenesis in Annelida Hirudinea. J. Submicroscop. Cytol. **6**, 245-255.

DOOHER, G. B. AND BENNETT, D. (1973) Fine structural observations on the development of the sperm head in the mouse. Am. J. Anat. **136**, 339-362.

DROCHMANS, P. (1962) Morphologie du glycogène. Étude au microscope électronnique de colorations négatives du glycogène particulaire. J. Ultrastru. Res. **6**, 141-163.

DUDEK, C. J., INJEYAN, H. S., SOUTAR, B., WEIR, G. Y. AND TOBE, S. S. (1980) The ovotestis of Aplysia californica: anatomy and egg release. Can. J. Zool. **58**, 2220-2229.

DUFRESNE-DUBE, L., PICHERAL, B. AND GUERRIER, P. (1983) An ultrastructural analysis of Dentalium vulgare (Mollusca, Scaphopoda) Gametes. J. Ultrastruct. Res. **83**, 242-257.

DUNLOP, W. F. AND ROBARDS, A. W. (1972) Some artifacts of the freeze-etching techniques. J. Ultrastruct. Res. **40**, 391-400.

DYM, M., AND D. W. FAWCETT (1970) The blood-testis barrier in the rat and the physiological compartmentation of the seminiferous epithelium. Biol. Reprod. **3**, 308-326.

EASTER, D. W., WADE, J. B. AND BOYER, J. L. (1983) Structural integrity of hepatocyte tight junctions. J. Cell Biol. **96**, 745-749.

ECKELBARGER, K. (1982) Undulating arrays of endoplasmic reticulum in the spermatids of an opisthobranch mollusc. Tiss. Cell. **14**, 289-295.

ECKELBARGER, K. J. AND EYSTER, L. S. (1981) An ultrastructural study of spermatogenesis in the nudibranch mollusc Spurilla neapolitana. J. Morph. **170**, 283-299.

ECKELBARGER, K. J. AND BLANDES-ECKELBARGER, P. I. (1989) Structure of the ovotestis and evidence for heterosynthetic incorporation of yolk precursors in the oocytes of the nudibranch mollusc, Spurilla neapolitana. J. Morph. **201**, 105-118.

ECKELBARGER, K. J., BIELER, R. AND MIKKELSEN, P. M. (1990) Ultrastructure of sperm development and mature sperm morphology in three species of commensal bivalves (Mollusca: Galeommatoidea). J. Morph. **205**, 63-75.

EMERSON, W. K. (1962) A classification of the scaphapod mollusks. J. Paleo. **36** (3): 460-482.

EVERETT, N. B. AND SIMMONS, B. A. (1958) Measurement and radioautographic localisation of albumin in rat tissues after intravenous administration. Circ. Res. **6**, 307-313.

FARQUHAR, M. G., AND G. E. PALADE (1963) Junctional complexes in various epithelia. J. Cell Biol. **17**, 375-412.

FAVARD, P. AND ANDRÉ, J. (1970) The mitochondria of spermatozoa. In "Comparative spermatology" (ed: B. Baccetti). New York: Academic Press.

FAWCETT, D. W., LEAK, L. V. AND HEIDGER, P. M. (1970) Electron microscopic observations on the structural components of the blood-testis barrier. J. Reprod. Fertil. Suppl. **10**, 105-122.

FAWCETT, D. W., ANDERSON, W. A., AND PHILLIPS, D. M. (1971) Morphogenetic factors influencing the shape of the sperm head. Dev. Biol. **26**, 220-251.

FAWCETT, D.W. (1975) The ultrastructure and functions of the Sertoli cell. Handbk. Physiol. Vol. **5**. Sect. **7**. Washington, D. C.: American Physiological Society, pp. 21-55.

FIELDS, W. G. (1965) The structure, development, food relations, reproduction and life history of the squid Loligo opalescens Berry. Calif. Fish Game Bull. **131**, 1-108.

FIELDS, G. W. AND THOMPSON, K. A. (1976) Ultrastructure and functional morphology of spermatoza of Rossia pacifica (Cephalopoda, Decapoda). Can. J. Zool. **54**, 908-932.

FLICKINGER, C. AND D. W. FAWCETT (1967) The junctional specializations of Sertoli cells in the seminiferous epithelium. Anat. Rec: **158**, 207-222.

FRANC, A. (1968) Sous-class des Opisthobranches. In "Traité de Zoologie" (eds: P. P. Grassé). Vol. II, Masson, Paris. pp. 608-893 and 1079-1082.

FRANCHI, E., CAMATINI, M. AND CURTIS, I. (1982) Morphological evidence of a permeability barrier in urodele testis. J. Ultrastruct. Res. **80**, 253-263.

FRANZÉN, Å. (1955) Comparative morphological investigations into the spermiogenesis among Mollusca. Zool. Bidr. Upps. **30**, 399-456.

FRANZÉN, Å. (1956) On spermiogenesis, morphology of the spermatozoon and biology of fertilization among invertebrates. Zool. Bidr. Upps. **31**, 355-481.

FRANZÉN, Å. (1967) Spermiogenesis and spermatozoa of the Cephalopoda. Ark. Zool. Ser. 2, **19** (16), 323-334.

FRANZÉN, Å. (1970) Phylogenetic aspects of the morphology of spermatozoa and spermiogenesis. In Comparative Spermatology (Baccetti, B. eds.). Academic Press, New York, London. pp. 29-45.

FRANZÉN, Å. (1983) Ultrastructural studies of spermatozoa in three bivalve species with notes on evolution of elongated sperm nucleus in primitive spermatozoa. Gamete Res. **7**, 199-214.

FRETTER, V. (1948) Structure and life histroy of some minute prosobranchs of rock pools. J. Mar Biol. Ass. UK. **27**, 597-632.

FRETTER, V. AND GRAHAM, A. (1949) The structure and mode of life of the Pyramidellidae, parasitic opisthobranchs. J. Mar. Biol. Ass. UK **48**, 493-532.

FRETTER, V. AND GRAHAM, A. (1962) British prosobranch molluscs. Ray Society, London. pp.755.

FUJIWARA, K. AND LINCK, R. G. (1982) The use of tannic acid in microtubule research. Meth. Cell Biol. **24**, 217-233.

GAINEY, L. F. , Jr. (1972) The use of the foot and the captacula in the feeding in Dentalium. Veliger **15**, 29-34.

GALANGAU, V., AND TUZET, O. (1968a) L'acrosome d'Octopus vulgaris Lmk: Observations au microscope électronique', C. R. Acad. Sci. Paris, **267**, 1462-1464.

GALANGAU, V., AND TUZET, O. (1968b) Les mitochondries pendent la spermatogenèse d'Octopus vulgaris Lmk: Recherches au microscope électronique', C. R. Acad. Sci. Paris, **267**, 1735-1737.

GALTSOFF, P. S., AND PHILPOTT, D. E. (1960) Ultrastructure of the spermatozoon of the Oyster, Crassostrea virginica. J. Ultrastruct. Res. **3**, 241-253.

GHISELIN, M. T. (1966) Reproductive function and physiology of opisthobranch gastropods. Malacologia **3**, 327-378.

GIUSTI, F. (1971) L'ultrastructtura dello spermatozoo nella filogenesi e nella sistematica dei molluschi gasteropodi. Atti. Soc. Ital. Sci. Nat. **112**, 381-402.

GIUSTI, F. AND SELMI, M. G. (1982) The atypical sperm in the prosobranch molluscs. Malacologia. **22**, 171-181.

GLADWELL, R. T. (1977) The effect of temperature on the potential difference and input resistance of rat seminiferous tubules. J. Physiol. London. **268**, 111-121.

GLAUERT, A. M., ROGERS, G. E. AND GLAUERT, R. H. (1956) A new embedding medium for electron microscopy. Nature, London. **178**, 803.

GRIFFOND, B. AND GOMOT, L. (1979) Ultrastructural study of the follicle cells in the freshwater gastropod Viviparus viviparus L.. Cell Tissue Res. **202**, 25-32.

GRIFFOND, B. (1980) Étude ultrastructurale de la spermatogenèse typique de Viviparus vivparus L. Mollusque, Gastéropode. Archs. Biol. Bruxelles. **91**, 445-426.

GRIFFOND, B., DADKHAH-TEHERANI, Z., MEDINA, A. AND BRIDE, M. (1991) Ultrastructure of Helix aspersa spermatogenesis: scanning and transmission electron microscopical contribution. J. Moll. Stud. **57**, 277-287.

GUYARD, A. (1971) Étude de la differentiation de l'ovotestis et des facteurs controlant l'orientation sexuelle des gonocytes de l'escargot Helix aspersa Müller. Ph.D. Thesis, University de Besancon.

HADFIELD, M. G. (1979) Aplacophora. In: Reproduction of Marine Invertebrates; Vol V. (Eds: A. G. Giese and J. S. Pearse). Academic Press, New York. pp. 1-25.

HAGENÄS L., PLÖEN, L., RITZÉN, E. M. AND EKWALL, H. (1977) Blood-testis barrier: maintained function of inter-Sertoli cell junctions in experimental cryptorchidism in the rat as judged by a simple lanthanum-immersion technique. Andrologia **9**, 250-254.

HAYAT, M. A. (1973) Specimen preparation. In Electron microscopy of enzymes. Principles and methods. Vol. I. Ch. 1. Ed. M. A. Hayat, New York and London: Van Nostrand-Reinhold.

HEALY, J. M. (1982a) Ultrastructure of the spermatozoa of an opisthobranch Tornatina sp. (Mollusca, Gastropoda, Retusidae). Zool. Scripta. **11**, 221-226.

HEALY, J. M. (1982b) Ultrastructure of spermiogenesis of Philippia (Psilaxis) oxytropis with special reference to the taxonomic position of the Architectonicidae (Gastropoda). Zoomorphlogy. **101**, 197-214.

HEALY, J. M. (1983) Ultrastructure of euspermiogenesis in the mesogastropod Stenothyra sp. (Prosobranchia, Rissoacea, Stenothyridae). Zool. Scripta. **12**, 203-214.

HEALY, J. M. (1986) Euspermatozoa and paraspermatozoa of the relict cerithiacean gastropod, Campanile symbolicum (Prosobranchia, Mesogastropoda). Helgol. Meeresunters. **40**, 201-218.

HEALY, J. M. (1988a) The ultrastructure of spermatozoa and spermiogenesis in pyramidellid gastropods, and its systematic importance. Helgoländer Meeresunters. **42**, 303-318.

HEALY, J. M. (1988b) Sperm morphology and its systematic importance in the Gastropoda. Malacol. Rev. suppl. **4**, 251-266.

HEALY, J. M. (1989) Spermiogenesis and spermatozoa in the relict bivalve genus Neotrigonia: relevance to trigonia relationships, particularly Unionoidea. Marine Biology. **103**, 75-85.

HEALY, J. M. (1990) Spermatozoa and spermiogenesis of Cornirostra, Valvata and Orbitestella (Gastropoda: Heterobranchia) with a discussion of valvatoidean sperm morphology. J. Moll. Stud. **56**, 557-566.

HEALY, J. M. AND JAMIESON, B. G. M. (1981) An ultrastructural examination of developing and mature paraspermatozoa in Pyrazus ebeninus (Mollusca, Gastropoda, Potamididae). Zoomorphol. **98**, 101-119.

HEALY, J. M. AND JAMIESON, B. G. M. (1989) An ultrastructural study of spermatozoa of Helix aspersa and Helix pomatia (Gastropoda, Pulmonata). J. Moll. Stud. **55**, 389-404.

HEALY, J. M. AND WILLAN, R. C. (1984) Ultrastructure and phylogenetic significance of notaspidean spermatozoa (Mollusca, Gastropoda, Opisthobranchia). Zool. Scripta. **13**, 107-120.

HILL, R. S. (1977) Studies on the ovotestis of the slug Agriolimax reticulatus (Müller), 2. The epithelium. Cell Tissue Res. **183**, 131-141.

HODGSON, A. N. (1986) Invertebrate spermatozoa: structure and spermatogenesis. Archives of Andrology. **17**, 105-114.

HODGSON, A. N. AND BERNARD, R. T. F. (1986) Observations on the ultrastructure of the spermatozoon of two mytilid bivalves from the South-west coast of England. J. Mar. Biol. Assoc. U. K. **66**, 385-390.

HODGSON, A. H. AND BERNARD, R. T. F. (1988) A comparison of the structure of the spermatozoa and spermatogenesis of 16 species of patellid limpet (Mollusca, Gastropoda, Archaeogastropoda) J. Morph. **195**, 205-223.

HODGSON, A. N. , BARTER, J. M. STURROCK, M. G. AND BERNARD, R. T. F. (1988) Comparative spermatology of 11 species of Polyplacophora (Mollusca) from the suborders Lepidopleurina, Chitonina and Acanthochitonina. Proc. Roy. Soc. Lond. B. **235**, 161-177.

HODGSON, A. N., BERNARD, R. T. F. and G. V. der HORST (1990) Comparative spermatology of three species of Donax (Bivalvia) from South Africa. J. Moll. Stud. **56:** 257-265.

HODGSON, A. N., BERNARD, R. T. F. AND LINDLEY, D. S. (1991) Comparative spermatology of four sympatric species of Siphonaria (Pulmonata: Basommatophora). J. Moll. Stud. **57**, 309-322.

HOU, S. T. AND MAXWELL, W. L. (1990) Desmosome-like junctions between Sertoli and Sertoli-germ cells in the ovotestis of Arion hortensis (Mollusca, Pulmonata). J. Morph. **205**, 325-333.

HOU, S. T. AND MAXWELL, W. L. (1991) Ultrastructural studies of spermatogenesis in Antalis entalis (Scaphopoda, Mollusca). Phil. Trans. Roy. Soc. Lond. B. **333**, 101-110.

HYMAN, L. H. (1967) The invertebrates. Vol. VI, Mollusca 1, McGraw-Hill, New York.

JOHNSON, M. H. (1970) Changes in the blood-testis barrier of the guinea pig in relation to histological damage following iso-immunization with testis. J. Reprod. Fertil. **22**, 119-127.

JOHNSON, M. H. (1973) Physiological mechanisms for the immunological isolation of spermatozoa. Adv. Reprod. Physiol. **6**, 279-324.

JOHNSON, M. H. AND SETCHELL, B. P. (1968) Protein and immunoglobulin content of rete testis fluid of rams. J. Reprod. Fertil. **17**, 403-406.

JONES, R. T. (1978) The blood/germ cell barrier in male Schistocerca gregaria: the time of its establishment and factors affecting its formation. J. Cell Sci. **31**, 145-163.

JONG-BRINK, M., WIT, A., KRAAL, G. AND BOER, H. H. (1976) A light and electron microscope study on oogenesis in the freshwater pulmonate snail Biophalaria galbrata. Cell Tissue Res. **171**, 195-219.

JONG-BRINK, M., H. H. BOER, T. G. HOMMES, AND A. KODDE (1977) Spermatogenesis and the role of Sertoli cells in the freshwater snail Biomphalaria glabrata. Cell Tiss. Res. **181**, 37-58.

JONG-BRINK, M., SCHOT, L. P. C., SCHOENMAKERS, H. J. N. AND BERGAMIN-SASEN, M. J. M. (1981) A biochemical and quantitive electron microscope study on steroidogenesis in ovotestis and digestive gland of the pulmonate snail Lymnaea stagnalis. Gen. Comp. Endocrinol. **45**, 30-38.

JONG-BRINK, M., WITH, N. D., HURKMANS, P. J. M. AND SASSEN, M. J. M. B. (1984) A morphological enzyme-cytochemical and physiological study of the blood-gonad barrier in the hermaphroditic snail Lymnaea stagnalis. Cell Tissue Res. **235**, 593-600.

JOOSSE, J. AND REITZ, D. (1969) Functional anatomical aspects of the ovotestis of Lymnaea stagnalis. Malacologia **9**, 101-109.

JOOSSE, J. (1988) The hormones of molluscs. In: Invertebrate Endocrinology (Eds: H. Laufer and G. H. Downer), Vol. II, Endocrinology of selected invertebrate types. Alan R. Liss, New York. pp. 89-140.

KADURA, N. AND KHRAPUNOV, N. (1988) Displacement of histones by sperm-specific proteins at different stages of spermatogenesis of squid. Eur. J. Biochem. **175**, 603-607.

KARNOVSKY, M. J. (1965) A formaldehyde-glutaraldehyde fixative of high osmolality for use in electron microscopy. J. Cell Biol. **27**, 137A-138A.

KESSEL. R. G. (1970) Spermiogenesis in the dragonfly with special reference to a consideration of the mechanisms involved in the development of cellular asymmetry. In "Comparative spermatology" (B. Baccetti ed.). Academic Press, New York. pp. 531-549.

KHAN, H. R., AND A. S. M. SALEUDDIN (1983) Cell contacts between follicle cells and the oocyte of Helisoma (Mollusca, Pulmonata). J. Morph. **177**, 319-328.

KHRAPUNOV, N., KADURA, N. AND DRAGAN, I. (1988) Rearrangements of chromatin structure during spermatogenesis of squid. Eur. J. Biochem. **175**, 609-613.

KITAJIMA, E. W. AND PARAENSE, W. L. (1976) The ultrastructure of mature sperms of the fresh-water snail Biomphalaria glabrata (Mollusca, Gastropoda). Trans. Am. Microsc. Soc. **95**, 1-10.

KOHNERT, R. AND STORCH, V. (1983) Ultrastrukturelle untersuchungen zur morphologie und genese der spermien von Archaeogastropoda. Helgoländer Meeresunters. **36**, 77-84.

KOHNERT, R. AND STORCH, V. (1984a) Vergleichend-ultrastrukturelle untersuchungen zur morphologie eupyrener spermien der monotocardia (Prosobranchia). Zool. Jahrb. Anat. **111**, 51-93.

KOHNERT, R. AND STORCH, V. (1984b) Elektronen-mikroskopische untersuchungen zur spermiogenese der eupyrenen spermien der monotocardia (Prosobranchia). Zool. Jahrb. Anat. **112**, 1-32.

KOIKE, K. (1985) Comparative ultrastructural studies on the spermatozoa of the Prosobranchia (Mollusca : Gastropoda). Sci. Repts. Fac. Educ. Gunma. Univ. **34**, 33-153.

KOUKOURAS, A. T. H. AND KEVREKIDIS, T. H. (1986) Benthic fauna of the North Aegean Sea. III. Dentalidae (Mollusca: Scaphopoda). Oebalia **13**, 185-194.

KUBO, M. (1977) The formation of a temporary-acrosome in the spermatozoon of Laternula limicola (Bivalvia, Mollusca). J. Ultrastruct. Res. **61**, 140-148.

KUBO, M. AND ISHIKAWA, M. (1981) Organization of the acrosome and helical structure in sperm of the Aplysiid, Aplysia kurodai (Gastropoda, Opisthobranchia). Differentiation **20**, 131-140.

LACROIX, M., SMITH, F. Z. AND FRITZ, I. B. (1977) Secretion of plasminogen activator by Sertoli cell-enriched cultures. Mol. Cell Endocrinol. **9**, 227-336.

LONGO, F. J. AND DORNFELD, E. G. (1967) The fine structure of spermatid differentiation in the mussel, Mytilus edulis. J. Ultrastruct. Res. **20**, 462-480.

LONGO, F. J. AND ANDERSON, E. (1969) Spermiogenesis in the surf clam Spisula solidissima with special reference to the formation of the acrosomal vesical. J. Ultrastruct. Res. **27**, 435-443.

LONGO, F. J. AND ANDERSON, E. (1970) Structural and cytochemical features of the sperm of the cephalopod Octopus bimaculatus. J. Ultrastruc. Res. **32**, 94-106.

LUCHTEL, D. (1972a) Gonadal development and sex determination in pulmonate molluscs. I. Arion circumscriptus. Z. Zellforsch. **130**, 279-301.

LUCHTEL, D. (1972b) Gonadal development and sex determination in pulmonate molluscs. II. Arion ater rufus and Deroceras reticulatum. Z. Zellforsch. **130**, 302-311.

MCINTOSH, J. R. AND PORTER, K. R. (1967) Microtubules in the spermatids of the domestic fowl. J. Cell Biol. **35**, 153-173.

MCGOWAN, J. A. AND PRATT, I. (1954) The reproductive system and early embryology of the nudibranch Archidoris montereyensis (Cooper). Bull. Mus. Comp. Zool. Harvard, **3**, 261-276. pls. 1 and 2.

MADARA, J. L. AND DHARMSATHAPHORN, K. (1985) Occluding junction structure-function relationships in a cultured epithelial monolayer. J. Cell. Biol. **101**, 2124-2133.

MANN, T., MARTIN, A. W. AND THIERSCH, J. B. (1970) Male reproductive tract, spermatophores and spermatophoric reaction in the giant octopus of the North Pacific, Octopus dofleini martini. Proc. R. Soc. Lond. B. **175**, 31-61.

MARCAILLOU, C. AND SZÖLLÖSI, A. (1975) Variations de perméabilité du follicle testiculaire chez le criquet Locusta migratoria migratorioides (Orthoptère) au cours du dernier stade larvaire. C. R. Hebd. Acad. Sci. Paris Series D, **281**, 2001-2004.

MARCAILLOU, C. AND SZÖLLÖSI, A. (1980) The "blood-testis" barrier in a nematode and a fish: a generalizable concept. J. Ultrastruct. Res. **61**, 271-283.

MARCUS, E. (1957) On opisthobranchia from Brizil. J. Linn. Soc. Lond. **43**, 390-486.

MARTIN, A. W., THIERSCH, J. B., DOTT, H. M., HARRISON, R. A. P. AND MANN, T. (1970) Spermatozoa of the giant octopus of the North Pacific Octopus dofleini martini. Proc. R. Soc. Lond. B. **175**, 63-68.

MAXWELL, W. L. (1974a) Spermiogenesis of Eledone cirrhosa Lamarck (Cephalopoda, Octopoda). Proc. Roy. Soc. Lond. B. **186**, 181-190.

MAXWELL, W. L. (1974b) Studies of spermiogenesis in molluscs. PhD Thesis, University of Bristol, England.

MAXWELL, W. L. (1975a) Spermiogenesis of Eusepia officinalis (L.), Loligo forbesi (Steenstrup) and Alloteuthis subulata (L.) (Cephalopoda, Decopoda). Proc. Roy. Soc. Lond. B. **191**, 527-535.

MAXWELL, W. L. (1975b) Scanning electron microscope studies of pulmonate spermatozoa. Veliger **18**, 31-33.

MAXWELL, W. L. (1976) The neck region of the spermatozoon of Discus rotundatus (Müller) (Pulmonata, Stylommatophora). J. Morph. **150**, 299-306.

MAXWELL, W. L. (1977) Freeze-etching studies of pulmonate spermatozoa. Veliger **20**, 71-74.

MAXWELL, W. L. (1980) Distribution of glycogen deposits in two euthyneuran sperm tails. Internat. J. Invert. Reprod. **2**, 245-249.

MAXWELL, W. L. (1983) MOLLUSCA. In K. G. and R. G. Adiyodi eds: Reproductive biology of invertebrates. Vol. II: spermatogenesis and sperm function. John Wiley & Sons Ltd. pp.175-319.

MAXWELL, W. L., IRVINE, A., STRANG, R. H. C., GRAHAM, D. I., ADAMS, J. H. AND GENNARELLI, T. A. (1990) Glycogen accumulation in axons after stretch injury. J. Neurocytol. **19**, 235-241.

MEDINA, A., MORENO, F. J. AND LóPEZ-CAMPOS, J. L. (1985) Acrosome evolution in Hypselodoris tricolor (Gastropoda: Nudibranchia). J. Submicrosc. Cytol. **17**, 404-411.

MEDINA, A., MORENO, F. J. AND LóPEZ-CAMPOS, J. L. (1986a) Nuclear morphogenesis during spermiogenesis in the nudibranch mollusc Hypselodoris tricolor (Gastropoda, Opisthobranchia). Gamete Res. **13**, 159-171.

MEDINA, A., GARCíA, J. C., MORENO, F. J. AND LóPEZ-CAMPOS, J. L. (1986b) Comparative studies on the histology of the ovotestis in Hypselodoris tricolor and Godiva banyulensis (Gastropoda, Opisthobranchia), with special reference to yolk formation. J. Morphol. **188**, 105-118.

MEDINA, A. AND GARCíA, J. C. (1987) Estudio histológico y funcional de la gónada de Hypselodoris tricolor (Gastropoda, Nudibranchia). Boll. Malacologico. **23**, 69-82.

MEDINA, A. MORENO, F. J. AND GARCíA-HERDUGO, G. (1988) Sperm tail differentiation in the nudibranch mollusc Hypselodoris tricolor (Gastropoda, Opisthobranchia). Gamete Res. **20**, 223-232.

MEISTRICH, M. L., TROSTLE-WEIGE, P. K. AND RUSSELL, L. D. (1990) Abnormal manchette development in spermatids of azh/azh mutant mice. Am. J. Anat. **188**, 74-86.

MILLER, M. C. (1977) Aeolid nudibranchs (Gastropoda: Opisthobranchia) of the family Tergipedidae from New Zealand waters. J. Linn. Soc. Lond. **60**, 197-222.

MINNITI, F. AND D'ANDREA, A. (1989) Histological and ultrastructural studies on the spermiogenesis of Philippia hybrida (Linnaeus, 1958) with special reference to the taxonomical position of the Architectonicidae (Mollusca, Gastropoda). Zool. Anz. **222**, 129-142.

MIZUHIRA, V. AND FUTAESAKU, Y. (1974) Fine structure of the microtubules by means of the tannic acid fixation. Proc. 8th Congr. Electr. Mic. Canberra. Vol. 2, pp.340-341. Australian Academy of Science, Canberra.

MOGENSEN, M. M., TUCKER, J. B. AND STEBBINGS, H. (1989) Microtubule polarities indicate that nucleation and capture of microtubules occur at cell surfaces in Drosophila. J. Cell Biol. **108**, 1445-1452.

MOOR, H., MUHLETHALER, K., WALDNER, H. AND FREYWYSSLING, A. (1961) A new freezing ultramicrotome. J. Biophys. Biochem. Cytol. **10**, 1-13.

MORTON, J. E. (1959) The habits and feeding organs of Dentalium entalis. J. Mar. Biol. Assoc. U. K. **38**, 225-238.

NEAVES, W. B. (1973) Permeability of Sertoli cell tight junction to lanthanum after ligation of ductus deferens and ductuli efferentes. J. Cell Biol. **59**, 559-572.

NEWELL, P. F. AND SKELDING, J. M. (1973) Studies on the permeability of the septate junction in the kidney of Helix pomatia L.. Proc. Fourth Europ. Malac. Congr., Malacologia **14**, 89-91.

NIIJIMA, L. AND DAN, J. C. (1965) The acrosome reaction in Mytilus edulis. J. Cell Biol. **25**, 243-248.

NISHIWAKI, S. (1964) Phylogenetical study on the type of the dimorphic spermatozoa in Prosobranchia. Sci. Rep. Tokyo Kyoiku Daigaku Ser B. **11**, 237-275.

OKAMURA, F. AND NISHIYAMA, H. (1976) The early development of the tail and the transformation of the shape of the nucleus of the spermatid of the domestic fowl, Gallus gallus. Cell Tiss. Res. **169**, 345-359.

O'DONOVAN, P. AND ABRAHAM, M. (1987) Somatic tissue-male germ cell barrier in three hermaphrodite invertebrates: Dugesia biblica (Platyhelminthes) Placobdella costata (Annelida) and Levantina hierosolyma (Mollusca). J. Morph. **192**, 217-227.

O'RAND, M. G., ROMRELL, L. J. (1977) Appearence of cell surface auto- and isoantigens during spermatogenesis in the rabbit. Dev. Biol. **55**, 347-358.

OSMAN, D. I., EKWALL, H. AND PLOEN, L. (1980) Specialized cell contacts and the blood-testis barrier in the seminiferous tubules of the domestic fowl (Gallus domesticuc). Int. J. Androl. **3**, 553-562.

PALADE, G. E. (1952) A study of fixation for electron microscopy. J. Exp. Med. **95**, 285-298.

PALMER, C. P. (1974) A supraspecific classification of the Scaphapod, Mollusca. Veliger. **17**, 115-123.

PARIVAR, K. 1980 Differentiation of Seroli cells and post-reproductive epithelial cells in the hermaphrodite gland of Arion ater (L.) (Mollusca, Pulmonata). J. Moll. Stud. **46**, 139-147.

PARIVAR, K. (1981) Spermatogenesis and sperm dimorphism in land slug Arion ater L. (Pulmonata, Mollusca). Z. Mikrosk. Anat. Forsch. **95**, 81-92.

PELLETIER, R.-M., HUGON, J. S., CALVERT, R. AND NEMIROVSKY, M. S. (1981) Effects of immunization with Freund's complete adjuvant and isologous spermatozoa on the seminiferous epithelium and blood-testis barrier in guinea pigs. Anat. Rec. **199**, 197-211.

PELLETIER, R.-M. (1988) Cyclic modulation of Sertoli cell junctional complexes in a seasonal breeder: the mink (Mustela vison). Am. J. Anat. **183**, 68-102.

PELLETIER, R.-M. (1990) A novel perspective: the occluding zonule encircles the apex of the Sertoli cell as observed in birds. Am. J. Anat. **188**, 87-108.

PERSONNE, P. (1971) Étude structural et cytochimique de la pièce intermédiaire du spermatozoïde des gastropodes pulmonés cas de spécialisation mitochondriale. D. Sc. thesis, Université de Paris Sud (XI).

PERSONNE, P. AND ANDRÉ, J. (1964) Existence de glycogène mitochondrial dans le spermatozoïde de la Testacella. J. Microscopie. **3**, 643-650.

PERSONNE, P. AND ANDERSON, W. (1970) Localisation miotchondriale d'enzymes liees au metabolisme du glycogene dans le spermatozoide de l'escargot. J. Cell Biol. **44**, 20-28.

PHILLIPS, D. M. (1970) Insect sperm: their structure and morphogenesis. J. Cell Biol. **44**, 243-277.

PHILLIPS, D. M. (1974) Nuclear shaping in the absence of microtubules in scorpion spermatids. J. Cell Biol. **62**, 911-917.

POCHON-MASSON, J. AND GHARAGOZLOU, I.-D. (1970) Particularité morphologique de l'acrosome dans le spermatozoide de Tapes decussatus L. (Mollusque, Lamellibranche). Ann. Sci. Nat. Zool. **12**, 171-180.

PONDER, W. F. (1973) Pseudoskenella depressa gen. et sp. nov., an ectoparasite on Galeolaria. Malacol. Rev. **6**, 119-123.

POON, P. (1987) The diet and feeding behavior of Cadulus tolmiei Dall, 1897 (Scaphopoda, Siphonodentalioida). Nautilus **101**, 88-92.

POPHAM, J. D. (1974) Comparative morphormetrics of the acrosome of the sperm of "externally" and "internally" fertilizing sperms of the shipworms (Teredinidae, Bivalvia, Mollusca). Cell Tissue Res. **150**, 291-297.

POPHAM, J. D. (1979) Comparative spermatozoon morphology and bivalve phylogeny. Malacol. Rev. **12**, 1-20.

POPHAM, J. D., DICKSON, M. R. AND GODDARD, C. K. (1974) Ultrastructural study of the mature gametes of two species of Bankia (Mollusca: Teredinidae). Aust. J. Zool. **22**, 1-12.

POPHAM, J. D. AND DICKSON, M. R. (1975) Location of glycogen in spermatids and spermatozoa of the shipworm Bankia australis (Teredinidae, Bivalvia, Mollusca). Cell Tiss. Res. **164**, 519-524.

PRICAM, C., HUMBERT, F., PERRELET, A. AND ORCI, L. (1974) A freeze-etch study of the tight junction of the rat kidney tubules. Lab. Invest. **30**, 286-291.

PRUVOT-FOL, A. (1960) Les organes génitaux des opisthobranches. Arch. Zool. Exp. Gen. **99**, 135-224.

RACOVITZA, E. G. (1894) Notes de biologie. 3. Moeures et reproduction de la Rossia macrosoma (D. Ch.). Arch. Zool. Exp. Gen. **3**, 491-539.

RATTNER, J. B. AND B. R. BRINKLEY (1972) Ultrastructure of mammalian spermiogenesis III. The organization and morphogenesis of the manchette during rodent spermiogenesis. J. Ultrastruct. Res. **41**, 209-218.

REINKE, E. E. (1912) A preliminary account of the development of the apyrene sperm in Strombus and of the nurse cells in Littorina. Biol. Bull. Mar. Biol. Lab. Woods Hole. **22**, 319-327.

RETZIUS, G. (1904) Zur kenntnis der spermien der Evertebraten. I. Biol. Untersuch. **11**, 1-32.

RETZIUS, G. (1905) Zur kenntnis der spermien der Evertebraten. II. Biol. Untersuch. N. F., **12**, Nr. 9, 101-102. Taf. XI-XIX.

RETZIUS, G. (1906) Die spermien der gastropoden. Biol. Unters. [N.S.] **13**, 1-36.

REVERBERI, G. (1970) The ultrastructure of the ripe oocytes of Dentalium. Acta Embryol. Exp. **1970**, 255-279.

REVERBERI, G. (1972) The fine structure of the ovaric egg of Dentalium. Acta Embryol. Exp. **14**, 135-166.

RIGBY, J. (1982) The fine structure of differentiation, spermatozoa and Sertoli cells in the gonad of the pond snail, Lymnaea stagnalis. J. Moll. Stud. **48**, 111-123.

ROBERT, E. (1888) Sur la spermatogénèsis chez les Aplysies. C. R. Hebd. Seances. Acad. Sci. **106**, 422-425.

ROBERTSON, J. G., LYTTLETON, P., WILLIAMSON, K. I. AND BATT, R. D. (1975) The effect of fixation procedures on the electron density of polysaccharide granules in Nocardia corallina. J. Ultrastruc. Res. **50**, 321-332.

ROBERTSON, R. (1973) The biology of Architectonicidae: gastropods combining prosobranch and opisthobranch traits. Malacologia **14**, 215-220.

ROBERTSON, R. (1978) Spermatophores of six eastern North American pyramidellid gastropods and their systematic significance (with the new genus Boonea). Biol. Bull. **155**, 360-382.

ROBINSON, G. (1982) Electron microscopy. 2: Transmission (A) Tissue preparation; (B) Sectioning and Staining. In Bancroft, J. D. and Stevens, A. (eds): Theory and Practice of Histological Techniques, 2nd edition, Churchill Livingstone, pp. 428-799.

ROKOP, F. J. (1974) Reproductive patterns in the deep-sea benthos. Science, N.Y. **186**, 743-745.

ROKOP, F. J. (1977) Seasonal reproduction of the Brachiopod Frieleia nalli and the Scaphopoda Cadulus californicus at bathyal depths in the deep sea. Marine Biology. **43**, 237-246.

ROOSEN-RUNGE, E. C. (1977) The process of spermatogenesis in animals. Cambridge University Press. pp. 37-50.

ROSS, M. H., AND DOBLER, J. (1975) The Sertoli cell junctional specializations and their relationship to the germinal epithelium as observed after afferent ductule ligation. Anat. Rec. **183**, 267-292.

ROSS, M. H. (1976) The Sertoli cell junctional specialization during spermiogenesis and at spermiation. Anat. Rec. **186**, 79-104.

ROSS, M. H. (1977) Sertoli-Sertoli junctions and Sertoli-spermatid junctions after efferent ductule ligation and lanthanum treatment. Am. J. Anat. **148**, 49-56.

RUSSELL, L. D., AND CLERMONT, Y. (1976) Anchoring device between Sertoli cells and late spermatids in rat seminiferous tubules. Anat. Rec. **185**, 259-278.

RUSSELL, L. D. (1977a) Desmosome-like junctions between Sertoli and germ cells in the rat testis. Am. J. Anat. **148**, 301-312.

RUSSELL, L. D. (1977b) Movement of spermatocytes from the basal to the adluminal compartment of the rat testis. Am. J. Anat. **148**, 313-328.

RUSSELL, L. D. (1977c) Observations on rat Sertoli ectoplasmic (junctional) specializations in their association with germ cells of the rat testis. Tiss. Cell **9**, 475-498.

RUSSELL-PINTO, F., AZEVEDO. C. AND BARANDELA, T. (1983) Fine structure of the spermatozoa of Chiton marginatus (Mollusca: Amphineura), with special reference to nucleus maturation. Gamete Res. **8**, 345-355.

RUSSELL-PINTO, F., AZEVEDO, C. AND OLIVEIRA, E. (1984) Comparative ultrastructural studies of spermiogenesis and spermatozoa in some species of Polyplacophora (Mollusca). Internat. J. Invert. Reprod. Dev. **7**, 267-277.

SABATINI, D. D., BENSCH, K. AND BARRNETT, R. J. (1963) Cytochemistry and Electron Microscopy. The preservation of cellular ultrastructure and enzymatic activity by aldehyde fixation. J. Cell Biol. **17**, 19-58.

SACHWATKIN, V. (1920) Das vrinogential-system von Ampullaria gigas Spix. Acta Zool. **1920**, 67-130.

SAKKER, E. R. (1983) Seasonal reproduction and gametogenesis in the chitons Onithochiton quercinus (Gould), Chiton pelliserpentis Quoy and Gaimard and Plaxiphora paeteliana (Thiele) (Mollusca: Polyplacophora). PhD Thesis, University of Sydney. (Refered from Sakker, 1984).

SAKKER, E. R. (1984) Sperm morphology, spermatogenesis and spermiogenesis of three species of chitons (Mollusca, Polyplacophora). Zoomorphology **104**, 111-121.

SALEUDDIN, A. S. M., L. E. WILSON, H. R. KHAN, AND G. M. JONES (1980) Effects of brain extracts on oocyte maturation in Helisoma (Pulmonata : Mollusca). Can. J. Zool. **58**, 1109-1124.

SCHITZ, V. (1925) Etudes sur l'évolution des éléments génitaux chez les Mollusques Ptéropodes. I. La spermatogénèse. Biol. Gen. **1**, 299-338.

SERTOLI, E. (1865) Dell'esistenza di particolari cellule ramificate nei canalicoli seminiferi del testicolo umano Morgagni. **7**, 31-40.

SETCHELL, B. P. AND WAITES, G. M. H. (1975) The blood-testis barrier. In: Male reproductive system (eds: Hamilton, D. W. and Greep, R. O.), Section **7**, Handbook of Physiology, Vol. **4**, Washington D. C.: American Physiology Society, pp. 143-172.

SETCHELL, B. P. (1980) The functional significance of the blood-testis barrier. J. Androl. **1**, 3-10.

SETCHELL, B. P. AND BROOKS, D. E. (1988) Anatomy, vasculature, innervation and fluids in the male reproductive tract. In: The physiology of reproduction (eds: Knobil, E. and Neil, J.). Raven Press, New York, pp. 735-835.

SHIMEK, R. L. (1988) The functional morphology of Scaphopod captacula. Veliger **30**, 213-221.

SHOUP, J. R. (1967) Spermiogenesis in wild type and in a male sterility mutant of Drosophila melanogaster. J. Cell Biol. **32**, 663-676.

SOUSA, M., CORRAL, L. AND AZEVEDO, C. (1989) Ultrastructural and cytochemical study of spermatogenesis in Scrobicularia plana (Mollusca, Bivalvia). Gamete Res. **24**, 393-401.

STEP, E. (1951) Shell life. An introduction to British mollusca. Frederick Warne and Co. Ltd., London & New York. pp. 403-435.

SUMMERS, R. G. (1970) A new model for the structure of The centriolar satellite complex in spermatozoa. J. Morph. **137**, 229-242.

SZÖLLÖSI, A. AND MARCAILLOU, C. (1977) Electron microscope study of the blood-testis barrier in an insect: Locusta migratoria. J. Ultrastruct. Res. **59**, 158-172.

TAKAICHI, S. AND SAWADA, N. (1973) An electron microscope study on sperm formation in Euhadra hickonis. Memoirs Ehime University series B (Biology). **7**, 17-34.

TAKAICHI, S. AND DAN, J. C. (1977) Spermiogenesis in the pulmonate snail Euhadra hickonis. I. Acrosome formation. Develop. Growth and Differ. **19**, 1-14.

TAKAHAMA, H., KINOSHITA, T., SATO, M. AND SASAKI, F. (1991) Fine structure of the spermatophores and their ejaculated forms, sperm reservoirs, of the Japanese common squid, Todarodes pacificus. J. Morph. **207**, 241-251.

TAKEDA, N. (1989) Hormonal centrol of reproduction in land snail. Venus **48**, 99-139.

THIÉRY, J. P. (1967) Mise en évidence des polysaccharides sur coupes fines en microscopie électronique. J. Microscopié. **6**, 987-1018.

THOMAS, R. F. (1975) The reproductive system of Bursatella leachi plei (Opisthobranchia, Aplysiacea) with special reference to its histology. Malacologia **15**, 113-121.

THOMPSON, T. E. (1961) The structure and mode of functioning of the reproductive organs of Tritonia hombergi (Gastropoda, Opisthobranchia). Quart. J. Microsc. Sci. **102**, 1-14.

THOMPSON, T. E. (1966) Studies on the reproduction of Archidoris pseudoargus (Rapp) (Gastropoda, Opisthobranchia). Phil. Trans. Roy. Soc. Lond. B. **250**, 343-375.

THOMPSON, T. E. (1971) Application to molluscan ultrastructure research of the Balzers 360M Freeze-Etching Plant. Veliger **13**, 367-368.

THOMPSON, T. E. (1973) Euthyneuran and other molluscan spermatozoa. Proc. Fourth Europ. Malac. Congr., Malacologia **14**, 167-206.

THOMPSON, T. E. (1975) Dorid nudibranchs from eastern Australia (Gastropoda, Opisthobranchia). J. Zool. London. **176**, 477-517.

THOMPSON, T. E. (1976) Biology of Opisthobranch molluscs. Vol. I. The Ray Society. pp. 1-197.

THOMPSON, T. E. AND BEBBINGTON, A. (1969) Structure and function of the reproductive organs of three species of Aplysia (Gastropoda: Opisthobranchia). Malacologia **7**, 347-380.

THOMPSON, T. E. AND BEBBINGTON, A. (1970) A new interpretation of the structure of the Aplysiid spermatozoon (Gastopoda, Opisthobranchia). Arch. Zool. Exp. Gen. **111**, 213-216.

TILNEY, L. G., BRYAN, J., BUSH, D. J., FUJIWARA, K., MOOSEKER, M. S., MURPHY, D. B. AND SNYDER, D. H. (1973) Microtubules: evidence for 13 protofilaments. J. Cell Biol. **59**, 267-275.

TUNG, P. S. AND FRITZ, I. B. (1978) Specific surface antigens of rat pachytene spermatocytes and successive classes of germinal cells. Dev. Biol. **64**, 297

TUZET, O. (1930) Recherches sur la spermatogenése des prosobranches. Arch. Zool. Exp. Gén. **70**, 95-229.

TUZET, O. (1939) La spermiogénèse d'Aplysia depilans Linné. Arch. Zool. Exp. Gén. **81**, 130-138.

VITALE, R., FAWCETT, D. W. AND DYM, M. (1973) The normal development of the blood-testis barrier and the effects of clomiphens and estrogen treatment. Anat. Rec. **176**, 333-344.

VOGL, A. W. AND SOUCY, L. J. (1985) Arrangement and possible function of actin filament bundles in ectoplasmic specializations of ground squirrel Sertoli cells. J. Cell Biol. **100**, 814-825.

VYE, M. V. AND FISCHMAN, D. A. (1971) A comparative study of three methods for the ultrastructural demonstration of glycogen in thin sections. J. Cell Sci. **9**, 727-749.

WADE, J. B. AND KARNOVSKY, M. J. (1974) Fractures faces of osomotically distrupted zonulae occludentes. J. Cell Biol. **62**, 344-350.

WAITES, G. M. H. AND GLADWELL, R. T. (1982) Physiological significance of fluid secretion in the testis and blood-testis barrier. Physiol. Rev. **62**, 624-671.

WALKER, M. H. AND MACGREGOR, H. C. (1968) Spermatogenesis and the structure of the mature sperm in Nucella lapillus (L.). J. Cell Sci. **3**, 95-104.

WEBSTER, P. M. AND RICHARDS, K. S. (1977) Spermiogenesis in the enchytraeid Lumbricillus rivalis (Oligochaeta: Annelida). J. Ultratruct. Res. **61**, 62-77.

WELCH, J. E. AND O'RAND, M. G. (1985) Identification and distribution of actin in spermatozogenic cells and spermatozoa of the rabbit. Dev. Biol. **109**, 411-417.

WELLS, M. J. (1977) Cephalopoda: Octopoda. In: Reproduction of marine invertebrates. (Eds: A. Giese and J. Pearse, eds.). Academic Press. pp. 291-336.

WILSON, E. B. (1904a) Experimental studies in germinal localization. I. The germ-regions in the egg of Dentalium. J. Exp. Zool. **1** (1): 1-72.

WILSON, E. B. (1904b) Experimental studies in germinal localization. II. Experiments on the cleavage-mosaic in Patella and Dentalium. J. Exp. Zool. **1**, 197-268.

WOLOSEWICK, J. J. AND BRYAN, J. H. (1977) Ultrastructural characterization of the manchette microtubules in the seminiferous epithelium of the mouse. Am. J. Anat. **150**, 301-332.

WOODARD, T. M. (1940) The function of the apyrene sperm of Goniobasis. J. Exp. Zool. **85**, 103-126.

WOUTERS-TYROU, D., MARTIN-POLDTHIEA, A., RICHARD, A., SAUTIERE, D. (1988) Charaterization of the nuclear basic proteins specific of spermiogenesis in cuttlefish, Sepia officinalis. Biochimica et Biophysica Acta. **953**, 86-94.

YASUZUMI, G., TANAKA, H. AND TEZUKA, O. (1960) Spermatogenesis in animals as revealed by electron microscopy. VIII. Relation between the nutritive cells and the developing spermatids in a pond snail, Cipangulopaludina malleata Reeve. J. Biophys. Biochem. Cytol. **7**, 499-504.

YASUZUMI, G. (1974) Electron microscope studies on spermiogenesis in various animal species. Int. Rev. Cytol. **37**, 53-119.

YASUZUMI, G., TAKAHASHI, Y., NISHIMURA, Y., YAMAGISHI, N., YAMAMOTO, H. AND YAMAMOTO, K. (1974) Spermatogenesis in animals as revealed by electron microscopy. XXVIII. Development of flagella of spermatozoa of Limax flavus L. Okajimas Folia Anatomica Japonica **51**, 11-28.

PART II

FIGURE PLATES

The originals for these plates are stored at the Department of Anatomy, University of Glasgow and may be examined there.

Sheng Tao Hou

30TH AUGUST 1991

FIGURES FOR CHAPTER I

FIGURE 1.

A transverse section through the testicular region of Antalis entalis, showing testicular follicules lying between the longitudinal muscle bands, kidney and large mantle cavity.

(Mag. x.75).

ABBREVIATIONS: K, kidney; M, mantle cavity;
Mu, muscle band; T, testis.

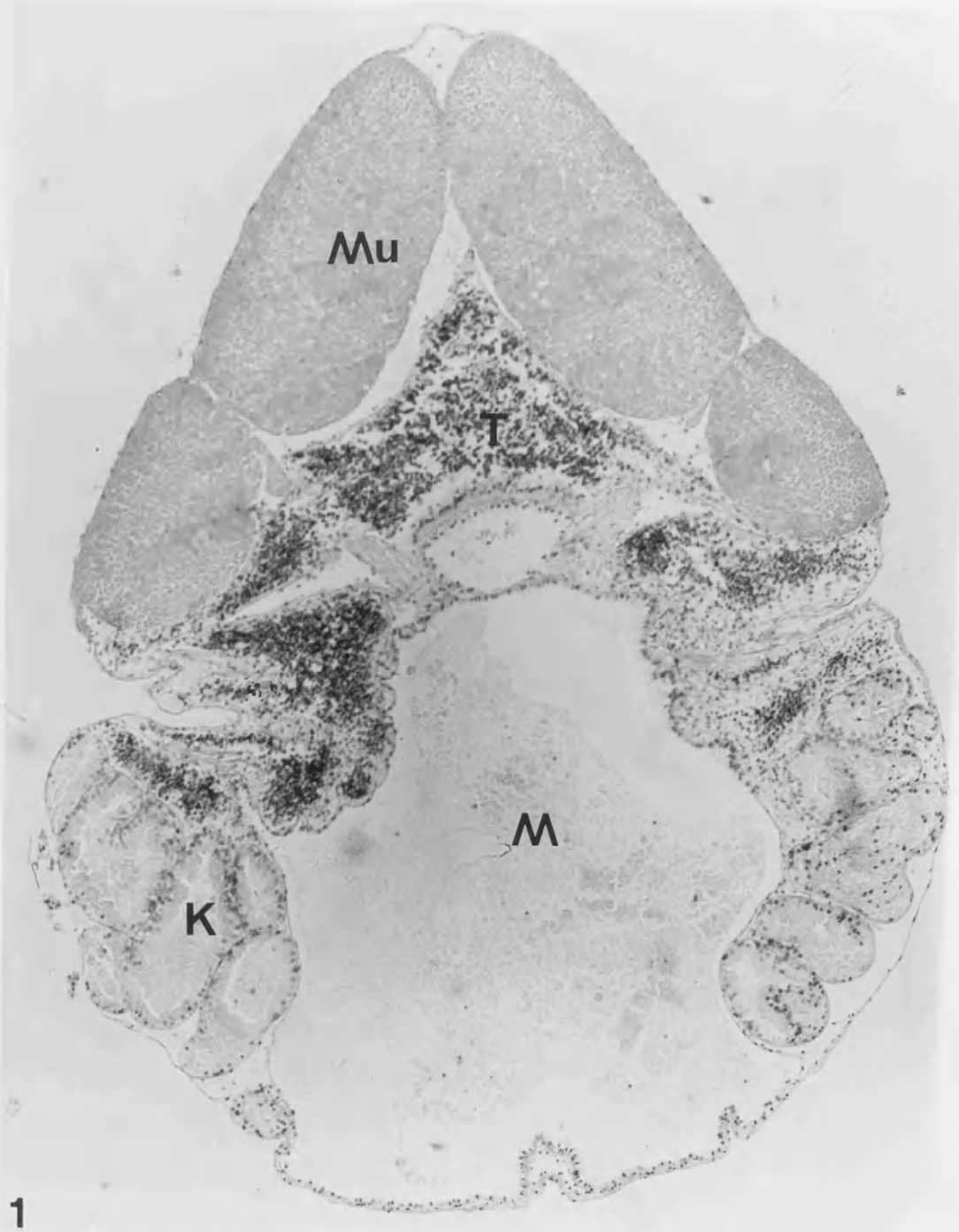

1

FIGURES 2 AND 3.

Sections of wax (FIGURE 2) and resin embedded (FIGURE 3) testes of Antalis entalis showing developing spermatogenic cells within a testicular follicle. The rectangule in Figure 2 is enlarged to demonstrate the ultrastructure of the basal lamina with a loose outer and dense inner layers.

(Mags.: FIGURE 2, x.240; inset, x.14,000; FIGURE 3, x.260).

ABBREVIATIONS: B, basal lamina; Sc, spermatocyte; Sd spermatid; Sg, spermatogonium; Sz, spermatozoon.

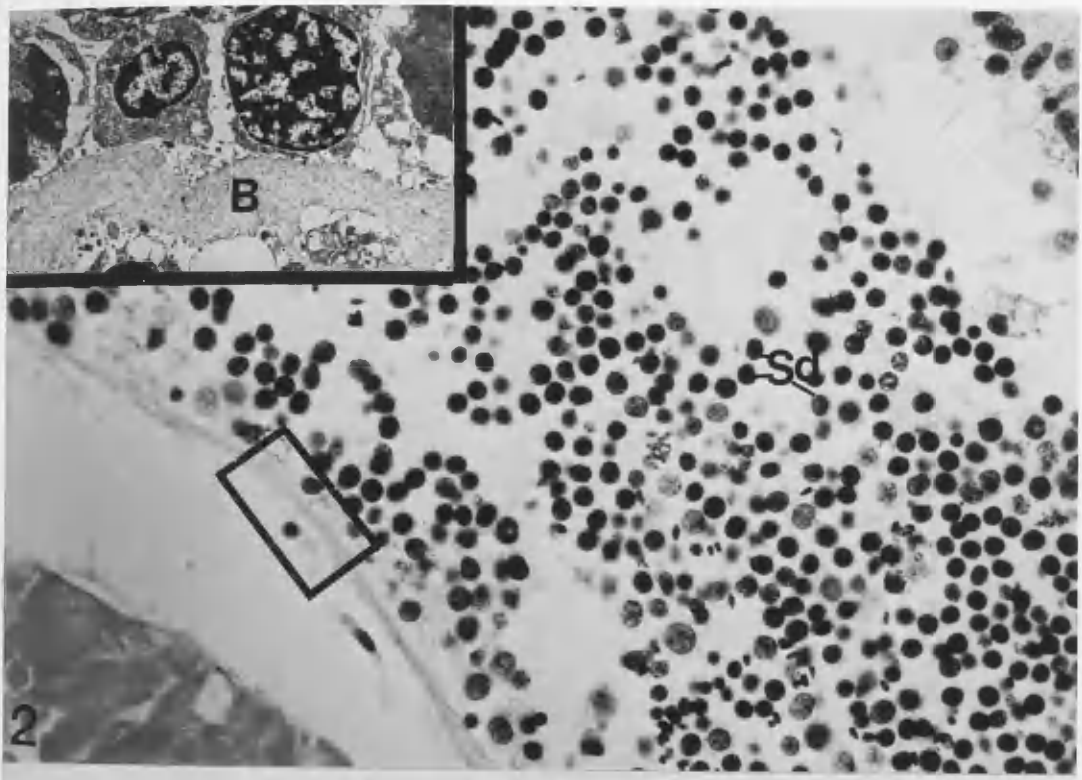
B
Sd
2

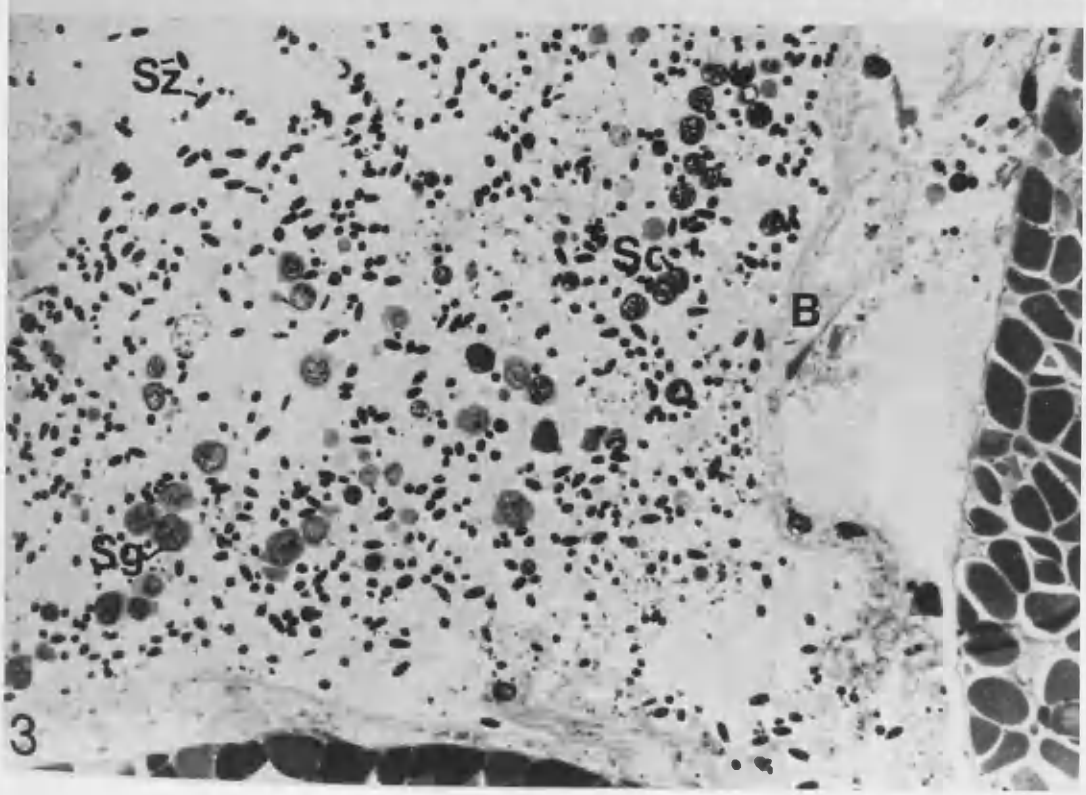
Sz
Sc
B
Sg
3

FIGURES 4, 5 AND 6.

Scanning electron micrographs of spermatozoa taken from testicular follicles, showing the acrosome (A) capping the elongate nucleus (Nu), five spherical mitochondria (M) and the cranial end of the tail (Tl). Arrowheads in Figures 5 and 6 indicate the invaginated pit of the acrosome.

(Mag.: FIGURE 4, x. 25,000; FIGURE 5, x. 25,000; FIGURE 6, x.75,000).

FIGURE 7.

A longitudinal thin section through the apex of the spermatozoan head showing the invaginated pit of the acrosome (arrowhead).

(Mag. x.45,000).

ABBREVIATIONS: A, acrosome; Nu, nucleus;
M, mitochondrion; Tl, tail.

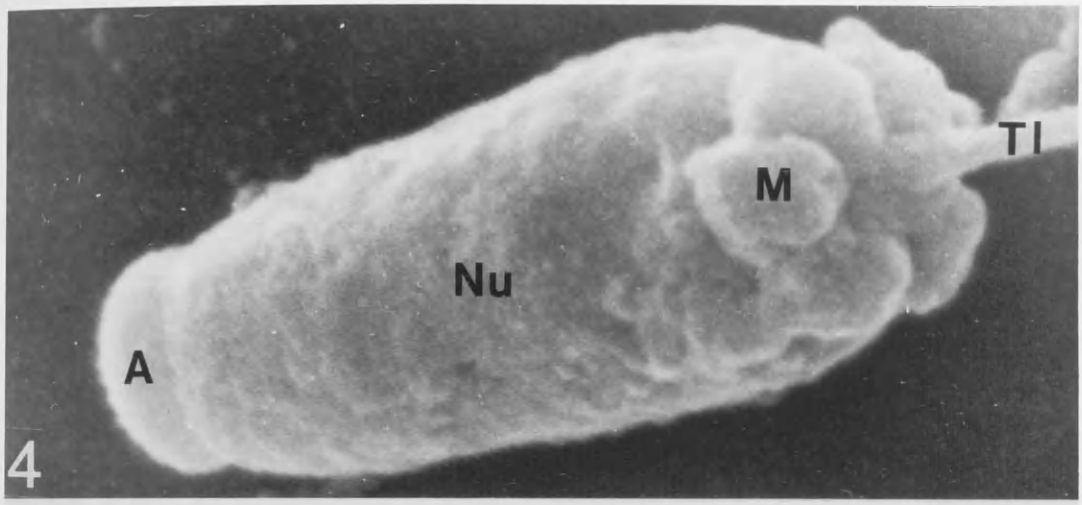

4

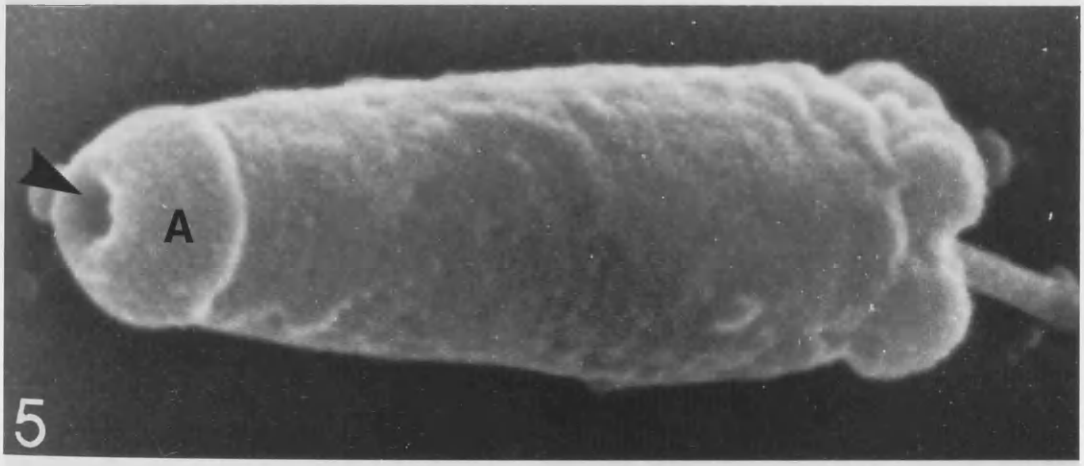

5

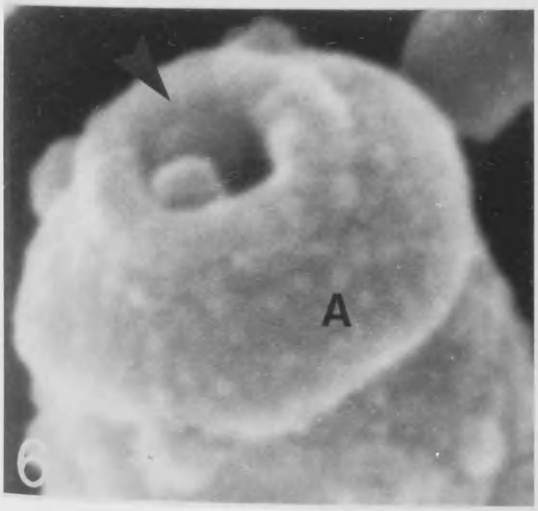

6

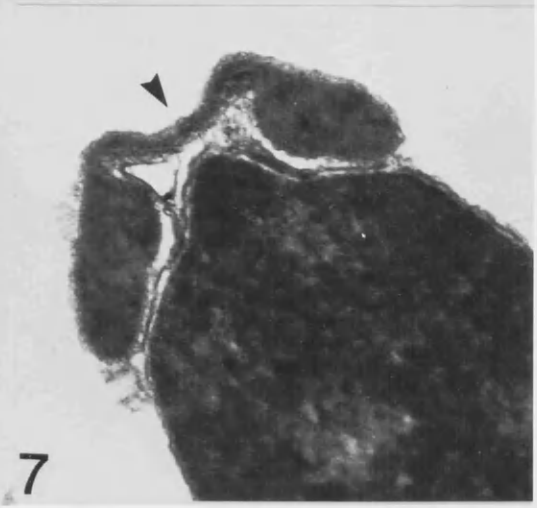

7

FIGURE 8.

A longitudinal section through the spermatozoan head, midpiece and cranial end of the tail. Arrowheads indicate the arms of the distal centrolar satellite.
(Mag. x.25,300).

FIGURES 9, 10 AND 11.

TEM micrographs of transverse sections through the acrosome (FIGURE 9), nucleus (FIGURE 10) and mitochondrial midpiece (FIGURE 11).
(Mags.: FIGURE 9, x.42,350; FIGURE 10, x.17,500; FIGURE 11, x.25,800).

FIGURES 12, 13 AND 14.

Longitudinal sections through the mitochondrial midpiece. Note the perpendicularly orientated distal and proximal centrioles, distal centriolar satellite (arrowheads in FIGURES 12 and 13).
(Mags.: FIGURE 12, x.21,000; FIGURE 13, x.35,000; FIGURE 14, x.35,000).

ABBREVIATIONS: A, acrosome; D, distal centriole;
N, nucleus; M, mitochondrion;
P, proximal centriole; T, tail.

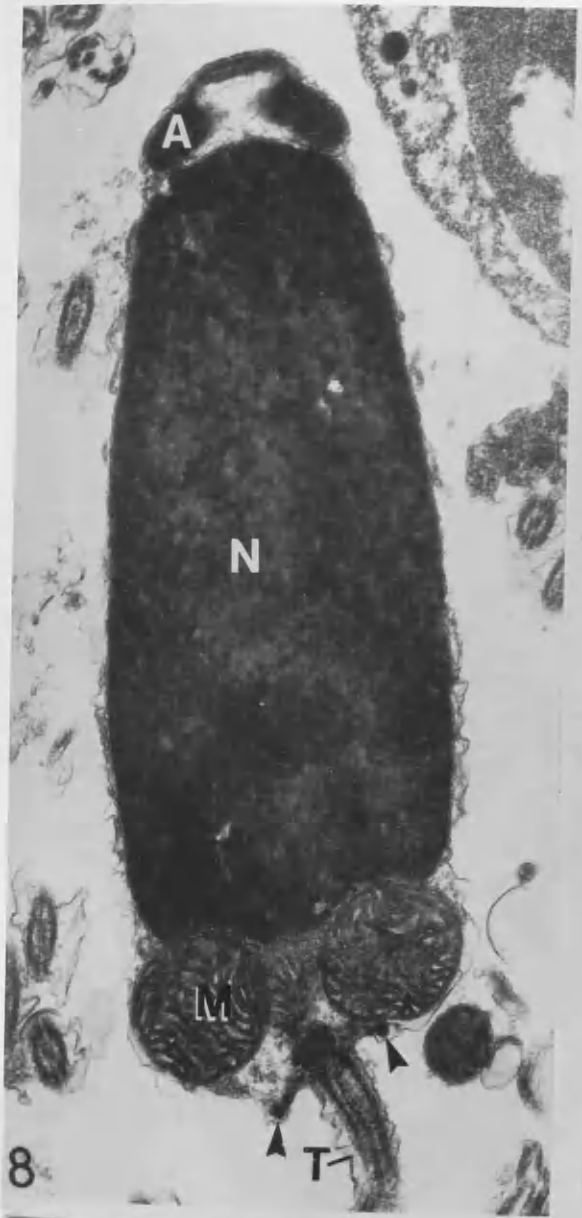

8

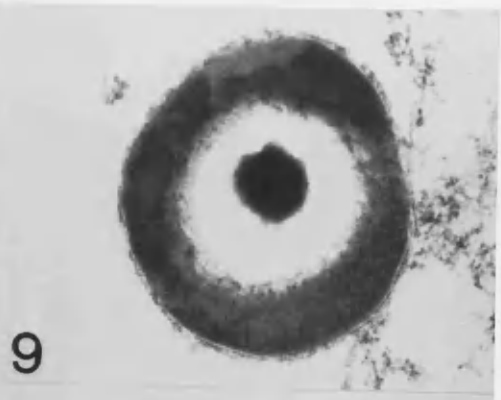

9

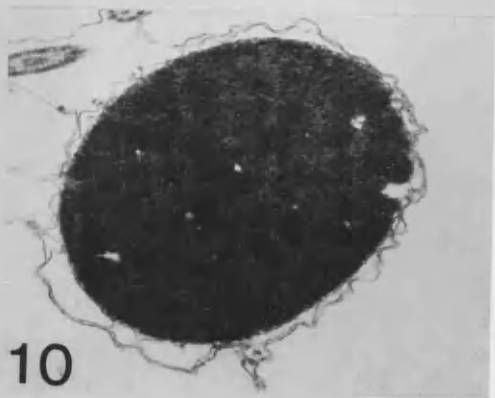

10

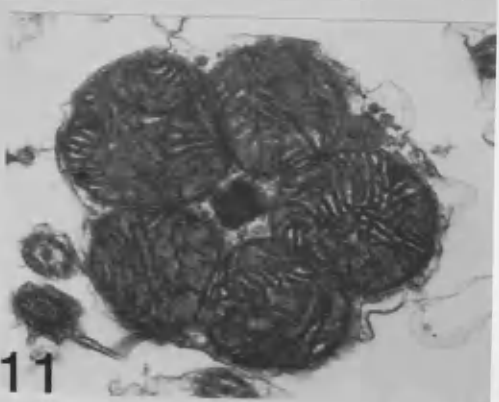

11

12

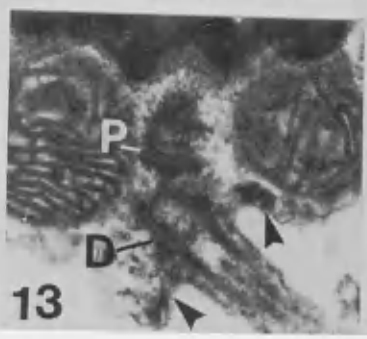

13

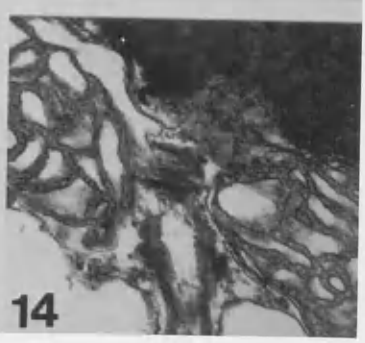

14

FIGURE 15.

A PA-TSC-SP treated thin section of a late spermatid. Dark glycogen granules (arrowheads) occur around mitochondria.

(Mag. x.44,000).

FIGURE 16.

A transverse section through the distal centriole showing the nine microtubular triplet structure.

(Mag. x.128,000).

FIGURES 17, 18 AND 19.

Transverse sections through the centriolar region showing the nine arms of the distal centriolar satellite (FIGURES 17 and 18) and their branched Y-shaped terminations (arrowhead in FIGURE 19).

(Mags.: FIGURE 17, x.70,000; FIGURE 18, x.21,000; FIGURE 19, x.28,000).

FIGURES 20 AND 21.

Transverse sections through the tail illustrating the typical "9 + 2" microtubular axoneme. Arrowheads indicate the spokes between the A and the central tubules.

(Mags.: FIGURE 20, x.157,000; FIGURE 21, x.55,000).

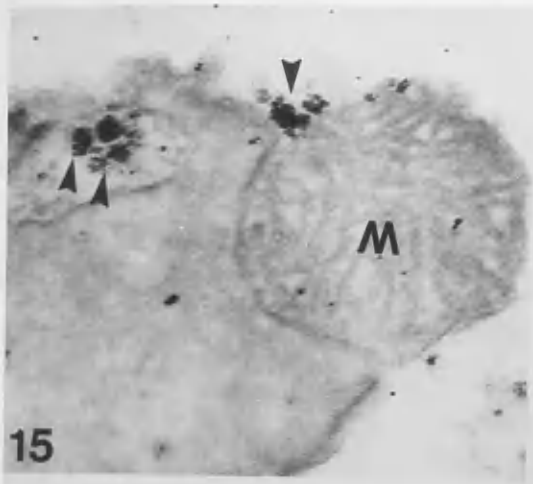

15

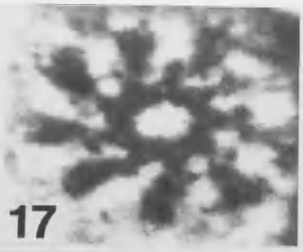

17

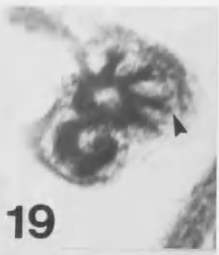

19

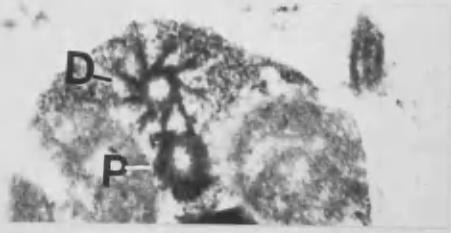

18

16

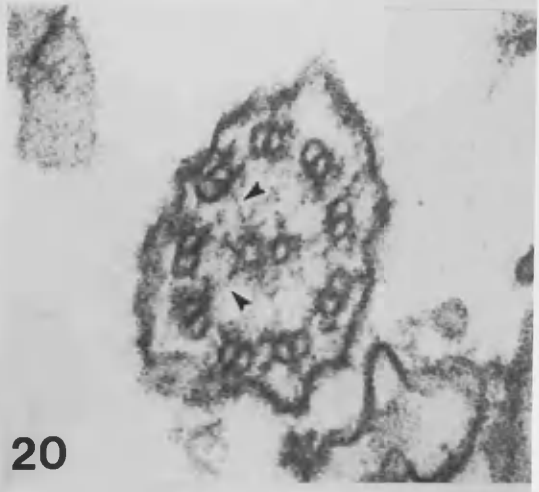

20

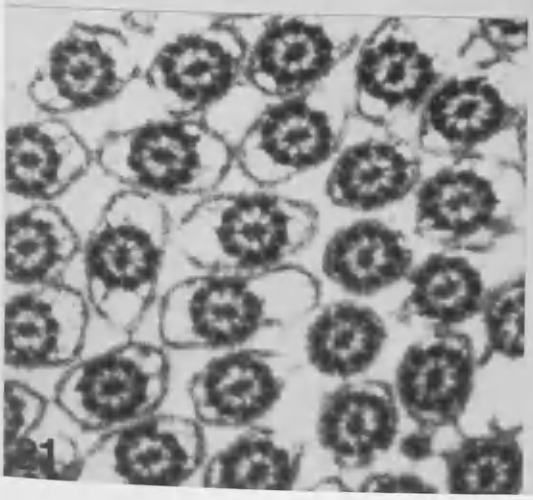

21

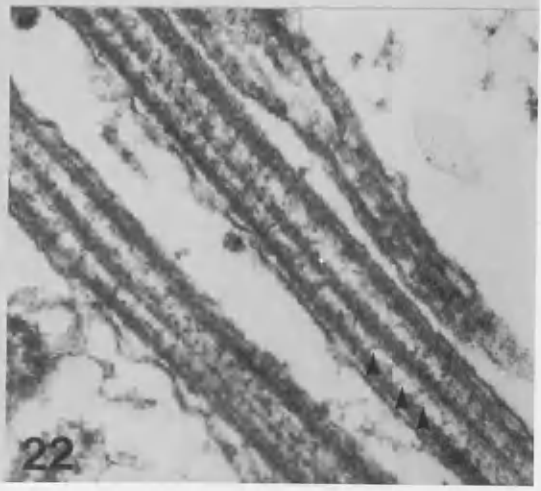

22

FIGURE 22.

Longitudinal sections of the tail showing arrays of spokes (arrowheads) between the central tubules and peripheral doublets.

(Mag. FIGURE 22, x.48,000).

ABBREVIATIONS: D, distal centriole; M, mitochondrion; P, proximal centriole.

FIGURE 23.

TEM micrograph of part of the testis. Developing spermatogenic cells form small groups close to the luminal side of the basal lamina in a testicular follicle.

(Mag. x.45,000).

ABBREVIATIONS: B, basal lamina;

Sc, spermatocyte;

Sd, spermatid;

Sz, spermatozoon.

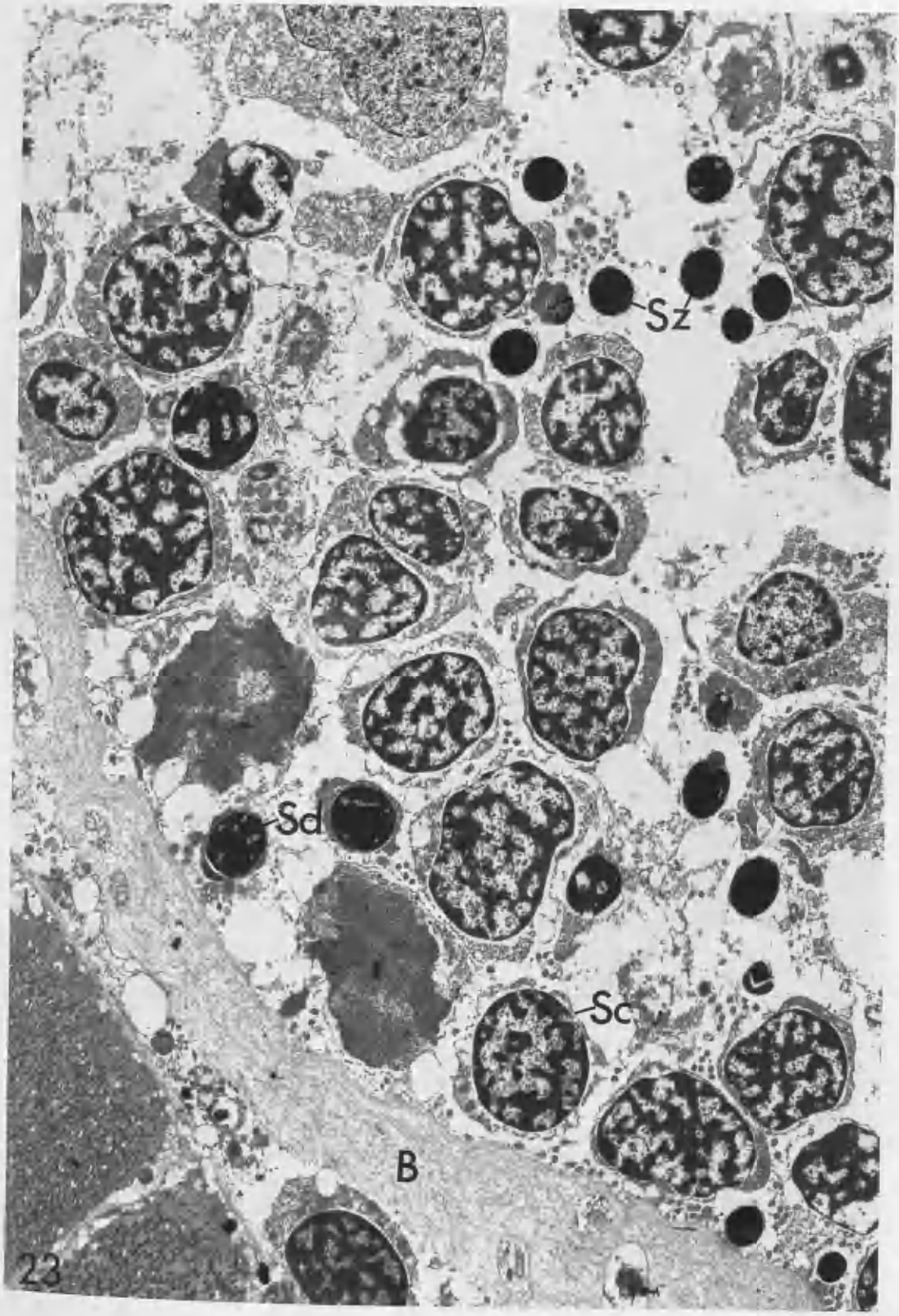
Sz
Sd
Sc
B
23

FIGURE 24.

A thin section of a spermatogonium with a prominent nucleolus and a large number of small mitochondria scattered in the cytoplasm.

(Mag. x.9,500).

FIGURE 25.

An enlargement of the nucleolus in the nucleus of a spermatogonium.

(Mag. x.35,000).

FIGURE 26.

A secondary spermatocyte with diffuse heterochromatin in the nucleus (Nu). The mitochondria (M) are small.

(Mag. x.11,000).

FIGURE 27.

Two nuclei (Nu) of early spermatids occur within a single mass of cytoplasm.

(Mag. x.6,125).

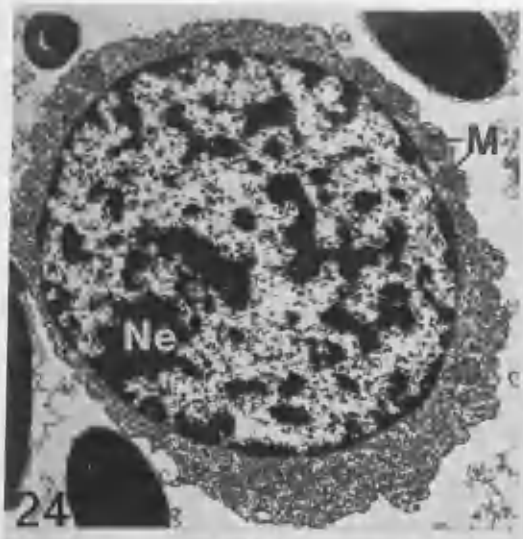

24

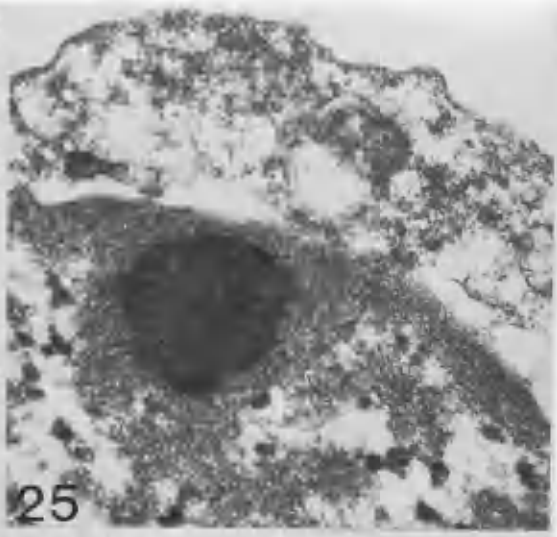

25

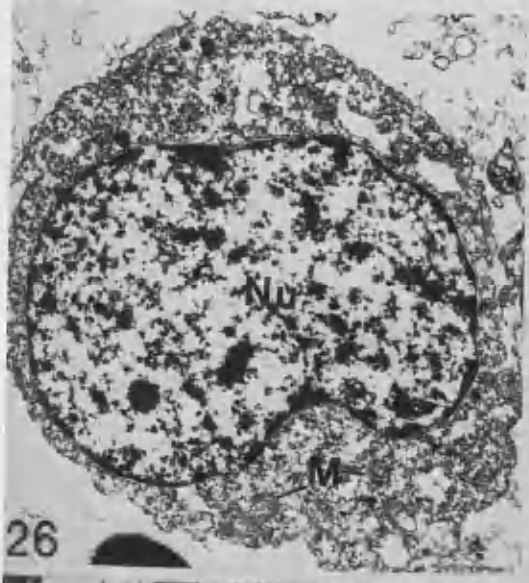

26

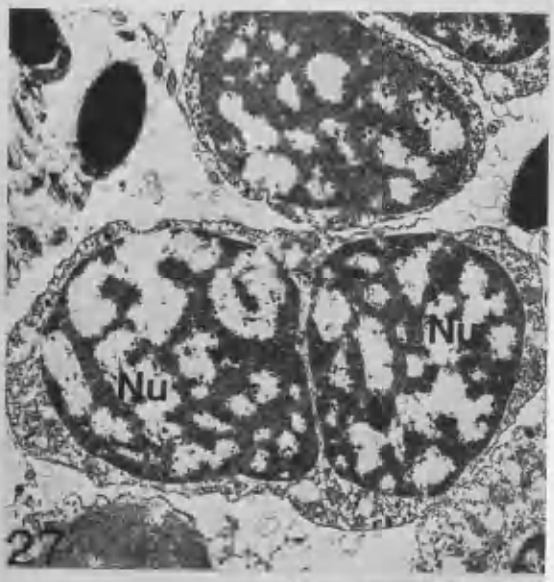

27

8

29

FIGURES 28 AND 29.

Sections through early (FIGURE 28) and late (FIGURE 29) spermatids, showing the granular heterochromatin (arrowheads in FIGURE 28 & inset) aggregating into an almost homogeneous state (FIGURE 29 & inset). Because of uneven chromatin condensation, small nuclear cavities remain (FIGURE 29).

(Mags.: FIGURE 28, x.11,800; inset, x.80,000; FIGURE 29, x.13,000; inset, x.90,000).

ABBREVIATIONS: G, Golgi complex; M, mitochondrion;
Nu, nucleus; NC, nuclear cavity;
Ne, nucleolus;

FIGURES 30, 31, 32, 33 AND 34.

Ultrathin sections of developing early spermatids (FIGURES 30 and 31) and late spermatids (FIGURES 32, 33 and 34). Nuclear morphogenesis results in a change from an oval shape (FIGURE 30) to an elongate one (FIGURES 33 and 34). The proacrosomal granule is in close relation to mitochondria, the axoneme and plasmalemma in the early spermatid (FIGURES 30 and 31) where the granular heterochromatin is still diffuse. Once the mitochondria are attached to the base of the nuclear envelope and increase in size (FIGURE 31), the proacrosome starts to move towards the presumptive anterior pole of the spermatid. FIGURES 32, 33 and 34 show further condensation and elongation of the nucleus of the late spermatid and the loss of excess cytoplasm.

(Mags.: FIGURE 30, x.11,000; FIGURE 31, x.15,000; FIGURE 32, x.14,000; FIGURE 33, x.15,000; FIGURE 34, x.16,000).

30

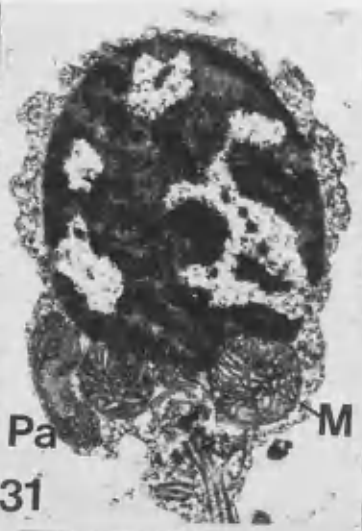

31

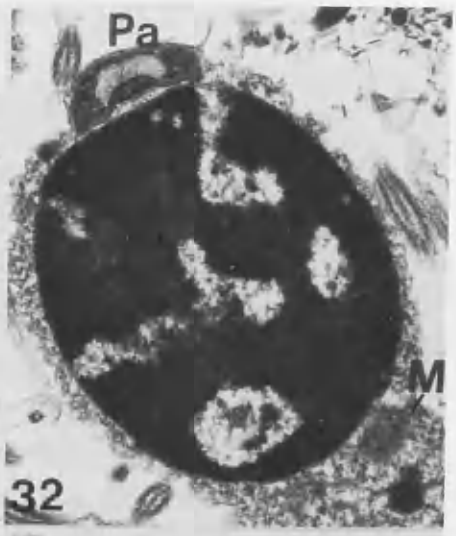

32

33

34

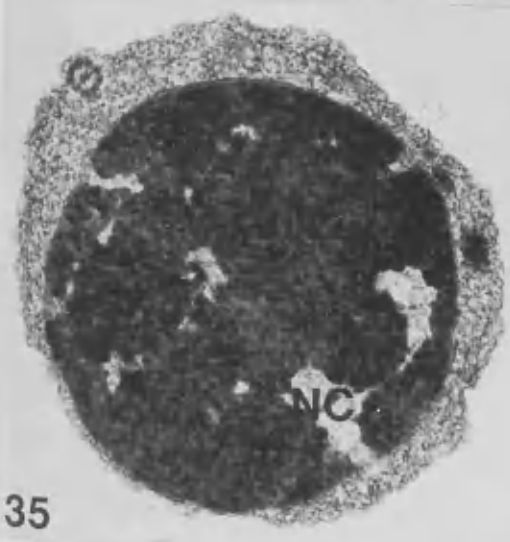

35

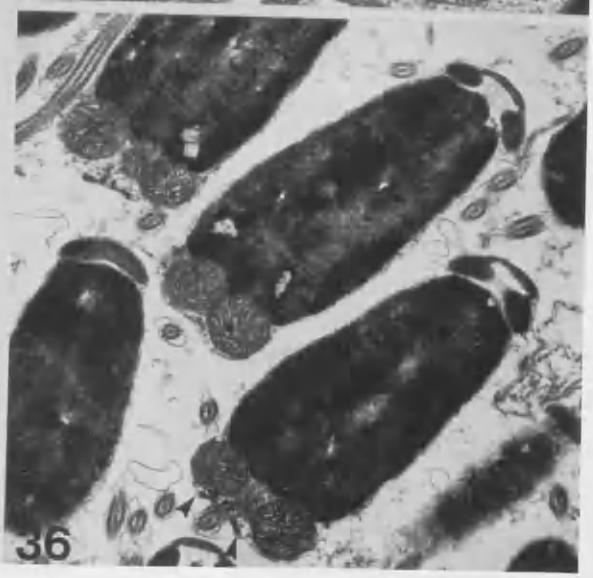

36

FIGURE 35.

A transverse section through the nucleus of a late spermatid. Note the prominent nuclear cavity.
(Mag. x.24,000).

FIGURE 36.

Longitudinal sections of several spermatozoa. The nucleus is further condensed. The proximal centriole and distal centriolar satellite with radial arms (arrowheads) are fully established at this developmental stage.
(Mag. x.11,000).

ABBREVIATIONS: Ax, axoneme; M, mitochondrion;
N, nucleus; NC, nuclear cavity;
Pa, proacrosome.

FIGURES 37, AND 38.

The proacrosome is secreted by the Golgi complex (G) which is in close association with mitochondria and the axoneme in the early spermatid. Both electron dense and lucent granules occur (arrowheads in FIGURE 38) The distal centriole (D) at this stage lacks a supporting satellite body (FIGURE 37).

(Mags.: FIGURES 37 and 38, x.32,000).

FIGURES 39, 40, 41, 42, 43 AND 44.

Electron dense granules and lucent vesicles (arrowheads in FIGURE 39) fuse to form a proacrosomal granule (Pa) (FIGURES 40 and 41). During the course of migration from the posterior to anterior pole of the spermatid, the electron-dense zone (arrow in FIGURE 40) becomes closely related to the nucleus and gradually disperses to form a layer of dense fibrous material (arrows in FIGURES 42 and 44). The proacrosome undergoes significant morphogenesis, changing from a spherical (FIGURES 40 and 41) to a cup-shape with an inverted central pit (arrowhead) into the underlying acrosomal fossa (FIGURE 44). Note a glycogen granule close to the acrosome.

(Mags.: FIGURE 39, x.45,000; FIGURE 40, x.40,000; FIGURE 41, x.38,000; FIGURE 42, x.41,000; FIGURE 43, x.27,000; FIGURE 44, x.32,000).

ABBREVIATIONS: Ax, axoneme; Af, acrosomal fossa; D, distal centriole; N, nucleus; G, Golgi complex; g, glycogen granule.

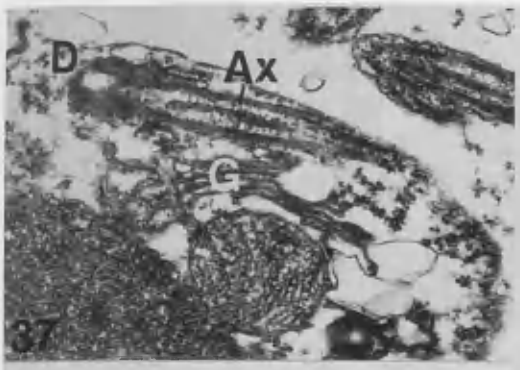
D
Ax
C
37

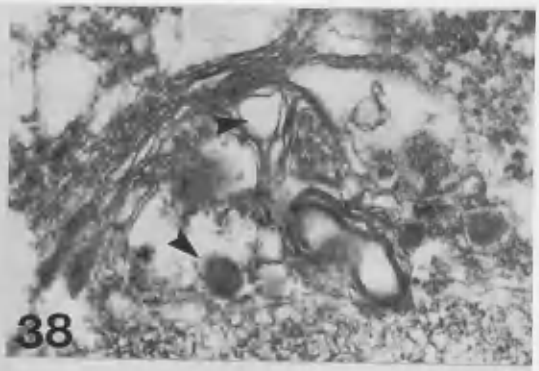
38

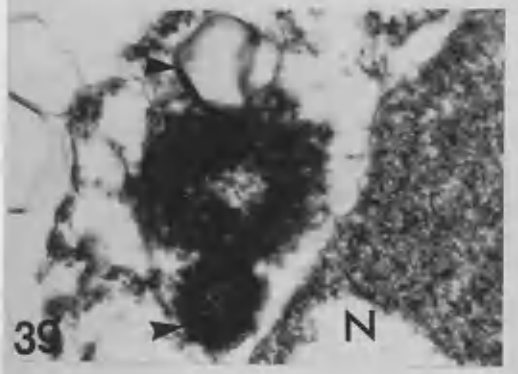
N
39

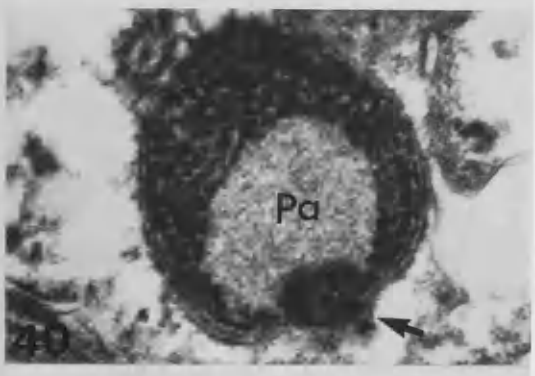
Pa
40

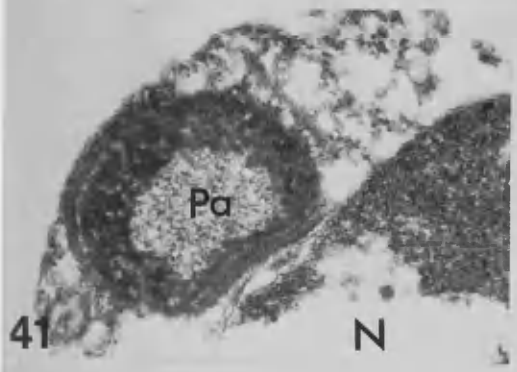
Pa
N
41

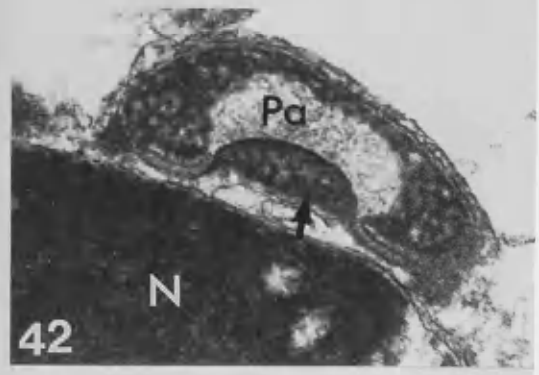
Pa
N
42


N
43


Af
g
N
44

FIGURES FOR CHAPTER II

FIGURE 1.

A transverse section of part of the testis of Rossia macrosoma, showing testicular tubules with a large number of developing spermatogenic cells in the luminal aspect of the tubule.

(Mag. x.200).

FIGURE 2.

An enlargement of part of three testicular tubules. A group of spermatogonia overlay the basement membrane. External to the basement membrane, small blood vessels occur in the interstitial connective tissue.

(Mag. x.310).

FIGURE 3.

A TEM micrograph of the basal portion of a testicular tubule, showing the basal lamina with a thickened inner layer and a loose outer layer. Note the blood vessel.

(Mag. x.8,800).

ABBREVIATIONS: B, basal lamina; Bl, blood vessel;
Sc, spermatocyte; Sd, spermatid;
Sg, spermatogonium; Sz, spermatozoon.

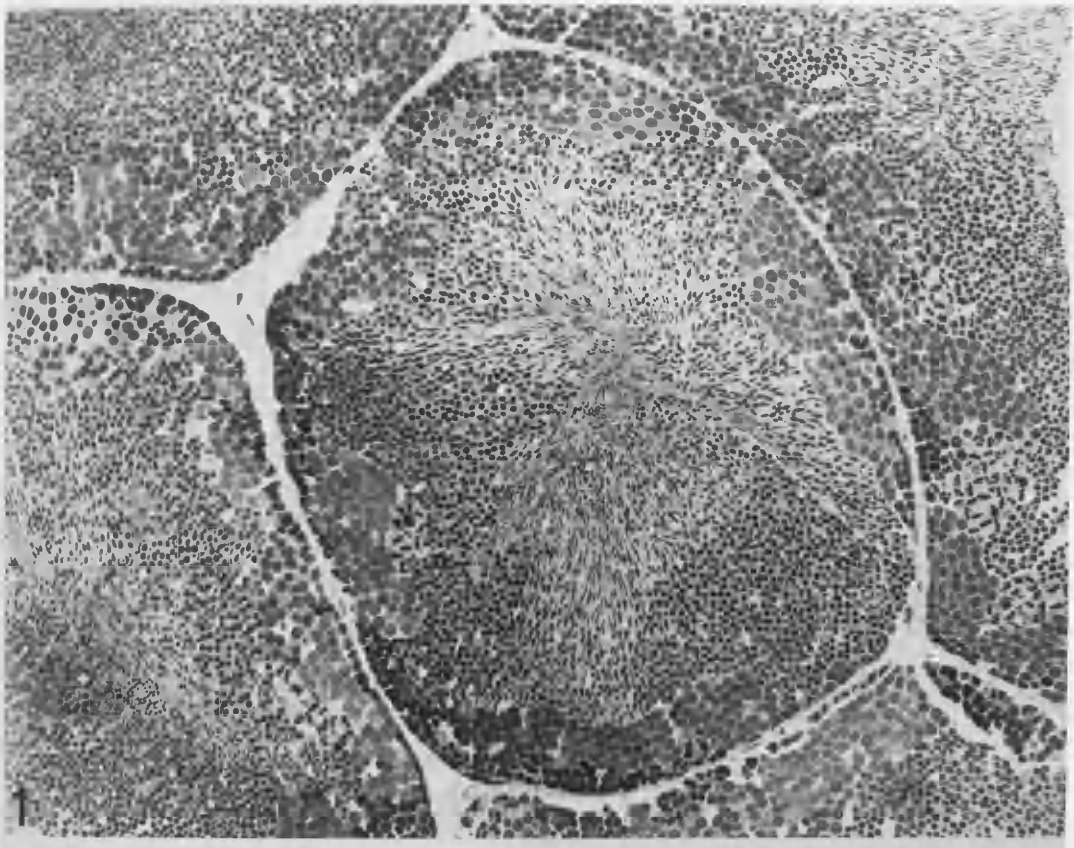
1

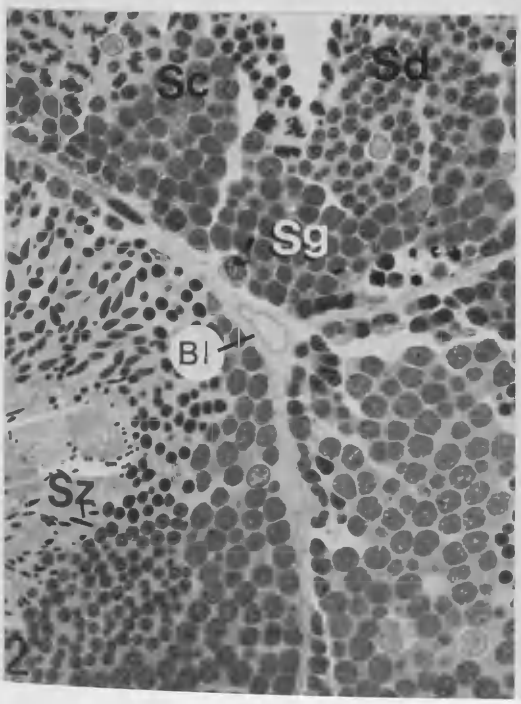

2

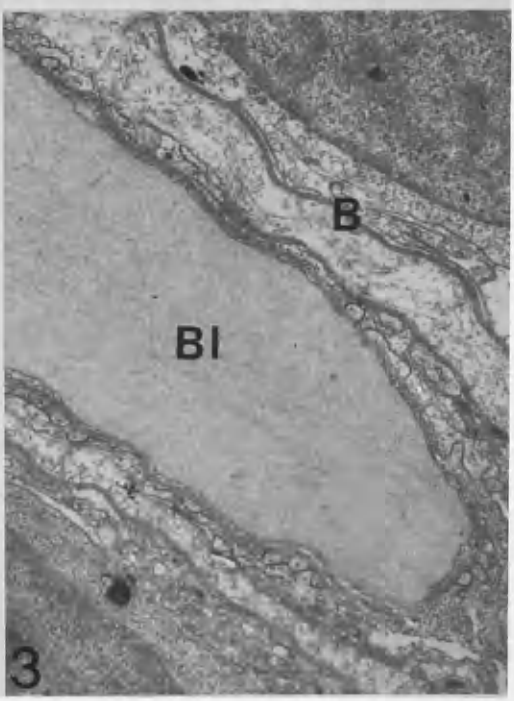

3

FIGURES 4, 5 AND 6.

Scanning electron micrographs of spermatozoa collected from the vas deferens. The spermatozoon consists of an elongate acrosome, nucleus and a mitochondrial sleeve. (Mags.: FIGURE 4, x.12,000; FIGURE 5, x.8,000; FIGURE 6 , x.20,000).

ABBREVIATIONS: A, acrosome; M, mitochondrial sleeve; N, nucleus; T, tail.

4

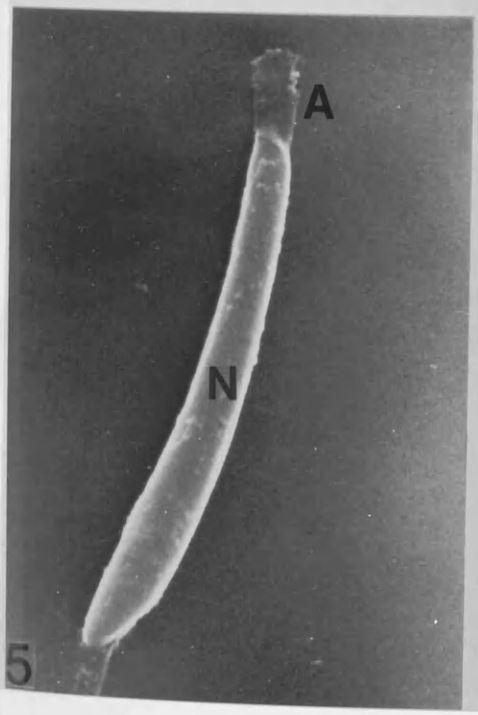

5

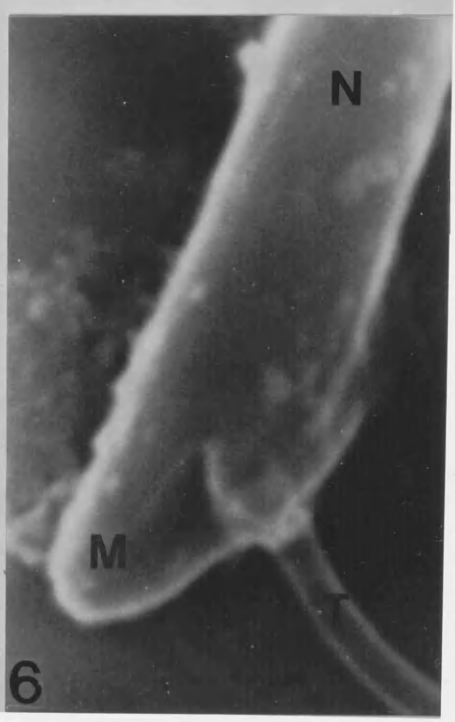

6

FIGURES 7, 8 AND 9.

Thin sections of a group of developing secondary spermatocytes. The nucleus at this stage is still spherical with a large amount of heterochromatin. Mitochondria remain small.

(Mags.: FIGURE 7, x.4,800; FIGURE 8, x.8,750; FIGURE 9, x.7,000).

FIGURE 10.

A thin section of two adjacent spermatids which are connected by an intercellular bridge (arrowheads) which is enlarged in the inset.

(Mags.: FIGURE 10, x.20,000; inset, x.25,000).

ABBREVIATIONS: N, nucleus; M, mitochondrion.

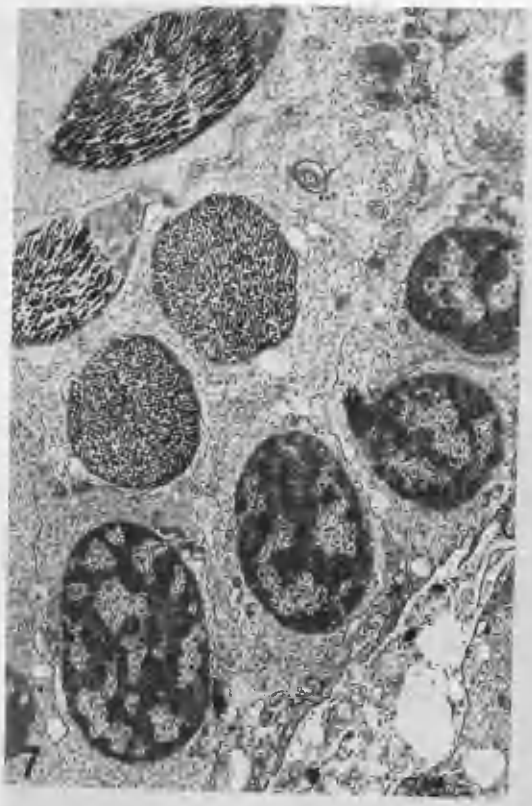

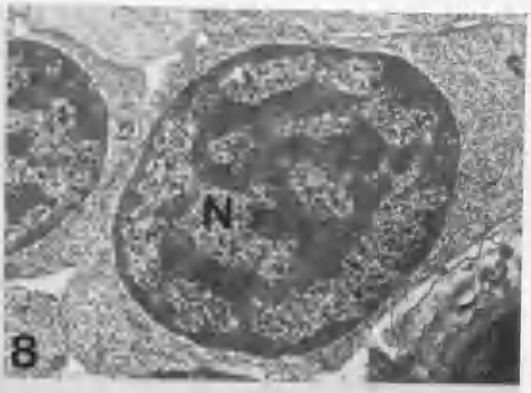
N

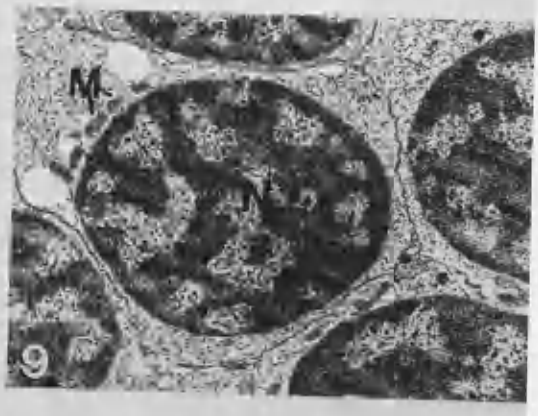
M
N

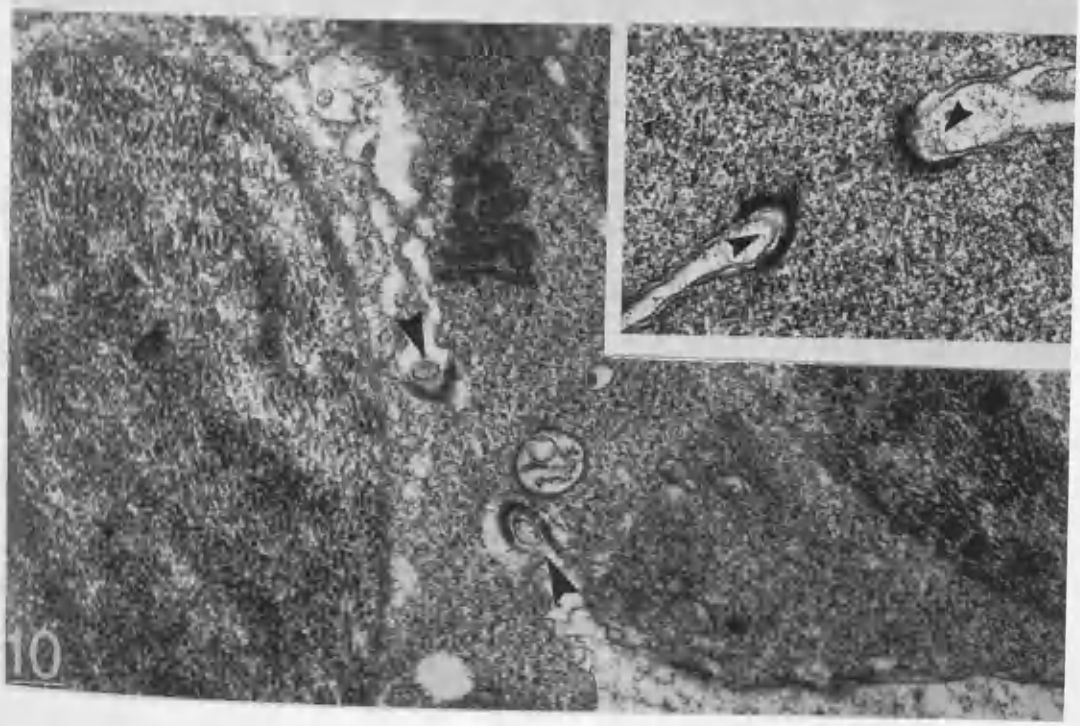

FIGURE 11.

A longitudinal thin section of a stage A spermatid. Chromatin forms thin fibrils and the nucleus starts elongation. The proacrosome caps the apex of the nucleus. (Mag. x.8,500).

FIGURE 12.

A transverse section of a stage A spermatid. Microtubules (arrowheads) forming a manchette are in close association with the nuclear envelope.
(Mag. x.58,000).

FIGURE 13.

An oblique section through the microtubular manchette. The section is stained with 1% tannic acid showing arrays of parallel arranged microtubules (arrowheads).
(Mag. x.36,000).

FIGURE 14.

A longitudinal section of a stage B spermatid. Chromatin fibrils aggregate into thin filaments and the nucleus further elongates.
(Mag. x.9,000).

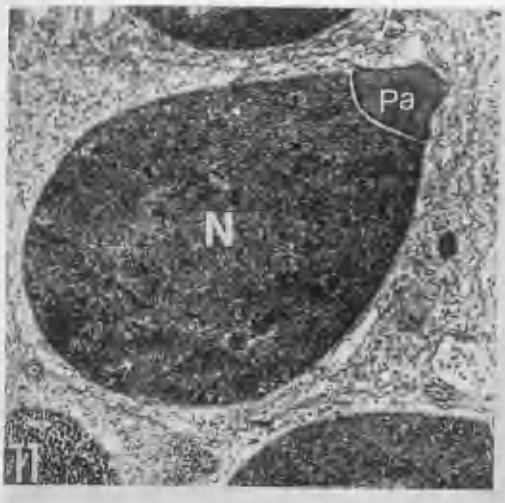
Pa
N
11


12

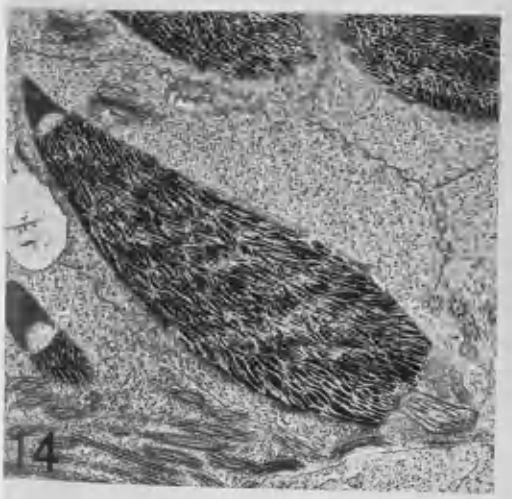
14

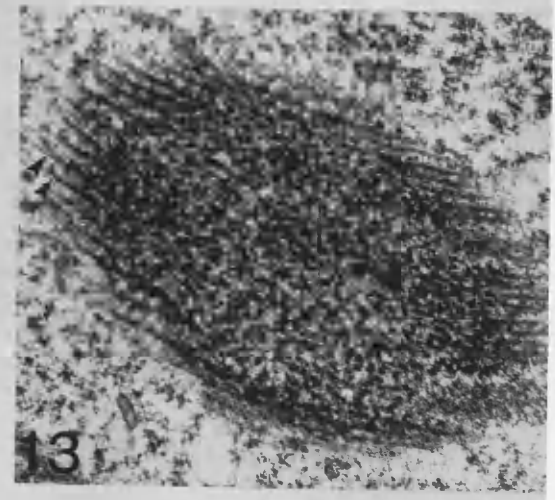
13

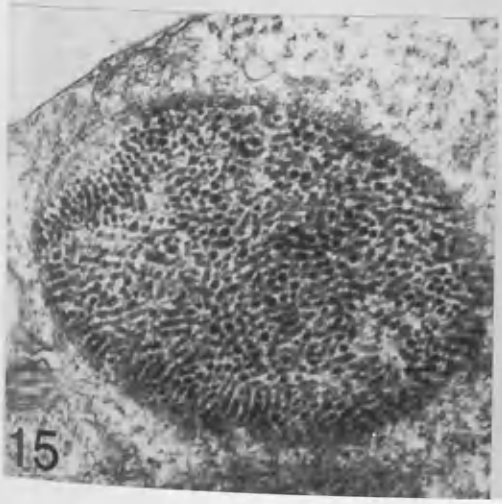
15

FIGURE 15.

A transverse section through the nucleus of an early stage C spermatid. Chromatin filaments are irregularly disposed. The majority lying parallel to the longitudinal axis of the nucleus.

(Mag. x.22,000).

ABBREVIATIONS: N, nucleus; Pa, proacrosome.

FIGURE 16.

An oblique section of a late stage C spermatid. Chromatin filaments condense into thick filaments and are oriented along the longitudinal axis of the nucleus.

(Mag. x.9,400).

FIGURE 17.

An oblique section of the anterior part of the head showing the well developed proacrosome and thick chromatin filaments.

(Mag. x.8,600).

FIGURE 18.

A transverse section of a spermatid at the stage similar to the one in FIGURE 17. The microtubular manchette is still associated with the nuclear envelope, but appears absent at places where there is no occurrence of chromatin filaments (arrowheads).

(Mag. x.36,400).

FIGURE 19.

A transverse section of a late stage C spermatid. Chromatin is almost condensed into a homogeneous state.

(Mag. x.15,000).

ABBREVIATIONS: N, nucleus; Pa, proacrosome.

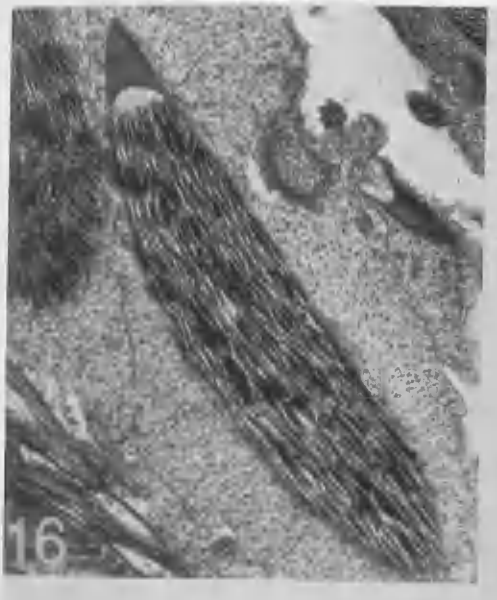
16

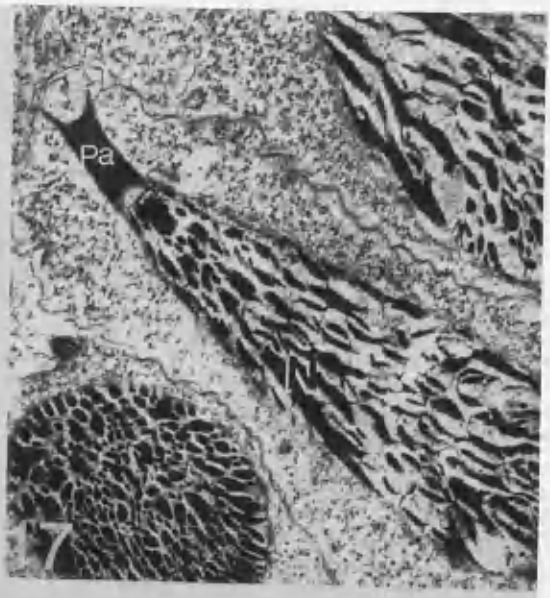
Pa
17

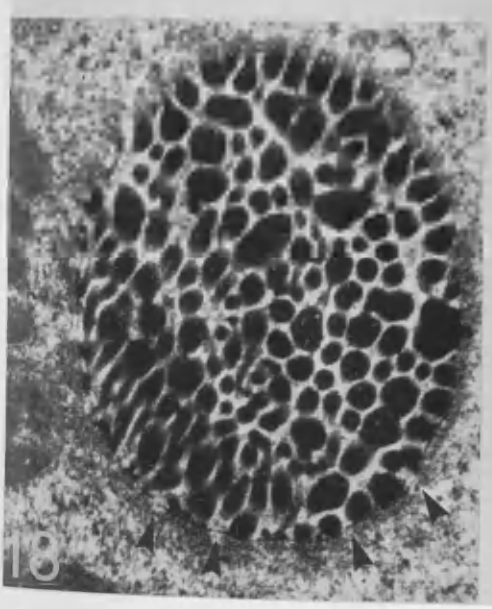
18

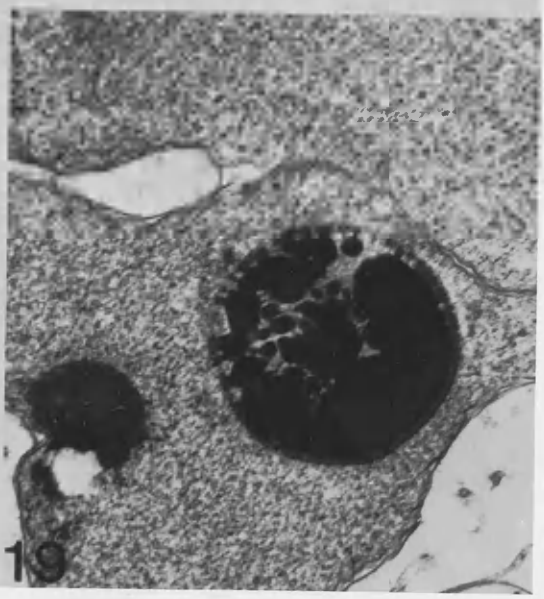
19

FIGURE 20.

A TEM micrograph of a spermatid showing two Golgi complexes. However, only one is involved in the production of a proacrosomal granule.

(Mag. x.50,000).

FIGURE 21.

The Golgi complex is in close association with a group of mitochondria.

(Mag. x.32,000).

FIGURE 22.

One of the Golgi cisternae at the maturing face forms a large proacrosomal granule.

(Mag. x.52,500).

FIGURES 23 AND 24.

The proacrosomal granule settles at the apex of the nucleus and its contents become electron dense. At this stage, the Golgi complex is still closely associated with the proacrosomal granule.

(Mags.: FIGURE 23, x.29,400; FIGURE 24, x.28,500).

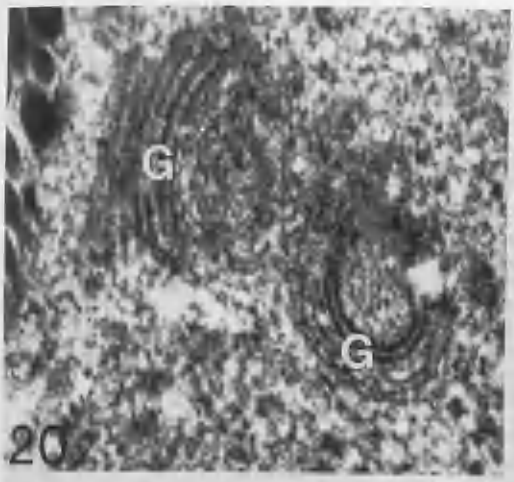
G
G
20

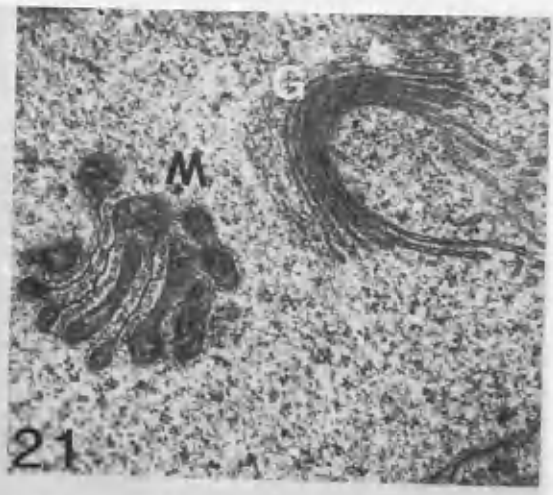
G
M
21

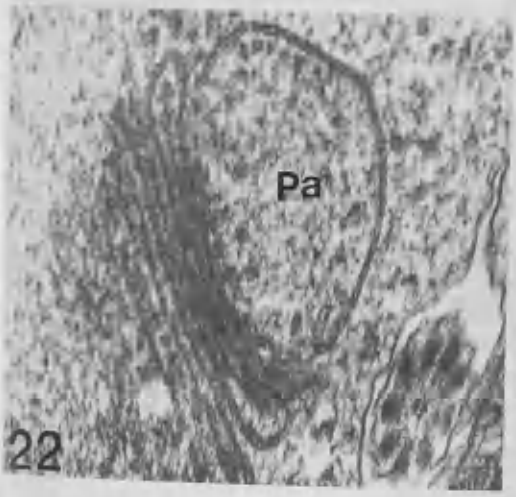
Pa
22

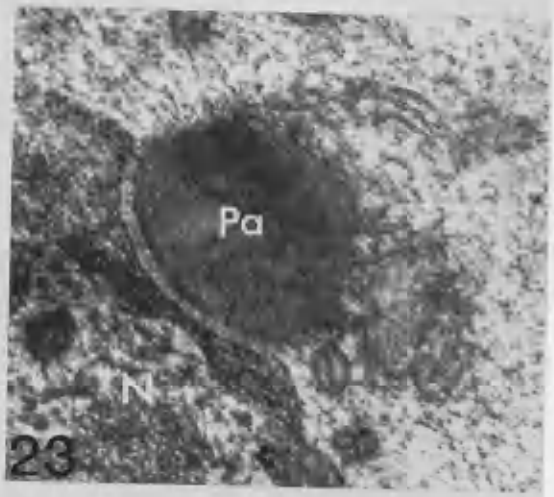
Pa
N
23

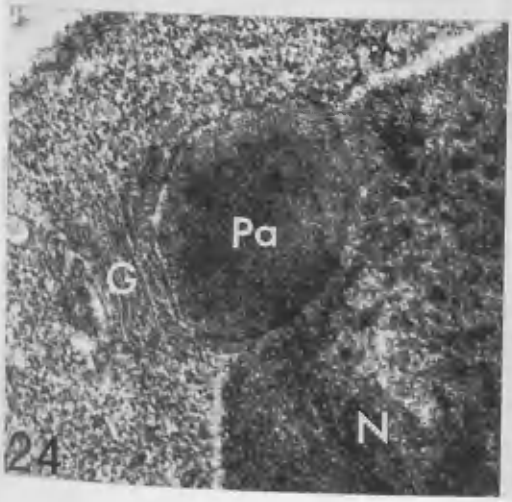
Pa
G
N
24

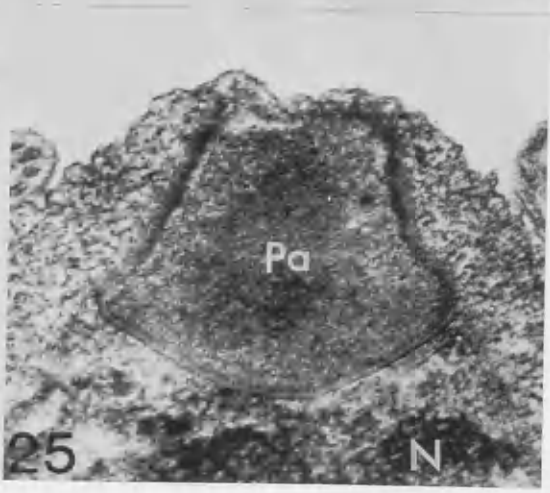
Pa
25
N

FIGURE 25.

The proacrosomal granule changes from a spherical into a trapezoid shape. The Golgi complex disappears. (Mag. x.35,000).

ABBREVIATIONS: G, Golgi complex; M, mitochondria; N, nucleus; Pa, proacrosomal granule.

FIGURES 26 AND 27.

Longitudinal sections throught the anterior region of the head. The proacrosome elongates and an anterior electron lucent vesicle is formed (arrowheads).

(Mags.: FIGURE 26, x.14,000; FIGURE 27, x.20,000).

FIGURES 28 AND 29.

Further development of the proacrosome. The basal aspect of the proacrosome separates from the underlying nucleus forming an electron lucent acrosomal fossa (arrow).

(Mags.: FIGURE 28, x.30,000; FIGURE 29, x.31,000).

FIGURES 30 AND 31.

Longitudinal sections of the proacrosome. The electron dense rod of the proacrosome (between the apical vesicle and acrosomal fossa in FIGURE 30) further differentiates into a thickened, electron dense peripheral layer, close to the acrosomal membrane, and a central less dense region (C). The microtubular manchette surrounds the elongated proacrosome (arrows).

(Mags.: FIGURE 30, x.27,000; FIGURE 31, x.40,000).


26


Ap
N
27

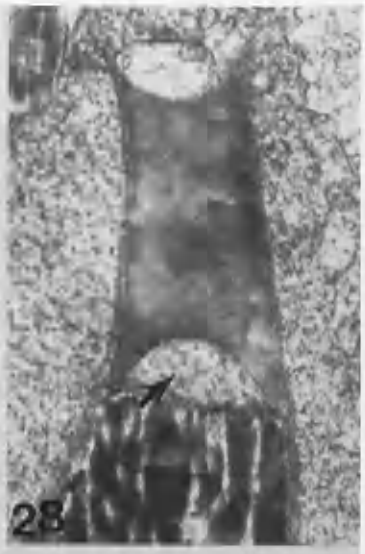
28


29

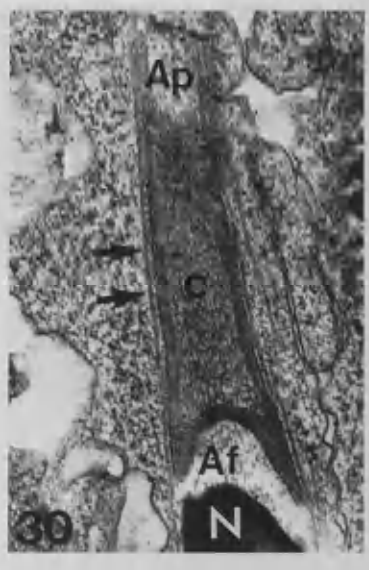
Ap
C
Af
N
30

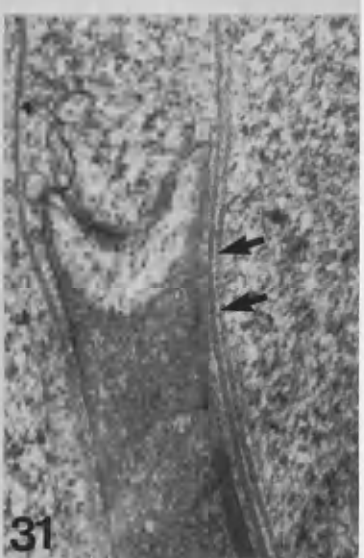
31

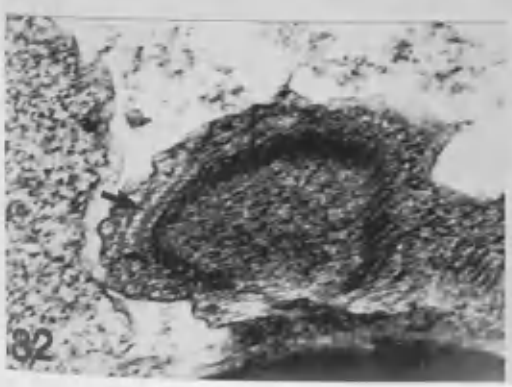
32


Af
33

FIGURE 32.

An oblique section of the proacrosome. The arrow indicates obliqually sectioned microtubules which are in close relation to the proacrosome.

(Mag. x.41,000).

FIGURE 33.

An oblique section of the basal part of the proacrosome, showing the electron lucent acrosomal fossa.

(Mag. x.39,000).

ABBREVIATIONS: Af, acrosomal fossa; Ap, apical vesicle;
C, electron lucent center; N, nucleus.

FIGURE 34.

A transverse section through the midpiece region, showing the microtubular manchette in the midpiece (arrowheads). (Mag. x.60,000).

FIGURE 35.

Mitochondria are closely associated with each other and their matrix becomes electron dense.
(Mag. x.28,500).

FIGURES 36 and 37.

Olique sections of the midpiece region of the spermatid, showing the thickened plasmalemma (arrowheads) of the mitochondrial sleeve which evelopes the cranial end of the flagellum, the proximal, distal centrioles and mitochondrial sleeve.
(Mags.: FIGURE 36, x.49,000; FIGURE 37. x.28,000).

ABBREVIATIONS: Ax, axoneme; D, distal centriole;
M, mitochondrion; N, nucleus;
P, proximal centriole.

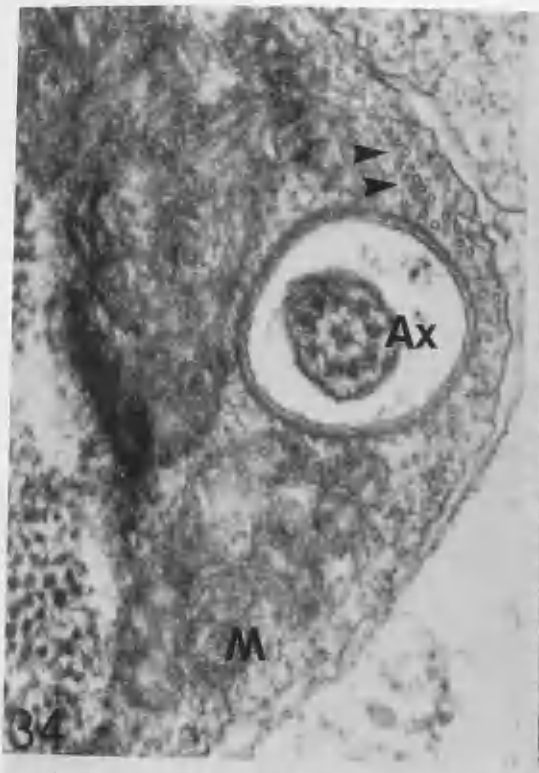
Ax
M
34

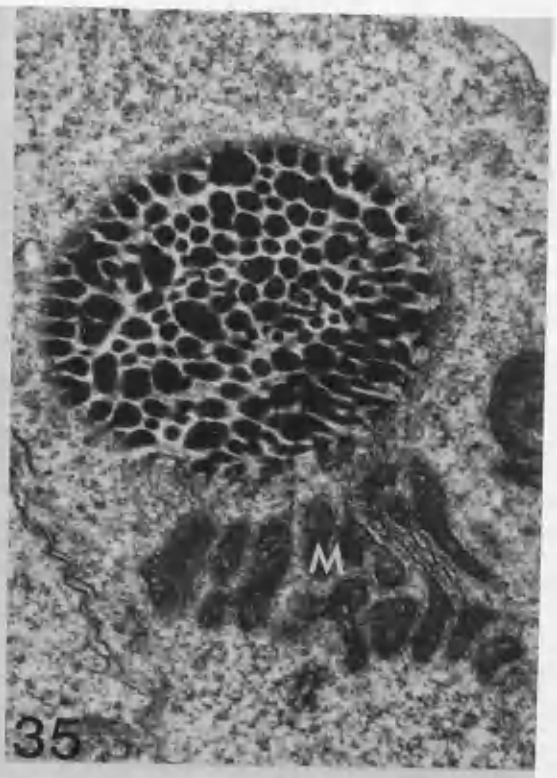
M
35


D
N
Ax
36

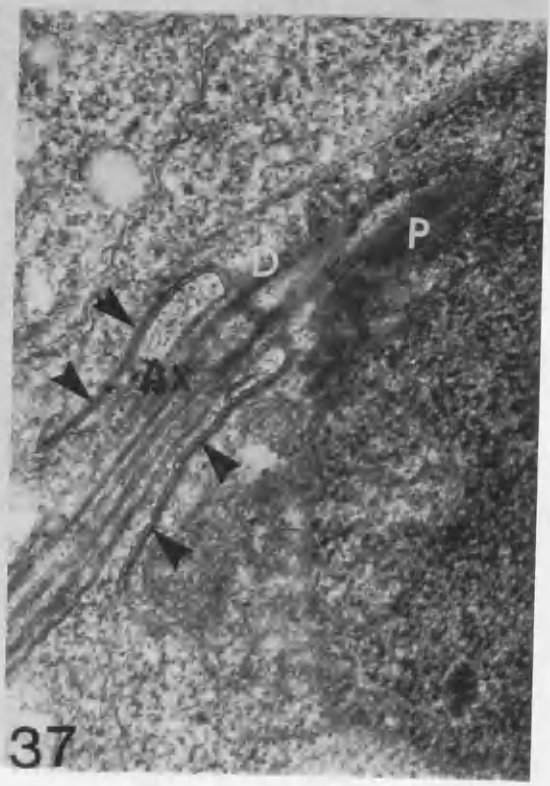
P
D
Ax
37

FIGURE 38.

An oblique longitudinal section of the midpiece region of a spermatid showing the folded membrane system and the centriole in a lateral pit.

(Mag. x.29,560).

FIGURES 39 AND 40.

Transverse sections through AA' (FIGURE 39) and BB' (FIGURE 40) regions in FIGURE 38. Microtubular structures are absent in the distal centriole. Nine electron dense masses occur (FIGURE 39). FIGURE 40 shows a section through the axoneme and associated membranous system. Note electron dense material is deposited on both sides of the plasma membrane limiting the axoneme (arrowheads).

(Mags.: FIGURE 39, x.83,000; FIGURE 40, x.83,000).

FIGURE 41.

A longitudinal section of a stage C spermatid showing the elongate proacrosome, nucleus and lateral centriolar pit (arrow).

(Mag. x.10,920)

ABBREVIATIONS: A, axoneme; D, distal centriole; M, mitochondrion; N, nucleus.

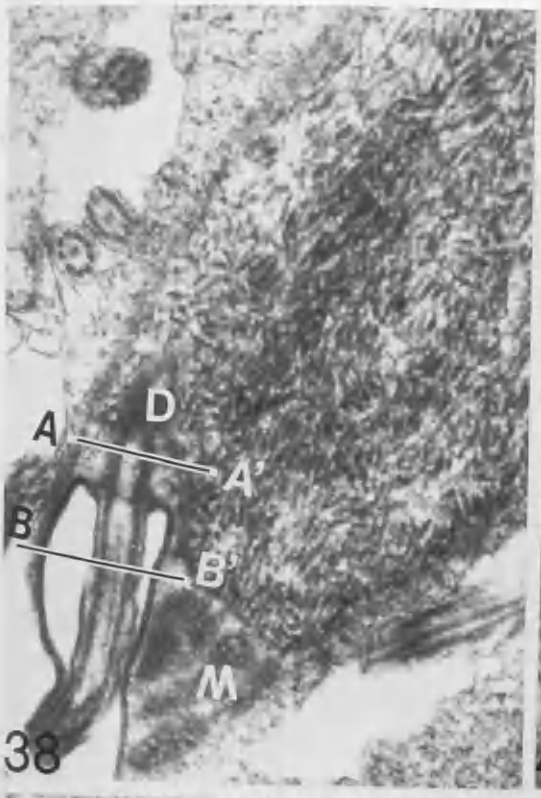
A
D
A'
B
B'
M
38


39


40


Pa
N
41

FIGURE 42.

A longitudinal section through the acrosomal region of a mature spermatozoon collected from the vas deferens. A large apical vesicle is present within the acrosome and the electron dense material has differentiated into a peripheral dense layer (arrowheads) and a electron lucent center (C). The subacrosomal fossa is filled with electron dense granules (arrows).

(Mag. x.25,000).

FIGURE 43.

An oblique section of the acrosome of a mature spermatozoon showing groups of transversely cut longitudinal filaments. Arrowheads indicate the bundles of filaments which are attached to the acrosomal membrane.

(Mag. x.45,000).

FIGURE 44.

An oblique section of the electron dense rod region of the acrosome. Note the longitudinal filaments (arrowheads).

(Mag. x.77,000).

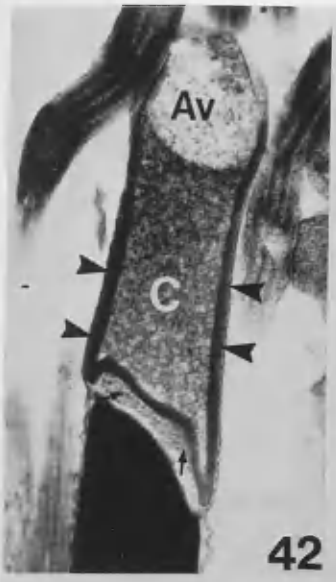
Av
C
42

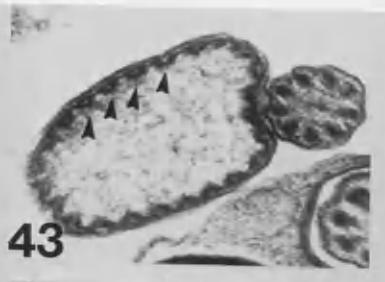
43


M
45


44


N
46


47


48

FIGURE 45.

A transverse section of a spermatozoon through the mitochondrial sleeve showing closely related mitochondria. (Mag. x.25,000).

FIGURE 46.

An oblique section of the distal centriole where no microtubular structures are visible.
(Mag.: x.76,000).

FIGURES 47 AND 48.

Transverse sections of the tail showing the "9 + 2" axoneme (FIGURE 47). At the distal end of the flagellum, the axial structure is lost resulting in a disarray of single tubules (FIGURE 48).
(Mags.: FIGURE 47, x.75,000; FIGURE 48, x.144,000).

ABBREVIATIONS: Av, apical vesicle; C, electron lucent centre; M, mitochondrium; N, nucleus.

FIGURE 49.

A transverse section of the mitochondrial midpiece (stained with PA-TSC-SP for glycogen). Most of the glycogen is distributed close to the sperm plasmalemma (arrowheads).

(Mag. x.74,000).

FIGURE 50.

A longitudinal section of the flagellum, treated with PA-STC-SP, showing glycogen distribution.

(Mag. x.250,000).

FIGURE 51.

A transverse section of the flagellum treated with PA-STC-SP, showing the peri-axonemal and intra-axonemal glycogen distribution.

(Mag. x.240,000).

ABBREVIATIONS: A, axoneme; M, mitochondria.

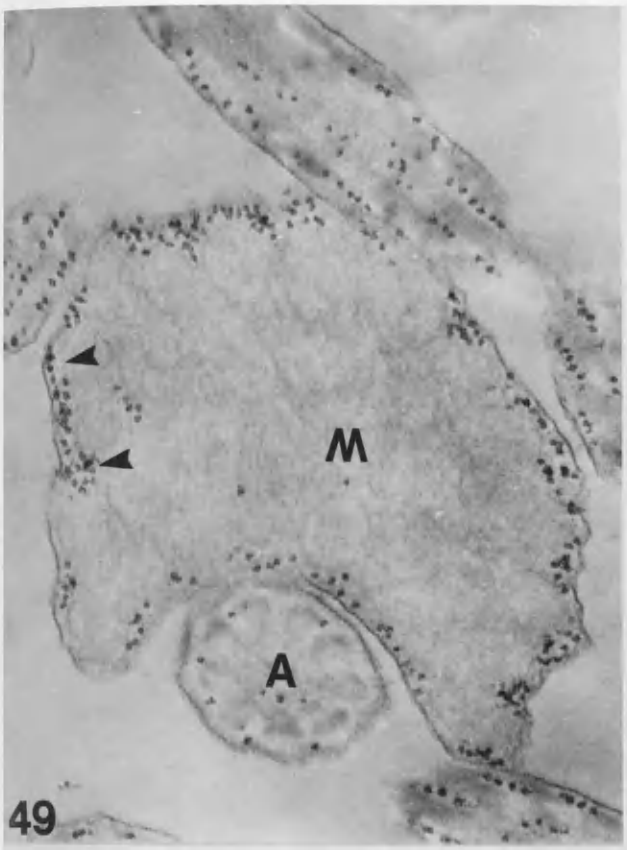
M
A
49


50

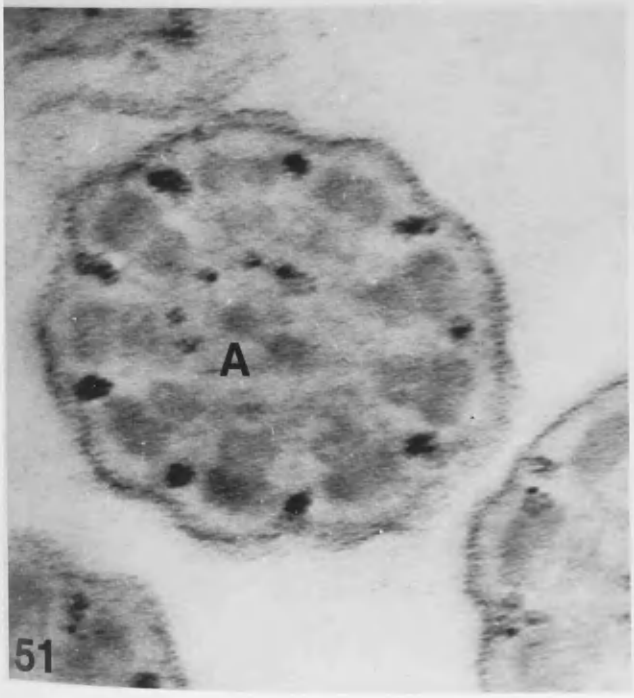
A
51

FIGURES FOR CHAPTER III

FIGURE 1.

A paraffin section of part of the ovotestis of Archidoris tuberculata. Most of the developing oocytes occur peripheral to the developing spermatogenic cells.
(Mag. x.195).

FIGURE 2.

A paraffin section of part of the ovotestis of Tritonia plebeia, showing the centrally located male germ cells and peripheral oocytes.
(Mag. x.200).

FIGURE 3.

A paraffin section of part of the ovotestis of Aplysia faciata. Developing oocytes occur peripheral to centrally located male germ cells.
(Mag. x.195).

ABBREVIATIONS: O, oocyte; T, spermatogenic cell;
D, digestive gland.

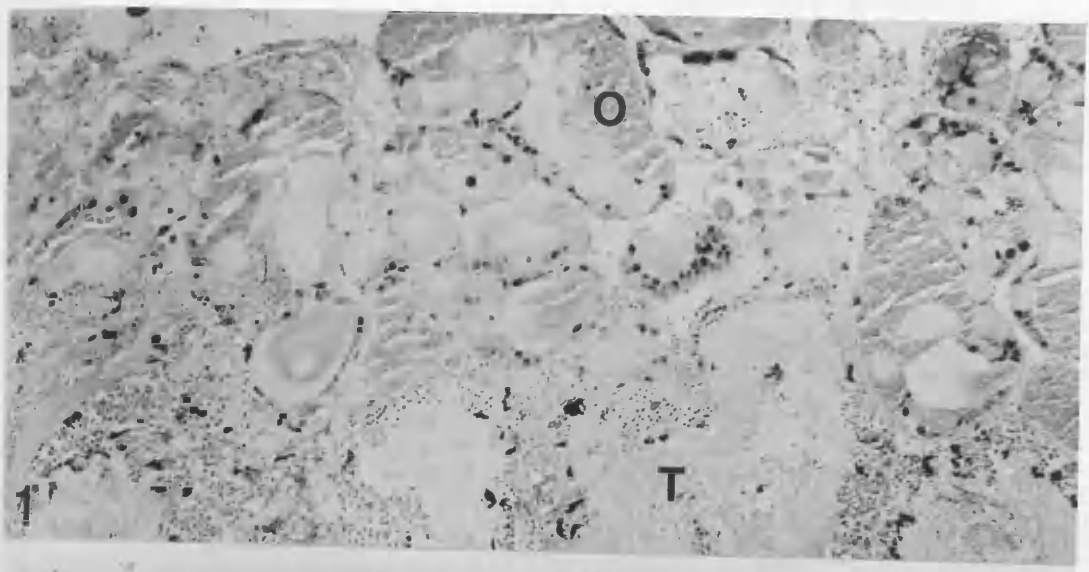
O
T
1

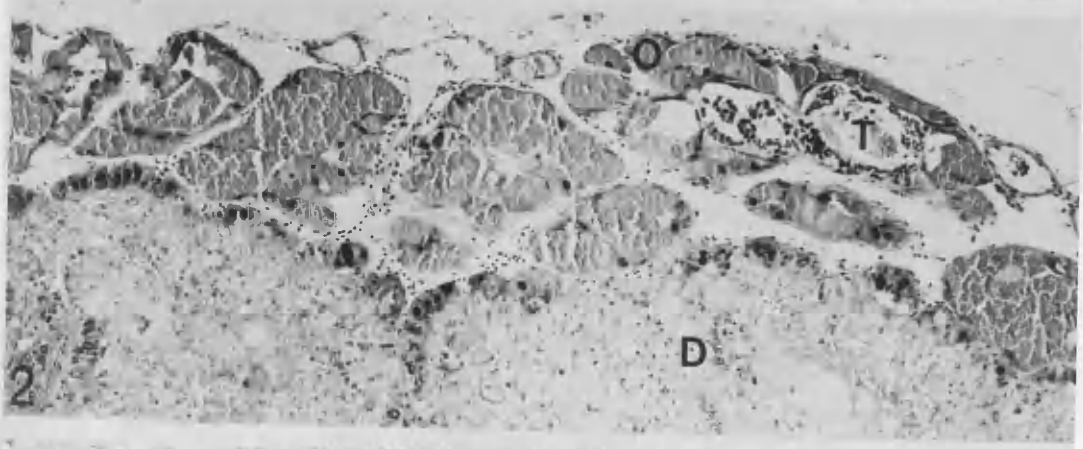
O
T
D
2

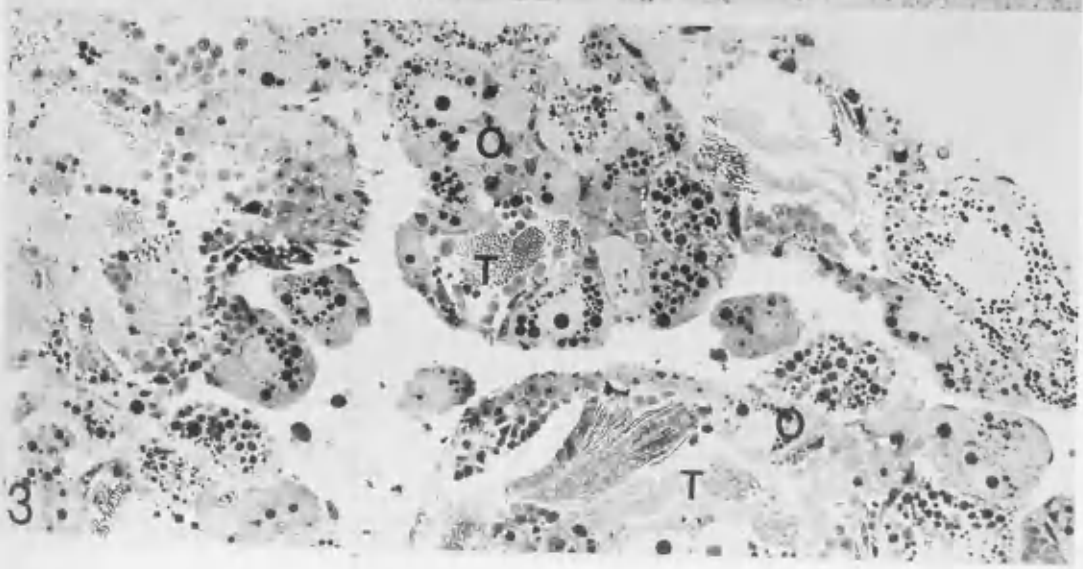
O
T
D
T
3

FIGURES 4, 5 AND 6.

Scanning electron micrographs of spermatozoa from Archidoris tuberculata.

(Mags.: FIGURE 4, x.5,000; FIGURE 5, x.1,200; FIGURE 6, x.3,000).

FIGURES 7, 8 AND 9.

Scanning electron micrographs of Tritonia plebeia spermatozoa, showing various parts of the spermatozoon. (Mags.: FIGURE 7, x.5,000; FIGURE 8, x.4,500; FIGURE 9, x.4,700).

FIGURES 10 AND 11.

Scanning electron micrographs of the head of Aplysia faciata spermatozoa.

(Mags.: FIGURE 10, x.3,750; FIGURE 11, x.3,500).

FIGURES 12, 13 AND 14.

Scanning electron micrographs of the head of spermatozoon from Archidoris tuberculata (FIGURE 12), Tritonia plebeia (FIGURE 13) and Aplysia faciata (FIGURE 14).

(Mags.: FIGURES 12, 13 and 14, 3,750).

ABBREVIATIONS: A, acrosome; H, head;
M, mitochondrial helix
T, tail piece.

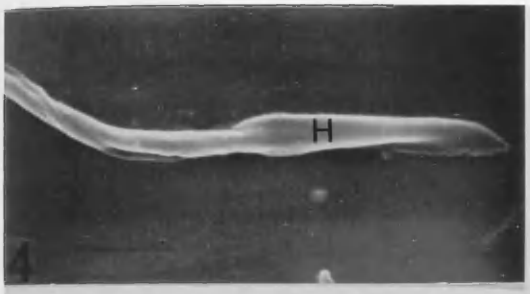
H
4

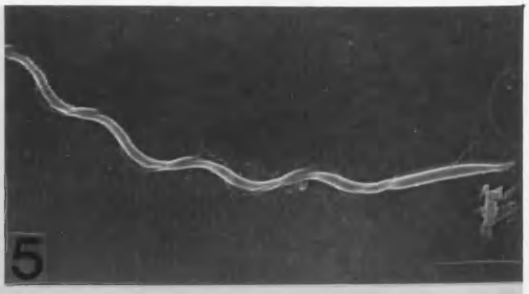
5

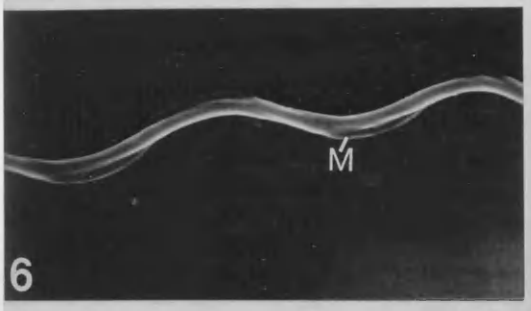
M
6

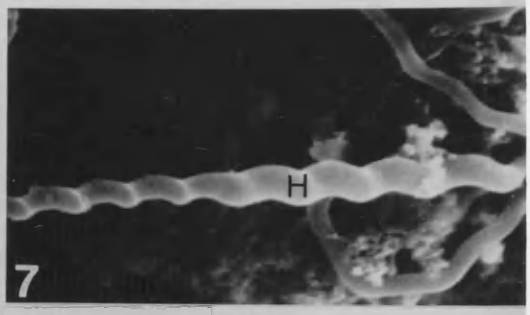
H
7

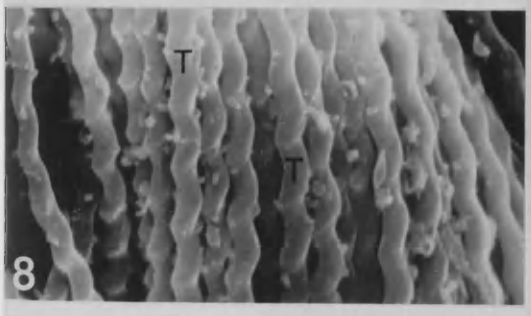
T
T
8

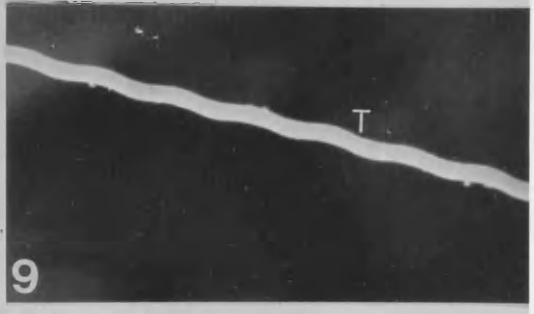
T
9

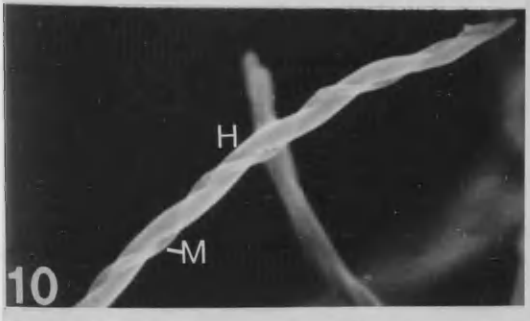
H
M
10


A
11


A
H
12


H
13


14

FIGURES 15, 16, 17 AND 18.

A group of transmission electron micrographs showing the basal lamina in the acinar wall of the ovotestis of Archidoris tuberculata (FIGURE 15, mag. x.12,250), Tritonia plebeia (FIGURE 16, mag. x.28,000) and Aplysia faciata (FIGURE 17, mag. x.20,000). A layer of myoepithelial cells occurs external to the basal lamina and a large number of myofilaments (arrowheads) are arranged parallel to the basal lamina (FIGURE 18, Archidoris tuberculata. Mag. x.28,000).

ABBREVIATIONS: B, basal lamina; Mo, myoepithelial layer; M, mitochondrion.

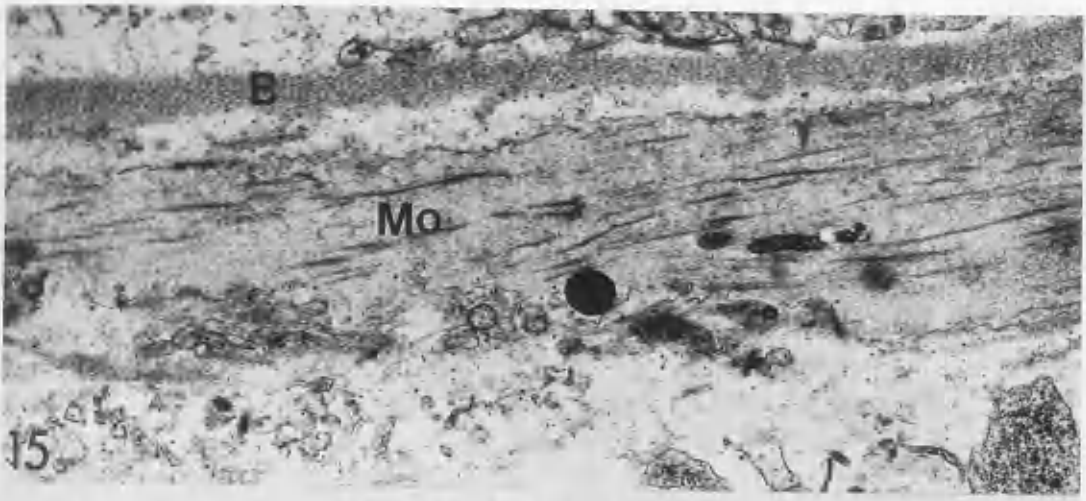
B
Mo
15

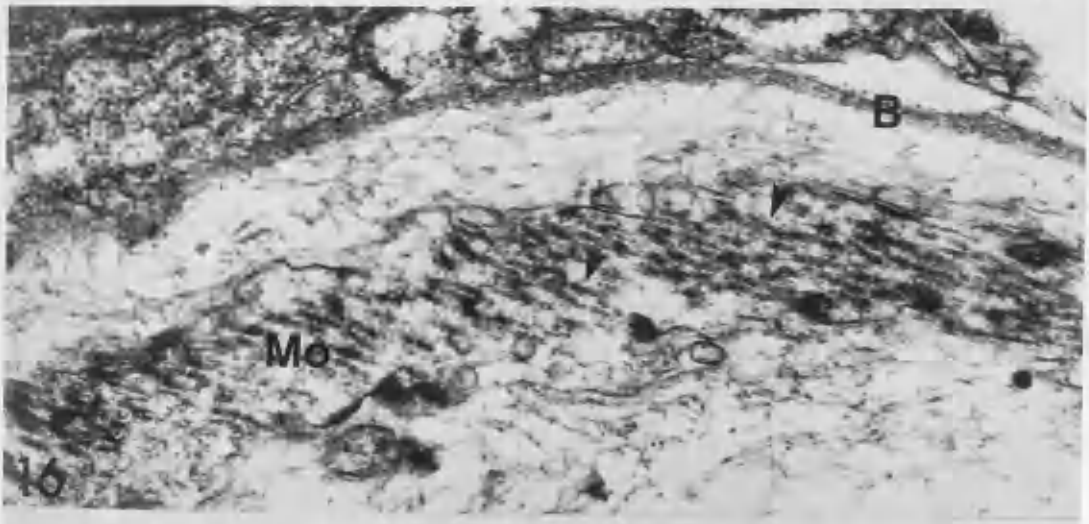
B
Mo
16

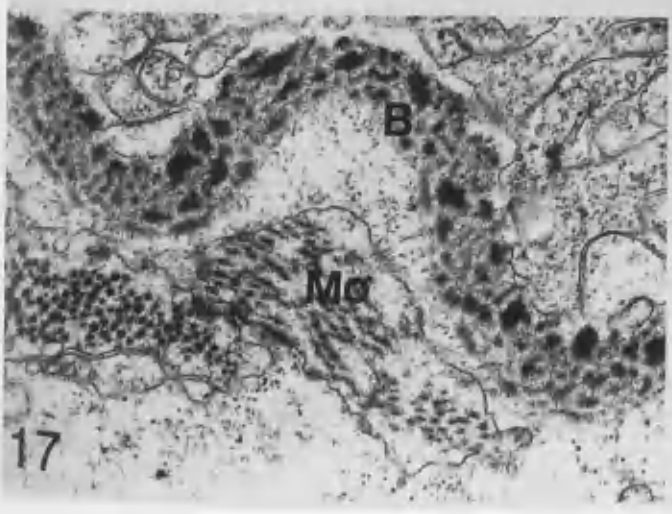
B
Mσ
17


M
18

FIGURE 19.

A TEM micrograph of part of the acinus of Archidoris tuberculata, showing a group of spermatogenic cells in close relation to the accessory cell which is resting on the basal lamina. A layer of myoepithelial cells with a prominent nucleus occurs external to the basal lamina. (Mag. x.5,000).

FIGURES 20 AND 21.

Archidoris tuberculata. Developing spermatogenic cells are in close association with an accessory cell (Mag. x.2,900). A large number of lipid droplets occur in the accessory cell cytoplasm. A lipid droplet is enlarged in Figure 21.
(Mag. x.25,000).

ABBREVIATIONS: A, accessory cell; L, lipid droplet;
B, basal lamina; Na, accessory cell nucleus;
Nm, myoepithelial cell nucleus;
Sd, spermatid.

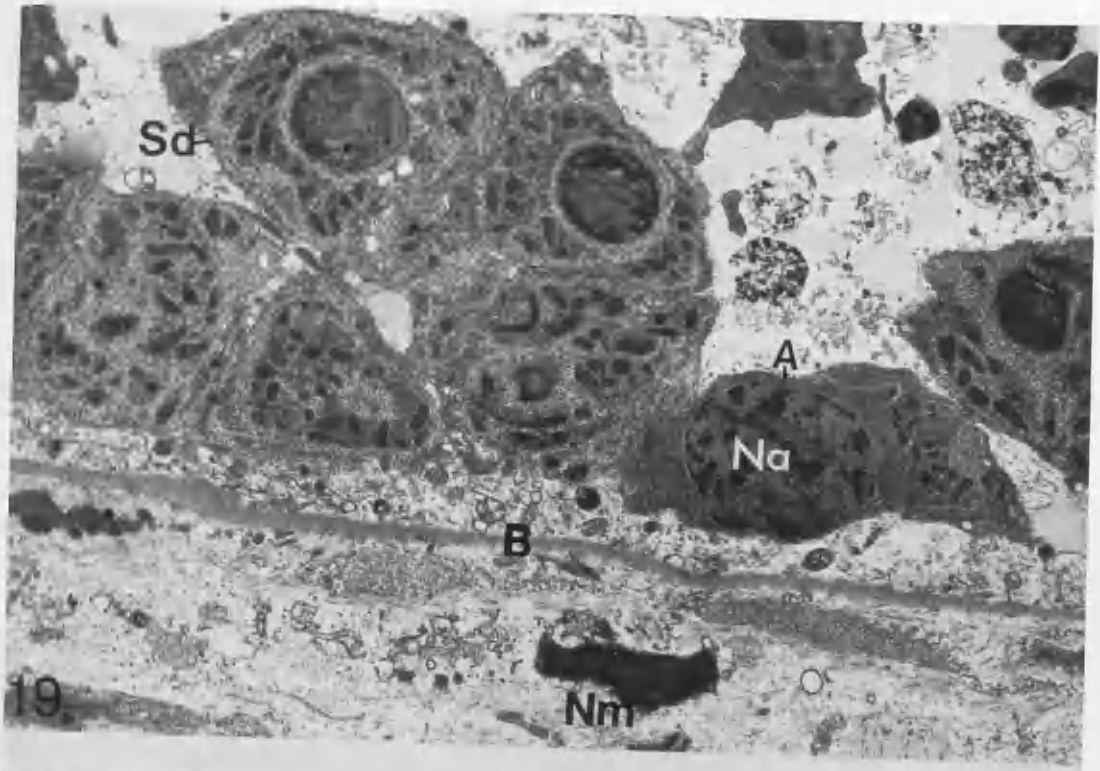
Sd
A
Na
B
Nm
19

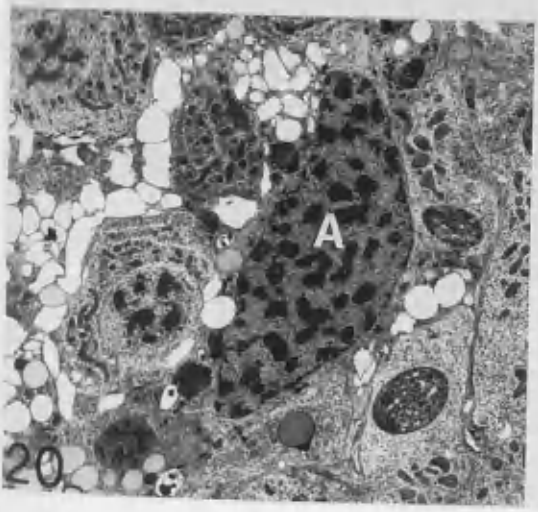
A
20

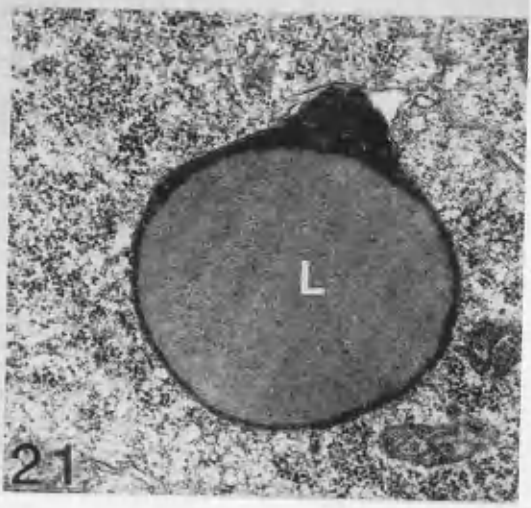
L
21

FIGURES 22, 23 AND 24.

TEM micrographs of spermatogonia of Archidoris tuberculata (FIGURE 22, mag. x.9,500), Tritonia plebeia (FIGURE 23, mag. x.6,700) and Aplysia faciata (FIGURE 24, mag. x.8,000). Note the spherical nucleus and small mitochondria.

FIGURE 25.

Adjacent spermatogonia are connected by an intercellular bridge (arrowheads). The cell membranes limiting the bridges appear thickened.
(Mag. x.11,200).

ABBREVIATIONS: N, nucleus; Ne, nucleolus;
M, mitochondrion.

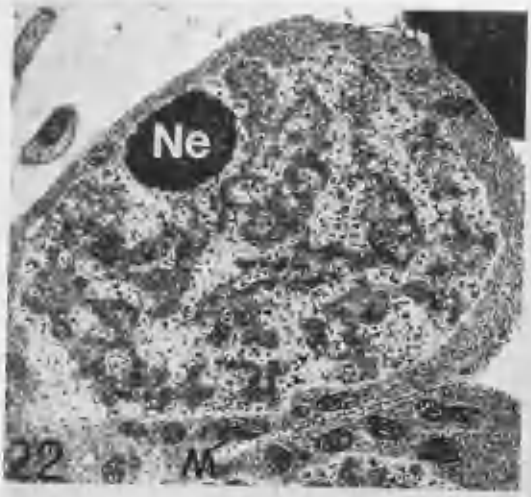

22

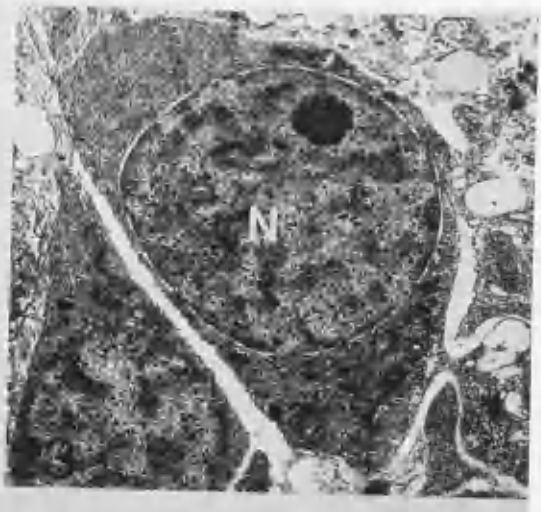

23

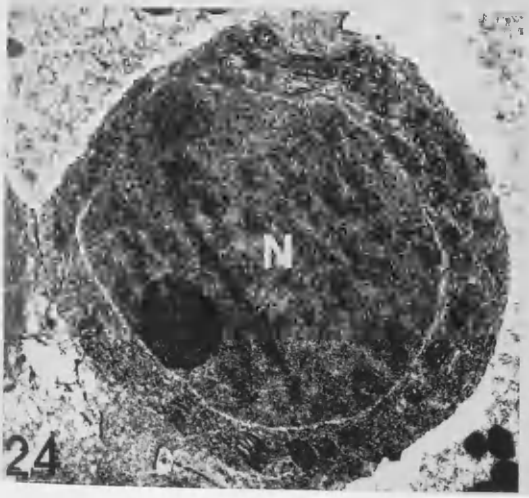

24

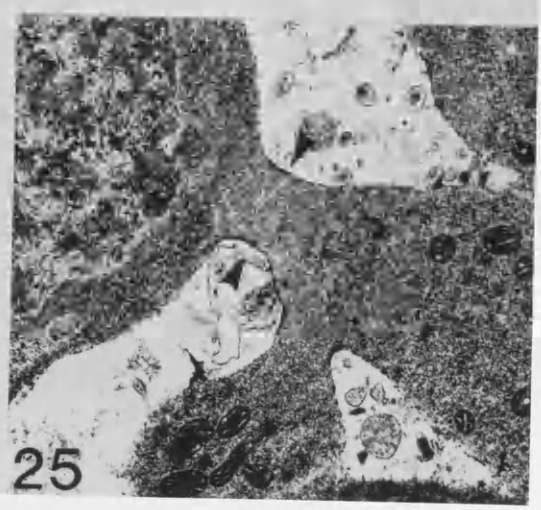

25

FIGURE 26, 27 AND 28.

TEM micrographs of primary spermatocytes of Archidoris tuberculata (FIGURE 26, mag. x.6,400), Tritonia plebeia (FIGURE 27, mag. x.4,500) and Aplysia faciata (FIGURE 28, mag. x.9,600). Note synaptonemal complexes inside the nucleus (arrowhead).

FIGURE 29.

A TEM micrograph showing groups of spermatocytes in Archidoris tuberculata.
(Mag. x.3,500).

FIGURES 30 AND 31.

An enlargement of synaptonemal complexes in the spermatocytes of Archidoris tuberculata (FIGURE 30, mag. x.17,500) and Aplysia faciata (FIGURE 31, mag. x.20,000).

ABBREVIATION: Sy, synaptonemal complex;


26

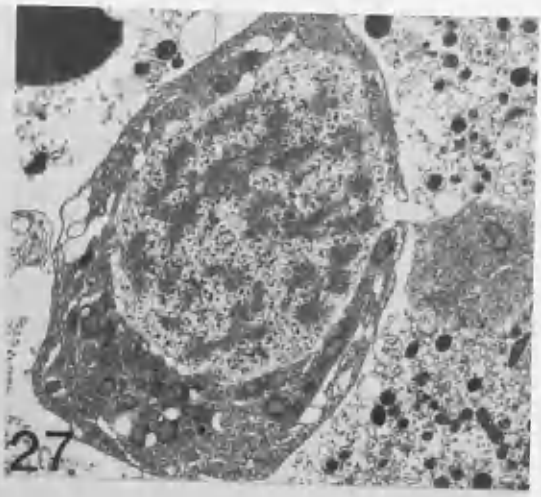
27


28

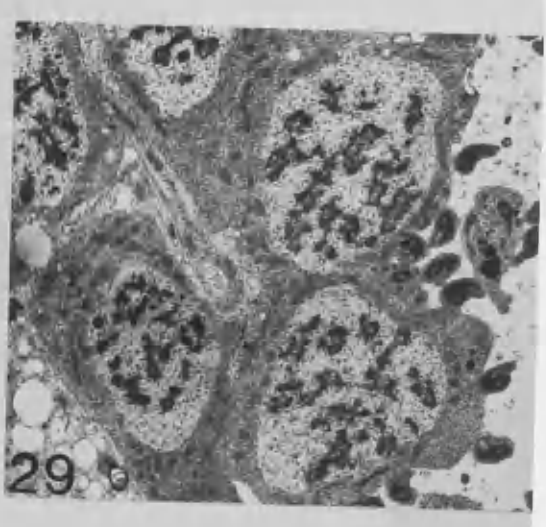
29

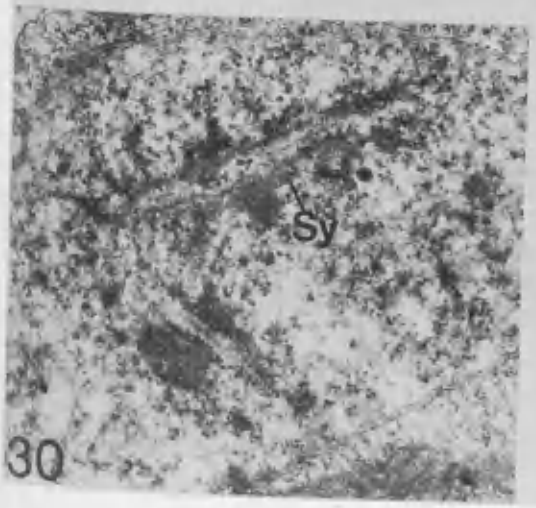
Sy
30

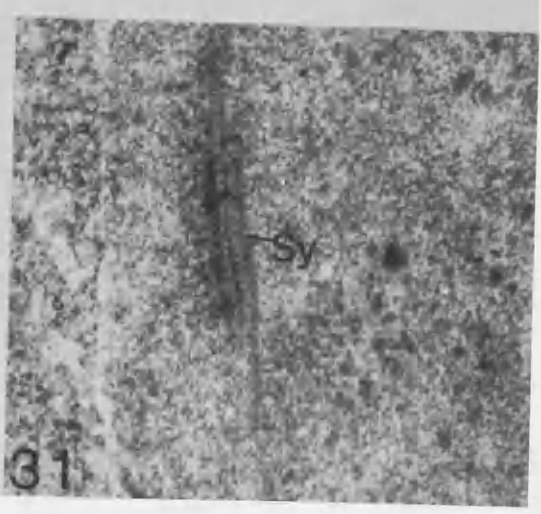
Sy
31

FIGURES 32, 33 AND 34.

Pre-cup stage spermatids of Archidoris tuberculata (FIGURE 32, mag. x.7,700), Tritonia plebeia (FIGURE 33, mag. x.18,660) and Aplysia faciata (FIGURE 34, mag. x.16,000). Adjacent spermatids are connected by intercellular bridges (arrow in Figure 32). Spermatid nuclei are still spherical and anterior (single arrowhead) and posterior (double arrowheads) nuclear plaques are established. However, note the ellipsoidal-shaped nucleus of Aplysia faciata (FIGURE 34) and the thick posterior nuclear plaque (about 0.3 μm).

FIGURES 35 AND 36.

The proacrosomal granule secreted by the Golgi complex is located at the anterior plaque of the nucleus (FIGURE 35, Archidoris tuberculata. mag. x.12,000). Initially the proacrosomal granule is associated with the Golgi complex (Figure 35). Later, the Golgi complex is separated from the proacrosomal granule and disappears (Figure 36, mag. x.14,000).

FIGURE 37.

High magnification (mag. x.140,000) of the anterior nuclear plaque (arrowheads) and adjacent normal double nuclear membrane (arrows). Note electron dense material is deposited at both internal and external aspects of the nuclear membrane at the anterior plaque (arrowheads).

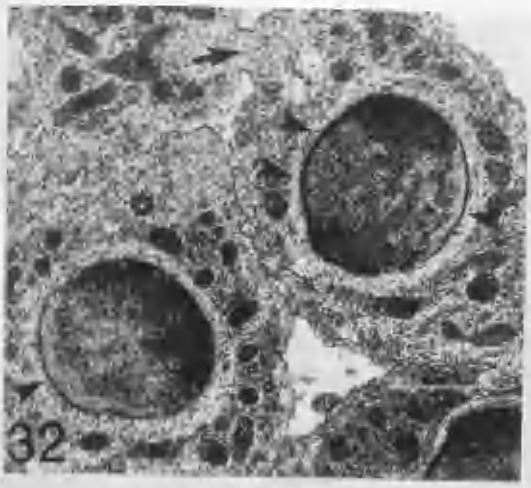

32

33

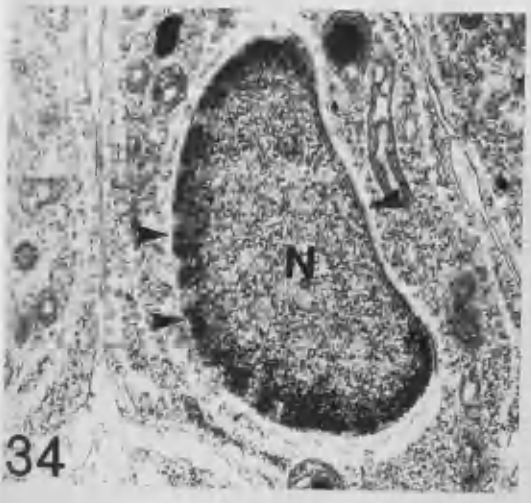

34

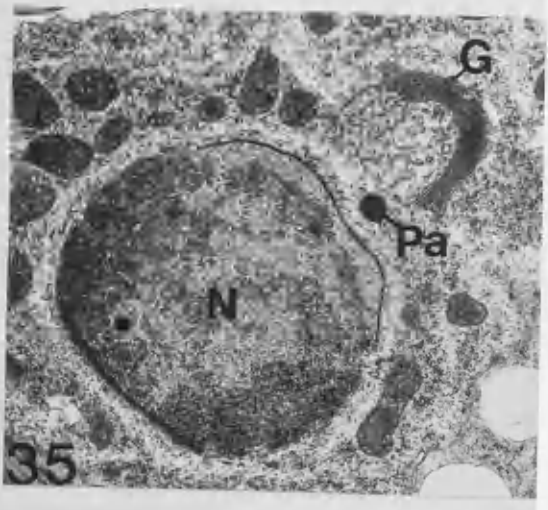

35

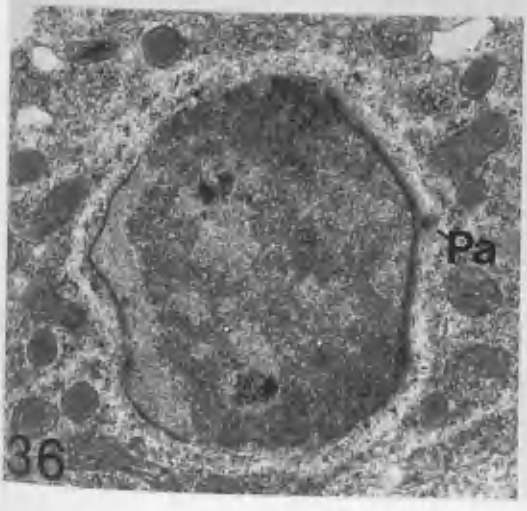

36

37

ABBREVIATIONS: G, Golgi complex; N, nucleus;
Pa, proacrosomal granule.

FIGURES 38 AND 39.

Cup-stage spermatids of Archidoris tuberculata. Chromatin forms fine fibrils orientated along the anterior-posterior axis of the nucleus and are most numerous near the anterior and posterior plaques (Figure 39).
(Mags.: FIGURE 38, x.5,800; FIGURE 39, x.14,000).

FIGURES 40 AND 41.

Cup-stage spermatids of Tritonia plebeia. Note the large number of thin chromatin fibrils near the anterior and posterior plaques. There is only an internal layer of electron dense deposit at the posterior plaque (arrowheads) (FIGURE 41).
(Mags.: FIGURE 40, x.11,000; FIGURE 41, x.27,000).

FIGURE 42.

A cup-stage spermatid of Aplysia faciata. Note the much thickened posterior nuclear plaque and the obliquely sectioned proacrosomal granule.
(Mag. x.13,700).

ABBREVIATIONS: AP, anterior plaque;
PP, posterior plaque;
Pa, proacrosomal granule.

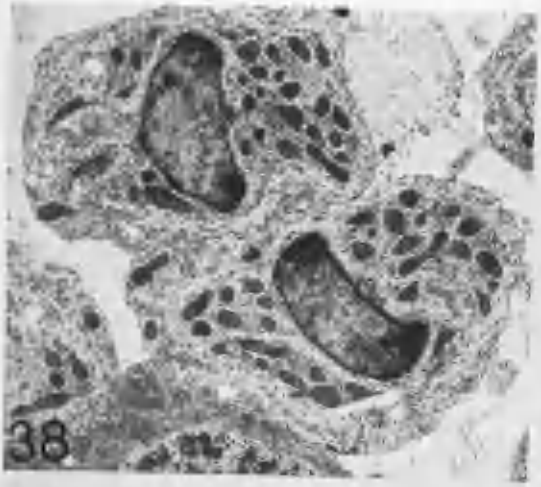
38


39

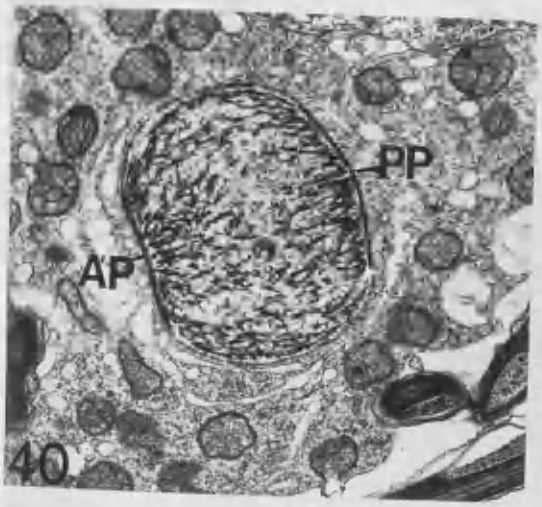

40

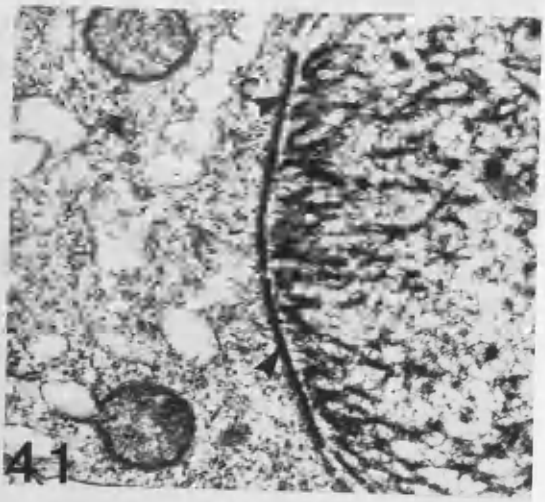
41

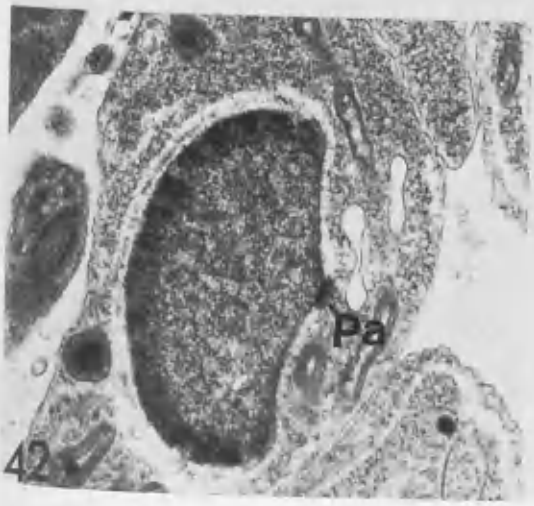

42

FIGURES 43, 44, 45 AND 46.

Archidoris tuberculata. Elongating spermatids. The proacrosome and centriole are attached to the anterior and posterior nuclear plaques, respectively (FIGURE 43) and chromatin fibrils aggregate into filaments (Figures 44, 45 and 46). The nucleus loses its cup shape, however. The anterior and posterior plaques are still visible (arrowheads in FIGURES 44 and 46). Differentiation of spermatids occurs in close association with the accessory cell (FIGURE 45).

(Mags.: FIGURE 43, x.13,000; FIGURE 44, x.34,000; FIGURE 45, x.14,000; FIGURE 46, x.30,000).

FIGURE 47.

Archidoris tuberculata. A TEM micrograph of an elongating spermatid midpiece, showing a single centriole and centriolar adjunt (arrowheads). Note the initial stage of mitochondrial wrapping around the axoneme.

(Mag. x.24,000).

FIGURES 48, 49 AND 50.

Tritonia plebeia. Elongating spermatids. The nucleus loses its cup shape. Chromatin condenses into thin filaments (FIGURE 48). Furthermore, the nucleus assumes a spiral form (FIGURE 49) and mitochondria wrap around the axoneme (FIGURE 50).

(Mags.: FIGURE 48, x.12,750; FIGURE 49, x.16,000; FIGURE 50, x.30,500)

43

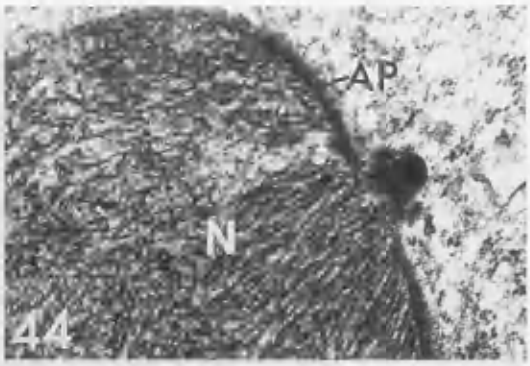

44

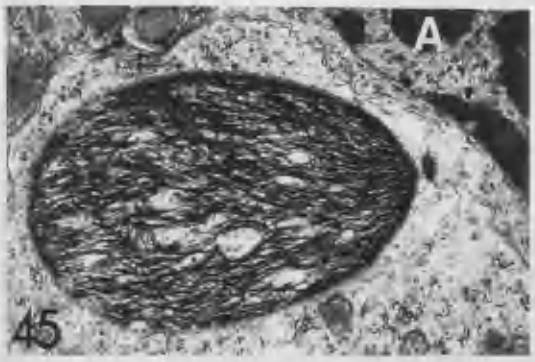

45


46

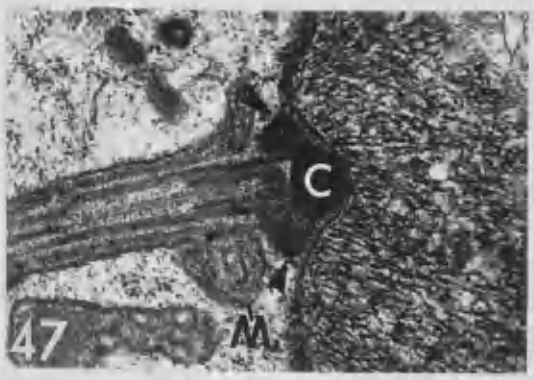

47


48

49

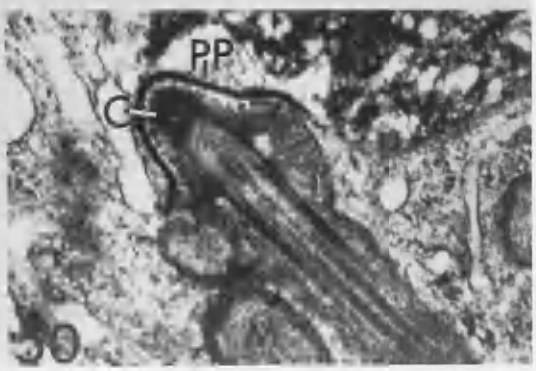

50

ABBREVIATIONS: A, accessory cell; AP anterior plaque;
PP, posterior plaque; Pa, proacrosome;
C, centriole; N, nucleus;
M, mitochondrion.

FIGURES 51, 52, 53 AND 54.

Aplysia faciata. Elongating spermatids. The nucleus assumes an irregular shape (FIGURE 51). Chromatin condenses into fine fibrils (FIGURE 53). A single centriole attaches to the base of the nucleus forming a centriolar fossa (FIGURE 52). There is no occurrence of a centriolar adjunct (FIGURE 54) comparable to that shown in FIGURE 47.

(Mags.: FIGURE 51, x.16,000; FIGURE 52, x.16,300; FIGURE 53, x.16,800; FIGURE 54, x.30,000).

FIGURES 55, 56 AND 57.

Archidoris tuberculata. TEM micrographs of spermatids showing the occurrence of multivesicular bodies (arrowheads) (FIGURE 55). The multivesicular body is secreted by the Golgi complex (FIGURE 56). It later migrates to the base of the nucleus close to the centriole (FIGURE 57).

(Mags.: FIGURE 55, x.8,750; FIGURE 56, x.19,000; FIGURE 57, x.23,000).

FIGURE 58.

Tritonia plebeia. A multivesicular body (arrowhead) occurs in close association with the centriolar fossa.

(Mag. x.32,000).

ABBREVIATIONS: C, centriole; N, nucleus;
G, Golgi complex.

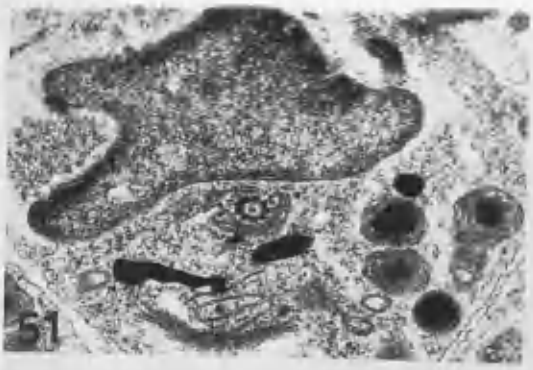
51

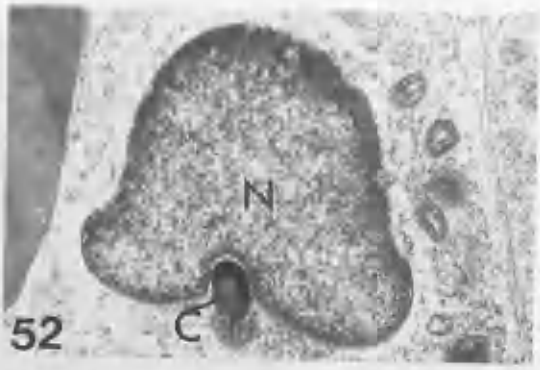
N
C
52

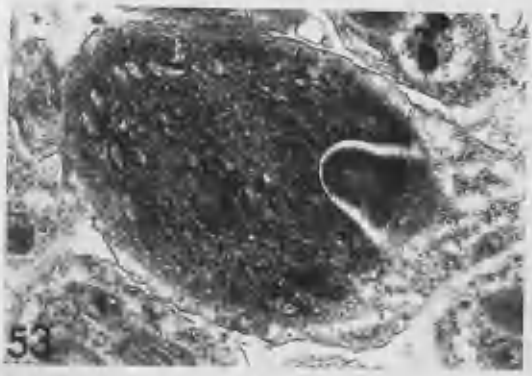
53

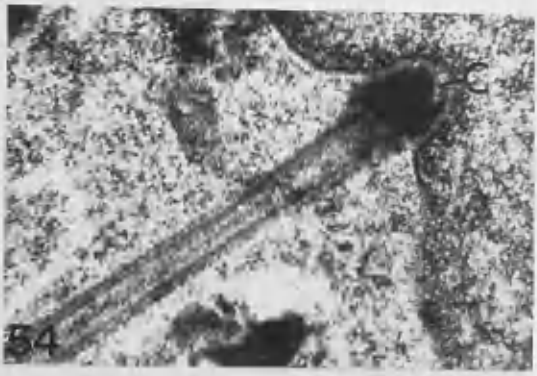
C
54

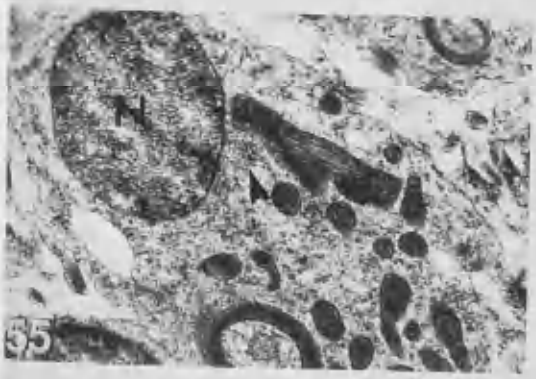
N
55


G
56


57

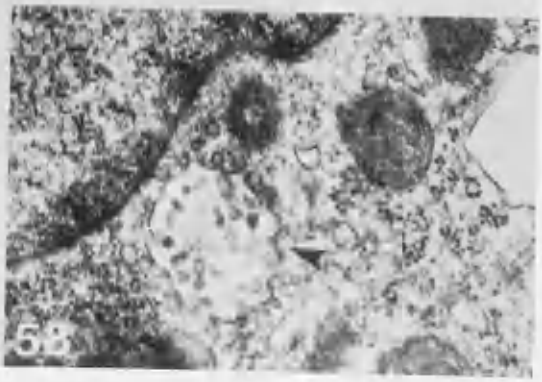
58

FIGURE 59.

Archidoris tuberculata. A transverse section through a condensing nucleus, showing the spiral arrangment of chromatin lamellae.

(Mag. x.34,000).

FIGURE 60.

Archidoris tuberculata. A longitudinal section through the centriolar region. Note the centriolar adjunct and mitochondria which are in the process of loss of intramitochondrial cristae and transformation into the mitochondrial derivative.

(Mag. x.45,000).

FIGURE 61.

Archidoris tuberculata. A transverse section through the centriolar region. Further condensation of chromatin lamellae is apparent.

(Mag. x.44,000).

FIGURES 62 AND 63.

Tritonia plebeia. Transverse sections through condensing spermatid nuclei, showing chromatin lamellae and the microtubular manchette (arrowheads) in a layer of electron dense material around the nucleus (FIGURE 62). The chromatin lamellae assume a helical arrangement, appearing transversely cut in one part of the nucleus, obliquely cut another part (FIGURE 62). Where chromatin lamellae are transversely cut, a banded chromatin pattern

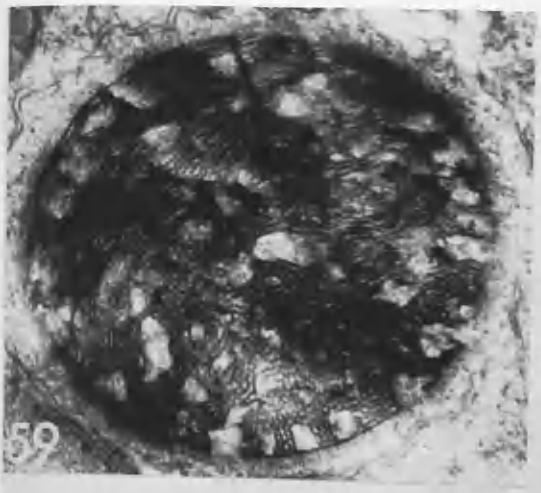

59

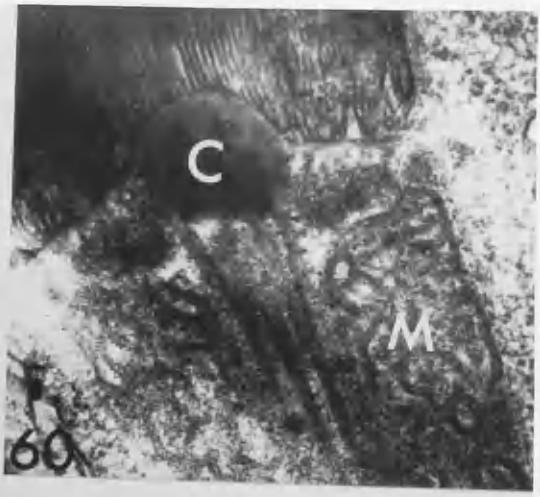

60

61

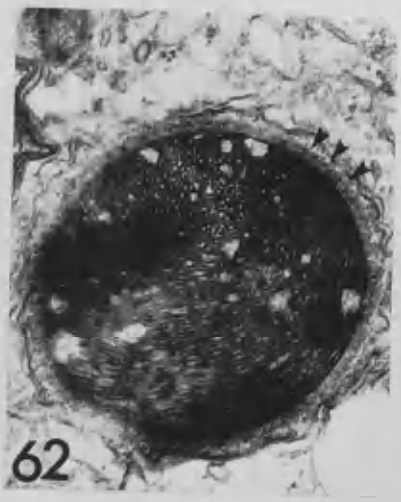

62

63

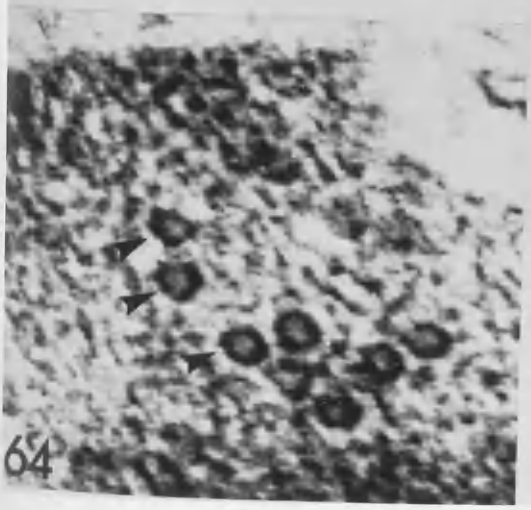

64

65

occurs near the nuclear membrane (arrowheads) (FIGURE 63). (Mags.: FIGURE 62, x.32,000; FIGURE 63, x.37,000).

FIGURE 64.

Aplysia faciata. A transverse section of a condensing nucleus showing tubular structures (arrowheads) within the chromatin.
(Mag. x.280,000).

FIGURE 65.

Aplysia faciata. A longitudinal section of the centriolar region. Chromatin has condensed into an almost homogeneous state. Note the single cap shaped centriole and absence of a centriolar adjunct.
(Mag. x.36,000).

ABBREVIATIONS: C, centriole; M, mitochondrial derivative; N, nucleus.

FIGURE 66.

Archidoris tuberculata. Transverse sections through spermatid nuclei. Chromatin condenses into an almost homogeneous state.

(Mag. x.18,000).

FIGURE 67.

Tritonia plebeia. Transverse sections through spermatid heads showing the prominent nuclear keels (arrowheads).

(Mag. x.25,500).

FIGURES 68, 69 AND 70.

Archidoris tuberculata. Tannic acid fixed spermatids. Glancing sections of spermatid nuclei showing arrays of microtubules (arrowheads, FIGURES 68 and 70) and intermicrotubular bridges (arrows, FIGURE 69).

(Mags.: FIGURE 68, x.35,000; FIGURE 69, x.93,000; FIGURE 70, x.87,500).

ABBREVIATION: N, nucleus.

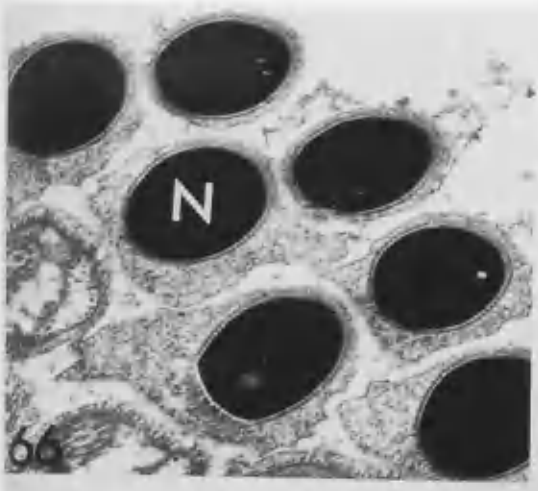

66

67

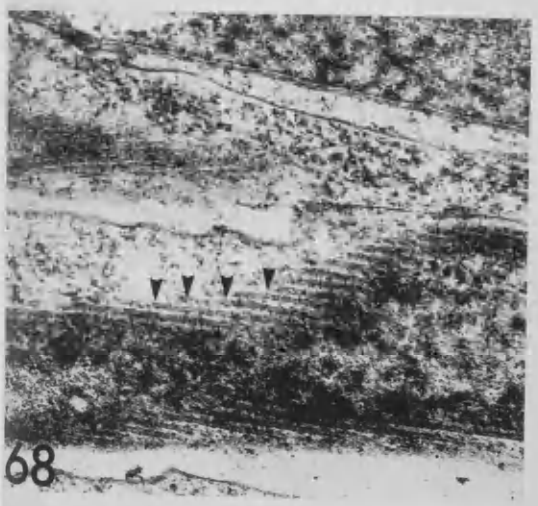

68

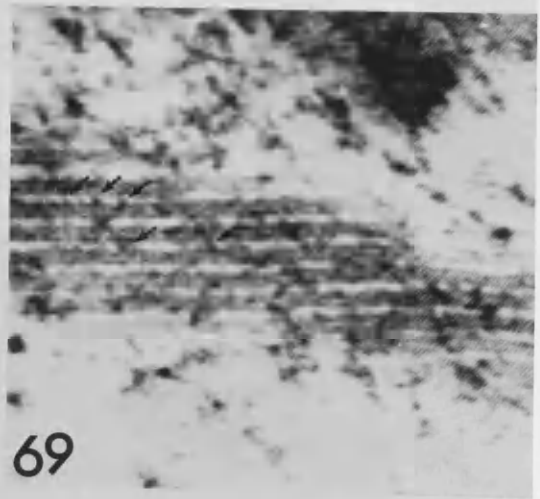

69

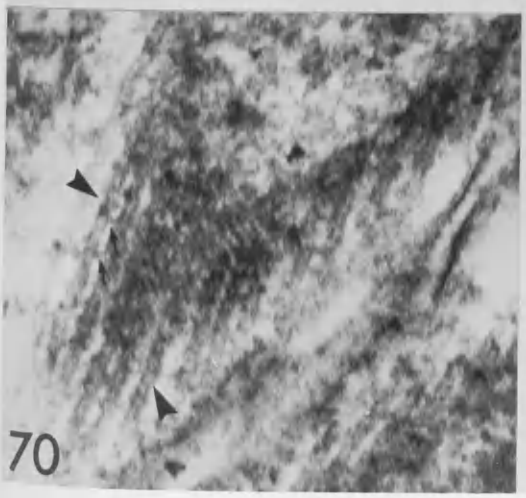

70

FIGURES 71 AND 72.

Aplysia faciata. Transverse sections through various parts of a group of spermatozoa. FIGURE 71 shows sections through the more anterior parts of spermatozoa and FIGURE 72 demonstrates the distal part of spermatozoa.

(Mags.: FIGURE 71, x.39,000; FIGURE 72, x.26,600).

ABBREVIATIONS: F, flagellum; N, nucleus.

N
F
7.1

N
F

FIGURE 73.

Archidoris tuberculata. A TEM micrograph showing two Golgi complexes within the spermatocyte cytoplasm.
(Mag. x.17,600).

FIGURE 74.

Tritonia plebeia. A TEM micrograph showing two Golgi complexes within the spermatocyte cytoplasm.
(Mag. x.15,000).

FIGURE 75.

Aplysia faciata. A proacrosomal granule is secreted by the Golgi complex. Note the extensive endoplasmic reticula in close relation to the Golgi complex.
(Mag. x.21,000).

FIGURE 76.

Tritonia plebeia. A proacrosomal granule is in close association with a transfer vesicle of the Golgi complex (arrowhead).
(Mag. x.39,000).

FIGURE 77.

Archidoris tuberculata. A proacrosomal granule (arrowhead) is in close relation to the Golgi complex.
(Mag. x.21,000).


73

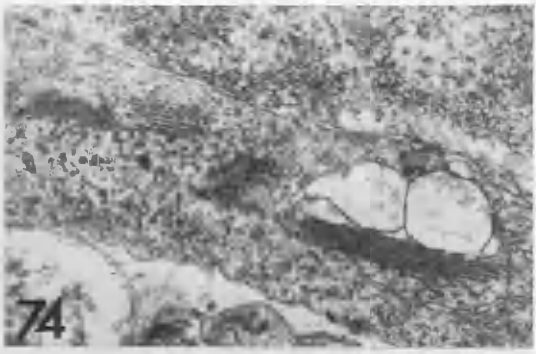
74

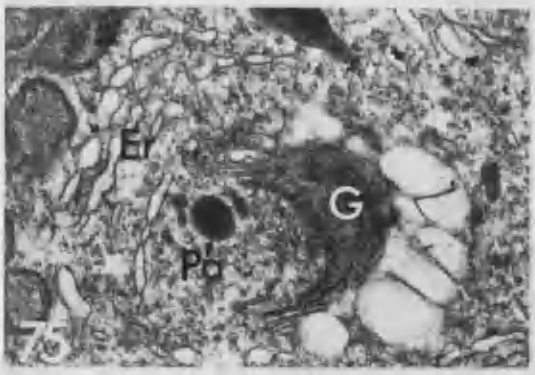
Er
G
Pg
75

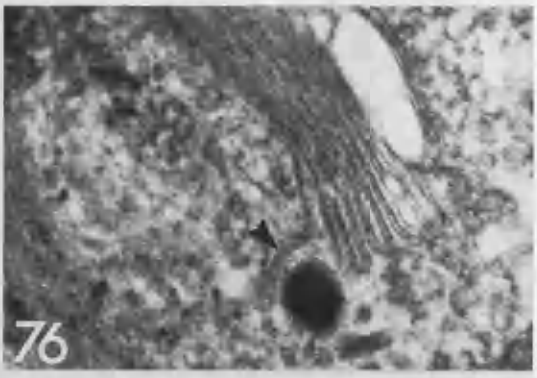
76


77

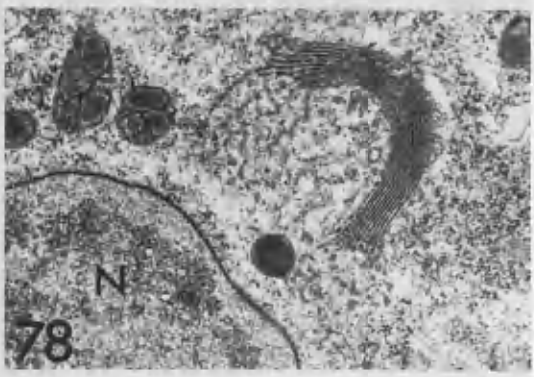
N
78


N
79

FIGURE 78.

Archidoris tuberculata. A pre-cup stage spermatid. The proacrosome is membrane bound and in close association with the Golgi complex and the anterior nuclear plaque. (Mag. x. 18,000).

FIGURE 79.

Archidoris tuberculata. The developing proacrosome. Note the membrane bound proacrosomal granule (arrowhead) and peripheral supporting acrosomal pedestal (arrows). (Mag. x.87,000).

ABBREVIATIONS: Er, endoplasmic reticulum;
G, Golgi complex;
N, nucleus;
Pa, proacrosomal granule.

FIGURES 80, 81 AND 82.

Longitudinal sections through the head of elongated spermatids, showing the acrosome located at the apex of the nucleus (FIGURE 80, Archidoris tuberculata; FIGURE 81, Tritonia plebei; FIGURE 82, Aplysia faciata). (Mags.: FIGURE 80, x.67,200; FIGURE 81, x.65,000; FIGURE 82, x.70,000).

ABBREVIATIONS: A, acrosome. N, nucleus.

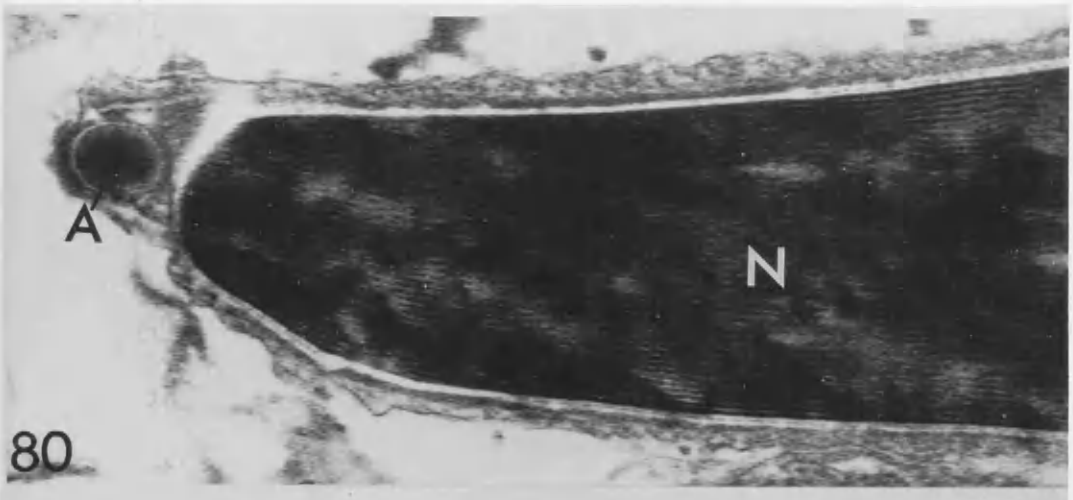

80

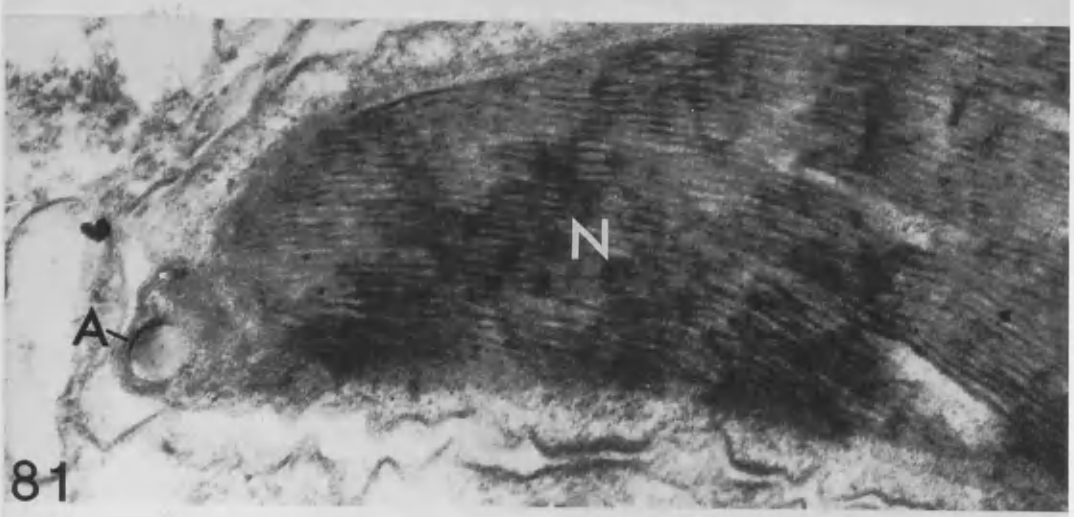

81

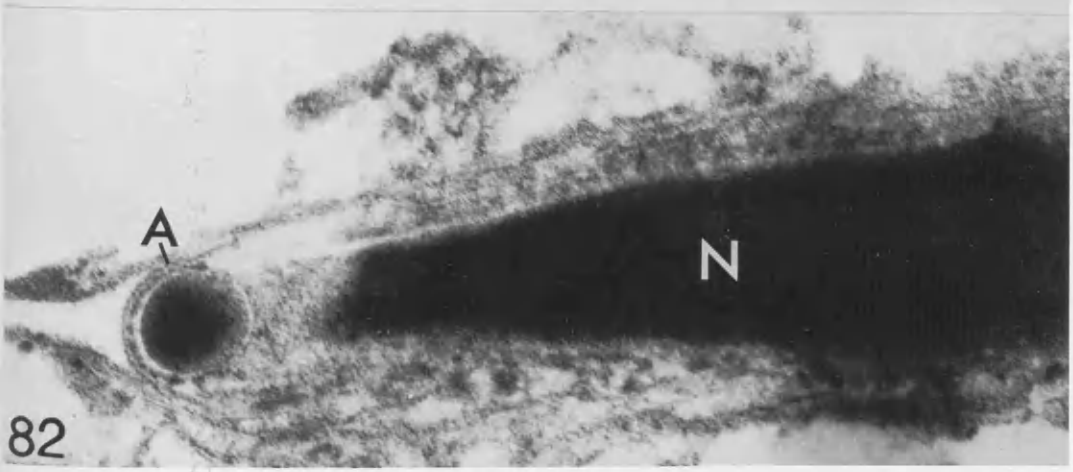

82

FIGURES 83, 84, 85 AND 86.

Mitochondrial morphorgenesis in the spermatogonia of Archidoris tuberculata (FIGURE 83 and 85), Tritonia plebeia (FIGURE 84) and Aplysia faciata (FIGURE 86). Electron dense intra-cristal bodies (arrowheads in FIGURES 85 and 86) replace the mitochondrial cristae (FIGURE 83) in Archidoris tuberculata and Aplysia faciata. In Tritonia plebeia, the number of mitochondrial cristae is reduced (FIGURE 84) and flocculent material accumulates within the mitochondrial matrix.
(Mags.: FIGURE 83, x.22,560; FIGURE 84, x.26,250; FIGURE 85, x.27,000; FIGURE 86, x.50,000).

FIGURE 87.

Tritonia plebeia. A longitudinal section of a spermatid showing the formation of the periaxonemal sheath by fusion of mitochondria.
(Mag. x.37,000).

FIGURES 88 AND 89.

Tritonia plebeia. Transverse sections through the axoneme showing the primary wrapping of the mitochondrial sheath (FIGURE 88) and wrapping of the secondary layer of mitochondria (arrows, FIGURE 89).
(Mags.: FIGURE 88, x.28,000; FIGURE 89, x.28,000).

ABBREVIATIONS: A, axoneme; M, mitochondrion.


83

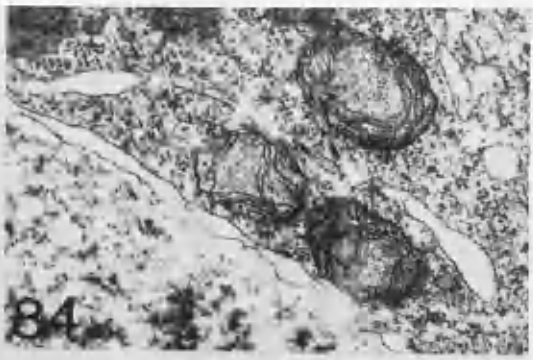
84

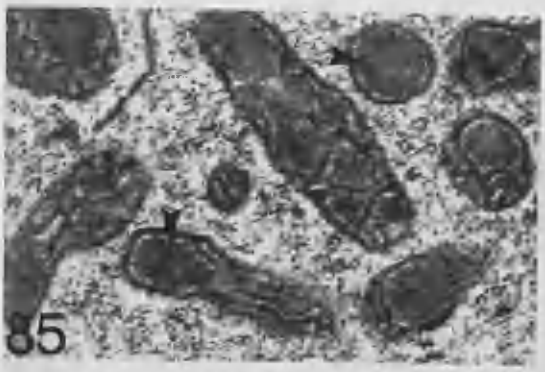
85


86

87

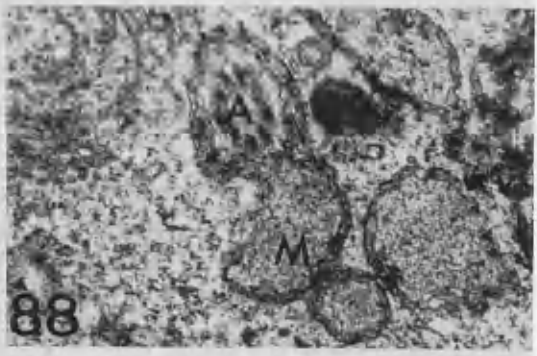

88

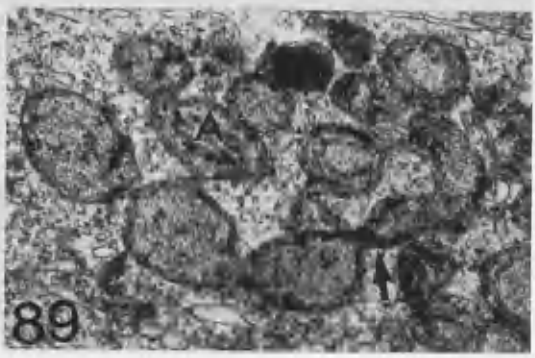

89

FIGURE 90.

Aplysia faciata. A transverse section through the axoneme showing the primary mitochondrial wrapping.
(Mag. x.42,000).

FIGURE 91.

Archidoris tuberculata. A longitudinal section through the axoneme. The primary mitochondrial wrapping starts from the nuclear-centriolar junction and spreads posteriorly along the axoneme.
(Mag. x.10,300).

FIGURE 92.

Archidoris tuberculata. A glancing section of the spermatid midpiece showing the mitochondrial derivative.
(Mag. x.18,700).

FIGURES 93 AND 94.

Aplysia faciata. Transverse sections of the spermatid midpiece showing secondary mitochondrial wrapping (arrows in FIGURE 93) and the mitochondrial derivative (FIGURE 94).
(Mags.: FIGURE 93, x.35,000; FIGURE 94, x.54,000).


A
M
90

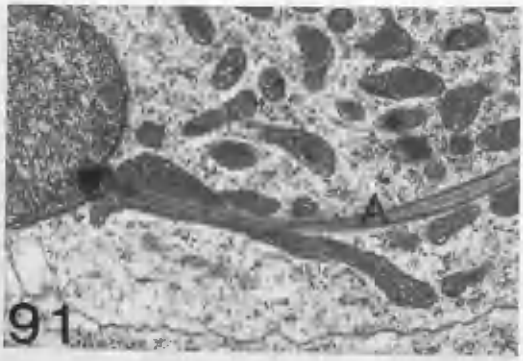
A
91

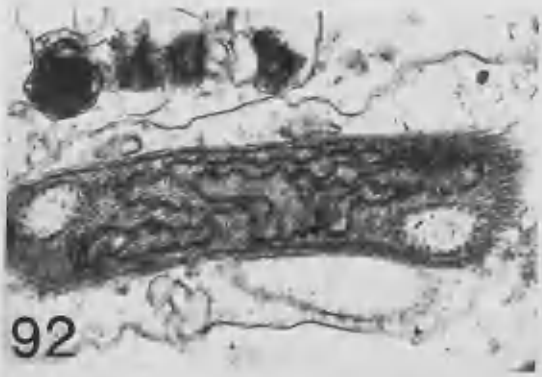
92


93

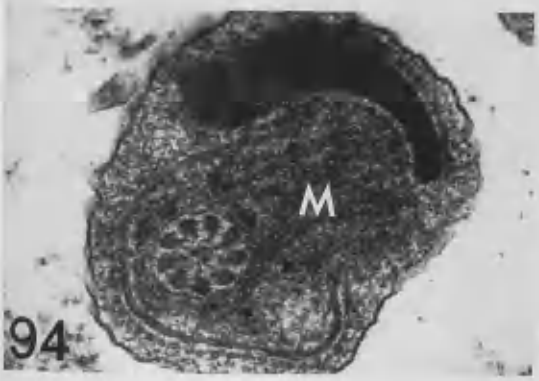
M
94

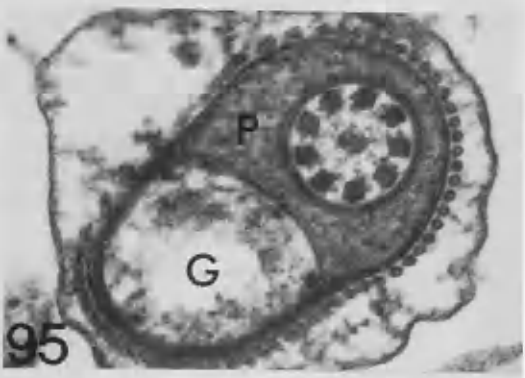
P
G
95


P
G
96

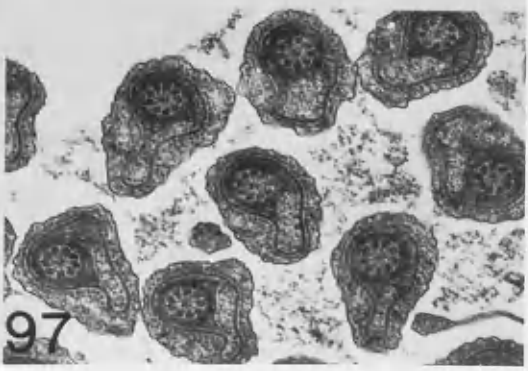
97

FIGURES 95, 96 AND 97.

Transverse sections through the midpiece of spermatozoa of Tritonia plebeia (FIGURE 95), Archidoris tuberculata (FIGURE 96) and Aplysia faciata (FIGURE 97). Note the axoneme, pseudo-paracrystalline material and the helical keel containing glycogen granules.

(Mags.: FIGURE 95, x.70,000; FIGURE 96, x.70,000; FIGURE 97, x.19,600).

ABBREVIATIONS: A, axoneme; G, glycogen helix;
M, mitochondrial derivative;
P, pseudo-paracrystalline material.

FIGURES 98, 99 AND 100.

Longitudinal sections through the flagellum of Archidoris tuberculata (FIGURE 98), Tritonia plebeia (FIGURE 99) and Aplysia faciata (FIGURE 100). Note the pseudo-paracrystalline material assuming 55-70 nm wide bands (arrows) spiralling around the axoneme and the glycogen helix.

(Mags.: FIGURE 98, x.50,400; FIGURE 99, x.40,000; FIGURE 100, x.20,000).

ABBREVIATIONS: Ax, aoneme; G, glycogen helix;
N, nucleus.

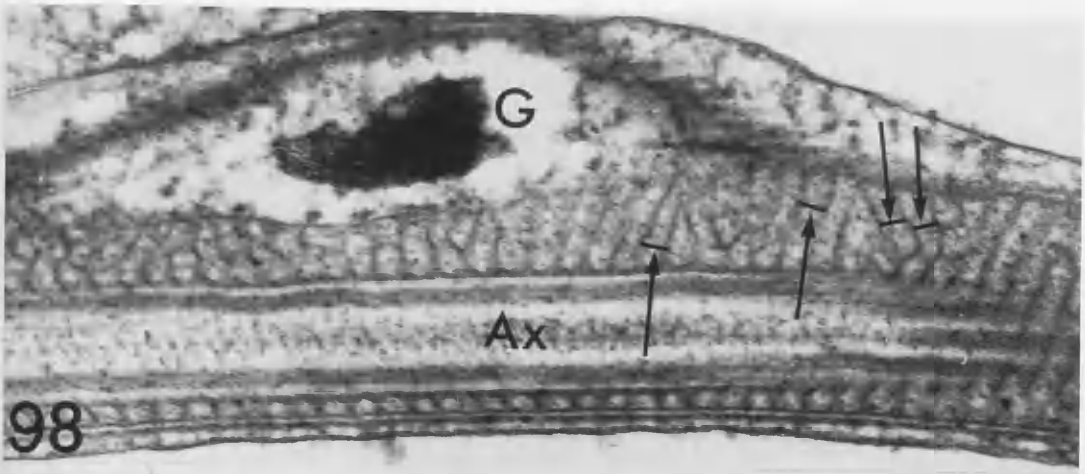
G
Ax
98

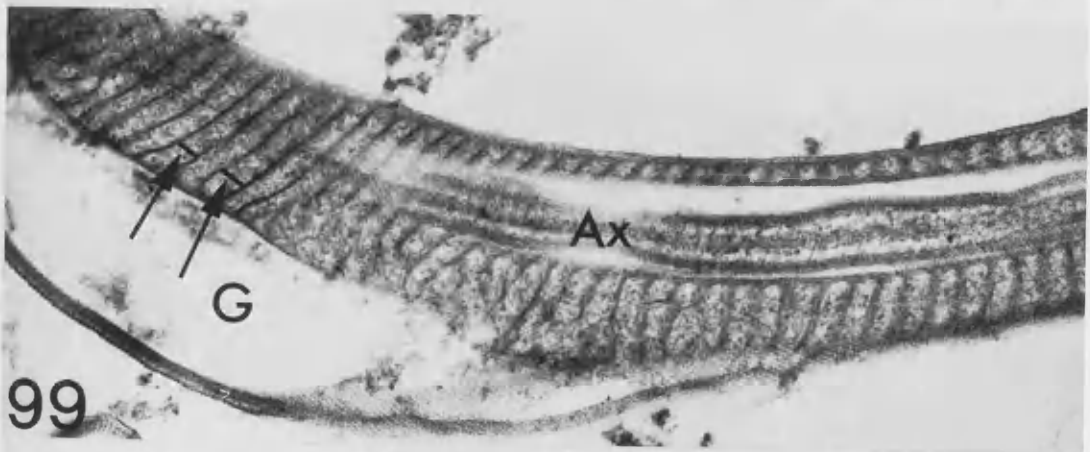
Ax
G
99

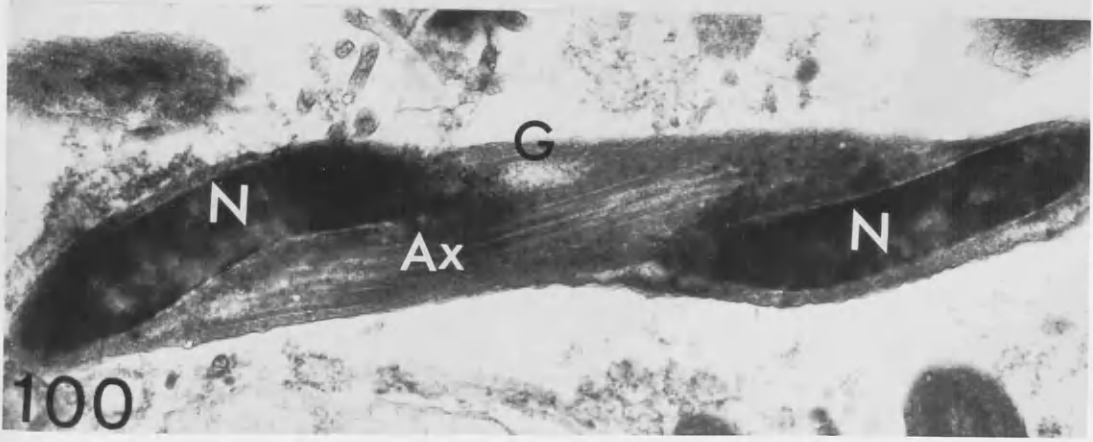
G
N
Ax
N
100

FIGURES 101 AND 102.

Archidoris tuberculata. PA-TSC-SP stained longitudinal (FIGURE 101) and transverse sections (FIGURE 102) of the spermatozoan flagellum, showing glycogen granules within the axoneme (arrowheads) and glycogen helix (arrows).
(Mags.: FIGURE 101, x.40,000; FIGURE 102, x.70,000).

FIGURE 103.

Aplysia faciata. PA-TSC-SP stained transverse section of the spermatozoan flagellum demonstrating the glycogen containing keel (arrow) and intra-axonemal glycogen (arrowheads).
(Mag. x.60,000).

FIGURE 104.

Tritonia plebeia. PA-TSC-SP stained transverse section of the spermatozoan flagellum. Note the strong glycogen staining in the glycogen helix (arrow). Arrowheads indicate intra-axonemal glycogen.
(Mag. x.90,000).

FIGURE 105.

Archidoris tuberculata. Transverse sections of the end piece of the spermatozoan flagellum.
(Mag. x.33,000).

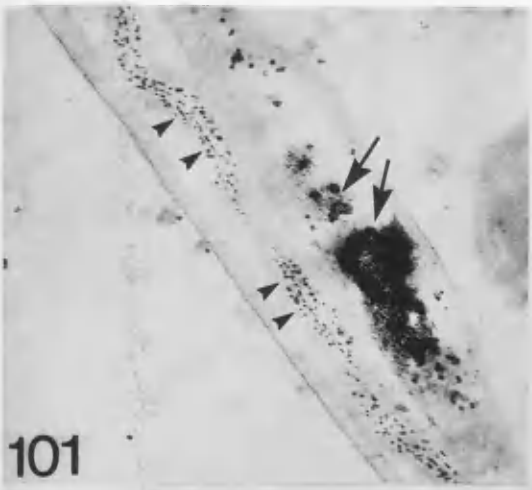

101

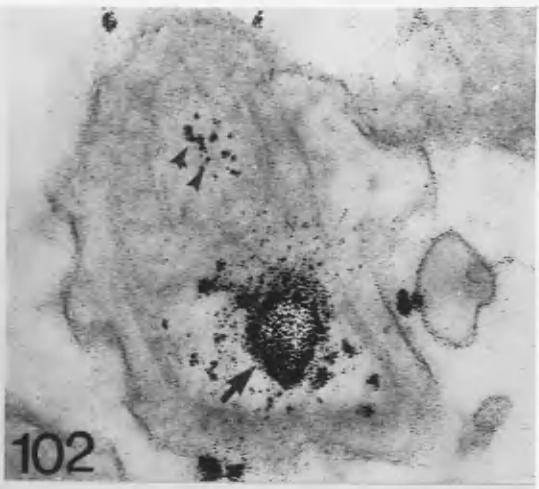

102

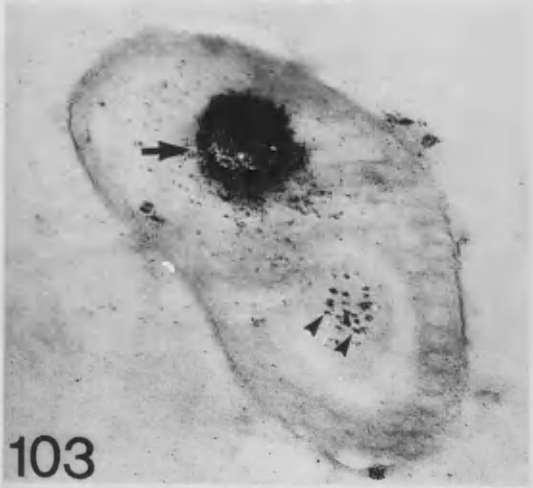

103

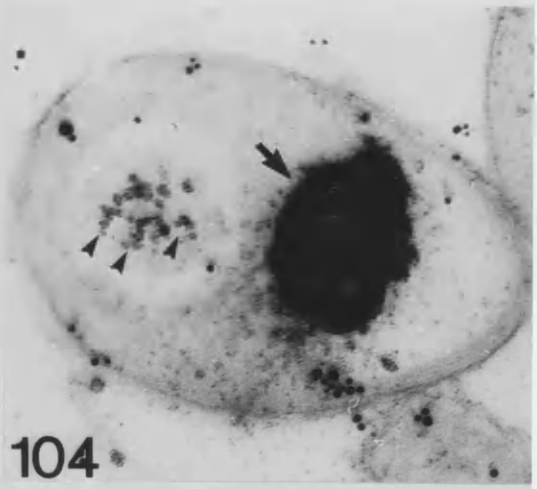

104

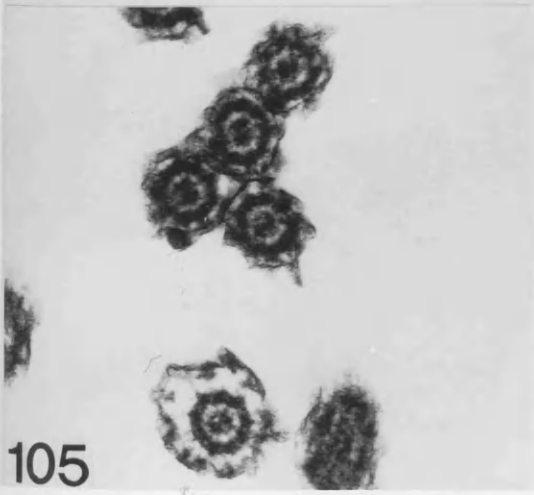

105

FIGURES FOR CHAPTER IV

FIGURES 1 AND 2.

Scanning electron micrographs of the ovotestis of Arion hortensis showing three lobules (FIGURE 1), with many acini within each lobule (FIGURE 2).

(Mags.: FIGURE 1, x.15; FIGURE 2, x.70).

FIGURES 3 AND 4.

Scanning electron micographs of the male compartment in an acinus. Note the large number of spermatozoa with their heads in close association with Sertoli cell cytoplasm.

(Mags.: FIGURE 3, x.750; FIGURE 4, x.1,900).

FIGURES 5 AND 6.

Scanning electron micrographs of the female compartment. The developing oocyte contains a large number of yolk granules (arrowheads). The oocyte is separated from the male compartment by a layer of follicular cells (arrows).

(Mags.: FIGURE 5, x.580; FIGURE 6, x.600).

ABBREVIATIONS: A, acinus; L, lobule; O, oocyte; S, Sertoli cell; Sz, spermatozoa.

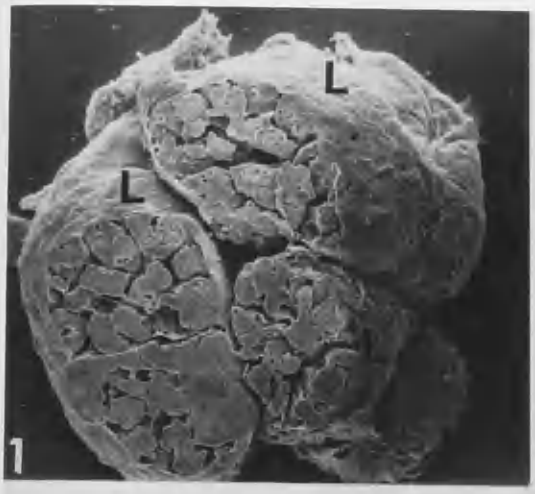
L
L
1

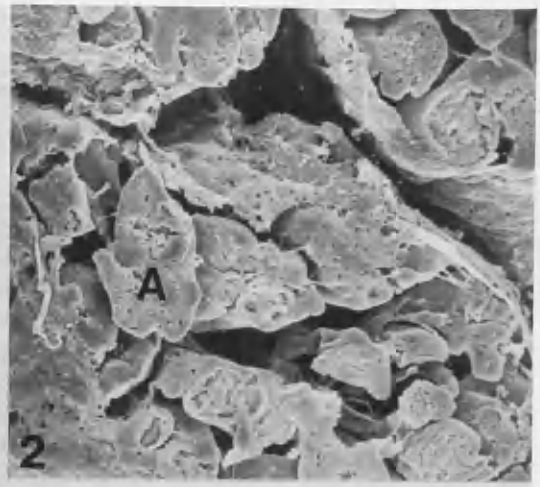
A
2

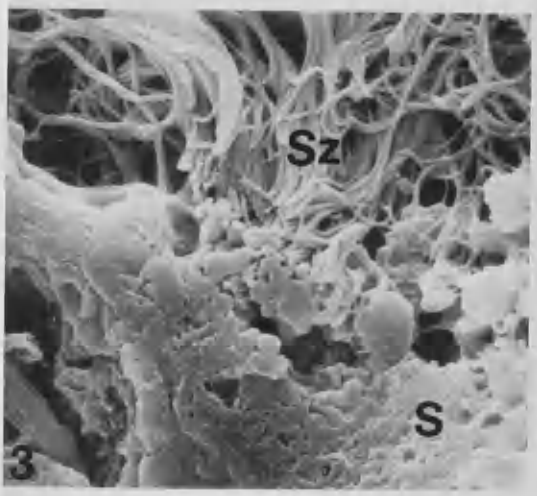
Sz
S
3

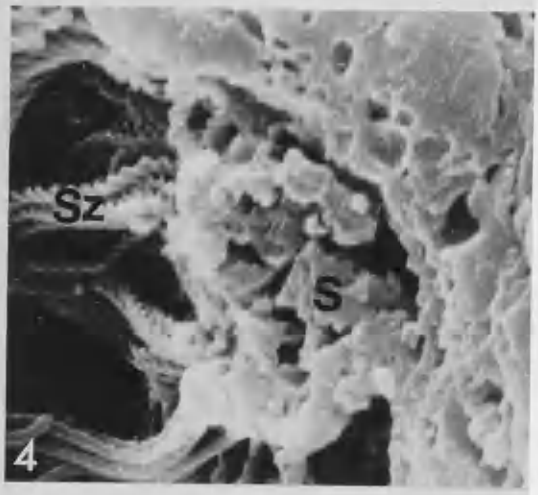
Sz
S
4

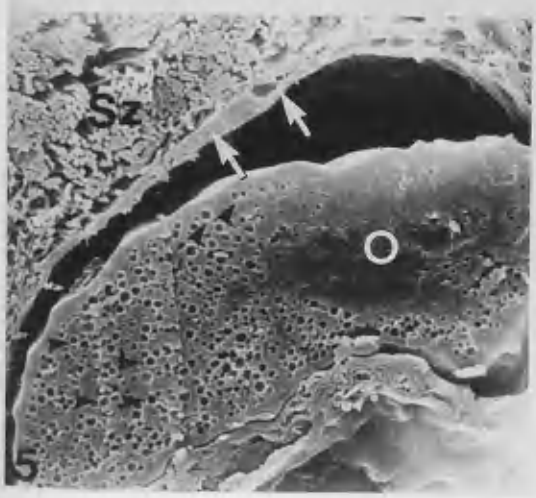
Sz
O
5


O
6

FIGURE 7.

A thin section through the wall of an acinus. A Sertoli cell body overlays the basement membrane. Developing male germ cells occur on the luminal aspect of the Sertoli cell. The irregular profiled Sertoli cell nucleus is filled with punctate heterochromatin. Many lipid droplets and vesicles occur in the cytoplasm.

(Mag. x. 9,200)

FIGURE 8.

A thin section of the cytoplasmic processes of two adjacent Sertoli cells, showing a desmosome-like junction (arrowhead) and closely associated long septate junction (arrow). Detail of the desmosome-like junction is shown in the inset.

(Mags.: FIGURE 8, x. 57,500; inset, x. 161,500).

FIGURE 9.

A freeze-fracture replica of the P-face of a Sertoli cell membrane. Desmosome-like junctions (arrowheads) occur on the membrane surface forming well defined groups (dotted lines and inset). The cytoplasm contains many membranous inclusions.

(Mags.: FIGURE 9, x. 20,000; inset, x. 46,700).

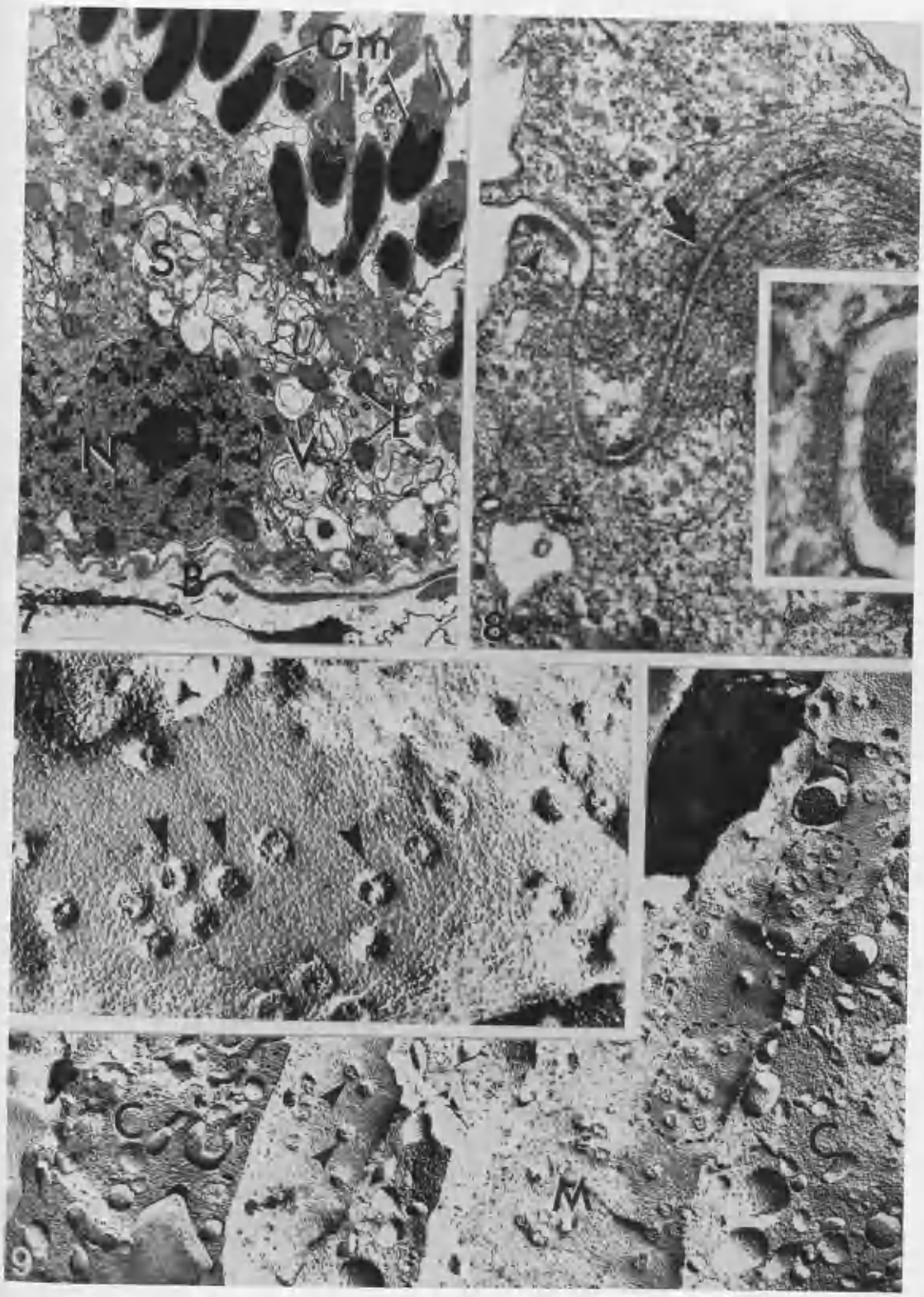
Gm
S
N
V
L
B
8
9
C
M
C

ABBREVIATIONS: B, basal lamina;

C, Sertoli cell cytoplasm

Gm, developing spermatogenic cells;

L, lipid;

M, Sertoli cell membrane;

N, nucleus;

S, Sertoli cell.

FIGURE 10.

A thin section of an area of desmosome-like junctions (arrowheads) between a spermatogonium and Sertoli cell, Detail of the junction is shown in the inset. No intermediate dense line is present.

(Mags.: FIGURE 10, x. 47,000; inset, x. 180,000).

FIGURE 11.

A thin section of an area of desmosome-like junctions (arrowheads) between a spermatocyte and Sertoli cell demonstrating the discrete intercellular space within the junction and well defined electron dense plaques on either side.

(Mags.: FIGURE 11, x. 24,500; inset, x. 132,000)

FIGURE 12.

An oblique thin section of an early spermatid and Sertoli cell. Well developed desmosome-like junctions (arrowheads) occur between the spermatid and adjacent Sertoli cell. Despite the slight obliquity of the section, a discrete intercellular space is apparent within the junction. The electron dense plaque is thicker on the germ cell side of the junction.

(Mag. x. 60,000).

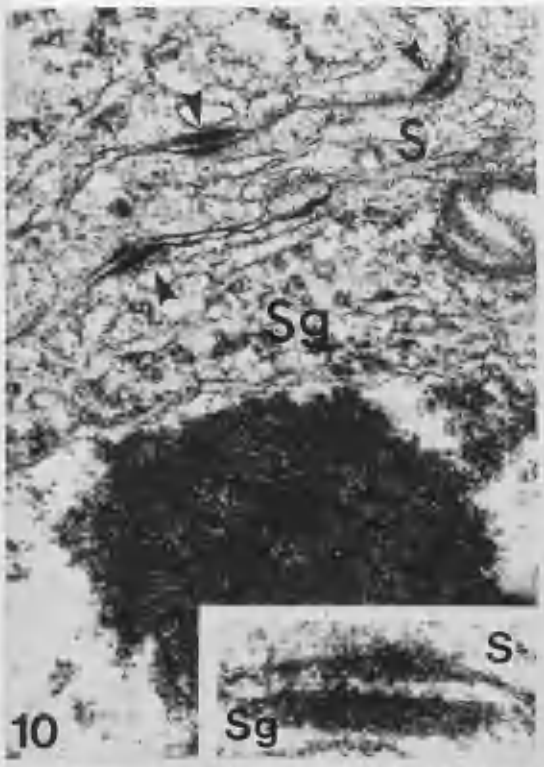
S
Sg
S
Sg
10

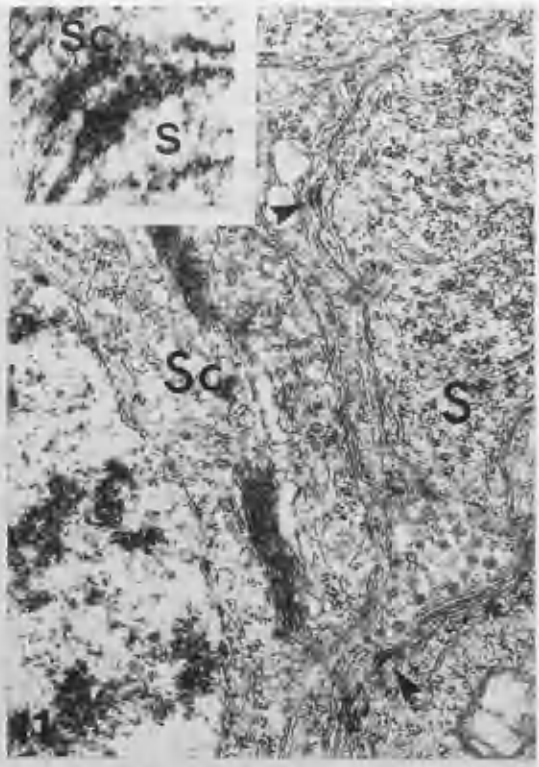
Sc
S
Sc
S
11

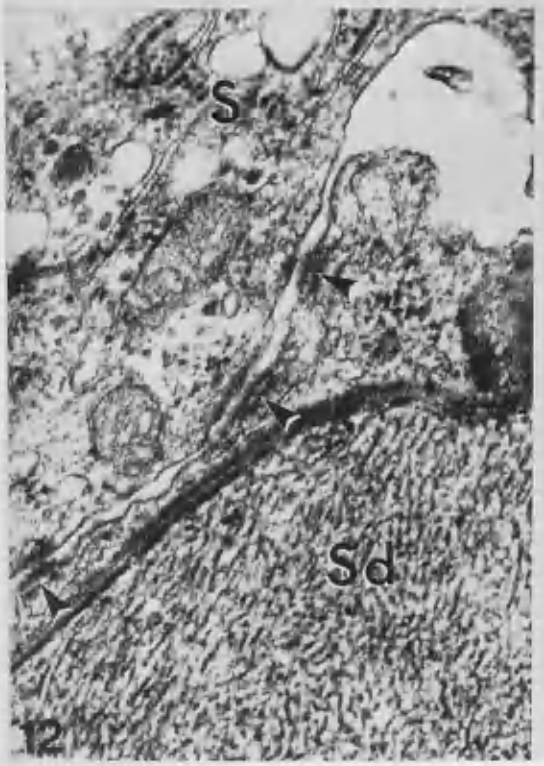
S
Sd
12

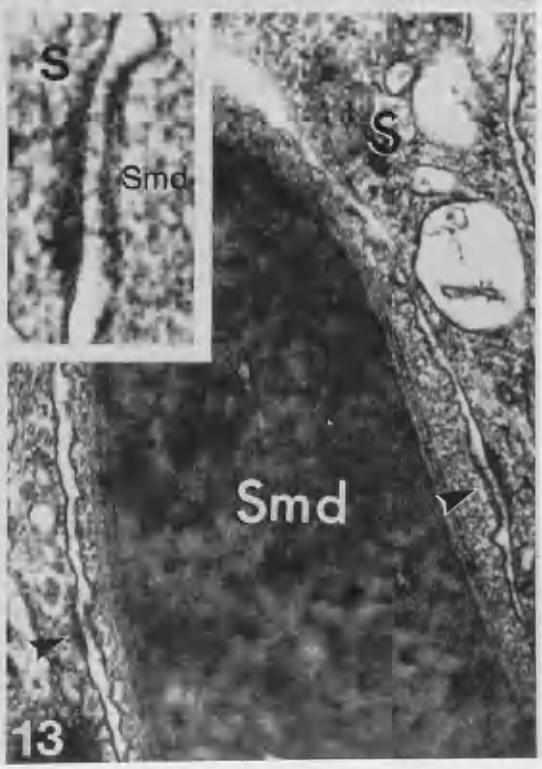
S
Smd
S
Smd
13

FIGURE 13.

A longitudinal thin section of a maturing spermatid in the region of the developing head. Two desmosome-like junctions (arrowheads) are present between the Sertoli cell and the maturing spermatid. The electron dense plaque on the Sertoli cell side is more prominent, a discrete intercellular space is present which is traversed by fine filaments.

(Mags.: FIGURE 13, x. 50,000; inset, x. 170,000).

ABBREVIATIONS: S, Sertoli cell; Sc, spermatocyte;
Sd, early spermatid; Sg, spermatogonium;
Smd, maturing spermatid;

FIGURE 14.

A freeze-fracture replica of the head of a late spermatid which is enveloped by the cytoplasm of a Sertoli cell. A desmosome-like junction occurs on the external surface of the membrane of the head (arrowhead).
(Mags.: FIGURE 14, x. 30,000; inset, x. 72,000).

FIGURE 15.

A longitudinal section of the head of a late spermatid. Only the apex of the nucleus is still intimately related to the luminal surface of the Sertoli cell where a desmosome-like junction occurs (arrowhead). The electron dense plaque on the spermatozoan side is reduced. A discrete intercellular space, bridged by fine filaments, is still present. A finger-like process (arrow) of the Sertoli cell lies in close relation to the spermatid.
(Mag. FIGURE 15, x. 40,000; inset, x. 190,000).

ABBREVIATIONS: C, Sertoli cell cytoplasm;
H, late spermatid head; S, Sertoli cell;
Sld, late spermatid.


H
C
14

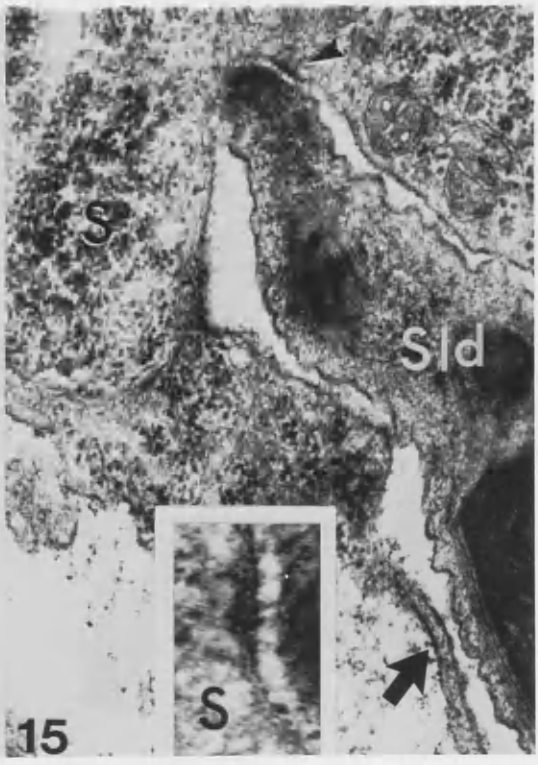
S
Sld
S
15

FIGURES 16, 17 AND 18.

Serial longitudinal thin sections through the head of a spermatozoon showing the intimate association of the spermatid head with Sertoli cell cytoplasmic processes. (Mags.: FIGURE 16, x.23,000; FIGURE 17, x.24,000; FIGURE 18, x.23,000).

FIGURES 19 AND 20.

Serial longitudinal sections through the head of a spermatozoon at the time of spermiation. Note finger-like Sertoli cell cytoplasmic processes (arrowheads) are in close association with the apex of the head.
(Mags.: FIGURE 19, x.29,000; FIGURE 20, x.29,000).

ABBREVIATIONS: A, acrosome; N, nucleus;
S, Sertoli cell.

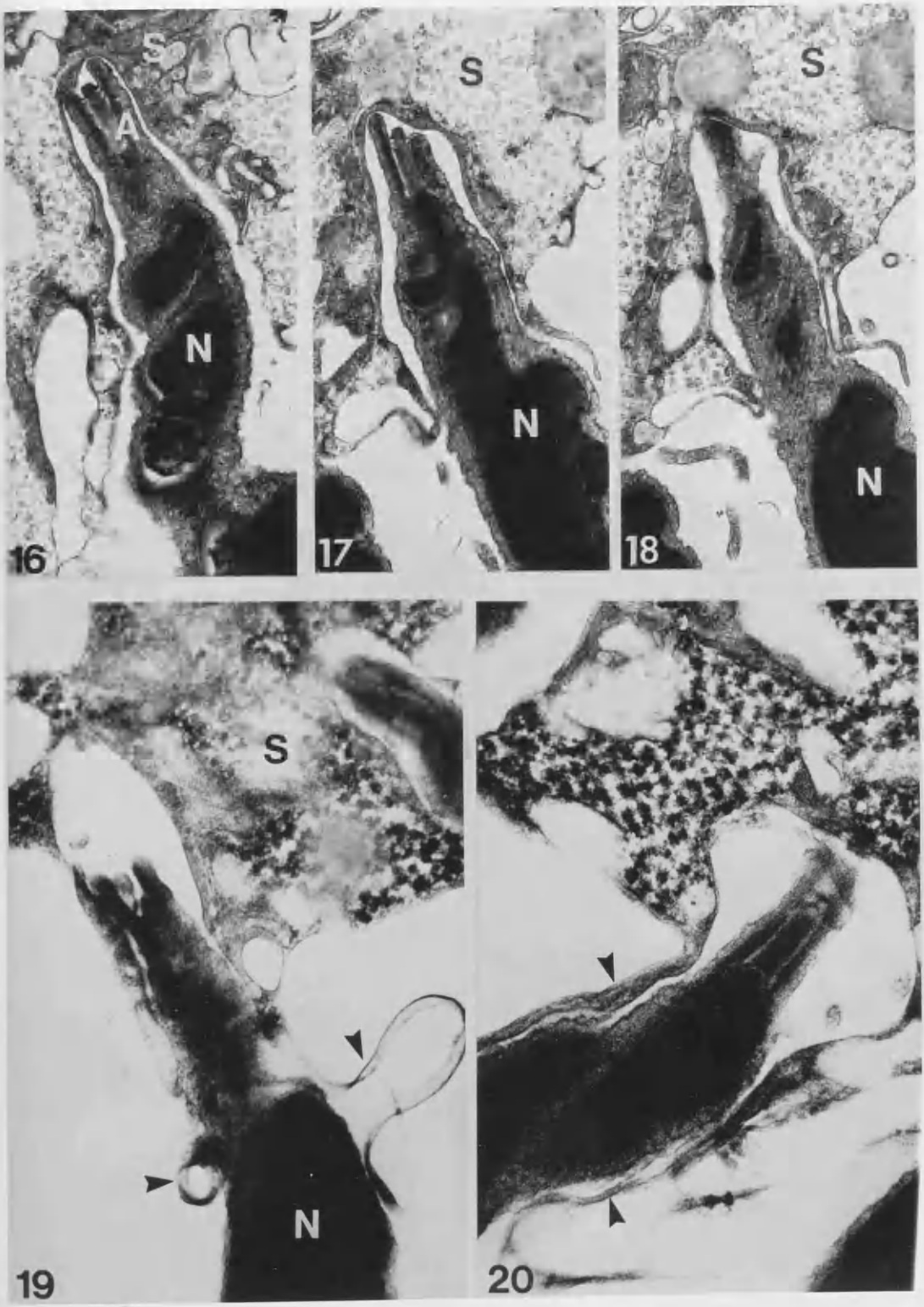
S
A
N
16
S
N
17
S
N
18
S
N
19
20

FIGURE 21.

A thin section through a desmosome-like junction between a spermatocyte and a Sertoli cell fixed in hypertonic medium (10% dextrose added). The intercellular space (*) is exaggerated, but the surfaces of two adjacent cells are still closely apposed at the junctional site (arrowhead) demonstrating its adherent role.

(Mag. x.132,000)

FIGURE 22.

Two desmosome-like junctions (arrowheads) between cytoplasmic fragments from a Sertoli cell and spermatocyte after treatment with strong hypertonic fixative solution (15% dextrose added). Despite cellular fragmentation, the desmosome-like junctions are intact with no change in the discrete intercellular space at the junctional sites and the dense plaque on the Sertoli cell.

(Mags.: FIGURE 22, x.52,000; inset, x.75,000).

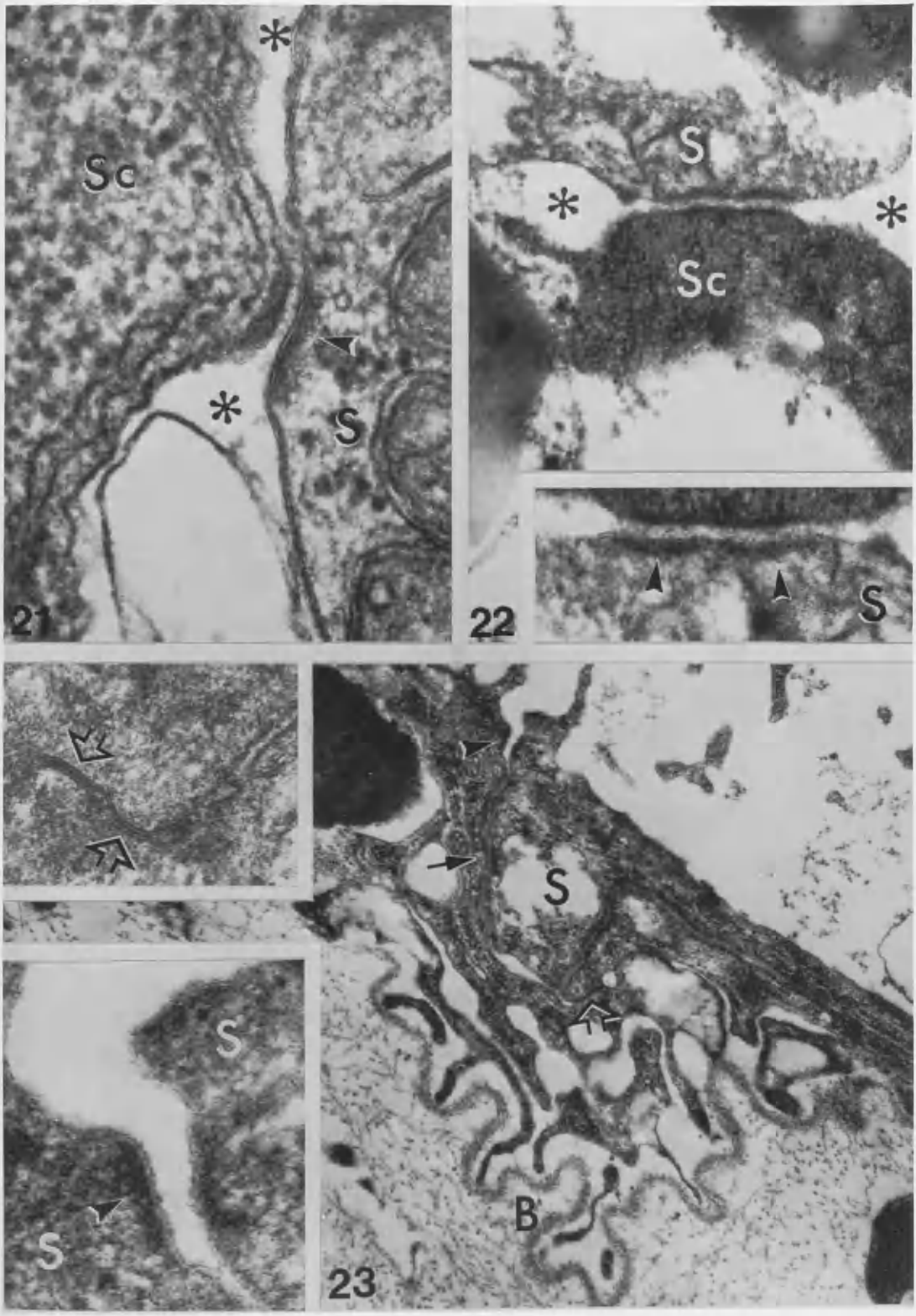
Sc
S
21
S
Sc
22
S
S
S
S
B
23

FIGURE 23.

A thin section of two Sertoli cells after treatment with fixative containing 15% dextrose. Although the cytoplasm is highly condensed and folding of the basal lamina suggests shrinkage, the adjacent Sertoli cells are still intimately linked by the desmosome-like junction (arrowhead, inset on the left bottom, mag. x. 126,000), septate junction (arrow, mag. x.25,000) and tight junctions (empty arrows, inset on the left top, mag. x.96,000).

ABBREVIATIONS: B, basal lamina; S, Sertoli cell;
Sc, spermatocyte;

FIGURES 24, 25 AND 26.

Sections through the germinal epithelium in the male compartment of an ovotestis treated with 5% lanthanum nitrate during fixation. Lanthanum nitrate (arrowheads) is visible within the intercellular spaces between Sertoli and developing germ cells.

(Mags.: FIGURE 24, x.5,000; FIGURE 25, x.3,300; FIGURE 26, x.9,500).

ABBREVIATIONS: B, basal lamina; L, lumen;
S, Sertoli cell; Sd, spermatid;
Sg, spermatogonium.

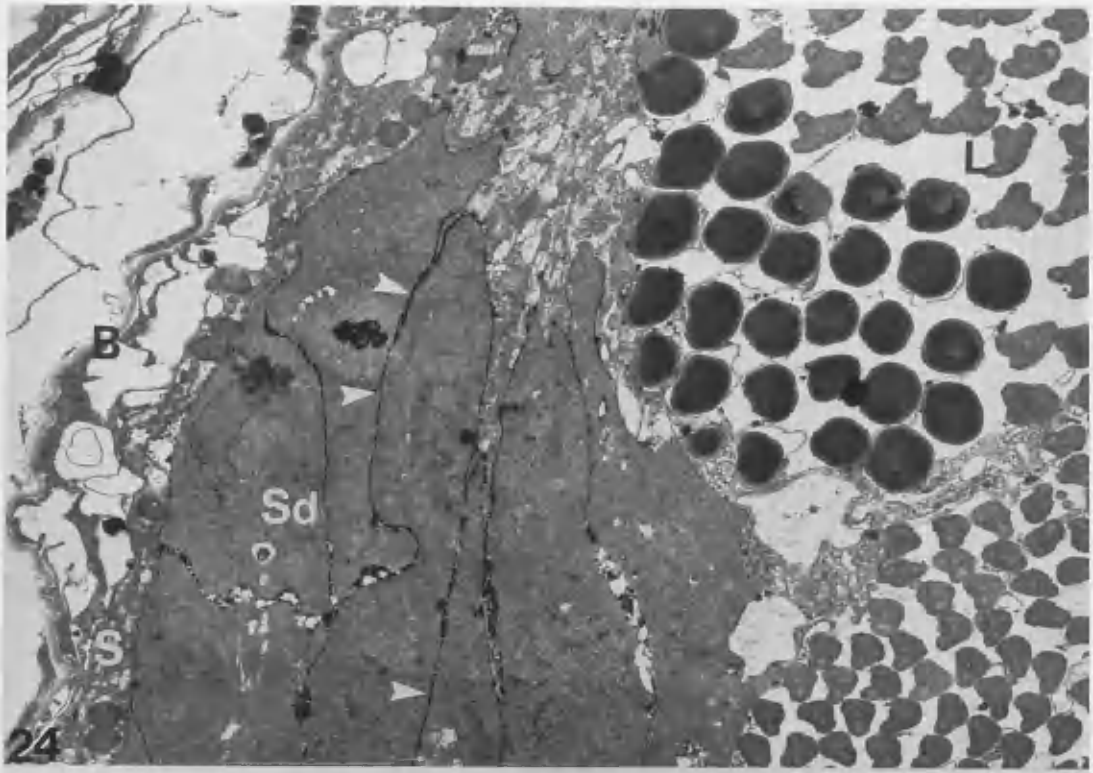
L
B
Sd
S
24

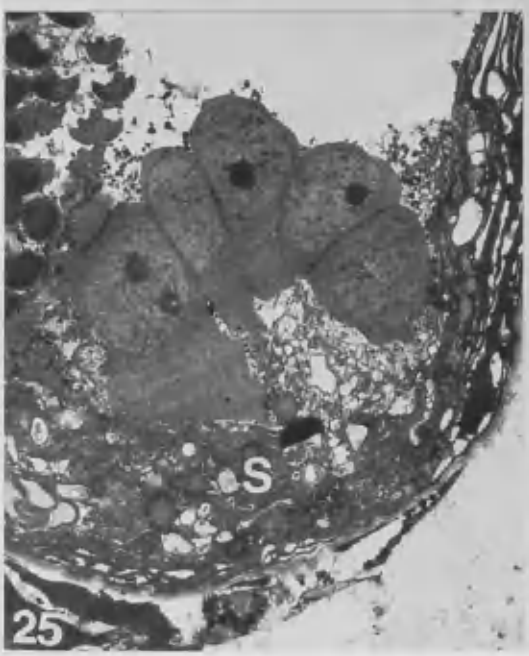
S
25

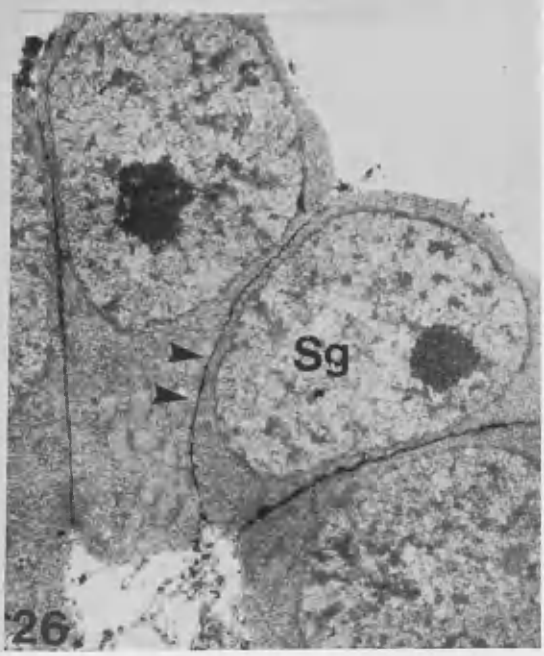
Sg
26

FIGURES 27 AND 28.

Lanthanum nitrate containing fixative treated ovotestis. Note that a large amount of lanthanum nitrate surrounds the elongating spermatids.

(Mags.: FIGURE 27, x.21,000; FIGURE 28, x.50,000).

FIGURES 29 AND 30.

Sections through Sertoli cells from an ovotestis treated with 5% lanthanum nitrate during fixation. Lanthanum nitrate penetrates between adjacent Sertoli cells (FIGURE 29) and also crosses the septate junction (arrow) (FIGURE 30).

(Mags.: FIGURE 29, x.46,000; FIGURE 30, x.70,000).

ABBREVIATIONS: L, lumen; S, Sertoli cell;
Sd, spermatid.

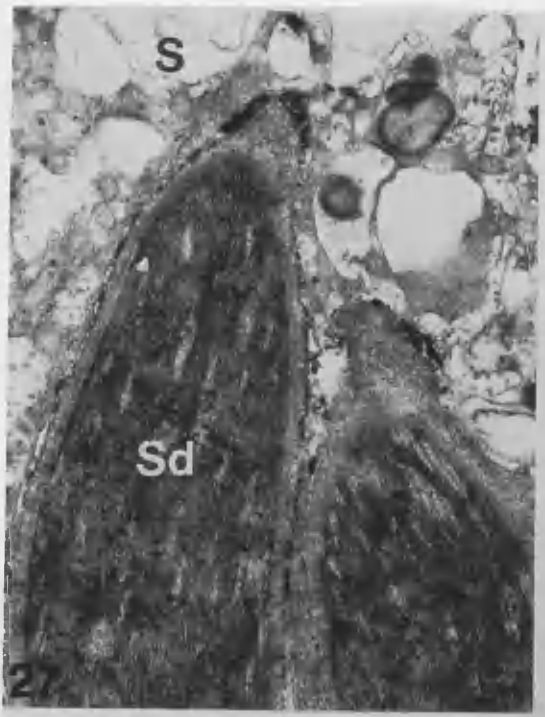
S
Sd
27

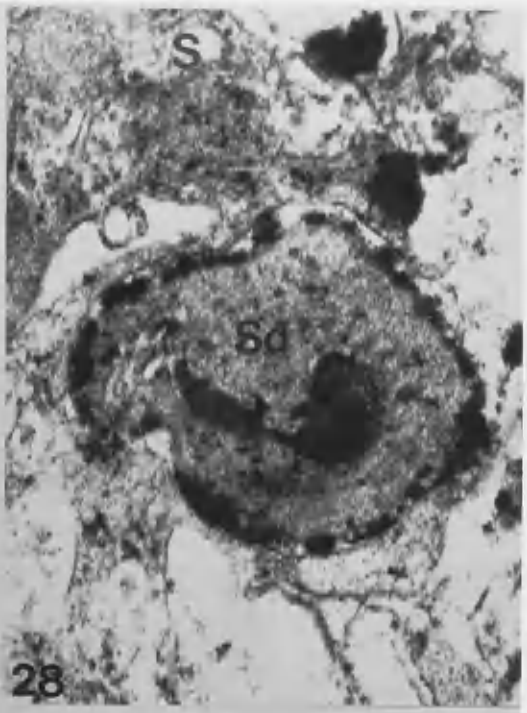
S
Sd
28

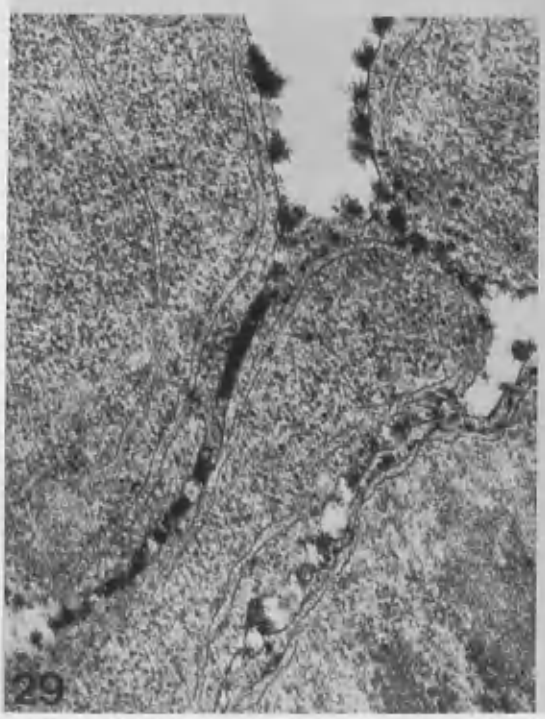
29

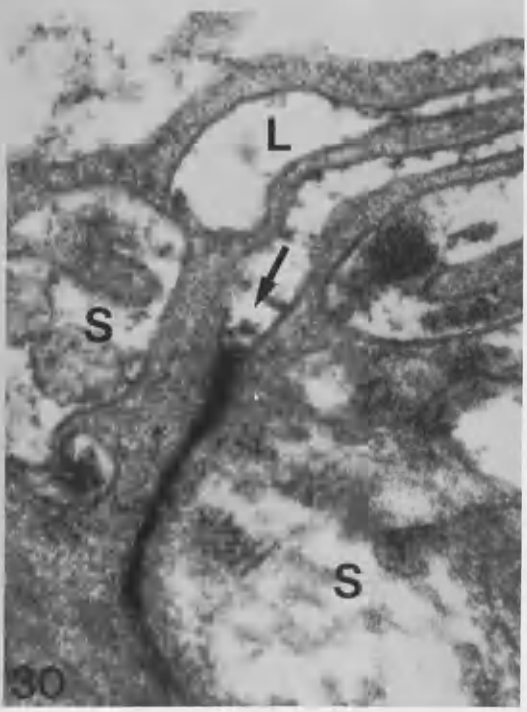
L
S
S
30

FIGURES 31 AND 32.

Thin sections through the basal portion of the Sertoli cells from an ovotestis treated with 5% HRP (horse radish peroxidase). Note HRP only penetrates partially into the inter-Sertoli spaces (arrowhead).

(Mags.: FIGURE 31, x.15,000; FIGURE 32, x.29,000).

FIGURES 33, 34 AND 35.

Thin sections through the distal part of Sertoli cells close to the lumen (also treated with 5% HRP containing fixative). HRP is partially blocked by the septate junction and failed to reach the acinar lumen (arrow).

(Mags.: FIGURE 33, x.125,000; FIGURE 34, x.44,000; FIGURE 35, x.80,000).

ABBREVIATIONS: L, lumen; S, Sertoli cell;
Sp, septate junction.


S
31

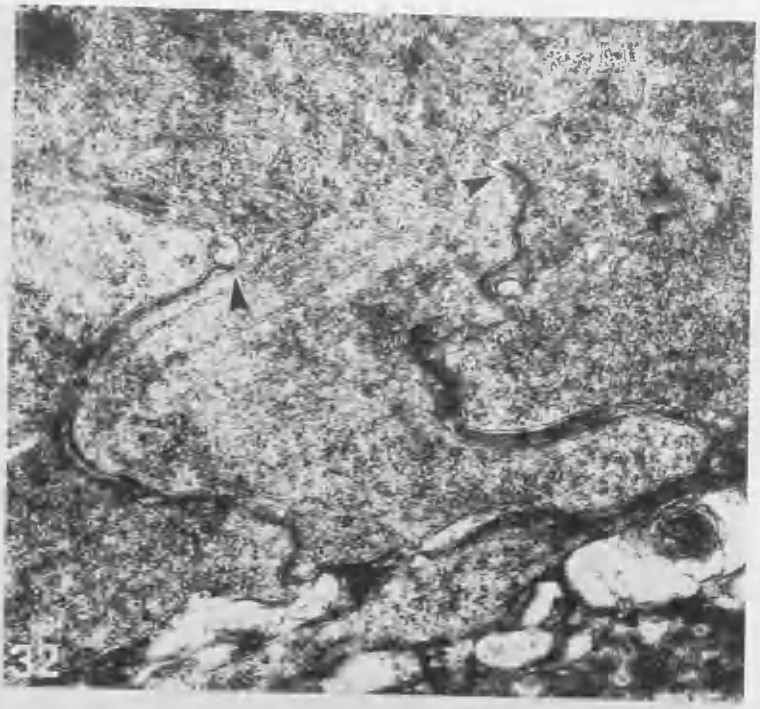
32

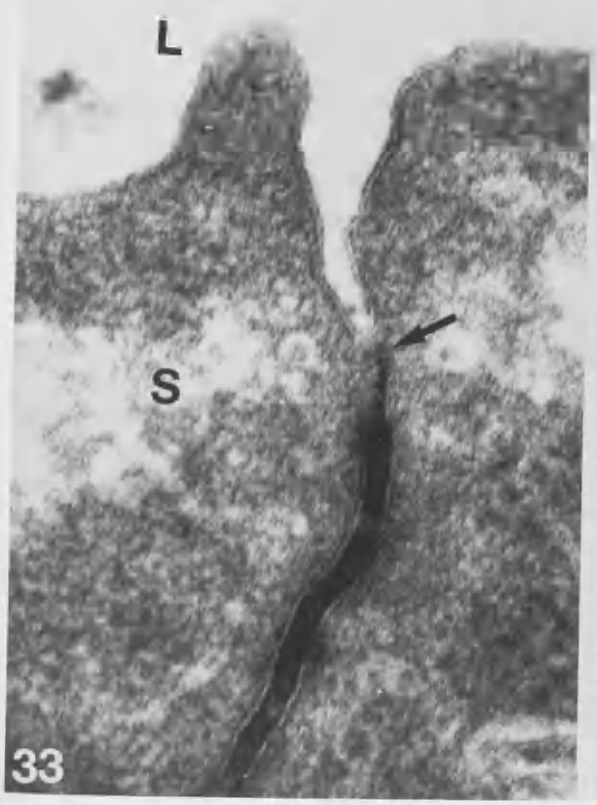
L
S
33

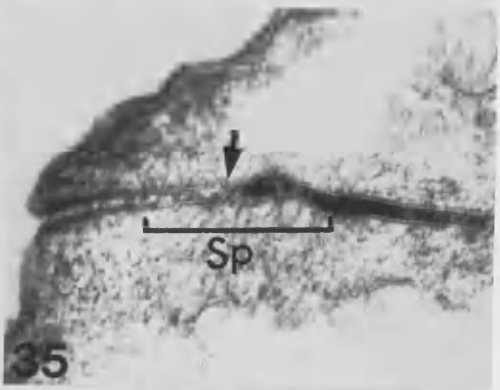
Sp
35


Sp
34

FIGURES 36 AND 37.

Thin sections through the basal portion of an acinus from an ovotestis treated with 5% Ferritin during fixation. Large ferritin particles (arrowheads) are blocked by the basal lamina and do not occur within intercellar spaces. (Mags.: FIGURE 36, x.46,000; FIGURE 37, x.47,000).

ABBREVIATIONS: B, basal lamina; S, Sertoli cell.

36

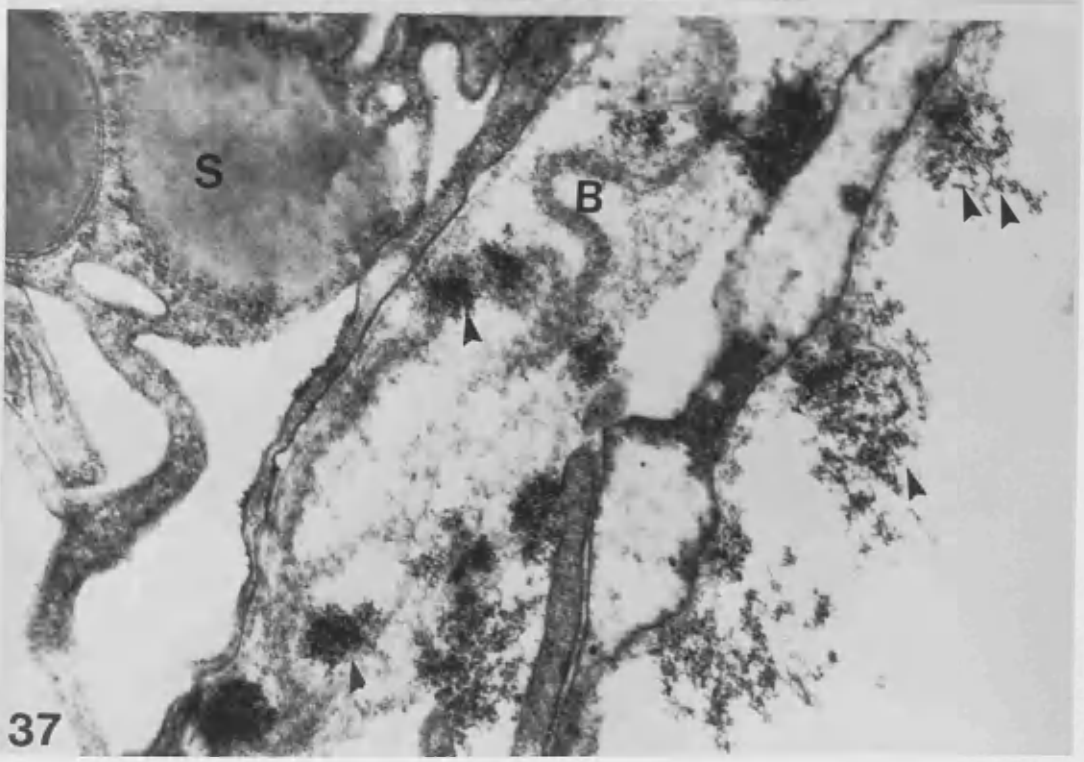

37